Production, Isolation and Characterisation of Fullerenes and Related Species

Robert James M^{c}Quillan

A thesis presented for the degree of
Doctor of Philosophy in the Faculty of
Science at the University of Edinburgh,
1997

To my Mum and Dad, thanks.

Abstract

This thesis describes the development and application of techniques for the production, isolation and characterisation of fullerenes and carbon nanotubes, and the attempted production of endohedral fullerenes.

A benchtop carbon arc reactor for the macroscopic production of these species was built. The construction and characterisation of this carbon arc reactor is described. Experiments aimed at optimising the productivity of the reactor by varying the operating conditions are described in relation to possible fullerene formation schemes.

These included the effect of experimental variables such as reactor buffer gas pressure, discharge current, internal dimensions and graphite electrode size on fullerene formation. The use of graphite electrodes packed with a possible fullerene precursor molecule, tri-indane, was also investigated as a means of probing fullerene formation mechanisms and increasing the quantity of fullerenes produced.

A wide range of techniques for the extraction of fullerene rich soot and for chromatographic separation and mass spectrometric characterisation of the resulting fullerenes have been investigated. A high yield extraction protocol is described involving preliminary large scale separation of fullerenes by competitive complexation with $AlCl_3$. Chromatographic studies led to the development of a novel stationary phase for separation of fullerenes using high performance liquid chromatography (HPLC). The characterisation of this stationary phase using on-line particle beam mass spectrometry is described. The change in enthalpy on adsorption of C_{60} and C_{70} on this stationary phase have been experimentally determined. A linear relationship between molecular weight and chromatographic retention time has also been established for fullerenes eluting from such a column.

Extensive use has been made of laser desorption/ionisation (LDI) time-of-flight mass spectrometry and MALDI for rapid characterisation of fullerene samples. The versatility of this technique is illustrated with examples of spectra demonstrating the high mass resolution and wide mass range that may be covered together with the use of MALDI, in conjunction with HPLC, to monitor the degradation of fullerene derivatives.

The use of the benchtop reactor for the production of endohedral fullerenes and carbon nanotubes is also described; although carbon nanotubes were successfully produced endohedral fullerenes could not be made. An examination of the factors that may affect the formation of these species in the reactor is given. The nanotubes produced were characterised using high resolution transmission electron microscopy (HRTEM) and were found to be multiwalled and occurred in disordered bundles.

Acknowledgements

The completion of this thesis would not have been possible without help and support from many sources. Firstly I would like to thank my supervisor Pat Langridge-Smith for introducing me to the field of fullerenes research, and for his help and advice throughout the course of this work. I would also like to thank my second supervisor Ian Gosney and Malcolm Banks for many valuable discussions on all aspects of this work.

This work would not have been possible without the assistance of many others. I would like to thank Youssef Ghaemi at Capital HPLC, Steve Davis at Kratos Analytical, Erik Williams at VG Analytical and Ian Mowatt for their help. In addition I would like to thank the departmental technical staff in particular Stuart Mains for his help in the design and construction of the fullerene reactor and for the use of their facilities including turning the welding room into a fullerene factory.

I would also like to thank my co-workers, Mike Dale, Craig Redpath, Scott Wright, and more recently Allison Hollingsworth, Angela Mudge and Michel Quiniou who although not directly involved in this work gave much support and provided a pleasant atmosphere in which to work. Thanks must also go for this to the rest of the room 5/6 crew and particularly to Gillian Sweeney for their cheerfulness in the face of my adversity.

Finally I would like to thank my Mother, Father Ruth and Rebecca for their support during my time at university.

Table of Contents

List of Figures

List of Tables

Chapter 1

Overview of Fullerene Research and Thesis Outline

1.1 Introduction

The discovery of Buckminsterfullerene, the unusually stable 60 carbon atom cluster, by Kroto *et al* [1] in 1985 and their proposal for the truncated icosahedral structure has led to major upheavals in the field of carbon cluster research.. Initial interest intensified further when in 1991 a method of producing C_{60}, and the other associated members of the fullerene family (C_{70}, C_{76}, C_{78}, C_{82}, *etc.*), in macroscopic amounts was discovered [2]. The structure for C_{60} as well as those for some of the higher fullerenes are shown in Figure 1.1

Fullerene science has from its earliest days been of interest to researchers with differing scientific backgrounds. The development by Kratschmer *et al* [2] of a method for producing fullerenes in macroscopic quantities opened the door further, so that today fullerenes are linked with research topics as diverse as astrophysical phenomena, high temperature superconductors, molecular wires and inhibitors of the HIV protease.

The behaviour of carbon, its reactions and the compounds it forms is the most studied area of chemistry. Carbon is one of the most abundant elements in the universe (after hydrogen and helium) and is believed to be the first stable element to be synthesised from the fusion reactions of hydrogen and helium produced in the original "big bang".

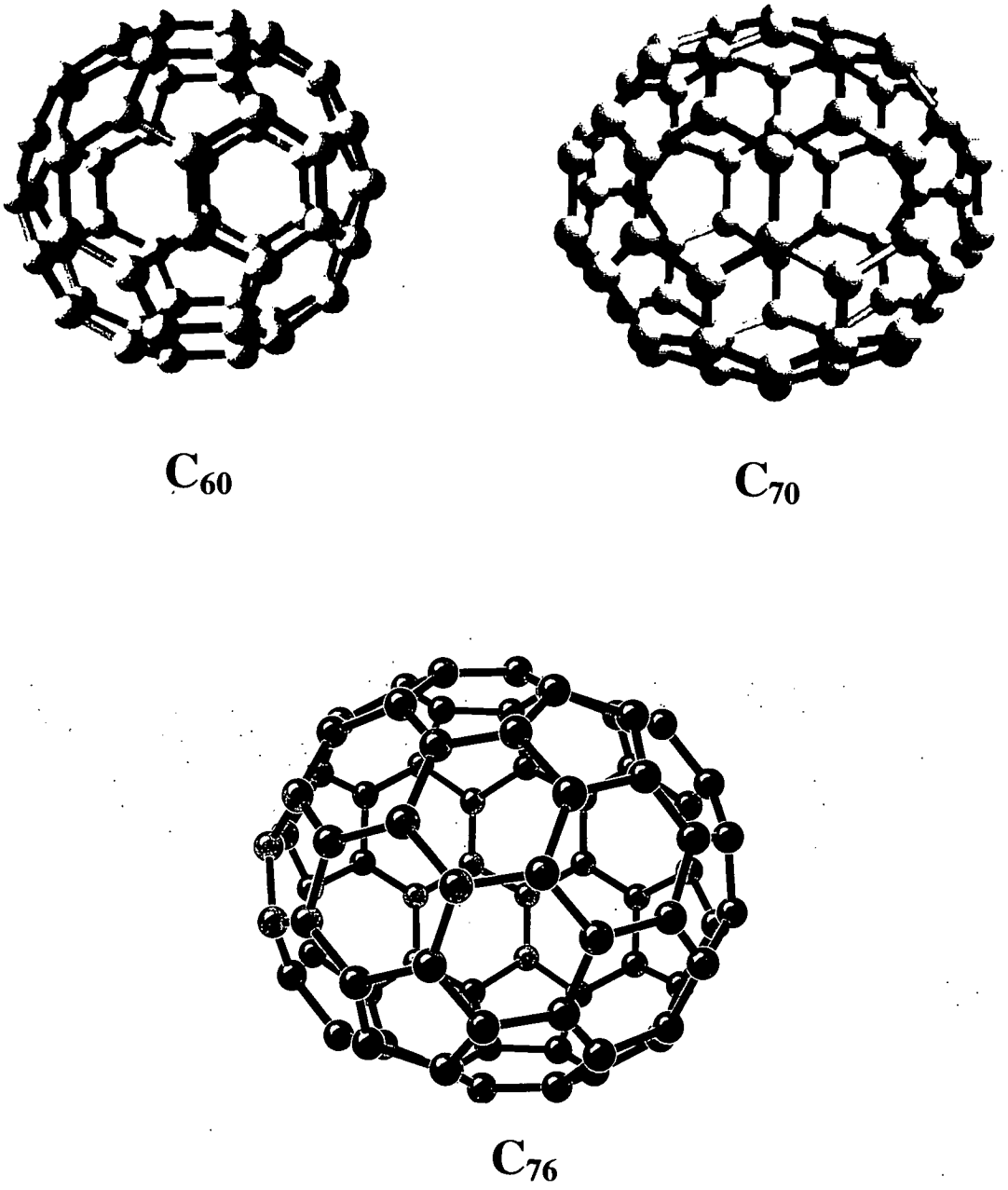

Figure 1.0: Molecular structure of C_{60}, C_{70} and C_{76}.

The importance of carbon chemistry explains the explosion of research into the fullerenes, which constitute a third allotropic form of carbon (diamond and graphite being the other two). The field of fullerene research has expanded at such a rate that it is no longer possible to give a full account of all aspects of fullerene chemistry. In the following sections aspects of fullerene research which are relevant to the work presented in this thesis are reviewed. A very general introduction to the field of fullerene research is given together with some practical and theoretical developments.

1.2 The Discovery of Buckminsterfullerene and Early Fullerene Research

The idea of a hollow carbon molecule is not a new one. It was first suggested by Jones [3] in a paper in 1966, writing under the pseudonym of Daedalus, in which he conjectured on the possibility of making large hollow carbon cages. The earliest recorded suggestion of the truncated icosahedral structure is contained in an article in *Kagaku* (in Japanese) by Osawa in 1970 [4], and was discussed further by Yoshida and Osawa [5] a year later in a chapter of their book on "superaromaticity". The structure was independently proposed in 1973 by two Russian chemists, Bochvar and Gal'pern [6], who carried out "Hückel" calculations on the molecule over a decade before the now famous paper in *Nature* appeared announcing the detection of C_{60}; further calculations were also carried out by Davidson in 1980 [7].

The impetus that would lead to the discovery of the fullerenes came, however, not from a chemist but from an astrophysicist named Douglas. In 1977 [8] he suggested that the "diffuse interstellar bands", unexplained features in the absorption/emission spectra of interstellar dust, might be due to some sort of carbon cluster. From work carried out at the University of Sussex by Kroto [9] in collaboration with Canadian radioastronomers the interstellar dust was known to contain long chain carbon molecules (the cyanopolyynes), found to be streaming out of red giant carbon stars.

The formation process for these species was believed to be related in some way to soot formation .

The subsequent development by Smalley and co-workers [10] of the laser vaporisation cluster beam technique, appeared to offer a means to simulate the high temperature conditions under which molecules might be formed in the atmospheres of stars. This led later to a collaboration between the Sussex group and Smalley's group at Rice University where the cluster beam technique had been developed. The laser vaporisation cluster source is based upon the principle that any material, no matter how refractory, can be volatilised at the focus of a high intensity laser pulse. The laser is fired at the material at the same time as a pulse (about 50-900 μsec long) of carrier gas, typically helium, is injected over the target. The laser pulse vaporises some of the target and superheats the volatalised material into a plasma. The plasma plume expands into the carrier gas where it is partly quenched. The carrier gas containing the entrained target material is then allowed to expand into vacuum, where it is cooled by supersonic expansion and clustering of the target material takes place. The degree of clustering that occurs is dependent on the conditions used and may be varied by altering factors such as the carrier gas backing pressure, the duration of the gas pulse and the time at which the vaporisation laser is fired relative to the carrier gas pulse. The resulting supersonic jet, containing the clusters, is then skimmed to form a molecular beam. The cluster species present in the beam can be investigated downstream using various mass spectrometric techniques. Nascent positive and negative cluster ions can be extracted by a pulsed electric field into the drift tube of a time-of-flight mass spectrometer, whilst neutral clusters can be photoionised using a second laser and the resulting positive ions similarly analysed with time-of-flight techniques.

Using this approach the collaboration between the Sussex group and the Rice group immediately showed that the long chain cyanopolyynes found in space [9] could be formed in a plasma produced by a laser focused on graphite [10][11]. By altering the clustering conditions, in an attempt to gain insight into formation processes, a

striking discovery was made. Under some sets of conditions the peak corresponding to C_{60} at m/z = 720 in the mass spectrum appeared to be extremely strong and its intensity could be varied dramatically to the point where it totally dominated the spectrum. Kroto *et al* [1] concluded that the cluster causing this peak must be stable to further nucleation and proposed that it had a truncated icosahedral structure, with all the atoms connected by sp^2 bonds and the remaining 60π electrons distributed in such a way that aromatic character would be highly likely. They also found that the C_{70} peak could be enhanced and under appropriate conditions the C_{60}/C_{70} ratio could be varied from *ca.* 20:1 to *ca.* 5:1.

The structure proposed for C_{60} was front cover news in the November 1985 issue of *Nature* and provoked a strong reaction from the scientific community. However, the structure was not initially universally accepted. Foremost among the sceptics was a group from Exxon research led by Kaldor. This group had also been investigating the laser vaporisation of graphite and had generated carbon cluster mass spectra a year before the Rice/Sussex group [12]. The Exxon group, however, explained their C_{60} atom carbon peak as merely a product of fortuitous clustering conditions, and not to some inherent property of the cluster itself [12][13]. This suggestion by Kaldor *et al* [12][13]was supported by Whetten *et al* [14] and by other workers at AT&T Bell Research Laboratories [15]. However, many scientists remained unconvinced by either argument and began to repeat the experiments performed by both the Rice/Sussex and the Exxon groups in order to determine just how special the C_{60} cluster was and to try and confirm or refute the hollow cage proposal.

Almost 5 years elapsed between the initial proposal of the truncated icosahedral structure for C_{60} by Kroto *et al* [1] and the isolation in 1990 of macroscopic amounts of the molecule by Kratschmer *et al* [2]. During this time the majority of research carried out into fullerenes was by mass spectroscopists and theoreticians. A brief summary of this early evidence for the truncated icosahedral structure of C_{60} is given below.

The structure proposed for C_{60}, in which all carbon valences are satisfied and any strain due to curving the polyaromatic system out of planarity is uniformly distributed over the surface, suggested that the molecule should be relatively chemically unreactive. Schmaltz *et al* [16] determined that there are over 12 500 Kekulé structures for the molecule showing resonance stabilisation. To test this behaviour Zhang *et al* [17], introduced gases such as CO, NO, SO_2, O_2, H_2, and NH_3 into the gas stream downstream from the nozzle where C_{60} is formed. In these experiments, the mass spectrum showed no features which could be attributed to chemical reaction of C_{60}, establishing its chemical inertness. Additional studies by McElvany *et al* [18] and by Weiss *et al* [19] further confirmed C_{60} and its analogues to be relatively unreactive.

However, when gases such as CO, NO, SO_2, H_2 were mixed with the driver gas in the nozzle reactions can take place before C_{60} is formed. Rohlfing [20], Hallet *et al* [21] and Doverstal *et al* [22], detected a wide range of hydrocarbon products when hydrogen was introduced in this way. The high resolution mass spectrometric studies of the reaction of C_{20}-C_{80} clusters with hydrogen by Rohlfing appeared to support the cage structure and suggested that the difference in reactivity of the different clusters was related to their structures [20]. The complementary studies by Hallet *et al* [21], and Doverstal *et al* [22], suggested, from the mass spectral patterns of the hydrogenated products, that clusters in the range C_{20}-C_{40} show at least three different types of reactivity. These observations are consistent with the suggestion that small fullerenes (*e.g.* C_{32}, C_{44}, C_{50} *etc.*) can also form [23].

The most obvious way to prove the hollow cage structure was to trap an atom inside it. The group at Rice University [24] were the first to demonstrate that such compounds, known as endohedral fullerenes, could exist. Heath, *et al* [24], vaporised carbon from a graphite disc soaked in $LaCl_3$. A peak in the mass spectrum at the correct mass for $C_{60}La$ was observed which was stable to photofragmentation even at high laser fluence, a strong indication that the La atom was inside the fullerene cage.

However, Cox *et al* [25] discussed these results in a paper in 1988, and concluded that the observations did not necessarily prove that $C_{60}La$ was a cage molecule.

From studies of the photofragmentation of carbon clusters [26], it was found that the fullerenes required a high laser fluence before fragmentation occurred, fragmentation proceeding *via* sequential loss of C_2 units to form the next smallest closed cage structure. Fragmentation continues in this fashion down to C_{32} when the steric strain becomes too great and the cage ruptures.

Further support for the closed cage structure for C_{60} came from applying these photofragmentation techniques to endohedral fullerene complexes [27]. $C_{60}K$ and $C_{60}Cs$ complexes were prepared by the laser ablation of graphite disks which had been soaked in alkali metal salt solutions. When these complexes were photofragmented it was found that the initial fragmentation occurred in the same manner as for normal fullerenes by loss of a C_2 unit. The fact that the metal atom was not lost in the initial fragmentation step indicated that it was on the inside of the carbon cage. It was also found that photofragmentation terminated, and the cage ruptured, at a higher internal radius for the endohedral complexes than for normal fullerenes. This was reasoned to be due to the increased steric strain incurred in the fullerene cage surrounding the encapsulated atom. The termination by sequential C_2 loss was found to occur at C_{44} for K and C_{48} for Cs, which is consistent with the known atomic radii of these species.

Between 1985 and 1990 while these mass spectrometric studies were being carried out, the fullerenes existed only in the gas-phase in highly sophisticated research instrumentation. While the search for a method to produce the fullerenes in macroscopic amounts went on, a great deal of work was carried out by theoreticians trying to predict the properties of this new molecule.

Theoretical calculations of the electronic properties of the fullerene family carried out by Fowler and Steer [28] indicated that they all had closed shell electronic structures.

As a guide to the aromaticity of C_{60}, the number of Kekule structures (12 500) was calculated by Schmaltz *et al* [16], Hosoya [29], and by Brendsdal and Cynn [30]. Hückel calculations on C_{60} have been carried out by many groups, e.g. Schmaltz *et al* [31] compared Hückel molecular orbital theory to resonant circuit theory and concluded that C_{60} should be less aromatic than benzene. The heat of formation of C_{60} was obtained by Luthi and Almlof [32] from Hartree-Fock calculations, whilst others such as Hale [33] calculated electronic properties and constructed orbital energy level diagrams for C_{60}. Newton and Stanton [34] provided initial details on the "normal vibrational modes of Buckminsterfullerene" which led to *ab initio* calculations of the vibrational properties of C_{60} and other fullerenes by Disch and Schulman [35].

Elser and Haddon [36] have investigated the magnetic response of C_{60} and found its magnetic ring susceptibility to be -0.21 that of benzene. This is an unusually small value and the calculated shielding effects of the π electrons on an atom placed in the centre of the cage were found to be less than 1ppm, due to cancellation of the diamagnetic and paramagnetic contributions. It was concluded from this study that C_{60} should not exhibit normal aromatic behaviour. These findings, however, have been disputed by Fowler *et al* [37], who have suggested the diamagnetic term has been underestimated and have extended their treatment [38] to predict chemical shifts in the N.M.R. spectrum of C_{70} that coincide well with observed values subsequently reported by Taylor *et al* [39].

1.3 Fullerene Production on a Macroscopic Scale

Although the theoretical predictions and insights gained from the early experiments, mainly carried out in mass spectrometry laboratories, were vital in order to try and obtain a proper understanding of the fullerenes, the study of this new species could not begin in earnest until a breakthrough in producing macroscopic amounts of the

fullerenes had been achieved. When this breakthrough was achieved, however, it was not made by chemists, but by researchers in a very different field. Huffman and Kratschmer were astrophysicists interested in interstellar dust. This dust is thought to consist mainly of short chain carbon molecules formed from carbon vapour in the atmosphere of stars. In the light of this Huffman, Kratschmer and their co-workers tried vaporising carbon in as many ways as possible. One method they used in 1983 was to evaporate a graphite rod by resistive heating in a helium atmosphere. The dust they produced showed an unusual "double hump" in the far UV region of its absorption spectrum which puzzled them since despite having examined many different samples from different sources they had never encountered anything like this before.

After reading in 1985 of the work of Kroto *et al* [1] and their discovery of C_{60}, Huffman and Kratschmer wondered if such a molecule could be the cause of their double-humped spectra. By 1989 they had convinced themselves sufficiently to examine the C_{60} hypothesis. They reproduced their original results and examined the IR spectra of their samples. Theoretical calculations for an icosahedral C_{60} molecule predicted that there should be four distinct bands in the IR spectrum. To their surprise, this is what they found in their experimental spectrum. They discovered a simple method of concentrating the C_{60} that they had produced in solid form. Following a basic dictum of organic chemistry, "like dissolves like", they found that fullerenes were soluble in benzene (the accompanying soot is not) thus giving further evidence of its aromaticity. The solvent was then evaporated leaving for the first time pure solid fullerenes [2].

In the time that has elapsed since Kratschmer *et al* [2] first published their results many improvements in the synthesis of fullerenes have been made. Reactors of many different types have been built, ranging from simple benchtop models (such as the one used in the current work), where a contact arc is set up between two graphite electrodes held together by gravity, to more elaborate plasma reactors [40], where a

gap between the electrodes is maintained by computer controlled stepper motors to form a plasma arc.

Other methods of producing the fullerenes have also been investigated. They have been detected in benzene/oxygen flames [41] and have been produced in reactors using hydrocarbons such as CH_4, C_2H_2, $CBrF_3$, CCl_2F_2, and C_2Cl_4 [42] Other techniquess for fullerene synthesis have employed hydrocarbon or carbon halides as starting materials. Coal has been used as an alternative to graphite, and has been shown to produce comparable yields of fullerenes at lower overall cost [43]. A solar powered fullerene reactor has also been constructed [44].

In addition to the exploration of different methods for producing fullerene rich soot the techniques for extracting the fullerenes have also been refined. An early development was the use of Soxhlet extraction with chromatographic separation techniques [45][46]. These techniques were further advanced by the development of different stationary phases. Flash chromatographic procedures using silica gel columns on which it is possible to separate gram quantities of C_{60} have also been introduced [47]. Commercially available HPLC columns have been developed [47][48] and chemical methods of separation also investigated. For example, host guest interactions have been investigated for C_{60}, such as the formation of complexes between C_{60} and water soluble macrocycles such as γ-cyclodextrin [49], and selective host guest interactions of fullerenes with calixarenes have led to techniques for separation of C_{60} and C_{70} [50].

The preparation of fullerenes in macroscopic amounts has led to significant developments in the field. Theoretical calculations on the structure and properties of C_{60}, and higher fullerenes, could be tested for the first time and experimentalists could begin to explore the chemistry and physics of these new materials.

1.4 Solid-State Properties

The structural and dynamical properties of the fullerene solids, and the many atomic and molecular species that are found to readily intercalate in the large interfullerene voids in these solids, have proved to be of immense interest.

In the solid-state at low temperatures, C_{60} exists in an orientationally ordered primitive cubic structure (Pa^3). There is an anisotropic electron distribution because there are two types of carbon-carbon bonds (i.e. "long" bond fusions of 5 and 6 membered rings, and "short" bond fusions of two 6 membered rings). The intermolecular bonding is predominantly van der Waals, with the electrostatic contribution optimised at low temperatures by aligning the electron rich regions ("short" carbon-carbon bond) of one molecule over the electron deficient regions pentagonal faces) of another.

At T_c (90-260K) the molecular dynamics of C_{60} in the solid-state change from a quasi-isotropic rotational distribution to "shuffling" between two distinct nearly degenerate orientations with "short" carbon-carbon bonds facing pentagonal or hexagonal faces. These two states are achieved by molecular "hops". On further cooling, (85-90K), the hopping motion freezes and a transition to an oriented glass-phase occurs.

There have been reports of the synthesis of polymeric forms of C_{60}. When C_{60} is exposed to visible or ultraviolet light (in the temperature range $250< T< 373$K), insoluble polymerisation products result [51]. The mechanism is believed to be a 2+2 cycloaddition forming a 4-membered carbon ring, fusing together adjacent molecules. Additionally rhombohedral polymeric forms of C_{60} have been identified in high hydrostatic pressure (5GPa) experiments at high temperature 500-800 °C [52][53].

Studies of solid-phase C_{70} have also been carried out, although this work has progressed at a slower pace. This has been due to the difficulty of producing large amounts of solid C_{70}, along with the greater complexity due to the lower degree of symmetry of the molecules (point group D_{5h}). Early X-ray and electron diffraction studies showed the coexistence of ccp and hcp crystalline phases with the hcp phase hard to eliminate [54].

1.5 Intercalation Compounds

Due to the large void space between the molecules in the solid fullerene structure (26% in solid C_{60}), small atoms or other molecules may be easily accommodated without significant distortion. Prolonged exposure to air, for example, can alter the properties of solid fullerenes through oxygen inclusion without drastically altering the structure. Intercalation of larger molecules is usually accompanied by a lowering in crystal symmetry and a change from cubic to hexagonal packing. This increases the volume of the interfullerene void space and allows the incorporation of such larger molecules. This is the case for certain simple intercalated systems such as $C_{60}(I_2)_2$ [55], $C_{60}I_2C_6H_5CH_3$ [56], $C_{60}(S_8)_2$[57], $C_{60}(P_4)_2$ [58]. Larger organometallic molecules like ferrocene can also be easily intercalated, *i.e.* $C_{60}(Cp_2Fe)_2$ [59]. Additionally an iodine-toluene intercalation compound of C_{60} involving co-ordinated I_2 molecules sandwiched between electron rich toluene, and electron deficient C_{60} molecules has been prepared [56]. The very short carbon-iodine distances imply that the I_2 molecules are acting as "molecular bridges" through which the C_{60}-toluene "donor-acceptor" interactions take place.

1.6 Alkali Metal Fulleride Intercalation

Some of the most interesting fullerene intercalation compounds yet produced are those formed by incorporation of electron donors like the alkali metals. This results in a mix of fulleride salts with well defined stoichiometries A_xC_{60}, where x can lie anywhere in the range 1 (*e.g.* CsC_{60}) to 12 (*e.g.* $Li_{12}C_{60}$). The highly ionic salts with the stoichiometry A_3C_{60} have been found to be superconducting with transition temperatures as high as T_c = 33K (e.g. $RbCs_2C_{60}$), [60]. The appearance of superconductivity in these compounds has led to extensive efforts to understand their electronic, structural and dynamic properties in order to account for their high T_c values and the superconducting mechanism. The fullerides are notably simpler systems than other high temperature superconductors and may be more easily amenable to theoretical modelling.

Deviations from the typical behaviour for A_3C_{60} type compounds occur when atoms with small atomic radii are introduced. For example, Li_2CsC_{60} is not superconducting [61]. This is perhaps due to the fact that the ionic radius of the lithium ion is smaller than the size of the tetrahedral interstice. Consequently, the C_{60}^{3-} ions are no longer confined to standard orientations allowing them to rotate more freely.

The geometry of the C_{60}^{n-} ions and their relationship to the observed superconductivity is an area of much interest. As previously mentioned, in C_{60} itself there are two different types of carbon-carbon bond; those that occur at the junction of two six-membered rings (6:6 bond) of length 1.40Å, and those that occur at the junction of five- and six-membered rings (6:5 bond) of length 1.45Å. Although a distortion from ideal icosahedral symmetry has been reported for C_{60}^{2-} in an iminium salt, the bond lengths are virtually unchanged [62]. This may be contrasted with the structural determination of C_{60}^{3-} ions in Na_2CsC_{60} [63], in which both types of bond are essentially equal (bond length 1.43Å) and an *ab initio* molecular dynamics

calculation [64] which predicts a smooth variation with the 6:6 bonds lengthening and the 6:5 bonds shortening on reduction.

Novel magnetic properties have also been reported for a number of C_{60} salts in which fullerene units carry a single negative charge. The simple salt RbC_{60} has been shown by X-ray diffraction to contain extremely close C_{60}-C_{60} contacts along one crystallographic direction; this is interpreted as one dimensional polymerisation of C_{60}^{-} ions through a 2+2 cycloaddition reaction forming a conduction pathway.

1.7 Inorganic and Organometallic Chemistry with Fullerenes

There have been two major trends in the synthesis of inorganic and organometallic fullerene derivatives. The first has involved the preparation of covalent addition products involving addition over a 6:6 ring junction. Because of the number of possible sites on C_{60} where this can occur (there are thirty 6:6 ring junctions), multiple additions are likely. The challenge, therefore, is to control the degree of addition, avoiding the formation of a wide variety of products which are difficult to separate into pure components. This has been possible in some cases and pure adducts have been obtained.

The other major area of synthetic activity has been the preparation of charge-transfer compounds, where the inorganic or organometallic partner functions as an electron donor and the fullerene as an electron acceptor. The degree of charge transfer depends on the redox potential of the donor. With suitable reductant components it is possible to obtain salts containing the fullerene anions (C_{60}^{-}, C_{60}^{2-}, *etc.*).

Pure crystalline samples of covalently bound addition products suitable for single crystal X-ray diffraction have allowed much information on the structure and reactivity of fullerenes to be firmly established. The adducts $C_{60}O_2OsO_2$(t-Bupy)$_2$

[65], $(\eta^2\text{-}C_{60})Pt(PPh_3)_2$ [63] and $(\eta^2\text{-}C_{60})Ir(CO)Cl(PPh_3)_2$ [66], characterised by X-ray crystallography in 1991, confirmed the proposed truncated icosahedral structure for C_{60}, whilst work using Vaska's compound, $(Ir(CO)Cl(PPh_3)_2$ produced the iridium adduct $(\eta^2\text{-}C_{70})Ir(CO)Cl(PPh_3)_2$ and established that the most reactive carbon atoms were those nearest the poles [66].

The reversible addition of Vaska's compound to the fullerenes made it possible to obtain a wide range of pure crystalline compounds with different members of the fullerene family and their derivatives. Crystallisation of the C_{84} adduct resulted in partial separation of two distinct isomers [67], while reaction with the fullerene epoxide $C_{60}O$, produced the compound $(\eta^2\text{-}C_{60}O)Ir(CO)Cl\ (PPh_3)_2$ [68].

A number of materials have been found to produce charge-transfer and salt-like compounds with C_{60}. Ferrocene, with a redox potential insufficient to generate C_{60}^-, forms the partial charge transfer compound $C_{60}\{(\eta^5\text{-}C_5H_5)_2Fe\}_2$ [69]. Polysilanes, not generally recognised as good electron donors, produce a fullerene doped form that displays charge transfer in the excited state [70]. Other inorganic reductants which are capable of reducing C_{60} include $\{Cr^{II}$ (meso- tetraphenylporphyrinole)$\}$, which enables reduction to C_{60}^- [71], and $(\eta^5\text{-}C_5H_5)Fe^I$ $(\eta^6\text{-}\ C_6Me_6)$ which allows reduction to C_{60}^-,C_{60}^{2-} and C_{60}^{3-} with stoichiometric control [72].

1.8 Electrochemistry and ESR Studies of Fullerenes

Numerous electrochemical and ESR studies have been reported for C_{60} and related molecules ever since large quantities of the fullerenes first became available in 1990. Although the electrochemical oxidation and reduction of these compounds has been well documented, the ESR studies of C_{60}^{n-} leave many unanswered questions and the spectra of species such as C_{60}^-, C_{60}^{2-}, *etc.* are open to several different interpretations.

Despite these unsolved problems in the spectra of C_{60}^{n-}, interest has moved on to the higher fullerenes with species such as C_{84}^{2-} attracting particular attention. Surprisingly the data appears to be more straightforward to interpret than that for C_{60} and, with better synthetic and isolation techniques for obtaining the higher fullerenes, they could eventually provide assistance with the assignment of the spectra for the corresponding C_{60} species.

The unique geometry of the fullerenes and their unusual electronic architecture with π orbitals radiating from the centre of the sphere have given rise to a number of theoretical and practical questions concerning the degree of conjugation and electron delocalisation.

The first studies of the electrochemistry of C_{60} demonstrated that it was possible to add two electrons reversibly to the molecule [73]. Subsequent to this observation, the corresponding tri-anion was also formed [74]. The triply degenerate nature of the LUMO of C_{60}, established from quantum mechanical calculations [75], prompted the search for more highly charged anions of C_{60} and has resulted in the detection of the tetra- [76] and penta-anions [77].

Studies of the anodic electrochemistry of the fullerenes have also been carried out. A chemically irreversible oxidation was observed for a C_{60} film, but the oxidised C_{60} was reported to be unstable [78]. However, this was disputed by Xie *et al* [79] who observed both chemically and electrochemically, reversible one-electron oxidations of C_{60}, and concluded that this was due to the solvent medium.

As the number of fullerene derivatives that have been produced has increased so has the number of measurements of their physical properties. Wudl *et al* [80-84] have carried out cyclic voltammetry on a wide range of derivatives, and have found that there are only minor perturbations in the electrochemistry of C_{60} due to the added derivative, even down to the fourth electron reduction. This was supported by studies

carried out by Suzuki *et al* [85]. However, Prato *et al* [86], have recently reported electrochemical behaviour beyond the fourth reduction wave.

In addition to this work the electrochemically induced isomerisation of a [5,6] methanofulleroid to a [6,6] methano-fullerene has been reported [87], suggesting possible means of using electrochemistry to effect structural transformations of fullerenes and their derivatives.

In contrast to electrochemical work, as yet there have been comparatively few ESR studies on anionic fullerene derivatives, despite the ease with which such compounds may be prepared and purified. This is an area of growing importance since such studies are necessary for comparison with those of free radical adducts of C_{60} in order to determine where the reduction electrons are located in the fullerene derivatives.

1.9 Derivatisation of Fullerenes

The development of fullerene chemistry has been hampered by a number of problems. Although these compounds undergo a number of different types of reaction and are potentially reactive, their unique geometry means that reaction products are often a complex mixture of isomers leading to difficulty in characterisation. The key, therefore, in the development of the chemistry of these compounds lies in the selective formation of single structural isomers in high yield. Even when this is possible, the lack of solubility of many fullerene derivatives leads to further complications, *e.g.* in characterisation using NMR spectroscopy.

Despite these difficulties there has been considerable progress in exploring the reactions of C_{60} and some underlying principles of the reactivity of the molecule have been established. Early theoretical studies [88], predicted high electron affinity for the fullerenes. This was supported by the early work of Wudl, Diederich and co-

workers [74] whose cyclic voltammetry studies showed that both C_{60} and C_{70} undergo reversible three electron reduction. Subsequently reversible four, five and six electron reduction of C_{60} has been achieved [76,77], [89].

Unlike the reduction experiments, oxidation of C_{60} has been found to be difficult and the oxidised products are chemically unstable [78]. Attempts to generate the diamagnetic cation in solution have been unsuccessful [90].

Miller and co-workers have used magic acid ($FSO_3H:SbF_5$) to oxidise C_{60} to the radical cation [91]. The oxidised C_{60} has been trapped with nucleophillic addition products with two, four and six groups adding symmetrically to the C_{60} radical cation. Species such as methanol, butanol and benzene have also been found to add to the C_{60} radical cation. Additionally, Christie and Wilson [92] have reported the oxidation of C_{60} to C_{60}^+ using XeF_2.

The first functionalisation of C_{60} and C_{70} *via* alkylation *(C-C)* was reported when the C_{60} polyanion was reacted with excess methyl iodide [93]. Analysis of the product using field ionisation mass spectrometry (FIMS) established the formation of methylated products containing 1 to 24 methyl groups (six and eight methyl groups predominating). However, the exact mechanism for methylation is still not clear.

1.10 Thesis Outline

As can be seen from this brief introduction to the field, fullerene research has rapidly become very diverse involving researchers from widely differing backgrounds. The research carried out in this work in some way reflects the way that the field has advanced. The initial goal was simply to produce fullerenes in macroscopic quantities. This was at a time when fullerene production in the laboratory was in its infancy and the design of our benchtop reactor was based on the first design of such a

reactor by Koch *et al* [94] who supplied us with details in advance of publication. The construction and characterisation of this carbon arc reactor is described in Chapter 2, including the design and modification of the reactor and initial experiments aimed at investigating the effect on fullerene formation of certain experimental variables, such as buffer gas pressure, discharge current and internal dimensions. Once this was accomplished experiments aimed at optimising the yield and increasing the efficiency and productivity of the reactor were carried out. Possible formation mechanisms are discussed in this chapter and experiments aimed at probing the formation of fullerenes are also described, some of these involving the introduction of a possible fullerene precursor molecule, tri-indane, to the graphite rods used in the reactor prior to combustion..

As the project developed and it became financially viable to buy in large quantities of fullerene rich soot, attention moved from the production of fullerenes in the reactor to the development of a high yield extraction protocol to separate and isolate the various fullerenes. This process contains many steps, from the extraction of the fullerene rich soot using different techniques and solvents to the separation and isolation of the different fullerenes and their identification. A full account of the range of techniques and instrumentation employed in this phase of the work is given in Chapter 3.

The experimental results arising from this work are collated in Chapter 4. These include the results obtained using different extraction protocols, as well as discussion on the temperature dependence of C_{60} solubility, the development and characterisation of a novel stationary phase for the chromatographic separation of fullerenes using high performance liquid chromatography (HPLC) and on-line LC-MS, studies of a non-chromatographic separation method and the characterisation of fullerene samples by laser desorption/ionisation time-of-flight mass spectrometry.

In addition to the production of fullerene rich soot the carbon arc reactor was also employed in experiments aimed at producing related species, namely endohedral

fullerenes and carbon nanotubes. Chapter 5 contains a description of the experimental procedures and a discussion of the results obtained, including an examination of the factors that may effect the formation of these species in the reactor. This chapter also includes images of the carbon nanotubes obtained by high resolution transmission electron microscopy (HRTEM) as well as a brief description of this technique.

Chapter 2

Production of Fullerene Rich Soot

2.1 Introduction

Immediately after the startling discovery of C_{60} and the proposal for the truncated icosahedral structure for the molecule by Kroto *et al* in 1986 [1], interest in the field became intense. Although the initial conclusions regarding the structure of C_{60} had been supported by extensive further experiments and theoretical calculations, no more than a few tens of thousands of these new molecules could be produced, sufficient to detect in sophisticated mass spectrometers but not enough to see or touch. The fullerenes existed only in the gas-phase in highly sophisticated instrumentation in research laboratories. It was necessary to try to understand how these highly symmetric molecules might form from condensing carbon vapour in order to find a method for producing macroscopic amounts of C_{60} so that studies of its properties could begin in earnest.

Kroto *et al* [95] originally postulated that C_{60} was formed in laser ablation experiments as layers of graphite were removed intact and re-arranged by two- and three-body collisions to incorporate pentagons into the "chicken wire" structure, so curving and eventually closing to form fullerenes. These ideas developed into the "pentagon road" mechanism which will be discussed in more detail later. Structures not incorporating enough pentagons to curve sufficiently to permit closure would simply continue to grow, the so-called "icospiral nucleation scheme", rather like a snowball rolling downhill.

The similarity between fullerenes and the proposed structures for soot precursors suggested that the formation schemes were related. This was verified when Gerhardt *et al* [96] found that C_{60} could indeed be detected during the soot formation process, leading to interest in different methods of vaporising graphite.

The breakthrough came when the astrophysicists Huffmann and Kratschmer and their co-workers, in their investigations into interstellar dust particles, attempted experiments aimed at simulating the conditions under which carbon nucleates in the atmosphere of stars. When a sample of soot prepared by the resistive heating of a graphite rod in an inert atmosphere was extracted with benzene they found that they had produced for the first time a macroscopic amount of pure fullerenes [2].

Since these results were first published in 1990, a great many fullerene reactors have been built. The majority of these are variations on the original technique, involving resistive heating of graphite in an inert (He) atmosphere, although fullerenes have also been produced in sooting flames (benzene/oxygen) [41], and in sputtering and electron beam experiments. A brief description of some of these different techniques follows.

2.2 Fullerene Production Techniques

2.2.1 Benchtop Reactors

The simplest of the reactors used in fullerene production are the "benchtop reactors". These have been used primarily in experiments aimed at probing reaction conditions or in the production of different types of species (*e.g.* endohedral fullerenes or carbon nanotubes), rather than in the large scale production of fullerenes. A diagram of a typical benchtop reactor is shown in Figure 2.1. This design was one of the first employed for fullerene synthesis and was published by Koch, Khemani and Wudl in

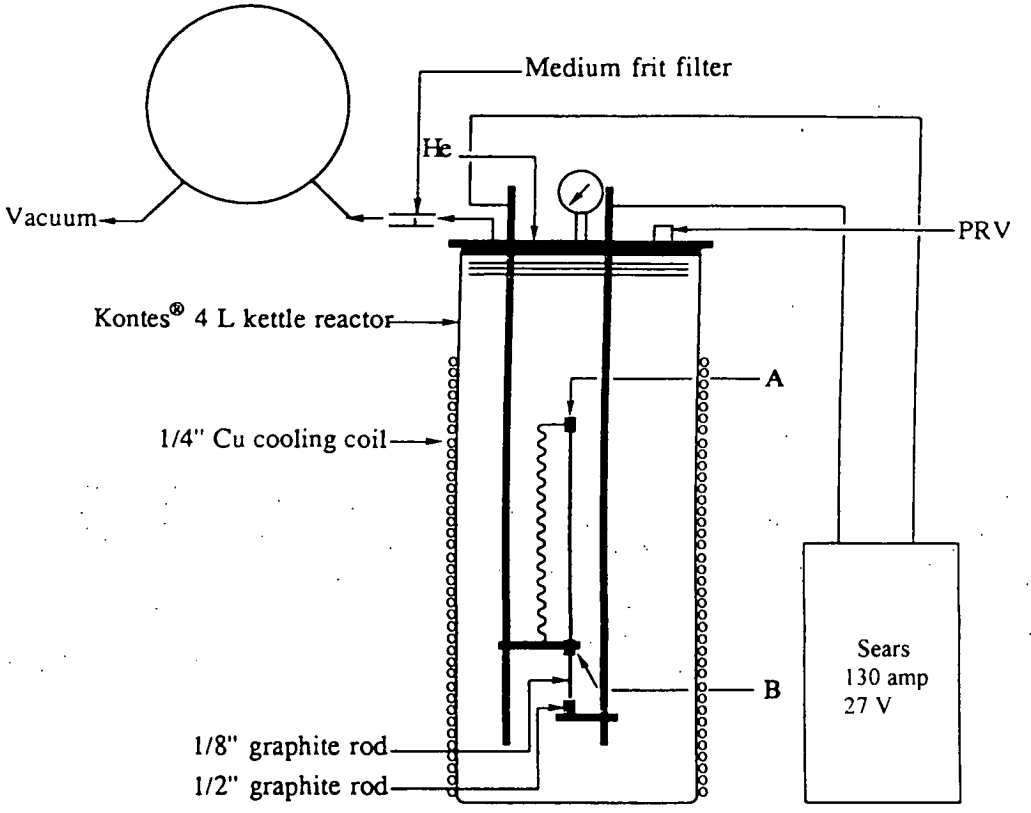

Figure 2.1: Benchtop reactor used for fullerene generation

1991 [94]. With this type of reactor a contact arc is set up between the upper 3 mm dia. consumable rod and the lower 6 mm dia. rod, using a current of 100-150 amp and a He pressure of 100 torr.

The design of this type of reactor is very simple. The apparatus is water-cooled by a 6 mm dia. copper cooling coil. The sacrificial graphite rod is gravity fed and the soot is all contained in the reaction vessel. Koch *et al* [94] reported yields of 1/4 gram C_{60} per day (1/2 gram soot extract per day). At a current of 55 amps they reported that it took 10 minutes to burn 150mm of the 3 mm graphite rod with approximately 20 minutes required for the apparatus to cool before the soot may be recovered. Using higher currents (120-150 amps), 150mm of graphite rod could be consumed in only one minute. However, there is a substantial decrease in the yield of fullerenes produced (1-2 %). The main advantage of this type of reactor is its simplicity. It can be assembled almost entirely from commercial components, having very few machined parts, at a relatively low cost and can easily fit into a fume hood. It is simple to use and the soot can be easily recovered with the production of useful amounts of fullerenes.

2.2.2 Plasma Reactors

The technique used for fullerene production with benchtop reactors is modified slightly for use with plasma reactors. Both reactors produce carbon soot from the evaporation of graphite rods in an inert He atmosphere. In a plasma reactor, however, a plasma discharge rather than a contact arc discharge is employed. This is achieved by moving the electrodes apart after the contact arc is initiated and maintaining this gap mechanically as the sacrificial electrode is consumed.

Figure 2.2 shows the plasma reactor used in the high yield synthesis of fullerenes by Parker *et al* [97] at the Argonne National Laboratory. The vacuum chamber is evacuated by a mechanical pump to a base pressure of 10^{-2} torr, and is then filled to a pressure of 200 torr with helium. The region near the graphite electrode is lined with

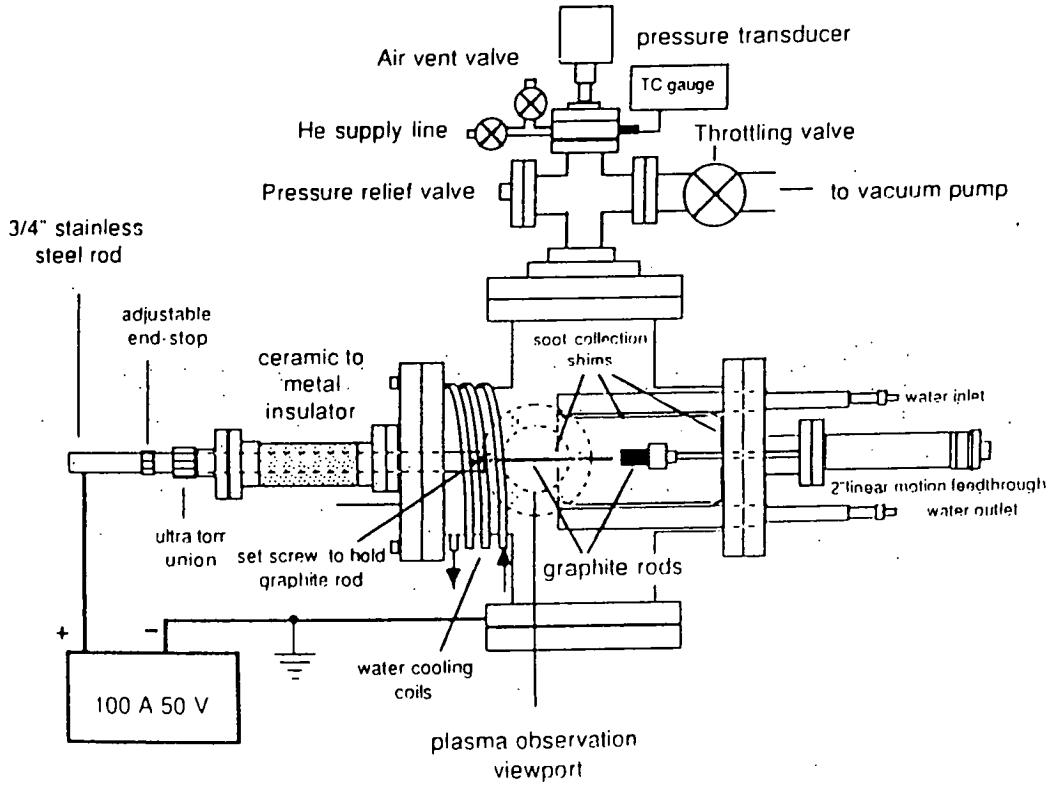

Figure 2.2: Plasma reactor used in the high yield synthesis of fullerenes at the Argonne National Laboratory [97].

water cooled stainless steel shims on which the fullerene rich soot collects, and the outer surface of the chamber is surrounded with copper cooling coils. At the end of a run, the shims can be easily removed and the soot recovered. A large 13 mm dia. graphite rod is attached to a 50 mm linear feedthrough drive. The smaller 6 mm dia. rod is held in a stainless steel holder, which can be fed into the chamber by means of a modified UltraTorr™ union. This design allows the entire length (305 mm) of the rod to be "burned" without breaking vacuum. The holder is attached to the positive lead of the power supply. A ceramic to metal insulator electrically isolates the smaller carbon rod from the chamber. The negative lead of the power supply is attached to the grounded vacuum chamber.

To generate fullerenes the two carbon rods are first positioned so that they are touching. The power supply is set for a current limit of 70 amps, and the voltage is set to 20 volts. Resistive heating occurs when the rods are touching. The rods are moved apart using the fine control provided by the linear motion feedthrough until the plasma is burning steadily. The plasma can be viewed indirectly through the viewport and the gap adjusted to maintain the maximum brightness of the plasma. The gap between electrodes is typically around 4 mm during operation. Typical operating conditions are 18 volts at 60 amps (1kW). Under these conditions the smaller 6 mm dia. electrode is consumed at the rate of 5 mm per minute. Using 3 mm dia. electrodes the power requirement is less (18V, 25A) but the electrodes tend to break.

2.2.3 Generation of Fullerenes using Solar Power

Remarkably, solar power has been used for production of fullerenes. Figure 2.3 shows the 10kW solar furnace used for fullerene production at the National Renewable Energy Laboratory (N.R.E.L.) in Colorado [44]. The instrument delivers a solar flux of 1200 W/cm^2 to a graphite pellet. Sunlight is channelled through two sets of concentrators and directed onto a 12cm diameter target in the exit aperture of

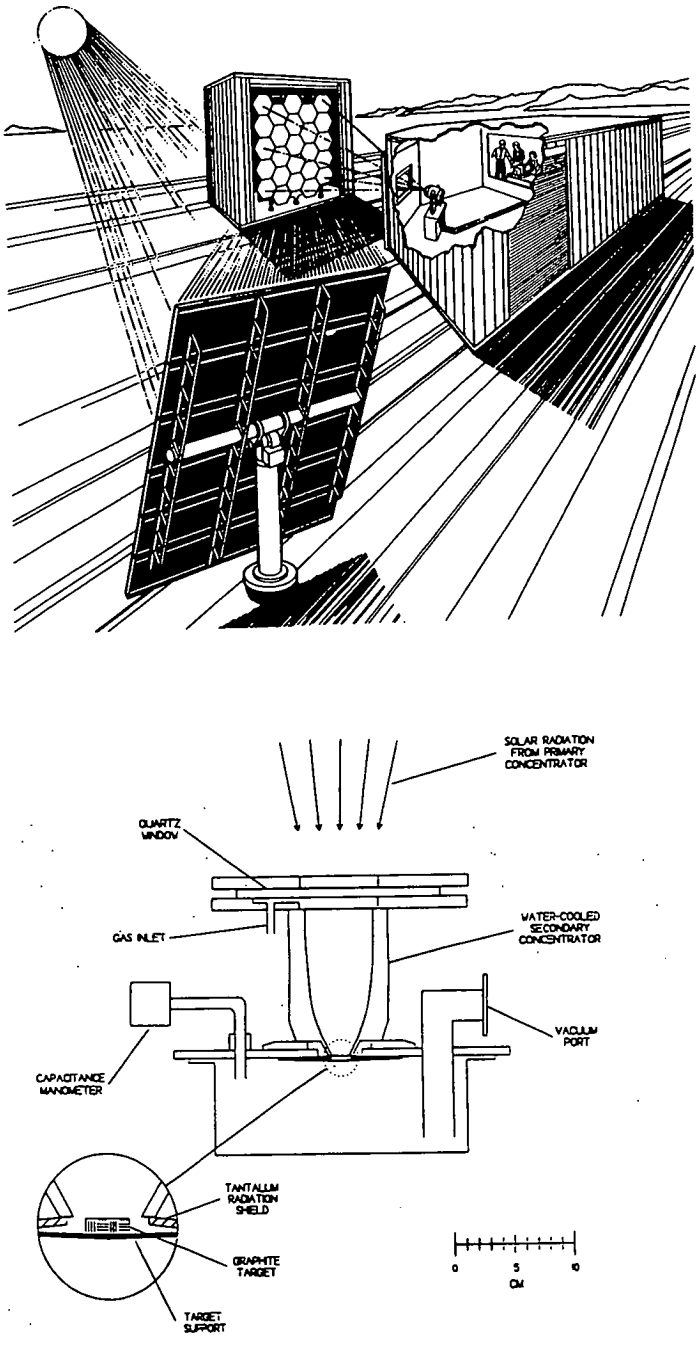

Figure 2.3: High flux solar furnace at the National Renewable Energy Laboratory used for fullerene production [44]. The upper figure a) shows the collection optics for the furnace. The lower figure b) shows the fullerene reactor in more detail; the graphite pellet is placed near the exit of the secondary concentrator.

the secondary concentrator. Argon gas flows through the secondary concentrator from the inlet over the graphite target and is removed by vacuum pump from the reaction chamber. This flow keeps the secondary concentrator clean by sweeping away vaporised carbon into the reaction chamber where it condenses into soot on the cool surface of the chamber. The pressure of argon is typically 50 torr and the graphite sample is exposed to the 1200 W / cm^2 solar flux for around 30 seconds.

2.2.4 Sputtering and Electron Beam Evaporation Techniques

Electron beam evaporation/deposition and sputter deposition are the basic physical vapour deposition (PVD) processes used extensively for thin film production. In the former technique, thermal energy is used to convert a solid target into vapour. In the latter, positive ion bombardment of negatively biased sputtering targets results in the ejection of the target atoms into the gas *via* momentum transfer.

Using this approach Bunshah *et al* [98] obtained a product in which isolable amounts of C_{70} rather than C_{60} were the predominant species (*ca.*70% C_{70}). The very different pressure ranges used to produce the fullerenes, and the isolation of fullerenes from the cathodic but not anodic substrate in the electron beam evaporation process, suggests the possibility of different formation mechanisms involving cationic intermediates.

A schematic diagram of the experimental set up employed for fullerene production using sputtering processes is shown in Figure 2.4. The system comprises a magnetron sputtering cathode and a ground plate with a graphite target in between. The graphite target is placed such that the magnetic field of the cathode confines the electrons from the discharge between the cathode and the ground plate in the vicinity of the target. A pressure of 3 torr helium is maintained and carbon species are sputtered from the graphite target by helium ions from the discharge. The flow of helium gas over the surface of the target serves to cool the sputtered species and to push material

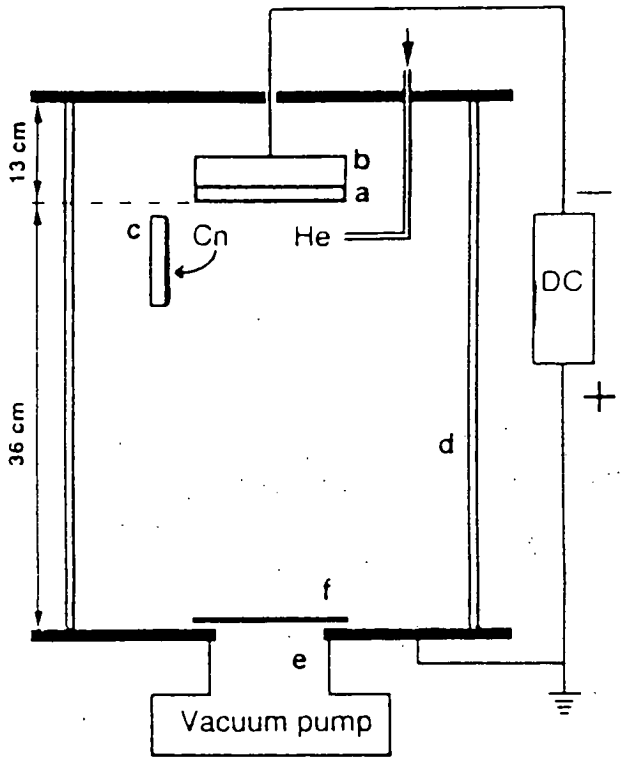

Figure 2.4: Schematic diagram of experimental apparatus for fullerene production by sputtering processes [98]. The figure shows the graphite target (a) attached to a magnetron sputtering cathode (b), a 30 cm diameter pyrex chamber (d) containing a liquid nitrogen cooled copper plate (c) and an aperture to the vacuum pump (e) partially covered by stainless steel plate (f).

formed in the direction of a liquid nitrogen cooled copper plate where it can be easily collected. Other material also collects on the walls of the bell jar in which the whole apparatus is housed. A stainless steel plate is placed over the entrance aperture to the vacuum pump to prevent loss of gaseous carbon species.

In the electron beam evaporation experiment [98], illustrated in Figure 2.5, a 10 kV electron beam is used to evaporate carbon from a 2.5 cm diameter graphite rod leaving a conical hole in the graphite rod approximately 5mm deep and 10mm in diameter in the surface of the rod. The electron beam emission current used was 0.2 A, which is necessary to maintain the high evaporation rate critical for fullerene formation. The operating pressure in the stainless steel bell jar was 2×10^{-5} Torr without the introduction of any working gas. The flux of carbon species evaporated from the rod was made to pass through an aperture in a horizontal plate. The charged carbon species were collected behind the aperture on quartz, silicon or copper substrates clamped to two electrodes 5.5 cm apart. The substrates were heated to 200°C by quartz lamps and a 1000 V potential supplied between anode and cathode. A liquid nitrogen cooled copper plate was placed directly above the aperture to collect those species which are not deviated by the electrostatic field.

Fullerene formation has also been found to occur in sooting hydrocarbon flames [41]. Under the proper conditions, atmospheric pressure benzene/oxygen flames have yielded gram quantities of soot with 20% yields of fullerenes within a few minutes. Similarly, the pyrolysis of species such as napthalene [99] has resulted in fullerene formation.

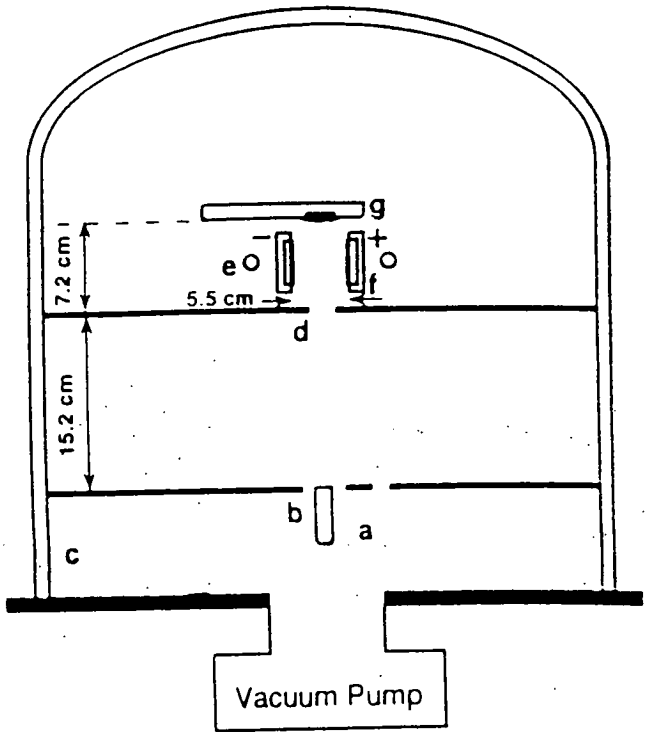

Figure 2.5: Experimental apparatus for fullerene production using electron beam evaporation [98]. The figure shows a 270° deflection electron gun (a), graphite rod (b), water cooled stainless steel chamber (c), aperture (d), quartz lamps for heating of substrates on the electrodes (e), electrodes (f), and a liquid nitrogen cooled copper plate (g).

2.3 Fullerene Formation Mechanisms

As described above, many different techniques have already been used to produce fullerenes. This wide variety of processes presents a considerable challenge when considering the mechanisms of fullerene formation since this occurs under very differing sets of conditions. As a further complication, even when using the same technique, *e.g.* vaporisation of graphite by electric arc discharge, the optimum conditions for fullerene formation often vary from one reactor to another leading to the emerging opinion that all of the important variables have not yet been identified, let alone their effects characterised.

It is possible, however, to identify some similarities between the different techniques employed. The laser ablation experiments, inductive heating of graphite in arc reactors and the sputtering or electron beam evaporation processes all occur under inert gas atmospheres and would appear to have related mechanisms, although the relationship between these methods and the production of fullerenes in sooting flames or from the bombardment of organic polymers by MeV atomic ions is not yet known. Given this wide range of conditions it seems likely that there are in fact several, perhaps many, different ways in which fullerenes might form with very different timescales and spatial domains.

The most puzzling aspect of fullerene synthesis has always been the formation of these highly symmetric molecules in condensing carbon vapour, primarily due to the complexity of this carbon vapour. In particular, none of the models can explain the very high abundance of C_{60}, compared to other carbon clusters, or the way in which its yield varies with experimental conditions. Perhaps the single most important fact when considering the mechanisms for formation of fullerenes is that C_{60} forms with such high efficiency; up to 20% of the carbon vaporised can often end up as C_{60}.

Energetically it is difficult to understand why formation of C_{60} is favoured over the higher fullerenes since, on a per atom basis, larger fullerenes are more stable. Increased size and an increased number of hexagons means that the higher fullerenes are more graphitic-like in structure and more stable. It has been postulated that the dominance of C_{60} is due to its high local stability. It is the smallest fullerene with no adjacent pentagons, and consequently is less strained than structures with abutting pentagons (the strain being due to bending of the sp^2 orbitals concentrates at the vertices of the pentagons), and its spherical form allows the strain to be evenly distributed over all the atoms.

Because of the extremely high degree of symmetry (and therefore low entropy) of C_{60} it is difficult to see, from thermodynamic considerations, why it should form under the violent high temperature conditions of a laser vaporisation source or electric arc reactor. Early studies by Kroto *et al* [1] involving the combination of laser vaporisation with a pulsed gas flow permitted the intermediate steps involved in carbon condensation to be studied in a controlled, systematic way. Kroto *et al* found that C_{60} is only dominant when carbon nucleation nears completion, suggesting that C_{60} is unreactive toward some sort of growth mechanism.

Initially, in their paper announcing the discovery of C_{60} [1], Kroto *et al* suggested that laser vaporisation removes intact pieces of the graphitic sheet from the surface of the carbon disk that was employed as a target. They speculated that these sheets are left in contact with high density helium and rearrange by two- and three-body collisions to eliminate dangling bonds thus forming the cage structures. However, this interpretation was ruled out when experiments on the laser ablation of other carbonaceous materials such as polyimides [100] and polycyclic aromatic hydrocarbons [101] demonstrated that pure carbon clusters could be generated with practically identical distribution to those produced using a graphite target.

2.3.1 The Icospiral Nucleation Mechanism

The first feasible nucleation scheme for C_{60} was proposed in 1986 by Zhang *et al* [17] and refined further by Kroto and McKay [95].This scheme, called the "icospiral nucleation mechanism", came from consideration of the original mechanism for soot formation proposed by Kroto *et al* [1] and the clustering processes occurring in the laser vaporisation nozzle source, in which C_{60} was obviously a survivor.

The scheme is illustrated in Figure 2.6 and predicts that fullerenes are formed as a by-product of soot formation. It is suggested that carbon radicals initially form into chains until they reach a size where they can "backbite", *i.e.* form polycyclic rings. Growth then continues in a manner resembling the formation of graphite sheets, up to the 25-35 atom size. The rings then rearrange into hexagons to try and build a graphite-like "chicken wire" structure. However, there is no hydrogen available to tie up the dangling bonds on the edges of the sheets. Clearly, the sheets could get rid of the dangling bonds and thus minimise their energy if the edges could curve round and join-up. This can be achieved by incorporating a pentagon into the hexagon "chicken wire" structure to form one good C-C bond from two dangling ones. This naturally causes the sheets to curl. As the pentagons tie up dangling bonds, the more that are incorporated into the structure the better (although they should not share a common edge as this is unstable). Therefore, as the sheet grows the edges naturally curve and this process has two possible outcomes.

The first is that the two edges of the growing sheet eventually meet and a fullerene is formed, *i.e.* C_{60}, C_{70}, etc.. The second and far more likely outcome is that the two edges miss each other (*i.e.* if not enough pentagons are incorporated to give sufficient curving). The leading edges continue to grow, rather like a snowball rolling downhill the structure becomes larger with the overlapping skin lying as close as possible to the underlying layer (*i.e.* around 3.4Å for the graphite interlayer spacing). As illustrated in Figure 2.6, the structure incorporates pentagons and curves as it grows

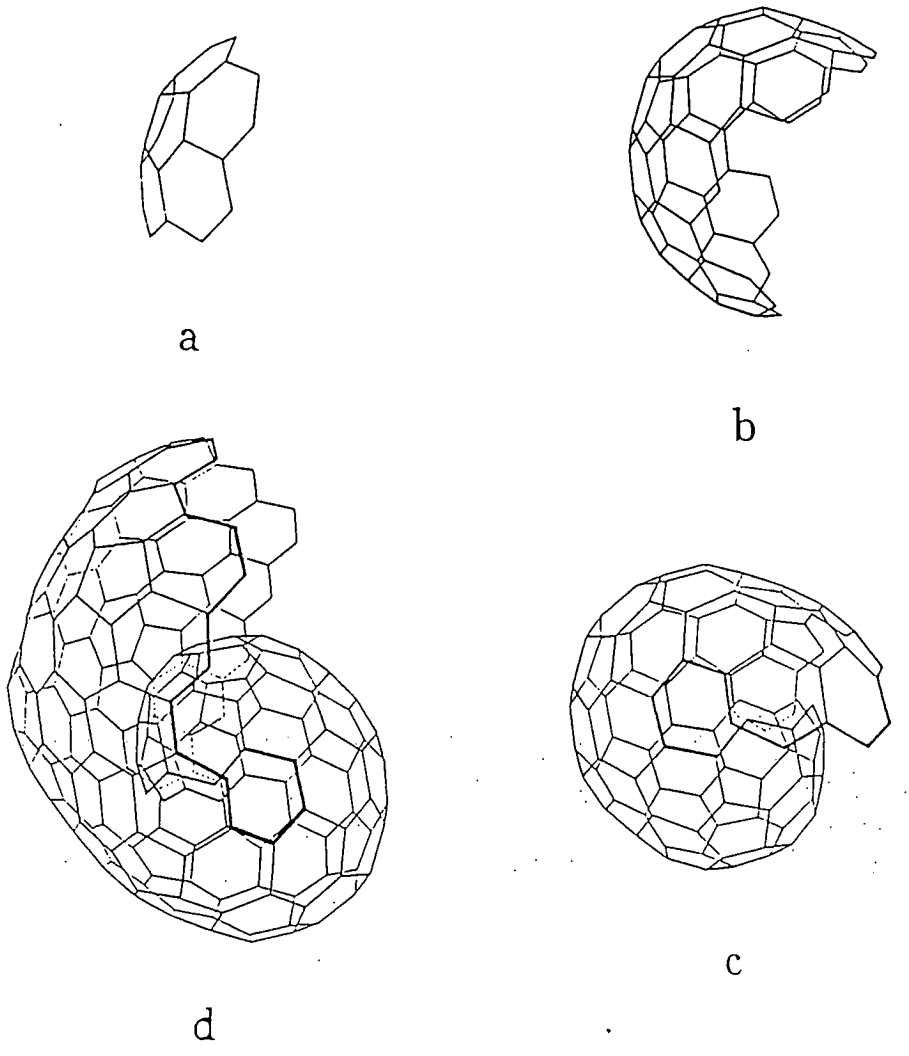

Figure 2.6: Diagrammatic illustration of the "icospiral nucleation scheme". This scheme was proposed for the formation of graphite microparticles. Structure **c** has overlapped and so trapped the trailing edge. The network continues to spiral (structure **d**) and 'snowballs' into a massive particle. C_{60} (and other fullerenes) may be formed by a modification of this process, when the edges meet and form a closed cage, thus halting further growth. These structures are thought to be intermediates in soot formation.

by addition of carbon species (**a** and **b**). However, in this instance an insufficient number of pentagons are incorporated and the edges overlap (**c**), growth continues and the structure snowballs (**d**).

This model explains why C_{60} and C_{70} are only dominant when nucleation nears completion. The fullerenes are formed by statistical closure during nucleation of a network with the correct disposition of pentagons. Once closed, the fullerene is unable to grow and is left behind as the other particles "snowball" into giant structures. This leaves C_{60}, C_{70} and the other fullerenes as survivors surrounded by giant particles. These giant particles are of too high a mass to be readily detected in the photoionisation mass spectra but they can be seen to be present from the fact that they can be photofragmented into smaller detectable species using higher laser power densities.

However, there were doubts about the validity of this mechanism. The process of pentagon incorporation in the correct position for closure as the carbon radicals rapidly condense appears unlikely to account for the high yields of fullerenes found.

2.3.2 The Pentagon Road Mechanism

By building on the "icospiral nucleation mechanism" and incorporating "annealing" of the clusters, Smalley *et al* put forward the "pentagon road" mechanism [102]. This was the first mechanism to receive widespread recognition. Smalley *et al* suggested that the fullerenes form from carbon clusters following the minimum energy path. The most energetically favoured form of any open graphitic sheet is one which (a) is made up solely of pentagons and hexagons, (b) contains as many pentagons as possible and (c) avoids adjacent pentagons. These criteria are called the "pentagon rule", and if followed, lead directly to C_{60} which is the first pentagon rule structure that can close. The "pentagon road" theory holds that given sufficient time to anneal, any carbon cluster will take on its favoured "pentagon rule" structure before growing

any further. Therefore, in principle, for high yield C_{60} synthesis all one needs to do is adjust the conditions so that each open cluster has ample time to anneal.

This mechanism can be used to explain the failure of attempts to produce fullerenes in macroscopic amounts by laser vaporisation. The pulsed laser generates a hot plasma of carbon radicals of extremely high density. The sheets initially grow extremely quickly, but since the surrounding gas is at room temperature the carbon vapour cools very quickly and thus has no time to anneal. Consequently, very few clusters have the chance to adopt their favoured "pentagon rule" structures and very little fullerenes are formed.

By contrast in a Kratschmer-Huffman reactor, where the carbon radicals are formed by the slow evaporation of a resistively heated graphite rod, the carbon vapour density is lower and the clusters can grow more slowly. More importantly, the rate of cooling of the vapour is less and so the clusters have more time to anneal. Adjustment of the buffer gas pressure also provides a measure of control over the rate of migration and therefore the time the clusters have to anneal may be optimised.

It has been found that the Kratschmer-Huffman method can be used with either an a.c. or d.c. arc. Although this method of vaporisation differs markedly from that of a resistively heated rod, the optimum pressure was found to be similar. Smalley *et al* [102] suggests this is an indication that it is not the vaporisation method that is important but the conditions under which the carbon vapour condenses.

Although the "pentagon road" mechanism accounts well for some observed experimental facts, it leaves several questions unanswered. The mechanism relies heavily on the formation of highly reactive cup-like fragments at an early stage of clustering when many small radicals remain that as yet have not been observed. However, this is not an insurmountable problem. Much of the chemistry of combustion is carried out by highly reactive free radical species that are never present in high concentration. Much more serious is the failure of the "pentagon road"

mechanism to account for the formation of C_{70}, even though under the right conditions (*e.g.* the sputtering or electron beam techniques) C_{70} can be produced in high yields and as the major product.

2.3.3 The Fullerene Road Mechanism

An alternative formation mechanism has been proposed by Heath [103]. In this "fullerene road" mechanism it is suggested that the graphite-like sheets, growing from small carbon radical addition, do not stay open but close to form fullerenes as soon as possible (C_{28}) despite breaching the "pentagon rule" by having adjacent pentagons. The driving force to form these fullerene structures is the need to get rid of the dangling bonds and the resulting structures may thus be the lowest energy species. It is suggested that the fullerene species that are initially formed continue to grow by addition of carbon radicals. The process terminates when the cluster size reaches the stable region (where there is no need for adjacent pentagons) with C_{60} being a special stopping place since it is the first structure without adjacent pentagons.

This mechanism has also been questioned. The growth of the precursor fullerene species initially formed requires the presence of sufficient amounts of small radical species. However, as the growth of the fullerenes requires extensive annealing, the larger molecules may form at a late stage when it is doubtful whether the carbon radicals will still be present. High yields of C_{60} have been reported using techniques such as laser vaporisation where there is no continuous source of new radical species [104].

An additional experimental finding that the "fullerene road" mechanism does not account for is the formation of endohedral fullerene species. One of the first experiments carried out in trying to prove the truncated icosahedral structure for C_{60} involved the technique of "shrink wrapping" an endohedral fullerene, $C_{60}La$ [24]. In order to determine the correct structure for $C_{60}La$, the Rice group performed

extensive measurements in the magnetic trap of an Fourier transform ion cyclotron resonance (FT-ICR) mass spectrometer in order to confirm that the lanthanum atom was indeed present inside the carbon cage. When the endohedral cluster was photofragmented, the primary fragment channel was found to be loss of C_2 units rather than loss of the metal atom. By successively knocking off pairs of carbon atoms the fullerene structure can be shrunk until it reaches a stage where it is too small to encapsulate the atom and further photofragmentation causes the cage to split apart. This minimum size was found to be C_{44} for an encapsulated potassium atom and C_{48} for the slightly larger caesium atom. The fullerene growth model of Heath suggests that the synthesis of a metallofullerene in high yield would be difficult since the encapsulated species would be too large to fit inside the cavity of the very small fullerenes initially formed (*i.e.* C_{32}) and once the fullerene had closed, it would be difficult to insert it from the outside (*e.g.* to insert He into a C_{60} fullerene cage requires 10 eV [105]).

2.3.4 Ring-stacking Models of Fullerene Formation

Other mechanisms proposed for the formation of fullerenes suggest that rather than growing out of two dimensional clusters until they reach a size where they rearrange to a closed form driven by energy gain from loss of dangling bonds, the fullerenes are formed from elementary building blocks of carbon which already have two dimensional structures. Two different groups have suggested mechanisms that start with the conversion of C_{10} monocyclic rings to a bicyclic napthalenic unit, their subsequent addition reactions with other similar sized structures leading to fullerene formation.

The Japanese workers, Wakabayashi and Achiba [106], proposed in their "ring-stacking model" that the fullerenes are formed by the sequential stacking of even numbered carbon rings. The rings must meet two criteria :a) the intermediates (the half-formed fullerenes) must consist of pentagons and hexagons only and, b) they must not contain adjacent pentagons.

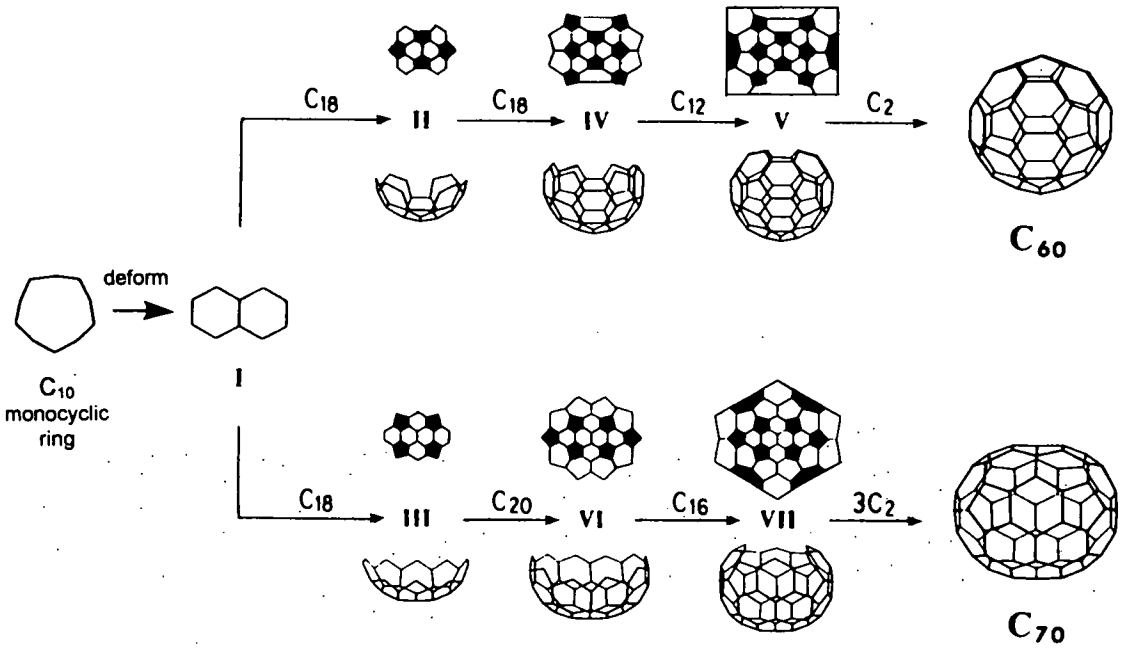

Figure 2.7: Schematic diagrams of the ring stacking processes for C_{60} and C_{70} formation. The C-C bond distances drawn are assumed constant.

The initial napthalenic unit contains two hexagons with a common edge and eight dangling bonds. The hexagon is then stacked with species such as C_{12}, C_{16}, C_{18}, C_{20}, *etc.*, as shown in Figure 2.7. In this model the rings are stacked such that all of the initial dangling bonds are converted into C-Cσ-bonds. By stacking the intermediates with rings that meet the above criteria C_{60} and C_{70} can be formed .

Broyer *et al* [107] have proposed an alternative "C_{10} monomer model". They believe that the cluster product abundance depends only on steric factors and the number of collisions, and they favour a process of homogeneous nucleation with only a few steps. Their model involves the six-fold combination of napthalenic C_{10} units. Like the model of Wakabayashi and Achiba, and the "pentagon road" mechanism of Smalley, their proposal requires saucer shaped intermediates of polyaromatic carbon molecules, which as yet have not been reported. In the case of the "C_{10} monomer model", when two naphthalene-type C_{10} units react they favour the formation of a connecting pentagon which produces the curvature of the intermediates. As a result any structure from C_{20} up is curved.

However, the main problem of both the "ring stacking" and the "C_{10} monomer" models is that they rely specifically on the combination of certain precursor carbon clusters, the napthalenic C_{10} units. The problem here is that this structure is actually higher in energy than monocyclic C_{10} and so would be expected to be present only in low concentrations. Thus these mechanisms rely on reactions between two mid-sized clusters present only in very low concentrations and it is difficult to see how such a mechanism could account for the formation of fullerenes in high yields.

2.3.5 Fullèrene Formation by Annealing of Bi- and Tri-cyclic Ring Systems

Recently, researchers from the University of California have proposed a further mechanism for fullerene formation. Bowers *et al* [108] have shown that high yields of C_{60} and C_{70} can be explained in terms of the collapse of larger structures. This

"collapsing mechanism" has been supported by molecular dynamics computer simulations performed by Chelikowsky [109] and by experimental results from studies by Hunter *et al* [110]. In this mechanism heating of the planar ring systems, that develop from the initial linear chains, above a certain temperature leads to 100% fullerene formation. It can be readily understood how linear carbon chains of a certain minimum size and energy can react with each other to form bi- and tri-cyclic rings. It is more difficult, however, to understand how these bi- and tri-cyclic ring systems can lead to the formation of fullerenes. There seems to be no mechanism by which planar cyclic rings can rearrange to fullerenes simply by adding new members. Bowers *et al* could also find no evidence of any type of "graphitic cup" fullerene precursor [111][112].

The initial experiments carried out by Bowers *et al* [108] were aimed at understanding the processes by which the ring systems lead to fullerenes, by providing long periods at high temperatures for the structural annealing processes that they believed occurred. This was achieved using the recently developed technique of gas-phase ion chromatography [113]. In this technique, a pulse of cluster ions are mass selected and injected into a high pressure drift cell containing helium at 2-5 Torr. The pulse contains different isomers which drift through the cell under the influence of a weak electric field. The ionic mobilities of different isomeric structures depend on their different collisional cross-sections with He. The isomers are therefore separated while drifting through the cell. A quadrupole detector is tuned to the appropriate mass and provides the arrival time distribution for the different isomers. The absolute value of the ionic mobility for a given cluster, together with computer simulations, allows determination of the cluster structure.

In the particular experiments which were concerned with studying the annealing processes, the pulse of mass selected ions was injected into the drift cell at fairly high energy rather than at very low energy as normal. This creates a transient internal energy increase that can allow isomerisation or even collision induced dissociation.

When the C_{39}^+ ion was injected into the cell at 50eV, a mix of mono-, bi- and tri-cyclic rings was found, as well as the presence of clusters which had adopted the fullerene structure. When the same sample was injected at 150eV, the fullerene peak was virtually unchanged. However, there was now only one monocyclic ring peak as this is the most stable planar ring structure. They also found that at this energy a substantial fraction of C_{39}^+ ions had been collisionally dissociated to form C_{38} or C_{36}, both of which possessed fullerene structures.

These observations are explained in the following way. When the C_{39} planar ring has insufficient energy to rearrange to a fullerene, it breaks one or two bonds and forms the more stable monocyclic ring structure. Injecting these structures at high energy into the drift cell induces a strong transient heating pulse, which collisionally heats the monocyclic rings above the threshold for isomerisation to a fullerene. This leads to rapid bond-breaking and rearrangement of the cluster to its most stable form (the fullerene). The newly formed cluster has massive internal energy (*e.g.* conversion of a tri-cyclic planar ring system into C_{60} fullerene liberates 45eV). The fullerene structures are therefore "superheated" and cool by evaporative loss of a carbon group; C_{39} loses either a single carbon atom or a C_3 molecule to form C_{38} or C_{36} fullerene, whereas C_{40} would lose a C_2 molecule to form C_{38}, an even numbered fullerene.

The possible outcomes of injecting the C_{39}^+ ion into the drift cell are illustrated schematically in Figure 2.8. The ions are energised by collisions, those with sufficient energy undergo collision induced dissociation (CID) and eject a C or C_3 unit to form the most stable fullerene structure. Those with insufficient energy to dissociate cool, by annealing, to form a monocyclic ring, the most stable planar monocyclic ring structure. Figure 2.9 shows the mono, bi- and tri-cyclic ring structures of C_{40} rearranging to form the C_{38} fullerene structure.

The first fullerenes are observed in small amounts when planar cyclic C_{33} ejects C_3 to form C_{30}. This is supported by *ab initio* calculations on the relative thermodynamic stabilities of fullerenes, cumulene and polyacetylene ring systems for species

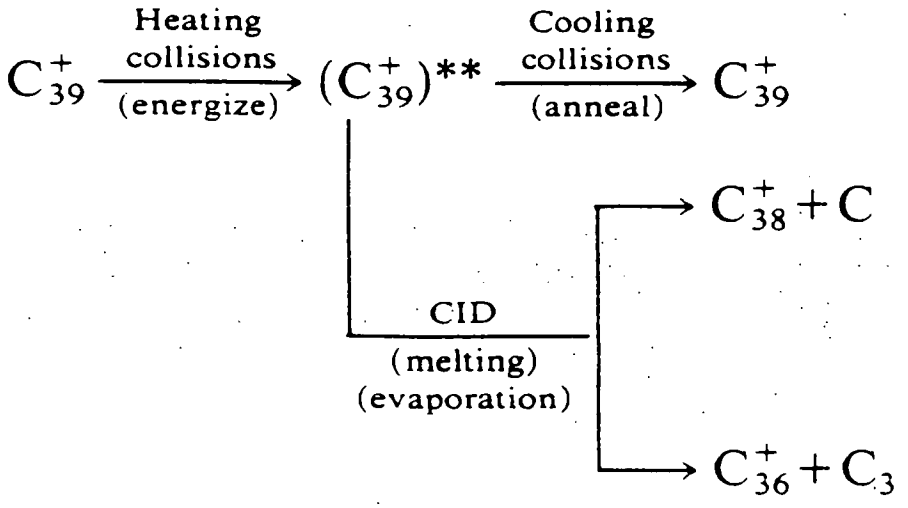

Figure 2.8: The mechanism for the pathway from monocyclic rings to fullerenes proposed by Bowers *et al* [108].

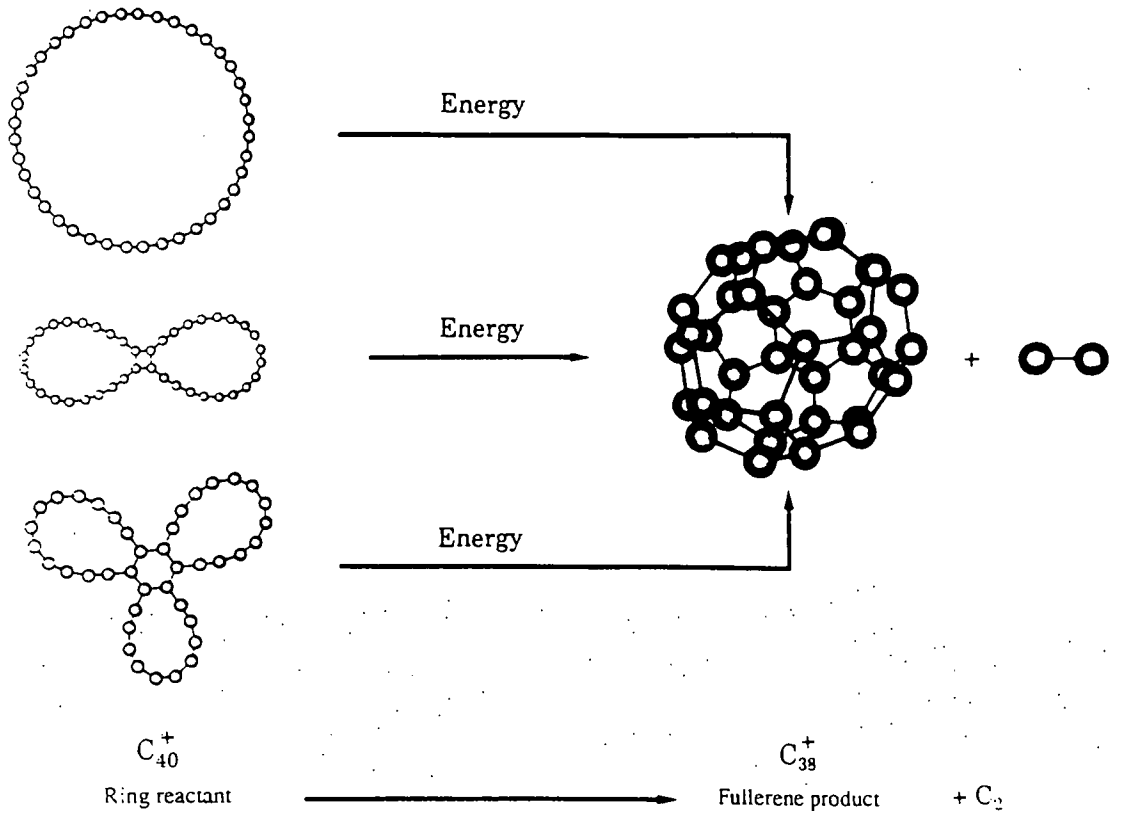

Figure 2.9: The "collapsing mechanism" proposed by Bowers *et al* [108] for fullerene formation. Planar monocyclic, bicyclic and tricyclic C_{40}^+ (ring reactant) forms C_{38}^+ (fullerene product) plus C_2 when collisionally heated above the isomerisation barrier for fullerene formation. All structures shown are minima on the potential energy surface according to semi-empirical PM3 electronic structure calculations. The bi- and tri-cyclic rings have lower isomerisation barriers to fullerene formation than the monocyclic ring.

containing between 24 and 60 carbons, and suggests that fullerenes become more stable than rings at around C_{30} [114]. As the size of the cluster increases the process accelerates, so that by the time 40 atom carbon clusters are reached the fullerene isomer dominates. The conclusion from this data is that the barrier for transforming planar ring systems to fullerenes decreases with size.

This model can be applied to the formation of C_{60} in carbon arc reactors. As is well known, efficient C_{60} synthesis occurs only over a narrow range of experimental parameters, suggesting fairly specific kinetics. As shown by the ion chromatography experiments of Bowers *et al* [108], C_{60} is synthesised from carbon atoms forming linear carbon chains and then planar ring systems, which through collisional heating isomerise to fullerenes [111][112][115][116]. These experimental results seem to rule out the possibility of a graphitic growth "pentagon road" type mechanism.

It is proposed that in the arc reactors the chains and then rings diffuse out of the initial carbon "soup". If the carbon density immediately surrounding the arc is high enough, these rings may coalesce to sizes larger than C_{60} and spontaneously rearrange to fullerenes due to the low rearrangement barrier for large systems and the hot environment. C_{60} would be formed preferentially to other fullerenes in a similar mass range *via* the evaporation of small particles from the newly formed fullerene because of its stability. The growth of planar rings to a size which would form C_{60} would be maximised only under certain conditions, but the abundance of C_{60} would be further enhanced by growth of smaller fullerenes (formed from smaller rings) *via* the "fullerene road" mechanism [103].

As yet there is no mechanism for fullerene production that is universally accepted. The different experimental results lend credence to a variety of schemes and it may be that there are several different pathways to fullerene formation. The most striking discovery has been that they are formed in such high yields by a method as simple as the evaporation of graphite by a contact arc. In the following section the construction,

characterisation and modification of the carbon arc reactor employed in the current work is decribed together with the experimental procedures used.

2.4 Design and Evaluation of a Fullerene Reactor

To produce fullerenes in the laboratory we chose a simple benchtop reactor design. The reactor is illustrated in Figure 2.10 and described in detail below. The advantages of this design are its simplicity, it may be easily assembled, has few machined parts and is easy to use. The small size of the reactor is a further advantage when retrieving the soot after a production run.

2.4.1 Construction of a Benchtop Reactor for the Production of Fullerenes

The reactor used for the production of fullerene rich soot in the present studies, shown in Figure 2.10, is based on a design by Koch, Khemani and Wudl [94]. A contact arc is set up between two graphite rods which are attached to 6mm dia. Cu electrodes which in turn are attached to an arc welding power supply. The arc causes the upper 3mm dia. graphite rod to combust. As the rod is consumed it falls under gravity and so the arc is maintained. The soot produced is contained within the reaction vessel which is cooled by circulating water through the 6mm dia. copper cooling coils surrounding the reaction vessel.

A Lincoln square wave AC/DC tig and stick welding power supply with high frequency stabilisation (Lincoln Electric Company, Cleveland Ohio, USA) was used as the power source. The graphite rods were supplied by Erodex Ltd (Unocal Poco 76 S55 POH21) and the four litre kettle jar used to house the reactor was obtained from Aldrich Ltd. The stainless steel reactor lid is 160mm diameter and 15mm thick. The underside of the lid has a 3mm deep, 150mm dia. groove for the O-ring which sits between the lid and the kettle jar to provide a vacuum seal. The lid also has ports

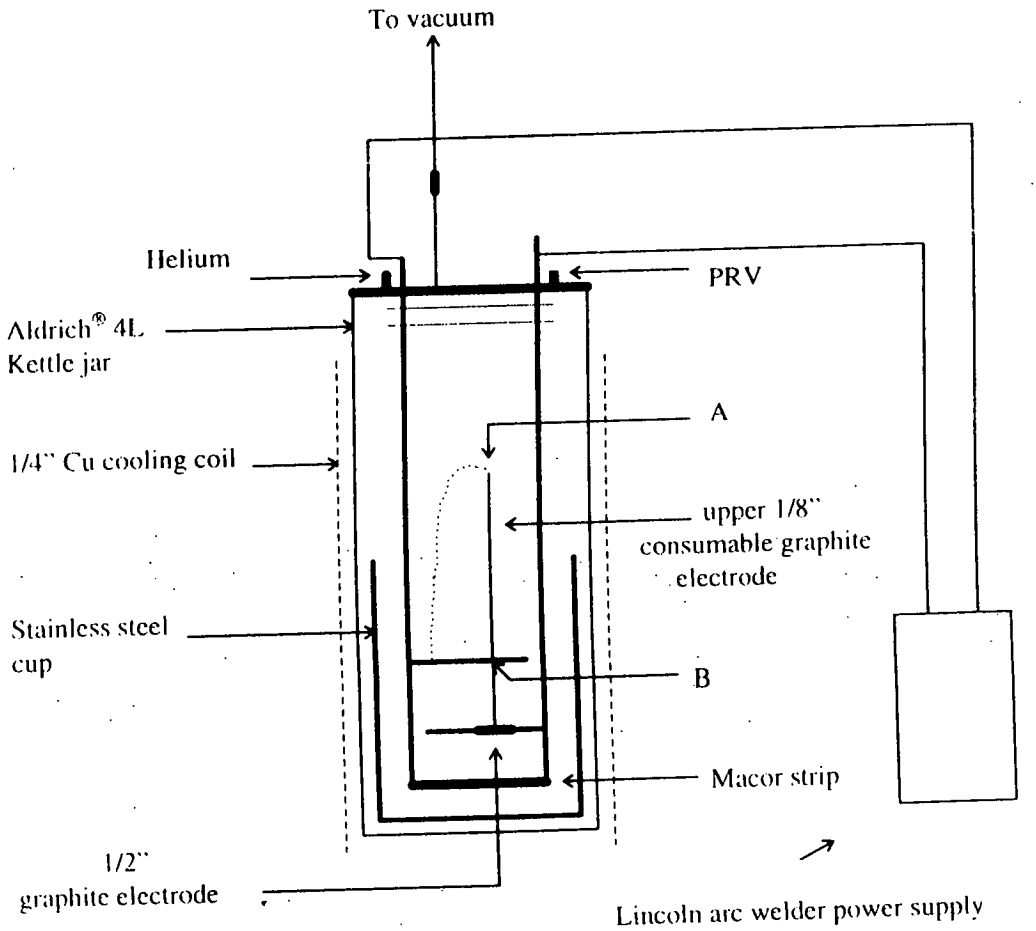

Figure 2.10: Diagram of the benchtop reactor used in the present work for the production of fullerene rich soot.

for the inlet of gas to the reactor and for connection to the vacuum pump, a pressure release valve (PRV) and a pressure/vacuum gauge. The 6mm dia. Cu electrodes were silver-soldered to the ceramaseal feedthroughs which were, in turn, silver-soldered to brass pipe threads. The cables from the power supply were modified so that they could be bolted onto the electrodes at the top of the reactor. One end of the upper sacraficial rod (3mm dia. 200mm length) was connected to the 6mm dia. Cu electrode by a 6mm braided flat Cu cable attached to the Cu support. The lower 12mm dia. graphite rod sits in a machined hole in the lower Cu support which is in turn attached to the other 6mm dia. Cu electrode. In later work a 100mm macor strip was bolted to the bottom of the two Cu electrodes to ensure the distance between them was maintained. A stainless steel cup 140mm dia. was also later placed in the bottom of the reactor to aid retrieval of the soot.

All machined components and modifications to the reactor were fabricated in-house. Latex gloves and dust masks were worn whenever handling the soot or extract. It should also be noted that the arc must not be observed directly during a production run, although once production is underway the glass walls become covered in the soot produced and only an orange yellow glow escapes.

2.4.2 Operating Procedure for the Production of Fullerene Rich Soot

A graphite rod (approximately 200mm length 3mm dia.) was sharpened to a point at one end with a pencil sharpener or file and weighed. The flat end of the rod was then secured to part A of the reactor (see Figure 2.10). The rod was placed through a copper guide hole at B so that the point was resting in an indent carved into a 12mm dia. graphite rod. The electrodes were connected to the power supply at the top of the reactor, which was also attached to an ultrapure helium gas cylinder and a vacuum pump. The reactor housing was surrounded by a copper cooling coil. Before use the reactor was purged five times with helium. The apparatus was then brought up to the required pressure of helium; (optimum pressure 130mbar or 100 Torr He, (see results

section)). The power supply was set to an upper current limit and turned on. The arc between the graphite electrodes was initiated by a burst of high frequency power (very high voltage, low current) and the current then controlled with a foot pedal. The high frequency capability of the Lincoln power supply was of great value since if the arc for some reason fails, the high frequency automatically activates to re-establish it. After approximately eight minutes enough of the rod was consumed to prevent it making contact with the bottom electrode and thus the arc failed. The reactor was brought up to atmospheric pressure of helium and allowed to cool for approximately 15 minutes. The amount of graphite consumed was calculated and the whole process was repeated. After 7-8 runs the soot was brushed off the electrodes, retrieved from the reactor and weighed so that the yields could be calculated.

Periodically, about once per run, grey "slag" formed on the bottom 12mm dia. graphite electrode. When this happened it was removed immediately since it could cause the upper electrode to burn non-uniformly and make it difficult to initiate the arc.

During the course of the initial runs on the reactor it was clear that some modifications to the original design were required. The first modification was to join the two 6mm dia. copper internal electrodes by a piece of Macor machineable glass ceramic. Macor does not conduct and is able to withstand high temperatures. Joining the electrodes ensured that the two graphite rods were kept in contact. This overcame the problem of having to realign the graphite rods before each run because of movement of the copper electrodes caused by a combination of dramatic temperature changes and wear and tear as the reactor was disassembled to remove and replace the graphite rods. Keeping the electrodes fixed also reduced the likelihood of an arc forming between the graphite and the copper supports.

The second modification was to introduce a steel cup. This had the combined advantage that it prevented any piece of the electrodes or their support falling through the bottom of the reactor if a meltdown occurred and it made the retrieval of the soot

considerably easier. The majority of the soot coats the inside of the cup and the rest may be brushed into it. The cup can then be easily removed and the soot retrieved. This process is considerably easier than taking the reactor apart, removing the cooling coils and attempting to retrieve the soot from the 4 litre kettle jar, and leads to a great reduction in the amount of soot lost.

2.4.3 Strategy and Objectives

Although the exact mechanism by which fullerenes are formed is unclear, there are factors common to all the mechanisms proposed. Each mechanism relies on an initial supply of carbon species that are kept close to each other by a quenching gas. It was therefore thought it might be possible to study what processes may be occurring within the reactor and how the operating conditions may effect formation by different schemes. The use of the simple resistive heating method provides the steady supply of small carbon species and radicals required from the evaporation of the graphite electrode and ensures that the consumption of the small linear carbon chains initially formed is low. The low concentration of these chains would be important in a "pentagon road" type mechanism since it would prevent them from adding too quickly to a growing cluster, and thus allow the cluster to correct imperfections within its own structure (*i.e.* to incorporate sufficient pentagons for closure). A low concentration of linear chains would also be important in a "collapsing type mechanism" where the process is initiated by carbon chains of just the right size forming rings which can then react with each other.

The helium buffer gas is also a critical element since it slows the migration of the carbon species. Keeping them near the arc has the combined effect of allowing the longer chains and larger clusters to develop and also providing the heat required to anneal the clusters. This would be important in a "pentagon road" type mechanism since the arc provides the heat necessary for the clusters to adopt their lowest energy form (*i.e.* obey the "pentagon rule"). In a similar way, helium is vital to the mechanism proposed by Bowers *et al* [108] By preventing rapid migration of the

carbon species, the buffer gas ensures that the density of the small carbon species immediately surrounding the arc is sufficiently high that the monocyclic rings that are thought to be initially formed would be able to grow and produce the bi- and tri-cyclic rings, which are the next stage towards fullerene formation.

In the following sections the way in which the reactor operating conditions, such as the pressure of buffer gas, were investigated in order to characterise the reactor and obtain maximum productivity are described together with the experiments that were undertaken to try and increase the yield of fullerenes.

2.5 Characterisation of the Fullerene Reactor

The optimum conditions for fullerene production are dependent on the exact nature of the technique and the design of the chamber used. Although there were certain conditions for running the reactor provided in the paper that outlined the original design [94], the fact that optimum operating parameters can differ from chamber to chamber, meant it was important to characterise the reactor by investigating the effects of varying the operating conditions. Experiments were conducted under different conditions and the effect on the quantity of fullerenes produced examined. The productivity of the reactor was based not just on the percentage yield of fullerenes extracted from the soot, but also how easily this soot could be generated and how labour intensive the method was. This included factors such as the ease of collection of the soot from inside the reactor chamber and the time needed for the reactor to cool down between runs (the turnaround time).

These studies involved variation of parameters such as buffer gas pressure and discharge current. The effect of a change in the internal geometry of the reactor was also investigated when the reactor was modified by the addition of a steel cup. The

variables that might effect fullerene production which were investigated are discussed below together with any effects their alteration had on the fullerene yield.

2.5.1 The Arc Discharge

The first variable considered was the arc itself, *i.e* .the nature of the power supply (a.c. or d.c.) and the optimum current. There are several inherent factors to consider outwith the actual yield of recoverable fullerenes from the soot. A relatively fast burn time (time for the rod to be consumed) means that a greater number of rods can be burned in one session, although the amount of heat generated must be minimised or the "turnaround time" (time lost between replacement of rods whilst reactor cools) becomes very long. The use of higher currents led to a faster burn time, however, there was found to be a drop in the yield of fullerenes produced when using currents in excess of 90 amps (3.6% fullerene yield at 90 amps, 3.2% at 110 amps). This could be an effect of the increase in temperature and therefore in the pressure inside the reactor at these higher current values, although it is more likely due to the electrode burning away too rapidly (*ca.*40 seconds to burn 150mm graphite at 90 amps). Despite the fact that the rods could be burned more quickly the decrease in yield coupled with the increased turnaround time meant that these conditions made the reactor less efficient to operate.

At current values below 45 amps it was found that the arc was difficult to initialise, and once started, hard to maintain. Also, the longer burn time was not really compensated for by the decrease in the heat within the reactor as this built up over a longer time period. The best conditions found for fullerene generation were between 55-60 amps. This had the advantage of providing relatively fast burn times (*ca.* 2 minutes to burn 150mm of graphite) with good turnaround times (*ca.* 10 minutes). It was found that the electrodes would burn more smoothly if the current was initially set at ~70 amps and then decreased to ~60 amps once the arc was initiated.

There was found to be no difference in the yield between using an a.c. or d.c. discharge. However, at higher current ratings with an a.c. discharge, the bottom graphite electrode overheated drastically and caused the copper support to melt. The resulting molten copper and the overheated electrode dropped to the bottom of the reactor causing the glass bell jar to implode on contact. To avoid further incidents of this nature, a d.c. discharge was used with the upper 3mm dia. graphite electrode set as the anode. This set-up prevented any heat build-up in the lower electrode since 90% of the power goes through the anode. It also made the arc easier to initialise since most of the power passes through the sharpened end of the thin rod ensuring combustion.

2.5.2 Effect of Steel Cup

The "meltdown" inside the reactor however highlighted the need for modifications to be made. The high temperature conditions within the reactor, coupled with the wear and tear of retrieving the soot led to the copper support electrodes becoming misaligned. This meant not only that it was difficult to maintain contact between the graphite electrodes, but also that there was the danger of misalignment, leading to an arc being set up between the upper graphite electrode and the copper support, which could again lead to a "meltdown" as experienced before.

Table 2.1 shows the percentage amount of soot recoverable before the steel cup was used. The results show a large variation (17%) in the values of the soot recovered over the three runs, an indication of the difficulties involved in trying to obtain reproducible conditions. Additionally, even in the most efficient retrieval only 64% by weight of the graphite consumed is recovered (on average over the three runs 56% of soot was recovered).

Modification of the reactor by the insertion of the steel cup made recovering the soot much simpler. Table 2.2 shows the percentage amount of soot that could be recovered by weight of graphite. Their is a vast improvement in the retrieval process,

Table 2.1: Results of preliminary reactor runs before the steel cup was in place

Run	Wt Graphite Consumed	Wt Soot Produced	% Yield Soot
1	11.12	5.32	47.8
2	12.25	7.94	64.8
3	11.5	6.38	55.5

Table 2.2: Percentage of soot recovered once the reactor had been modified by the introduction of the steel cup.

Run	Wt Graphite Consumed	Wt Soot Produced	% Yield Soot
4	13.02	13.00	99.8
5	11.50	10.52	91.5
6	12.29	11.86	96.5

Table 2.3: Yield of fullerenes from toluene extraction of soot produced in the reactor. Runs 1-3 show results obtained for extraction of soot produced prior to the introduction of the steel cup. Runs 4-6 show results for soot produced with the cup in place.

Run	Wt Soot Produced	Wt Fullerenes Extracted	% Yield Fullerenes
1 - 3	19.64	2.18	11.11
4 - 6	36.81	1.61	4.17

with as much as 99.8% of the soot being recovered in one run. In addition there is much less variation in results between runs (8.3%), with, on average over the three runs, 95.9% of the soot recovered.

An interesting result was discovered when samples of soot produced in the reactor were Soxhlet extracted with toluene to yield fullerenes and analysed by HPLC on a semi-preparative silica column, (the Soxhlet extraction technique is described in section 3.3.1). In Table 2.3 the percentage of fullerenes recovered from the soot for samples produced with or without the cup in place are compared. The results in the table show that there is a significant drop in the yield of fullerenes from the soot when the cup is in place; soot produced without the cup in place gave an 11% yield of fullerenes which dropped to around 4% when soot recovered with the cup inside the reactor was extracted.

These results illustrate the effect of another important aspect in characterising a fullerene reactor. Since most fullerene reactors are converted vacuum chambers, of one type or another, their internal geometries differ greatly and the effect of these geometries on the fullerene formation mechanism is difficult to determine. It is evident from the results in Table 2.3 that the cup is having an effect on the fullerene formation mechanism. Thus, addition of the cup could disrupt conditions inside the reactor in two ways. Firstly, as shown in Figure 2.10 the cup changes the shape within the chamber and therefore interferes with the convective flow through the reactor. At present the convective processes inside the reactor and their relevance to fullerene production is not well understood. Haufler *et al* [104] report that placement of a water-cooled "chimney" above the arc contributed to beneficial convection patterns within the chamber and significantly increased the fullerene yield. Similarly, Parker *et al* [123] report markedly different yields depending on whether or not a set of soot collection surfaces, "shims", are in place or not.

The second alteration to reactor conditions caused by the introduction of the cup concerns the heat produced inside the reactor. Heat minimisation is one well-defined

objective in reactor design, not just because of its possible effects on fullerene growth processes but also for its importance in the overall productivity of the reactor; time spent waiting for the reactor to cool down between runs is an important consideration. Additionally, the extremity of conditions inside the reactor will dictate its lifetime.

When the cup is in place inside the reactor its walls are not directly cooled but merely rest close to the glass walls which are cooled by the copper coils. This makes it more difficult for heat generated by the arc within the cup to escape, and leads to an increase in temperature and pressure inside the cup, both of which could interfere with the formation mechanism. There is a large change in the pressure reading inside the reactor when it is operated with the cup in place. Pressure rises of 70-80 torr within the first 30 seconds of operation are normal, and rises of up to 180 torr over a period of 7-8 minutes were sometimes recorded. It is known that an increase in the current producing the arc leads to a drop in the yield of fullerenes. This could possibly be an effect that is partially associated with the rise in temperature and pressure that the higher current produces, although other factors such as the electrode burning away more also need to be considered. A further possibility is that wall reactions play some part in the nucleation process. It could therefore be possible that replacing the glass wall with the steel wall of the cup negates some wall processes involved in fullerene formation or introduces an inhibitory effect on the process.

Whatever the reason, it is clear that the yield of fullerenes is diminished once the cup was introduced. However, the desirability for a high yield has to be balanced with the relative ease of use and the percentage of soot recoverable when the cup is used. A great amount of care was taken to retrieve the soot produced in the initial runs without the cup. Even so, only 55% of the soot, from the weight of graphite consumed, was recovered. The recovery process took upwards of two hours since it was necessary to disassemble the reactor, remove the copper cooling coils which are difficult to replace when the reactor is used again, and wash the soot out using toluene. This compares poorly to the 20 minute process of brushing the soot into the

cup and removing it, a procedure by which 99.8% of the soot was recovered. It is advantageous therefore, if the reactor is to be in continuous use, to operate with the cup in place, not merely to speed up the recovery process so that a new run may begin but also to reduce wear and tear.

2.5.3 Buffer Gas

The next consideration was the nature of the quenching gas. Fullerenes have been found to form in a variety of inert atmospheres, helium, nitrogen, argon, *etc.* However, it was decided to continue with the use of helium since the reported yields with this quenching gas have been found to be substantially higher [118].

Probably the most obvious step in characterising the reactor was to find the optimum helium pressure for fullerene production. In order to investigate the effect of helium pressure the reactor was run at a range of different pressures between 20 and 200 Torr. The results obtained are given in Table 2.4 and show the percentage yield of fullerenes after Soxhlet extraction with toluene of the soot produced at these different pressures. In each case the soot was produced with the steel cup in place using a current of 55Amps, and a similar amount of graphite was consumed (*ca.* 60mm). There was no appreciable difference in the length of time taken for the rods to be consumed at the different pressures.

Table 2.4: Yield of fullerenes for different helium pressures in the reactor.

Pressure of Helium (Torr)	% Fullerenes Extracted
20	3.3
60	3.5
100	4.37
160	4.02
200	3.81

NOTE: Yields shown in table represent percentage of fullerenes recovered after Soxhlet extraction using toluene.

The results show the optimum pressure of helium for fullerene production using our reactor to be around 100 Torr. At 20 Torr He pressure 3.3% of the soot is recovered as fullerenes. This rises slightly as the pressure is increased to 60 Torr and then more rapidly peaking at 100 Torr (4.37% yield of fullerenes). The yield then slowly decreases as the pressure is raised but remains moderately high; 3.8% at 200 Torr.

The relevance of helium pressure to fullerene formation has been mentioned earlier, although high yields have been reported with a range of different values. Shinohara *et al* [119] have reported yields up to 13% at a helium pressure of 20 torr, whilst Scrivens and Tour [120] found that their highest yield occurred at a pressure of 450 torr.

2.6 Further Experiments to Increase the Fullerene Yield

Once the reactor had been characterised and optimum conditions found, experiments were undertaken to try and increase the yield of fullerenes, with the overall productivity of the reactor in mind. The first experiment was to try to increase the amount of soot produced by simply burning bigger rods. This was attempted primarily because fullerene production is such a time consuming procedure that the ability to produce a greater quantity of soot from the same production run would greatly increase the overall efficiency of the system. Additionally however, some of the subsequent planned reactor experiments required drilling out the sacrificial 3mm dia. graphite carbon rod, a task which would be made considerably easier if thicker 6mm dia. rods could be used. In these experiments 6mm dia. rods were used, which when burned should provide four times the volume of soot as the 3mm dia. rods.

A second series of experiments involved seeding the sacrificial carbon rod with an organic substrate, tri-indane. The structure of this molecule is shown in Figure 2.11. This C_{15} species is in effect one quarter of a C_{60} molecule, and comprises a hexagon surrounded by 3 pentagons. It was thought that this species might act as a template for the growth of fullerenes. The "ring stacking model" and the "C_{10} monomer model" in which the fullerenes are proposed to form from elementary building blocks of two dimensional carbon structures, as well as the "pentagon road" mechanism all predict the formation of cup-like fragments at an early stage of clustering when many small radical species are also present. It was therefore hoped that the presence of tri-indane, a quarter-formed fullerene, might promote the growth of fullerenes and lead to increased yields.

2.6.1 Effect of Increased Electrode Size

In these experiments the 3mm dia. sacrificial electrode was replaced with a 6mm dia. rod. The experimental procedure was the same as before except that in order to maintain the arc a current of 140 Amps was required. In addition the guide hole at point B in the reactor (see Figure 2.10) had to be enlarged to accommodate the larger electrode.

The main reason for using the larger electrodes was to increase the amount of soot produced in a single run. The 3mm dia. electrodes produced 1.2g per rod on average, whilst burning a similar length of the larger diameter rod should produce four times this quantity. However, the increased amount of heat required to burn the larger volume of graphite in the 6mm dia. rods meant that the reactor took longer to cool down between runs, thereby decreasing its overall productivity.

The yield of fullerenes after Soxhlet extraction with toluene of the soot produced with the larger electrodes are given in Table 2.5. Surprisingly it was found that the

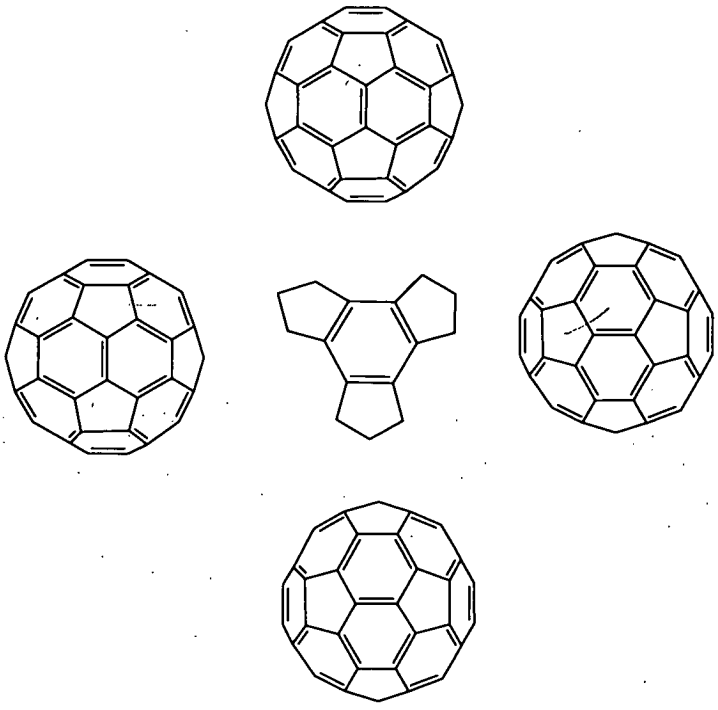

Figure 2.11: Structure of C_{15} tri-indane (centre) surrounded by C_{60} structures. Tri-indane is in effect a quarter of a C_{60} molecule which is evident from examination of the C_{60} structures.

yield of fullerenes recoverable from the soot rose from 4% to 7%. HPLC analysis of these extracts using HPLC system 1 (ChiralCap® column, mobile phase 15% chloroform in hexane, for details of the system see section 3.7) revealed an increase in the overall fraction of C_{60} in the fullerene mixture; 80% C_{60} as compared to 64% with the 3mm dia. rods. The reasons for this are not immediately obvious. The conditions inside the reactor when burning the larger rods are altered most obviously due to the increased power required. This increase in power means an increase in both temperature and pressure within the reactor. Increases in pressure to over 400 torr have been observed during a burn. The extra heat could assist in the annealing processes suggested for the "pentagon road" or the "collapsing mechanism" and lead to increased fullerene formation. However, it should be noted that when using the 3mm dia. rods there was a decrease in the yield of fullerenes at higher currents, although this could have been due to the rod burning too rapidly. Alternatively, the increased yield using the larger rods could be due to the higher carbon density immediately surrounding the arc leading to an increase in formation of the fullerene precursor structures. Such structures are important in a variety of proposed mechanisms, *e.g.* the naphthalene structures of the "C_{10} monomer model" and the "ring stacking model", or the large bi- and tri-cyclic ring systems which then rearrange to form fullerenes in the "collapsing mechanism". However, the dependence of fullerene formation on carbon density is not clear-cut since the presence of too many carbon species may cause any growing structure to form too quickly and leave less time to anneal to the most energetically favoured fullerene structure.

From Table 2.5 it can be seen that there is also a surprising fall in the amount of fullerenes other than C_{60} produced when using the larger graphite electrodes. The reasons for this decrease are unclear but may involve the increased carbon density which prevents any annealing to the higher fullerene structures.

Although the increased power required to burn these larger rods did provide some interesting results, it also posed serious problems in dealing with the heat produced.

Rod Diameter (mm)	**% Fullerenes Extracted**	**% C_{60}**	**% C_{70}**	**% Higher Fullerenes**
6	7.02	79.8	19.1	1.1
3	4.37	64.2	34.1	1.7

Table 2.5 Amount of fullerenes extracted using different diameter graphite electrodes

NOTE: Yields represent percentage of fullerenes recovered after Soxhlet extraction using toluene.

Experiment	**% Extract Yield**	**% C_{60}**	**% C_{70}**	**% Higher Fullerenes**
Tri-indane	4.48	84.3	14.6	1.1
Drilled rod	8.27	------	-------	----
Standard	4.37	64.2	34.1	1.7

Table 2.6 Yields of fullerenes from graphite rods seeded with tri-indane following Soxhlet extraction with toluene.

When burning 3mm dia. rods, a current of 60 amps is required, whereas thicker 6mm rods contain four times the volume of graphite and therefore require four times the current to burn. By experimentation it was found that it was possible to burn these rods at a lower current setting (140 amps), but the reactor was still running at a current level higher than that it was designed for. The heat generated from the arc is proportional to the square of the current multiplied by the resistance, and therefore, at these higher current settings there can be a substantial heat build-up. During one reactor run this led to the melting of the copper support which caused the glass kettle jar to crack. In order to burn rods of this size on a regular basis the reactor would have to be redesigned to accommodate a steel body which would be able to withstand the heat generated. An alternative support system for the base electrode would also have to be used to prevent the "meltdown" which occurred.

2.6.2 Experiments Using Seeded Electrodes

A further attempt to increase the yield of fullerenes from the reactor and to investigate their formation mechanism involved seeding the carbon rods with an organic substrate tri-indane, the structure of which is shown in Figure 2.11. From the figure it can be seen that the C_{15} carbon skeleton of tri-indane is in effect one quarter of a C_{60} molecule. It was hoped that this species when seeded into the graphite rods used in the carbon arc reactor might increase the amount of fullerenes formed by acting as a precursor. Ten 3mm diameter graphite electrodes were drilled out to a depth of around 30 mm and half of them packed with a 1:1 mix of tri-indane and graphite. The rods were then heated in an oven for twenty four hours at 150°C to ensure they were solidly packed. The remaining electrodes were packed with graphite only, to act as an internal standard, and heated in the same way. The conventional procedure for burning these rods in the reactor was then followed. The results obtained are shown in Table 2.6 and represent the percentage of fullerenes recovered after Soxhlet extraction of the soot formed with toluene. The percentage of different species present in the fullerene mixture was determined by HPLC analysis of the extract on a 4.6mm × 250mm FullereneSep® column using a 4% ether in hexane

mobile phase carried out on HPLC system 4 (see section 3.7 for details). From these results there is little difference in the overall amount of fullerenes extracted; 4.48% with the tri-indane seeded rods compared to 4.37% with the standard rods.

These results show little difference in the overall yield of fullerenes produced but do show a change in the composition of the fullerene mixture, with the percentage of C_{60} produced increasing for the seeded rods. In interpreting this result it is important to try to estimate the temperature inside the reactor to determine whether the tri-indane molecules are actually present and thus able to serve as preliminary building blocks for C_{60}, or if they are atomised by the power of the arc. If the latter is true they may still affect the growth mechanism by altering the carbon density surrounding the arc. A similar result of increased C_{60} formation was found when the larger 6mm diameter rods were used.

It is difficult to envisage how fullerenes can form from precursor hydrocarbon molecules such as tri-indane since it contains hydrogen atoms. If one considers models of carbon cage growth which imply energetic considerations such as the adoption of most favoured "pentagon road" type structures to minimise the number of dangling bonds, then it is obvious that the presence of hydrogen atoms would impair such a growth process by tying up any dangling bonds. De Vries *et al* [121] and Wilson *et al* [122] have shown that hydrogen impurities, whether in the rod or the quenching gas, in both arc-discharge and laser vaporisation experiments significantly decrease the yield of fullerenes formed even when the carbon concentration is considerably higher than that of the hydrogen; *e.g.* 10% fraction of hydrogen completely kills off any fullerene formation.

2.7 Conclusions

The initial aims of this phase of the present work were to construct and develop a reactor whereby macroscopic amounts of fullerenes could be produced with the maximum of efficiency in terms of the greatest yield in the shortest time. This was accomplished by investigating the operating parameters of the chosen design of the benchtop reactor to optimise the yield of fullerenes, whilst bearing in mind other factors that effect overall productivity, *i.e.* the factors affecting the reactor downtime such as the ease of retrieval of soot and the dissipation of heat produced during a production run. By careful examination of the various experimental variables, conditions were found for the optimum productivity and yields of up to 0.75g fullerenes per day were obtainable. The pressure of the buffer gas was altered to give the best fullerene yield and the discharge current adjusted until a value was found that gave a reasonable yield of fullerenes and also allowed the maximum number of rods to be burnt in the shortest time. During the course of these initial experiments it became evident that certain modifications had to be made to the reactor design. These were carried out with the overall productivity of the system in mind

The effect on the yield of fullerenes after the addition of a steel cup had altered the internal geometry of the reactor indicates the importance of convection patterns to the fullerene growth process and illustrates how the particular internal dimensions of the reactor may effect the yield of fullerenes

After the initial experiments aimed at characterising the reactor were complete, further experiments aimed at increasing the yield and understanding the formation mechanisms of fullerenes were carried out. The use of larger graphite rods to produce an increase in the amount of soot resulted in a higher percentage yield of fullerenes, but the increase in power required to burn these rods meant that the overall productivity of the reactor was reduced.

Attempts to increase the yield of fullerenes by seeding the graphite rods with an organic substrate had no noticeable effect on the total yield of fullerenes although it did affect the C_{60}/C_{70} ratio.

The benchtop reactor used in the initial phases of this work provided an extremely valuable source of fullerene rich soot at a time when macroscopic quantities of this material were extremely scarce and enabled a number of more speculative experiments to be carried out. Although the initial aims of the project were accomplished and fullerenes were successfully produced in macroscopic amounts using this reactor, the rapidly developing nature of the field meant that it soon became financially viable to obtain commercially raw soot. This changed the emphasis of part of the project to the development of a high yield extraction protocol for fullerenes and the investigation of HPLC techniques for their separation and isolation. However, this did not mean that the reactor became obsolete, instead its role changed. As the field developed species related to the fullerenes were discovered Endohedral fullerenes and carbon nanotubes became of as much interest to researchers as the fullerenes, and their formation mechanisms a matter of equal debate. The carbon reactor was now used in attempts to produce these species. These experiments are described in Chapter 5.

CAUTION

It should be noted that great care should be taken when harvesting the soot particularly when hydrocarbon species have been seeded into the reactor due to the possibility of the formation of carcinogenic polycyclic aromatic hydrocarbon (PAH molecules).

Chapter 3

Techniques for Extraction, Separation and Characterisation of Fullerenes

3.1 Introduction

The process of obtaining samples of purified, characterised fullerenes from the fullerene rich soot produced in a carbon arc reactor involves several stages that require a variety of techniques. The soot is initially extracted with solvent producing a mixture of soluble fullerenes. This mixture must then be separated into its component fullerenes and the different components characterised.

During the course of this work considerable use has been made of high performance liquid chromatography (HPLC) used both on- and off-line with a variety of different mass spectrometric techniques for the characterisation of fullerene mixtures. In the following chapter some background information on the different protocols for extraction and characterisation of fullerenes that have been described in the literature are given. The techniques employed in the present work are then described. The technical details of the extraction procedures as well as the HPLC and mass spectrometric instrumentation that have been used to characterise the fullerenes are summarised for clarity in this chapter. The experimental results obtained are presented together in Chapter 4.

3.2 Fullerene Solubility and Extraction Methodologies

Since Kratschmer *et al* [2] reported the first practical preparation of fullerene rich soot by resistive heating of graphite under a helium atmosphere, the huge growth in fullerene chemistry has been aided by the development of purification and extraction methods. Typically, the fullerene-rich soot, sometimes referred to as "fullerite", obtained from the resistive heating of carbon electrodes yields around 8-12% fullerenes of which 80% is C_{60} and 17% is C_{70} with the remainder being higher fullerenes, such as C_{76}, C_{78}, C_{84}, *etc* in smaller amounts. However, the isolation of pure samples of fullerenes remains a laborious process containing many steps, from the choice of initial production method and source of carbon, to the choice of extraction and purification techniques. Such choices may affect the type of fullerenes which will finally be isolated.

A major problem in the extraction and purification of fullerenes is that they have low solubility in most low boiling organic solvents, making such processes inefficient and costly. Moreover, the presence of impurities, whether residual solvents or molecules created during synthesis (e.g. polyaromatic compounds), the formation of solvates resulting from the strong affinity between the fullerenes and solvent molecules commonly used in their extraction, or the formation of fullerene adducts, particularly with oxygen, poses additional difficulties which must be overcome to produce high purity samples.

In order to develop the extraction and purification techniques needed to produce fullerenes on a large scale, an understanding of their interaction with solvents is required. This would enable choice of solvents that can provide cheap, scaleable methods for fullerene extraction. Solubility data additionally have a role in the choice

of stationary phase and type of chromatography employed for the separation of fullerene mixtures into their component species. The unique structure of fullerenes means that they interact with solvent molecules in interesting ways making solubility difficult to predict. Their rigid construction means there are no conformational degrees of freedom; their shape will be essentially the same in gas, liquid, solution or solid phases. As a consequence it might be thought that the process of C_{60} dissolution and its differential solubility would be to some degree predictable. An estimate of fullerene solubility in various solvents has been made [123] using parameters such as polarizability, polarity, cohesive energy density, and two aspects of the geometry of the fullerene molecule, namely molecular surface area (the area available for the fullerene to interact with the solvent) and molecular volume (the volume of the cavity created in the solvent liquid).

Ruoff *et al* [124] measured the solubility of C_{60} in 47 solvents and attempted to correlate the data with solvent properties such as index of refraction, dielectric constant, Hildebrand solubility parameter and molar volume. The molecule is poorly soluble in polar and hydrogen-bonding solvents. This is a result of the disruption of the solvent structure caused by the introduction of the non-polar C_{60} molecule, which does not participate in such bonding. However, no real correlation was found, and they concluded that although the different solvent parameters provided information concerning the solubility of C_{60}, there was no "universal parameter" that could be used to predict the solubility of fullerenes in different solvents.

This was also found to be the case by Beck *et al* [125], who carried out a similar study in which the solubility of C_{60} in more than 100 solvents was measured. They reasoned that the solubility of C_{60} was strongly influenced by molecular complex formation with the different solvents.

C_{60} was found to be sparingly soluble in alkanes [126,127], with the solubility increasing with the number of carbons in the alkane and the solubility in cyclohexane and cyclopentane was found to be very low [124]. Surprisingly, this was not the case

in decalin which was found to solubilise C_{60}. The solubility of C_{60} was found to be higher in halogenated alkanes than in the parent alkane [124]. Aromatic solvents are better solvents for C_{60}, with electron-donating substituent groups increasing the solubility and withdrawing groups decreasing it. Generally the solubility increases with the number of aromatic rings.

A further example of the unpredictable nature of fullerene solubility was discovered by Ruoff *et al* [128]. Experiments on temperature-solubility relationships for C_{60} in a variety of solvents revealed an unexpected discontinuity near 280K. The expected behaviour would be a monotonic increase in solubility with temperature, as is shown when an aromatic molecule or polycyclic aromatic hydrocarbon is dissolved in toluene. Instead for C_{60} solubility was shown to decrease with temperature over 280K. Ruoff *et al* [128] proposed that this was due to a phase change in solid C_{60}.

Ruoff *et al* [129] made further measurements on the solubility of C_{60} at different temperatures by using calorimetric measurements of the enthalpies of dissolution. They found that at lower temperatures the enthalpy of dissolution is positive; dissolution is endothermic and so there is a monotonic increase in solubility with temperature. Above a transition temperature of 285K, this behaviour changes; enthalpy of dissolution becomes negative, dissolution is exothermic and an increase in temperature leads to decreased solubility. In a simple experiment these authors demonstrated that when a saturated solution of C_{60} in toluene was filtered and sealed, upon heating the solution C_{60} was precipitated.

The negative temperature dependence of C_{60} solubility in toluene was verified by Smith, Li, King and Zimmerman [130]. They proposed that the commonly observed formation of C_{60} solvates might play a role in explaining such behaviour. Kumar and co-workers [131] have suggested that C_{60} has a larger solvation shell than previously thought and thus larger heats of solvation may explain this behaviour. Whatever the reasons these results have obvious implications when considering practical applications, whether it is the extraction of fullerenes from the soot matrix, or the

chromatographic solvent system required to purify and separate the extracted fullerenes.

The methods initially used for fullerene extraction involved hot solvent or Soxhlet extraction. As the solubility of C_{60} is at a maximum at ambient temperature, these methods have been modified by the introduction of cooling-fluid exchangers to maintain the temperature in the maximum solubility range. Temperature also plays a role in extraction kinetics, and other physical phenomena such as diffusion into the soot and absorption into pores must also be considered. The choice of solvent and technique is therefore guided by the type of species to be extracted with a rough trend that the higher boiling-point solvents extract the higher molecular-weight fullerenes.

The choice of solvent for extraction of the fullerene-rich soot is an important consideration. The starting soots are a complex mixture of materials with the exact distribution of fullerene species and the presence of impurities, such as polycyclic aromatic compounds or fullerene adducts, depending mainly on the production method used. In addition to this, the solvent used can be quite selective toward the extracted fullerenes. Consequently, it should be noted that straightforward extraction by any solvent will not reveal the true distribution of fullerenes present. Initial extractions therefore may be thought of as a pre-purification step.

3.3 Techniques Employed for the Extraction of Fullerenes from Soot

The first step in the isolation of separate fullerene species from soot is the extraction of the fullerene mixture. As indicated in the previous section there are different techniques by which this may be achieved and different solvents which can be used. The choice of the exact method will effect the yield and composition of the fullerene species recovered. In the course of this work two techniques were used for the initial recovery of fullerenes from soot, Soxhlet extraction and ultrasound extraction.

3.3.1 Soxhlet Extraction

This is a simple and effective technique for extracting a solid organic product from a solid mixture containing other materials. The soot produced in the reactor was first ground with a mortar and pestle and placed in a porous thimble, which is in turn was placed in the chamber of the Soxhlet extractor. Figure 3.1 shows a diagram of such a Soxhlet continuous extractor. The solvent in the round bottom flask is heated to boiling, and after condensation distils into the extraction chamber. When the chamber is full it empties *via* the siphon tube into the round bottom flask. Thus by prolonged repetition in a continuous cycle any soluble material is removed from the porous thimble into the round bottom flask. This method has the advantage over boiling under reflux in that the material is being washed with a fresh portion of solvent each time.

The fullerene extracts are deep red in colour, thus the progress of the extraction could easily be monitored from the colour of the solution in the extraction chamber. When there was no change in colour of the solvent as it entered the extraction chamber the extraction was deemed to be complete. The solvent was finally removed on a rotary evaporator to yield a mixture of C_{60} and C_{70}.

3.3.2 Ultrasound Extraction

The second extraction method that was employed was ultrasound extraction. This technique involved the use of an ultra-sound bath to sonically agitate material to be extracted causing any soluble components to dissolve. The soot was first ground with a mortar and pestle and placed in a round bottom flask with the selected solvent. The flask was then placed in an ultrasound bath (Ultrasons P Selectra® Model 513 240V, 150W, 50Hz manufactured by Lag Plant Ltd. Huddersfield) filled with water and switched on. The vibration caused by the bath agitates the material in the flask and the soluble material dissolves. The non-dissolved soot was finally filtered off and

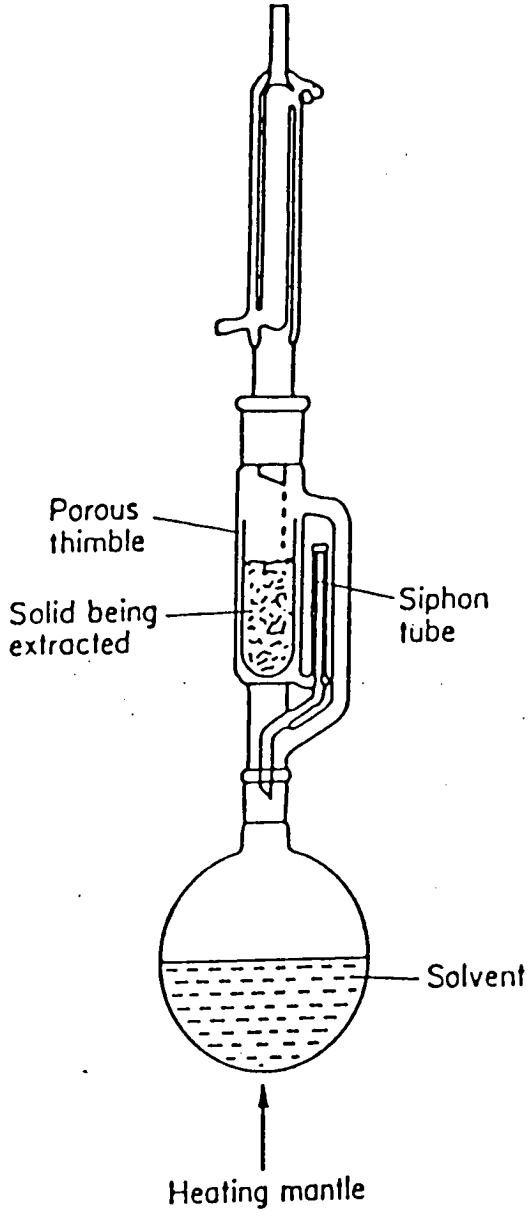

Figure 3.1: Soxhlet continuous extractor for the extraction of solids.

the solvent evaporated in vacuo to yield a mixture of fullerenes containing mainly C_{60} and C_{70} but also a small percentage of higher fullerenes.

Since the material in the flask is agitated it gradually causes the solvent to be heated. By stopping the reaction at different times and examining the yield of fullerenes produced, the point at which the maximum solubility of C_{60} occurs could be found. This is an important consideration when investigating the extraction of fullerenes as C_{60} solubility is known to decrease with temperature over 280K [128].

3.4 Separation Techniques for Fullerene Mixtures

Whatever synthesis and extraction method is employed, the soluble extract will be a complex mixture requiring further purification steps to produce the high purity samples required. The major technique used for such separation is liquid chromatography, both for analytical and preparative separation of solubilised extracts.

3.4.1 Liquid Chromatography and High Performance Liquid Chromatography (HPLC)

In these techniques the sample to be separated is loaded onto the top of a column packed with the stationary phase. The liquid mobile phase passes down the column and elutes at the bottom. The different fractions in the mixture are carried down the column at different rates depending on their relative affinities for the stationary phase and mobile phase and may be collected as they exit the column. In high performance liquid chromatography (HPLC) the mobile phase (eluting solvent) is supplied by a high pressure pump. Different fractions are detected as they exit the column by a detector which measures UV absorption at a pre-set wavelength. The absorbance is recorded as a function of time so that it is possible to tell by looking for peaks on the

detector when a fraction is leaving the column, thus allowing different fractions to be collected.

Many different chromatographic studies on the fullerenes have been conducted using different stationary and mobile phases to try and achieve increased selectivity, productivity and lower cost.

Initial attempts at production of purified fullerenes centred around extraction with toluene followed by separation with column chromatography on alumina [45,46]. Although this is an efficient method for the separation of C_{60} and C_{70}, the technique is time consuming and expensive because of the large volumes of solvents required, and at best, yields are less than one gram of purified extract per day. Silica columns have also been employed [132,133], although the retention times of the major fullerenes (C_{60} and C_{70}) are low and the selectivity is poor.

The main approach has been to employ reversed phase chromatography. Although primarily used for the separation of polar molecules this is a technique often employed for the separation of components which are poorly resolved by adsorption chromatography. Octadecyl silica phase (ODS), either monomeric or polymeric, is commonly used as a stationary phase in reversed phase HPLC. Aromatic solvents can be employed rather than hexane since their increased solubility for C_{60} allows a greater quantity of fullerenes to be injected onto the column.

The monomeric and polymeric phases show slight differences in separation; for instance, the D_3 isomer of C_{78} can be observed on polymeric ODS but not on monomeric ODS, and in order of elution, C_{76} and C_{78} ν' (an isomer of C_{78}) elute in different orders on the two columns [134]. Experiments with polycyclic aromatic compounds (PAC) suggest that polymeric ODS has a higher capacity for "topological" recognition. Consequently the retention differences of fullerenes are a factor of their sphere diameters and of their general geometry.

Dinitroanilinopropyl silica (DNAP) columns have provided good separation [135,136]. Ruoff *et al* [137] examined several different commercially available DNAP columns and found they were able to separate fullerenes using a mobile phase of 80% toluene and 20% hexane although the separation was somewhat degraded when raised to the preparative scale.

Many Pirkle-type columns have also been synthesised and tested. One of the best of this type appears to be tetrachlorophthalimidopropyl (TCPP) modified silica. The TCCP is a π acidic phase normally used for the separation of π electron rich polycyclic aromatic compounds. Separations carried out at ambient temperature with a dichloromethane/hexane mobile phase show excellent separation of C_{60}/C_{70} with the higher fullerenes up to C_{84} being separated with baseline resolution [138]. The nature of the separation is due to both the interactions with the π acidic dinitrophenyl groups and to a steric effect. The dinitrophenyl groups have a cone-shaped arrangement which leads to the formation of a "cavity". This in turn provides a base for multipoint interactions with the fullerenes leading to increased selectivity.

The major advantage to be gained in using a stationary phase which exhibits a stronger and more selective interaction with the fullerenes is that it allows the use of better solvent systems. With conventional stationary phases where there is only a weak interaction it is necessary to use solvents such as hexane, in which fullerenes are only sparingly soluble, to achieve reasonable separation. Use of better solvents such as toluene leads to a loss of separation and retention. Therefore, the amount of fullerenes that may be loaded onto the column is limited. Stationary phases which interact more strongly with the fullerenes allow the use of better solvents and thus more sample may be loaded.

Using a stationary phase of immobilised tetraphenylporphyrins (TTP) on silica with a 100% toluene mobile phase, Martin *et al* [139] achieved very high C_{60}/C_{70} separation factors. Like the TCCP column this stationary phase appears to separate the fullerenes through π-π interactions, which are enhanced by the creation of a pocket in

the extended aromatic structure of the tetraphenylporphyrin into which the lower molecular weight fullerenes can fit.

This steric effect also plays a part in the separation of fullerenes by a stationary phase of silica bonded to γ-cyclodextrins. γ-Cyclodextrins have been used as a complexing agent to produce water-soluble C_{60} complexes [140] and have been shown to form inclusion complexes with different substrates [141]. When a C_{60}/C_{70} mixture is eluted using an *n*-hexane mobile phase, greater retention is observed for C_{70} owing to its stronger interaction with the stationary phase. This system is limited by the low solubility of the fullerenes under these conditions. The solubility may be improved by the addition of toluene to the mobile phase. A toluene concentration of 30% has raised the possibility of preparative applications even though the retention of fullerenes was lowered by the addition of toluene. The mechanism of interaction has been explained as being due to inclusion of the fullerenes in the cavity created by the γ-cyclodextrine [141] with the lower retention when toluene is used being due to the competition between the fullerenes and solvent molecules for inclusion within the cavities. The higher retention of C_{70} is probably due to a more favourable geometry for inclusion.

Activated charcoal has also been used as a stationary phase to try to separate the fullerenes [142]. A flash chromatographic column with activated charcoal Norit A on silica gel allowed purification of gram quantities of fullerenes per day. The drawback with using this material, however, is that it tends to irreversibly absorb fullerenes. Mixing the charcoal with silica gel tends to lessen the adsorption forces, although even under the most favourable conditions, around 20% of C_{60} and 50% of C_{70} was retained irretrievably on the column.

An improvement on this method has recently been proposed [143]. Modification of the charcoal characteristics by increasing the proportion of hydrophilic groups and by manipulation of the solvent system, conditions has enabled 95% of the original fullerene sample by weight to be recovered.

Gel permeation chromatography, in which components are separated using size exclusion, would seem to be a useful method for separating the fullerenes with their different geometries and molecular diameters and this approach has been investigated quite intensively [144-148]. Although the technique has been used successfully to separate fullerene species, the mechanism of separation is not yet understood. Meyer and Selegue believe it has to do with hydrophobic interactions [145].

3.4.2 Other Separation Methods

Other methods for the purification of fullerenes that do not involve chromatography have also been investigated. Purification of fullerene rich soots has been achieved by a process of sublimation when the crude soots are heated to a temperature of 1050°C [149]. A temperature gradient applied to a mix of fullerenes leads to rough separation without a high degree of purity. This technique is extremely useful in the separation of metallofullerenes that are insoluble in common chromatographic solvents.

Molecular sieves with a cage aperture of 10Å have been found to capture C_{60} [150] and molecular sieve filtration could be used for the separation of fullerenes from polycyclic aromatic compounds (PACs), which are present in large amounts in soot produced using combustion techniques.

A further purification method investigated is recrystallisation. Coustel *et al* [151] produced 99.5% C_{60} from two recrystallisations of toluene extracted soot. Fullerenes mixtures have also been separated by capillary zone electrophoresis [152].

Fullerenes have additionally been extracted from the soot matrix with toluene and CO_2 in a 1:1 ratio as a subcritical fluid by Jinno *et al* [153]. These experiments showed there is a strong matrix effect of the soot with only the surface being extracted whilst the smaller the particle size, the higher the yield of extracted fullerenes.

3.5 Chromatographic Separation of Fullerene Mixtures

After extraction of the fullerene mixture from the soot produced in the reactor the next stage in the process of producing purified fullerenes was the separation of this mixture into its individual components. In the present work this was carried out chromatographically using both preparative and analytical scale techniques. Additionally, the use of differential complexation with Lewis acids for the rapid large scale separation of fullerenes was investigated as discussed in Section 3.8.

The raw fullerene crystals that are the product of the extraction process are a mixture of different fullerenes (C_{60}, C_{70}, C_{76}, C_{78}, *etc.*). The exact components in the mixture depends on the solvent(s) used in the extraction. These initial samples, however, contained a large mixture of different fullerene species. To achieve better separation a pre-purification step was introduced to break the fullerene mixture down into more convenient fractions prior to HPLC analysis. This was achieved by passing the raw fullerene samples down a preparative scale flash chromatography column containing neutral alumina and eluting with boiling hexane. The resulting fractions were then collected and examined by HPLC.

A schematic diagram of the essential components of an HPLC system is shown in Figure 3.2. The system consists of a column, containing the stationary phase, through which the liquid mobile phase (eluting solvent) is pumped. Sample mixtures are injected onto the column by the injector valve and separate as they move down the column at different rates depending on their relative affinity for the stationary phase and the moving eluent. The separated solutes are detected as they exit from the column by a sensitive detector, typically a UV/vis absorbance detector, and the detector signal is recorded to give a quantifiable record. A peak integrator is commonly employed and in most modern integrated HPLC instruments the entire system is under computer control with computerised data logging and processing.

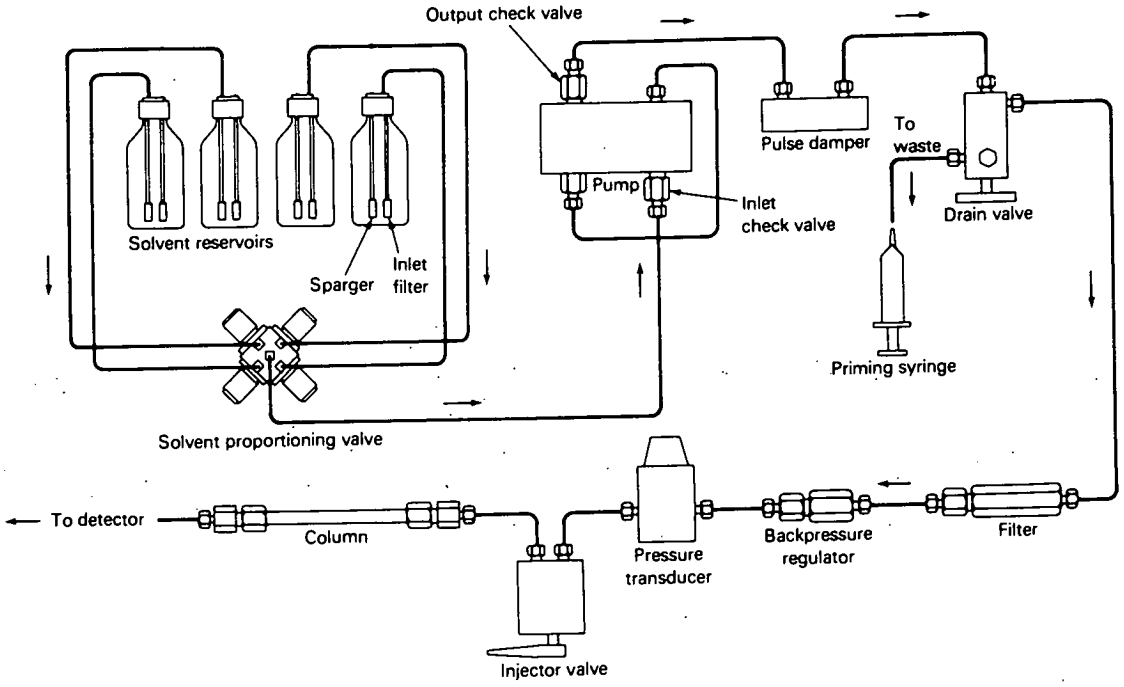

Figure 3.2: Schematic diagram of HPLC apparatus.

Several other features are common to most modern HPLC systems. The guard column (not shown), contains the same stationary phase as the main column and is located directly before it. This column is much shorter than the main column and is used in analytical HPLC to filter any dust or other insoluble impurities out of the solution before they reach the main column. The pulse dampener regulates the flow of the eluent ensuring the pressure is constant throughout the system. The proportioning valve allows different solvents to be mixed together in a pre-programmed and continuously variable way. The backpressure regulator prevents a build up of pressure occurring as solvent is pumped through the column. These features together allow the pulse free pumping of variable mobile phases through analytical or preparative scale columns with the minimum of wear on the column.

The performance of a chromatography column can be determined in different ways. Obviously, the first consideration is workable retention times. Although in HPLC the selectivity may be readily adjusted by variation in the nature of the eluent, it remains important to ensure that workable retention times are obtainable without recourse to forcing conditions.

Quantitatively the separating power of the column can be measured using capacity factors (k′) and the separation factor (α). Additionally the number of theoretical plates or the height equivalent to a theoretical plate can be found and used as a comparison with other columns.

The capacity factors, or phase capacity ratios as they are sometimes called, are a measure of the degree of retention of a solute by a column.

$$k' = (t_a - t_o) / t_o \qquad 3.1$$

where t_a is the retention time of component a, and t_o is the retention time of an unretained solute (i.e. one that behaves like eluent).

The separation factor (α) describes the ability of a chromatography column to separate two components in a mixture. It is a ratio of the capacity factors of the two components a and b (where a is eluted from the column before b).

$$\alpha = k'_a/k'_b \qquad 3.2$$

As a rule of thumb, for a column to be of use in separating a mixture of two components α should have a value greater than 1.2.

The performance of any new chromatography column may also be determined qualitatively. Good peak shape is very important and the chromatograph should contain sharp peaks with minimal tailing. The amount by which a peak tails is a measure of how well packed the column is.

As all molecules passing through the column have slightly different path lengths, they will take different times to pass down the column and so will exit at slightly different times causing the peak to broaden. Peak broadening will be increased by any regions of irregular packing that may occur in the column. The important areas where these regions are likely to occur are the entrance/exit of the column and the regions close to the wall. The importance of the entrance/exit regions decreases as the column length increases; in addition, the wall effects may be negated by making the column sufficiently wide. This technique is called the infinite diameter effect when the column is of sufficient width that sample molecules injected onto the top will traverse the entire length without reaching the walls. In order to obtain the best quality peak shapes it is important that the column is of the right dimensions.

3.5.1 Initial Studies of Fullerene Separation Using HPLC

As mentioned previously, the separation of fullerenes by HPLC using silica or alumina stationary phases suffers from poor separation factors and lengthy retention times. This led to the investigation of other materials which might enhance separation

and in particular, the development of a stationary phase specifically for use with fullerenes.

Chromatographic separation of π electron rich polycyclic aromatic hydrocarbons on π electron deficient stationary phases has been known for some time [154]. It was reasoned that such a stationary phase might be of use in separating the π electron rich fullerenes. Therefore, initial studies were carried out simply to see if enhanced separation was possible and, if so, to find conditions under which the technique might be optimised. These HPLC studies were carried out using a semi-preparative ChiralCap® column (2.5cm × 25cm ID cartridge) purchased from Capital HPLC, Bathgate. This is a commercially available chiral chromatography column, although the chirality plays no part in separating the fullerenes. The stationary phase is available as (R) or (S)-N-3,5-dinitrobenzoylphenylglycine (DNBPG) bonded covalently to 10μm aminopropylsilica, as shown in Figure 3.3 a). The electron withdrawing nature of the nitro groups gives the stationary phase its π acidity.

As described in Chapter 4 section 4.4.1, useful separation factors for C_{60} and C_{70} were obtained using this column and the effect of addition of chloroform to the mobile phase was investigated in an attempt to obtain workable retention times. However, the majority of further work was carried out using a new stationary phase for the separation of fullerene mixtures developed in collaboration with Capital HPLC Ltd.

3.5.2 HPLC Separations Using FullereneSep® Column

FullereneSep© is a novel stationary phase designed specifically for the separation of fullerenes. It was developed in collaboration with Capital HPLC Ltd, Bathgate. A more extensive series of HPLC studies were carried out using this column in order to investigate the efficiency of this phase in the separation of fullerene mixtures and to

a)

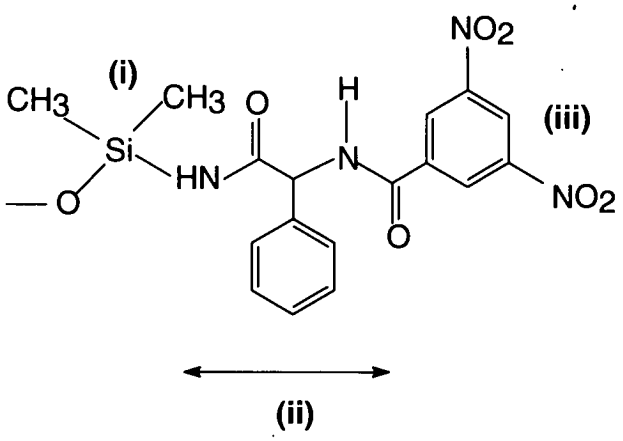

b)

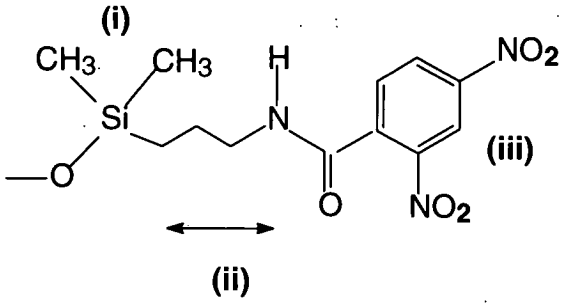

Figure 3.3: **a)** Structure of ChiralCap® Stationary phase **b)** Structure of FullereneSep© stationary phase. The figure shows the three parts of the stationary phase, (i) the adsorbent material, (ii) the linking group and (iii) the fullerene binding agent.

compare it against both the DNBPG ChiralCap® column used previously as well as other commercially available columns. These experiments involved investigation of the influence of mobile phase composition on capacity factor, column characterisation using on-line particle beam mass spectrometry, studies of the effect of column temperature on fullerene retention and an investigation of the relationship between the phase capacity factor and fullerene carbon number.

Initial chromatographic studies using the DNBPG stationary phase had shown it was of some use in separating fullerenes. Investigations aimed at increasing the interaction of the fullerenes with the stationary phase led to the development of the stationary phase FullereneSep®, shown in Figure 3.3b). The phase consists of three parts. An adsorbent material, hydrated silica in the form of particles typically of diameter 3-5μm, bonded to an alkyl amino linking group, which is joined in turn *via* an amide bond to a fullerene binding agent (a benzoyl moiety). Alkyl chains of varying length may be used in the linking group including C_3 , as shown in the figure, C_6, C_8, and C_{18}.

The fullerene binding agent is the part the of the stationary phase that is responsible for effecting any separation. On FullereneSep® this is the 2,4-dinitrobenzoyl moiety. As mentioned, separation is based on the interaction between the π-electron rich fullerenes and the π-electron deficient (π-acidic) stationary phase. Placing the nitro groups at the 2,4- positions, rather than the 3,5- positions as they are on the DNBPG column, maximises their electron withdrawing effect and so gives the molecule its strongest π-acidity. This is caused by the co-operative effect that occurs when substituents are placed at the *ortho-* and *para-* positions of a benzene ring.

In the DNBPG stationary phase the π acidic ring is linked to the silica support through a phenyl glycine unit, from which it derives its chirality. This chirality plays no part in fullerene separation. Indeed the bulky phenyl substituent in the chiral carbon centre may actually hinder the interaction between the fullerenes and the π

benzene ring. Therefore, the FullereneSep® stationary phase was designed with a simple alkyl linking unit to avoid the possibility of any steric interferences.

Separations on FullereneSep® are termed reversed phase. When applied to the separation of polar molecules the term reversed phase implies the use of a non-polar stationary phase in conjunction with a polar eluent. Although the separation of non-polar fullerenes proceeds by a different mechanism it is called reversed phase as it involves chromatography on non-polar alkyl bonded supports and results in the least polar molecules being eluted from the column first.

3.7 Technical Details of HPLC Systems Employed

Over the course of the present work, three different HPLC systems were used. Initial HPLC studies were carried out on a system which consisted of a Waters 6000A pump and a Spectroflow 773 absorbance detector connected to a Goerz Metrawatt BBC SE 120 chart recorder and a Hewlett Packard 3390A integrator. This work focused on the separation of fullerenes by a semi-preparative ChiralCap® column (Capital HPLC). The stationary phase consisted of 10μm (R)-DNBPG packed in a 2.5cm × 25cm ID cartridge, flow rate 9.9ml/min, detection wavelength 254nm column. For brevity in the following chapters this system will be subsequently referred to as HPLC system 1.

Subsequently work was undertaken using proprietary columns filled with a novel stationary phase called FullereneSep® (particle size 3μm, column sizes 4.6mm × 150mm and 4.6mm × 250mm). These columns were developed in collaboration with Capital HPLC Ltd, Bathgate. The HPLC employed for this phase of the work consisted of a Spectra Physics isocratic pump, a Rheodyne 7125 injector with a loop volume of 20μl and an LDC variable wavelength UV detector coupled to an LDC integrator. This system will be referred to as HPLC system 2.

On neither of these systems was there any facility for computerised data logging or data reprocessing so that some of these earlier chromatograms are reproduced directly from the original chart recordings.

During this period negotiations to purchase a new integrated HPLC system equipped with a computer interface were taking place and for a short period of time, a SpectraSYSTEM™ HPLC system from Spectra Physics was provided on evaluation. This highly integrated system consisted of an SCM400 solvent conditioning module, P4000 quaternary gradient pump, AS3000 variable-volume autosampler and a UV2000 dual wavelength UV/vis detector. One of the principal advantages of this system was the capability of the UV2000 detector to carry out on-the-fly spectral scanning enabling peak separation to be examined at multiple wavelengths. This system will be referred to as system 3. An example of such a spectrum recorded with this system is shown in Figure 4.12

Unfortunately the Spectra Physics system was eventually ruled out on the grounds of cost. Instead, an integrated HPLC system manufactured by Merck-Hitachi was purchased. This system consisted of a Merck-Hitachi L-6250 intelligent pump, equipped with low pressure gradient accessory, an AS-2000A autosampler, an L5025 column oven, an L-4250 UV/vis detector and L5200 fraction collector. The system was interfaced to a Dell System 433L PC equipped with an HP DeskJet 550C printer. The HPLC units were controlled through a Merck-Hitachi D-6000 interface module via the PC on which was mounted the D-6000 HPLC Manager chromatography data station software. All subsequent HPLC studies, such as investigations of the effect of temperature, column length and mobile phase composition were carried out using this system. This system will be referred to as system 4.

The various components in the system, pump, autosampler, detector and automatic fraction collector, can be controlled centrally from the PC (although all may be individually programmed), and the whole process from sample injection to fraction collection is automated, controlled by D-6000 HPLC Manager software. Sample

injection was carried out using the AS2000A autosampler, which has a capacity of 50 vials. The injection volume is variable in 0.5µl steps between 1 and 400µl. The L-6250 preparative pump is a dual reciprocating piston pump with electronic pulse dampening for pulse free flow. The preparative pump heads are capable of delivering flow rates between 3 and 30 000 µl/min. The L-4250 UV/vis detector is fitted with deuterium and tungsten lamps allowing a wavelength range of 190-700nm. The L-5200 automated fraction collector allows fractions to be collected by a variety of methods, according to time, peak number or solvent volume. Columns themselves were housed in the L-5025 thermostated oven guaranteeing a uniform programmeable temperature (range: ambient-100^{0}C) for every injection.

In studies involving the semi-preparative ChiralCap® column on HPLC system 1 and initial investigations of FullereneSep® using HPLC system 2 manual injection of samples was required. This was achieved using gas tight syringes, with 1ml capacity for injections on the ChiralCap® column and 50µl for the FullereneSep® column. The fullerene samples were thus injected into either a 100µl loop (ChiralCap® column) or a 20µl loop (FullereneSep® columns). Unless otherwise stated, all HPLC UV/vis detectors were set to a wavelength of 254nm.

The HPLC systems were calibrated with stock solutions of C_{60} and C_{60}/C_{70} which had been characterised by mass spectrometry. Standard solutions were made up at a range of concentrations and used to calibrate the HPLC instruments on a daily basis. They were also used to determine lower limits of detection for individual species and provided a means of regularly checking on column performance. Further details of the running conditions for the different samples examined are given in the individual figure captions.

The eluent solution was de-gassed and filtered through a sintered glass filter-funnel and filter paper. Saturated fullerene solutions were also filtered to remove any solid particles. The eluent was pumped at a set flow rate (9.9ml/min for the semi-

preparative ChiralCap® column and 1-2.5ml/min for the FullereneSep® column). Before use, columns were equilibrated for one hour at the required flow rate. Unless otherwise indicated the separations were carried out at ambient temperature. The fullerene solutions were loaded *via* the syringe into the sample loop and injected down the column.

3.8 Separation of Fullerenes by Competitive Complexation with $AlCl_3$

Because of the major difficulties involved in purifying the fullerenes by chromatographic techniques, especially on the preparative scale, other non-chromatographic methods were also investigated in the present work. One such method is competitive complexation. C_{60} and C_{70} have been successfully separated by selective complexation with calixarenes by Atwood *et al* [155]. In the light of this the feasibility of separating fullerenes by competitive complexation with $AlCl_3$ was studied.

Lewis acids, such as $AlCl_3$,, may be defined as substances which can accept an electron pair to form a covalent bond, thus filling their own outer shell. Primary interest in the fullerenes was originally sparked by the possibility of three dimensional organic chemistry. Although it has since been recognised that C_{60} does not react exactly like a three dimensional benzene ring, the electron rich nature of this compound has prompted interest in the reactivity of fullerenes with Lewis acids. As one ascends the fullerene series, moving from the perfectly symmetrical C_{60} upwards to C_{70}, C_{76}, C_{78}, and so on to the other higher fullerenes, the molecules become gradually more ellipsoid in shape and are thus more polarisable. This increase in polarisability should lead to an increase in reactivity and, therefore, as different species react at different rates, competitive complexation represents a possible method of separating fullerenes. The detailed results from these studies are

presented in Chapter 4, Section 4.7, and show that separation of fullerenes on a preparative scale can be achieved by complexation with $AlCl_3$.

3.9 Characterisation of Fullerenes Using Mass Spectrometry

Once the fullerene samples have been extracted from the soot they may be characterised by mass spectrometry. The techniques used in laser mass spectrometry have played a key role both in the discovery of the fullerenes and in their characterisation. The initial experiments that led to the discovery of C_{60} involved laser vaporisation cluster supersonic beam mass spectrometry. This is based on the principle that any material, no matter how refractory, will be vaporised when placed at the focus of a sufficiently intense laser pulse. The vaporised material is entrained into an inert gas pulse and is quenched by mixing with the gas stream. This allows clustering to take place for 30-200μs, producing clusters up to several hundred atoms large. The gas stream undergoes supersonic expansion into a vacuum, terminating further clustering and cooling the clusters to a few degrees Kelvin. The supersonic jet is skimmed into a molecular beam and probed by time-of-flight mass spectrometry. Residual positive or negative ions from the vaporisation plasma may be observed, or neutrals in the beam can be photoionised and the resulting positive ions detected.

Using this technique Rohlfing *et al* [156] first observed the distribution of even carbon clusters starting around the 40 atom size, a range that is now known to be due to closed fullerene cages. When clustering is allowed to proceed to a greater extent, a distribution in which C_{60} is far more prominent than its neighbours is obtained. It was just such a spectrum obtained under similar conditions that led to the proposal of the truncated icosahedral C_{60} structure [1].

This technique for generating clusters is very similar to that used in laser desorption mass spectrometry. In two-step laser desorption ionisation mass spectrometry the sample is initially desorbed by one laser. The desorbed neutral species can then be

ionised by a second laser and their time-of-flight mass spectrum subsequently recorded. In single-step laser desorption/ionisation mass spectrometry samples are desorbed from a substrate and the nascent ions, either positive or negative ions, formed during the desorption/ablation step are directly analysed by time-of-flight mass spectrometry.

Between 1985 and 1990, prior to the development of a macroscopic production technique, C_{60} and the other fullerene species were generated solely using laser ablation techniques. Since 1990 and the development of high yield fullerene production techniques the analytical aspect of mass spectrometry has been the most powerful tool in the characterisation of fullerene samples. At present mass spectrometric techniques are also being used to study the unique gas-phase physical and chemical properties of the fullerenes. A brief review of some of the work in this field is given below.

3.9.1 Previous Mass Spectrometric Studies

One of the earliest mass spectrometry experiments on C_{60} involved adding a reaction tube to the end of a laser vaporisation cluster source and injecting reagents such as NO, H_2, CO, SO_2, O_2, and NH_3 into the carrier gas stream [17]. The fact that this did not alter the C_{60} peak intensity in the cluster mass spectrum demonstrated the inertness of this species supporting the proposal for a closed cage structure.

Other laser ablation experiments led to the discovery of the first endohedral fullerene species. Attempts to purposely encapsulate an atom inside the fullerene cage were first carried out by Heath *et al* [24]. They used a disk of low density graphite which was soaked in a solution of $LaCl_3$, dried and employed as a laser target. When a high fluence ionising laser was used, sufficient to cause extensive photofragmentation with only the most stable species surviving, the resulting mass spectrum showed a prominent $C_{60}La^+$ peak. The survival of this species using such high laser fluence was a strong indicator that the La atom was inside the fullerene cage.

Tandem time-of-flight mass spectrometry has been used to investigate fullerene fragmentation. This technique allows the selection of ions of a single mass which may then be photofragmented using a second laser. The fragmentation of several even C_n^+ clusters, containing 60 or more carbon atoms, was investigated using this approach [26]. These species were all found to fragment by loss of an even number of carbon atoms, leaving a closed cage ion product. As the cages get successively smaller the steric strain increases until at C_{32} the cage ruptures. The C_{60} ion itself was found to be highly resistive to photofragmentation, as would be expected for the truncated icosahedron structure. In such a structure, all the atoms are equivalent with no weak point in the cage.

The photofragmentation of endohedral fullerenes was also investigated [27]. In experiments performed by Smalley *et al* [27] it was found that the fragmentation of $C_{60}M^+$ clusters proceeded by loss of an even number of carbon atoms, in the same way as for pure carbon clusters. This was strong evidence that the metal atom was inside the cage. If the metal atom were on the outside then fragmentation would be expected to proceed initially *via* loss of the metal atom, as this is the weakest bond. The cage was also found to rupture at a larger size with a metal atom present inside. This is as expected because of the repulsive force between the hard core of the metal ion electrons and the carbon atom cores. The size of the cage when it ruptured was found to agree well with the size predicted from the atomic radius of the atom inside the cluster.

Although the techniques used in laser mass spectrometry were responsible for the initial discovery of fullerenes, at present the most important application of mass spectrometry in fullerene research is as a tool in the optimisation of extraction techniques, by providing a method of rapidly characterising the different fullerene species and fullerene adducts, and in the characterisation of endohedral fullerenes and fullerene derivatives

3.12 Techniques of Mass Spectrometry for the Analysis of Fullerenes

Many different mass spectrometric studies have been carried out on the fullerenes. Techniques employed for their characterisation have included fast atom bombardment (FAB), electron impact (EI), chemical ionisation (CI), secondary ion (SI) and laser desorption mass spectrometry (LDMS). With these different techniques, the mass spectra of the same sample can differ quite markedly. In particular, the C_{60}/C_{70} ratio can vary significantly depending on the technique employed. One problem encountered in characterising fullerenes is fragmentation due to excess energy supplied either by the desorption or ionisation process. This fragmentation can affect the resulting spectra both qualitatively and quantitatively. The break-up of fullerenes present in the initial sample obviously affects the observed ratios of the different species. Additionally, reaggregation of these fragments into other fullerene species can produce signals in the mass spectrum arising from species not originally present in the sample.

For the analysis of samples by EI mass spectrometry, the sample must be present in the gaseous state. Typically this is achieved by applying the sample, as a liquid or solution, to a wire loop which is then dried in air and inserted into the instrument where it is heated to a temperature sufficiently high to produce gaseous molecules. The volatile molecules are then ionised by an electron beam of variable intensity. In such studies, Dunsch *et al* [157] observed high fragmentation and multiple ionisation at electron energies of around 70eV. By decreasing the electron energy to 15 eV the fragmentation and multiple ionisation disappeared, but the sensitivity also diminished distinctly.

A similar lack of sensitivity with a high degree of fragmentation is observed when using FAB mass spectrometry with caesium ions. In this case, correct interpretation

of the spectra is further complicated by adduct formation with the embedding matrix as well as with additional matrix signals below m/z = 600.

In comparison to these methods Dunsch *et al* [157] have found that CI mass spectrometry is about one thousand times more sensitive than other ionisation methods and may also be used to detect traces of higher fullerenes and endohedral fullerenes. The molecules are heated to put them into the gaseous state as in EI mass spectrometry and the ionisation gas is methane. This method does suffer from the disadvantage that the fullerenes also form adducts with the ionisation gas (M+14, M+16, *etc.*), making the detection of other addition products, such as those with oxygen, difficult.

The use of lasers in the mass spectrometric characterisation of fullerenes has been widespread, both as a desorption technique combined with ionisation methods such as CI or EI, and as a combined desorption ionisation technique as in single step laser desorption ionisation (LDI) and matrix assisted laser desorption ionisation (MALDI).

One problem in characterising fullerenes by laser desorption mass spectrometry is the formation of new fullerene species from reaggregation of carbon fragments caused by the desorption laser itself. An illustration of the problem is shown by the laser desorption studies of Ulmer *et al* [158]. In these experiments a sample of fullerenes were desorbed using either 308nm or 248 nm output at a range of different laser fluences. The resulting species were studied in two ways, either by direct examination of the positive ions produced by the desorption process, or by ionisation of the neutral species with a second laser. It was found that an increase in the fluence of the desorption laser led to a significant increase in fragmentation of the C_{60} and particularly the C_{70} species initially present, and that the fragmented species could reaggregate to give new fullerenes, as shown by an increase in the intensity of the signals for species higher than C_{70} and a corresponding decrease in the signals for C_{60} and C_{70}.

Meijer and Bethune [159] had previously produced similar mass spectra using a two step laser desorption/ionisation set-up very similar to that used by Ulmer *et al.* The mass spectra that they obtained from a carbon sample were interpreted as evidence that a range of fullerenes up to mass 2000 were present in the original sample. Nonetheless, they used only one laser fluence for desorption (120 $mJcm^{-2}$) which Ulmer *et al* has since shown [158] caused significant fragmentation and reaggregation.

Although these effects are well documented for positive ion mass spectra [160] it has been reported that the growth processes do not occur for negatively charged fullerene ions [161]. From mechanistic considerations, it is expected that the negative ion mass spectra of fullerenes should be more immune to both fragmentation and growth processes than the positive ion mass spectra. This is due to the competition between fragmentation and electron detachment that occurs for energetic negative ions. The excess energy required for fragmentation is easily sufficient to detach the extra electron on the negative ions. The electron affinity of C_{60} is 2.6-2.8 eV [162] whilst the threshold energy for fragmentation is 4.5 eV [163]. As a result any cluster that is hot enough to fragment is easily capable of losing the extra electron.

Similar considerations affect the growth processes. The addition of carbon units is also a heating process adding energy to the cluster. This would also tend to detach an electron. Therefore the hot negative ions formed in a growth process, like the negative ions that are hot enough to fragment, would detach an electron and therefore not be seen in the negative ion mass spectrum.

As a result it can be seen that the negative ions that are detected are the least energetic ions. These ions are more representative of the species which are desorbed intact, have less internal energy and undergo fewer gas-phase interactions. Consequently these ions have less chance of taking part in growth or fragmentation processes and should be more representative of those species initially present in the extract. By contrast the positive ions have no such corresponding neutralisation

processes and their spectra can therefore contain species which have been formed after growth or fragmentation processes have occurred.

There are however other processes involved in the generation of negative ion spectra which may skew the observed distribution. The abundance of the different fullerene anions may be affected by the electron-capture cross-section. The process of electron attachment may involve collisional cooling, implying some gas-phase interactions may take place. This process could also be affected by the presence of impurities with high electron affinities in the ablation plasma. For example large concentrations of chlorine atoms could have a scavenging effect on the electrons and consequently, lead to a decrease in the probability of fullerene anion formation. This means that the fullerenes would be desorbed but not observed as negative ions. The presence of residual solvent in the sample is therefore an important consideration.

Since the mechanisms for the formation of positive and negative ions are very different it is unlikely that the same interferences will affect both types of spectra. Thus, differences observed between the positive and negative ion spectra, are likely to indicate some of the processes mentioned are taking place. For example, absence of a negative ion distribution could indicate that peaks present in the positive ion spectrum are formed by growth reactions, or that the corresponding negative ions are not being formed due to competing effects. From these considerations it seems that the observation of similar positive and negative ion mass spectra provides a reasonable criterion for concluding that fullerene species detected in the mass spectrum derive from similar species in the input sample, and importantly are not created by the laser conditions.

3.10 Technical Details of Mass Spectrometers Employed for the Characterisation of Fullerenes

In this study characterisation of fullerenes was primarily achieved using laser desorption ionisation (LDI) time-of-flight mass spectrometry. These studies were carried out on a range of instruments. Additionally on-line particle beam liquid chromatography mass spectrometry was employed for the conclusive identification of fullerenes eluting from an HPLC column. A brief description of these techniques along with technical details of the instruments is given in the following sections.

3.10.1 Single-Step Laser Desorption/Ionisation Time-of-Flight Mass Spectrometry (LDI and MALDI)

Single-step LDI TOFMS was originally developed to provide a rapid yet gentle desorption technique for the direct analysis of high molecular-weight polymers. In this technique a single laser is used for both sample desorption and ionisation. The ionisation yield, particularly for high mass ions is considerably improved by the use of a matrix which is strongly absorbing at the incident laser wavelength. This technique is now known as matrix assisted laser desorption ionisation, or MALDI for short, and has rapidly become one of the most powerful techniques for recording mass spectra of proteins, peptides and synthetic polymers.. However, in certain instances, it is not always necessary to use a matrix in order to obtain a reasonable ion yield and in the majority of this work spectra were recorded without the use of a matrix. The sample signal is optimised by variation of the position and power of the laser beam and the ions generated, M^+, M^-, MH^+ or $(M-H)^-$. In the simplest form of time-of-flight mass spectrometry the ions are accelerated from the source into a field free drift region where they are allowed to drift over a fixed distance until they reach a detector; their mass can then be deduced from the measured flight time.

The "soft" ionisation involved in LDI TOFMS means there is little fragmentation and consequently the spectra are not complicated and data analysis is unambiguous. In addition the speed of analysis, including both sample preparation and data acquisition, meant LDI was the most convenient technique for the characterisation of fullerene species.

3.10.2 Characterisation of Fullerene Mixtures using LDI TOFMS and MALDI

The laser desorption ionisation mass spectrometry studies were carried out using an instrument constructed in-house at Edinburgh as well as several different commercial instruments, namely a VG TofSpec, a Kratos Kompact MALDI III and a Bruker Reflex. The work on the VG and Kratos instruments was performed at VG, Manchester, and Kratos Analytical, Manchester. The data on the Bruker instrument was obtained by Dr Pat Langridge-Smith while on sabbatical at the ETH Zürich. Although there are individual differences between the systems (technical details are given below), in each case the sample is desorbed and ionised using a single laser and the resulting ions are analysed by time-of-flight mass spectrometry.

Initial studies were carried out using the TOF mass spectrometer constructed at the University of Edinburgh. This instrument, details of which have been published elsewhere [164], was developed primarily for MALDI studies on synthetic polymers. A schematic diagram of the apparatus is shown in Figure 3.4. It is based on a coaxial linear reflectron of the "fountain" design. The sample probe, ion optics, reflectron and detector are cylindrically symmetrical and are contained within a single stainless steel vacuum chamber 50cm in length. The laser used for desorption/ionisation is a Lambda Physik K600 pulsed nitrogen laser. The laser output at 337nm has a pulse-width of 4ns and a typical pulse energy of 1.2mJ when running at a repetition rate of 10Hz. The sample holder is maintained at a positive potential and the extraction cone, 3mm in diameter, is at ground potential so that any positive ions formed by the laser pulse are extracted by this field into the field-free

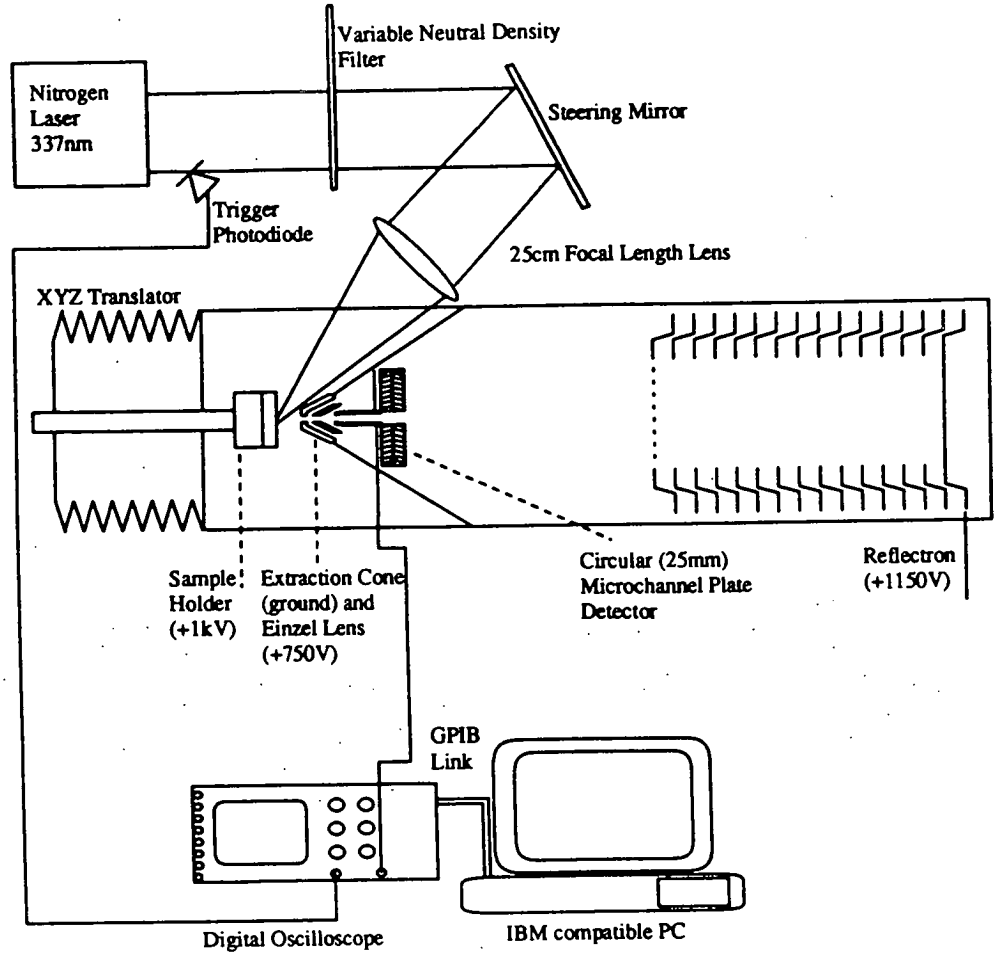

Figure 3.4: Schematic diagram of the LDI TOF mass spectrometer constructed in-house at the University of Edinburgh.

region of the mass spectrometer. The ions fly through a 4mm central hole in a circular 25 mm diameter dual microchannel plate assembly are reflected in the single field electrostatic reflectron and finally strike the microchannel plate detector. The waveforms are acquired using a LeCroy digital oscilloscope Model 9310M, with a digitisation rate of 100Msamples per second, *i.e* every 10 ns.

The sample holders used in these experiments were 2cm diameter copper or stainless steel disks onto which approximately 10 separate samples could be placed. Samples were deposited on the holder from toluene solutions, typically 1-4 μl of solution was applied. An apparently homogeneous layer formed easily as the toluene rapidly evaporated. No matrix was used in these experiments to assist ionisation. Sample locations could be chosen for analysis by viewing the sample holder through a window in the vacuum chamber and moving the area of interest into the laser focus with an XYZ manipulator.

The VG TofSpec, Kratos Kompact MALDI III, and Bruker Reflex time-of-flight mass spectrometers are commercially available instruments, functionally similar in design. These instruments have been developed specifically for MALDI experiments. On all three systems desorption/ionisation is carried out using the 337nm output of a nitrogen laser and on all three instruments both positive and negative ion mass spectra can be recorded.

Figure 3.5 (a) shows a schematic diagram of the VG TofSpec mass spectrometer in linear mode. In this configuration the instrument is typically operated with the sample holder at 25kV (source voltage). Ions generated by the nitrogen laser pulse are accelerated by the source to the analyser, where they are allowed to drift over a fixed distance; the drift path length to the linear detector is 650 mm. When the nitrogen laser is fired it triggers a start mechanism and the time taken for the laser-generated ions to arrive at the detector is measured by sampling the detector output at either 250 or 500Mhz. The detector is a tandem microchannel plate detector with impedance matched anode. The source and analyser are differentially pumped using

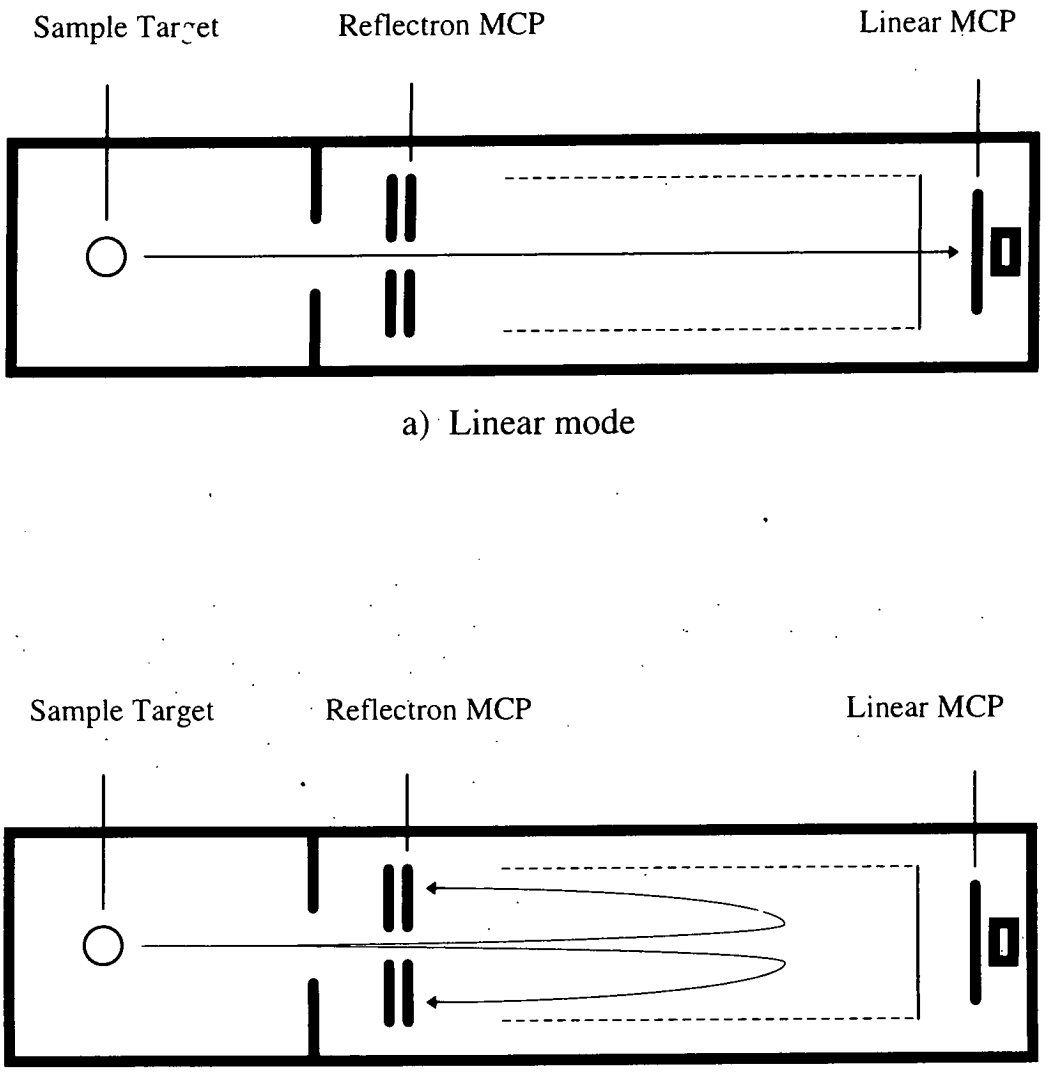

Figure 3.5: Schematic diagram of the VG TofSpec mass spectrometer.
a) linear mode of operation, b) reflectron mode of operation.

turbomolecular pumps (250 ls^{-1}), allowing the mass analyser to remain under high vacuum even on sample loading, thus protecting the detector. The sample stage can accommodate up to 20 samples at once, with automatic pumpdown and automatic sample selection. Additionally samples can be viewed in real time using a video CCD camera focused onto the sample stage. In addition to the linear mode of operation a reflectron is available when a higher degree of mass resolution and accuracy is required. Figure 3.5 (b) shows a schematic diagram of the instrument in reflectron mode. The reflectron lens assembly is located in front of the linear detector, and reflects ions back along the instrument axis to the annular reflectron MCP detector before they reach the linear MCP detector. This has the effect of doubling the flight path of the ions, and the reflectron itself compensates for the small, random energy differences between the ions as they emerge from the source. These two factors have the combined effect of producing better resolved data with a mass accuracy (assuming accurate calibration) of 0.02% compared to the 0.2% mass accuracy achievable in the linear mode. The mass resolution in reflectron mode is *ca.* 2000 (FWHM) compared to *ca.* 200 (FWHM) in linear mode. Instrument control, data acquisition and processing is carried out using a DEC VAXstation™.

The Kratos Kompact Maldi III mass spectrometer is slightly different. A schematic diagram of the instrument layout is shown in Figure 3.6. The principal difference is that in reflectron mode ions are deflected by a deflector plate into the reflectron which is offest by a small angle from the ion axis in linear mode. The length of the flight path is 700 mm in linear mode and 1.4 m in reflectron mode. Data can be acquired at 300 Msamples per second. Mass resolution is *ca.* 400 (FWHM) in linear mode and *ca.* 2000 (FWHM) in reflectron mode. Instrument control, data acquisition and processing is carried out using a SUN SPARCstation™. Again up to 20 samples may be deposited onto a disposable sample slide, which is mounted on a probe and drawn into the vacuum system by software control.

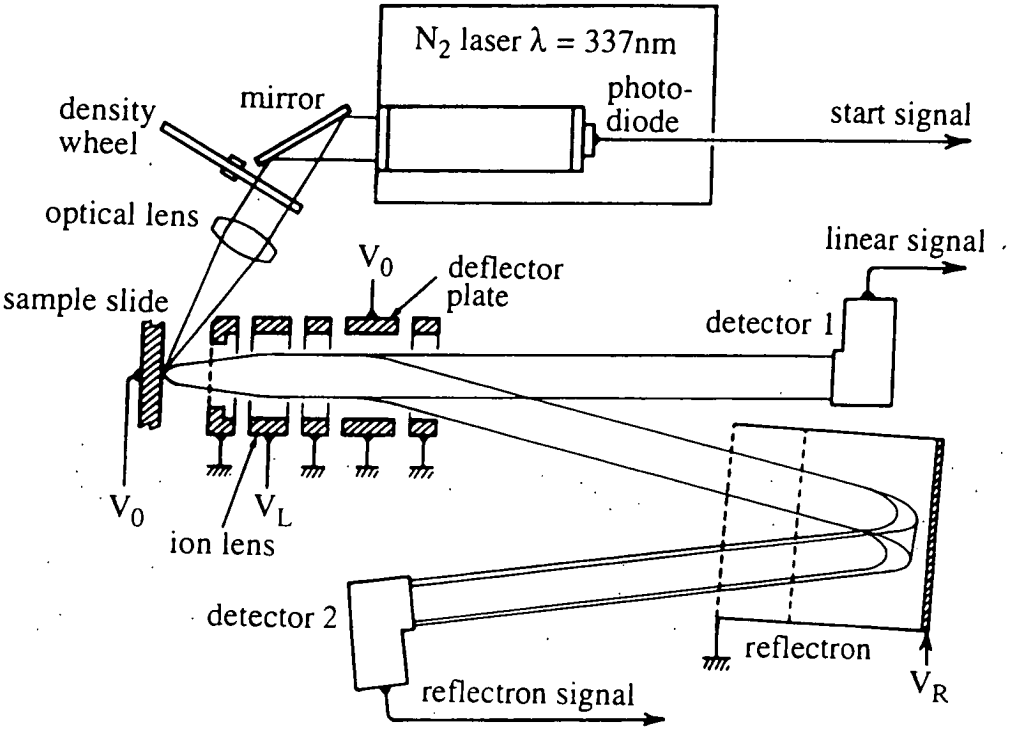

Figure 3.6: Schematic diagram of Kratos Kompact III mass spectrometer.

Finally the Bruker Reflex mass spectrometer is shown in Figure 3.7. In this instrument the reflectron is offset at a small angle relative to the overall instrument axis. In linear mode, when no voltages are applied to the electrostatic mirror, ions are accelerated out of the source, traverse the flight path and impact on a detector (not shown) behind the ion mirror. In reflectron mode these ions are reflected at an angle to their incident direction and strike the off-axis detector. The total drift length is 1.65m in reflectron mode and 1.45m in linear mode. Resolution in both modes of operation is similar to that on the other instruments, although somewhat higher ion acceleration energies can be employed (35 kV). Data acquisition is at 200 Msamples per second. Instrument control, data acquisition and processing is carried out using a SUN SPARCstation™. As in the VG instrument multiple samples can be loaded simultaneously and their position computer controlled. The instrument is also equipped with a video CCD camera for sample viewing in real-time.

As will be seen from the results presented in Chapter 4, laser desorption/ionisation has been found to be a very useful technique for volatilisation and ionisation of fullerenes. The combination of resistance to photofragmentation and relatively low ionisation potentials of the fullerenes makes them ideal candidates for the LDI technique.

3.10.3 Characterisation of Fullerenes Using On-line Particle Beam Liquid Chromatography Mass Spectrometry (LCMS)

In order to be able to fully characterise fullerene mixtures it is desirable to separate the species chromatographically and characterise each fraction by mass spectrometry. This can be a very time-consuming process if the mass spectrometric analysis is carried out off-line, especially when dealing with small concentrations of complex mixtures. With on-line liquid chromatography mass spectrometry, individual fractions eluted from the chromatography column pass directly into the mass

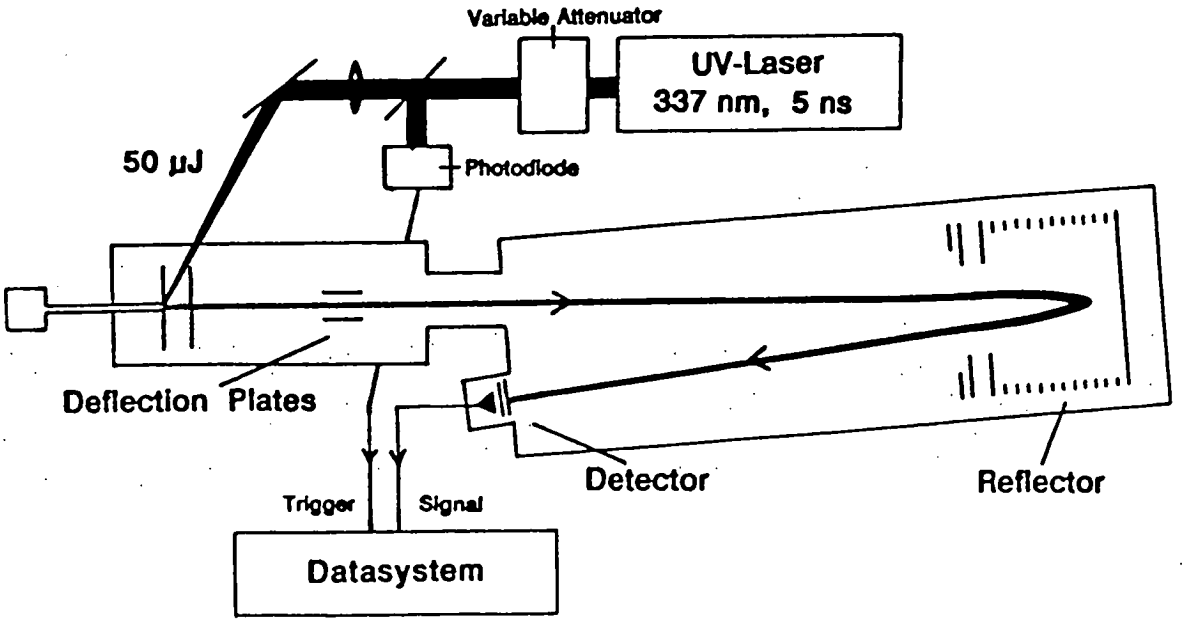

Figure 3.7: Schematic diagram of Bruker Reflex mass spectrometer.

spectrometer for analysis. The arrival of each separate fraction into the mass spectrometer can be observed by monitoring the total ion-current (TIC) and correspondingly, mass spectra can be displayed at any chosen retention time. Such studies were carried out during the course of this work in collaboration with Kratos Analytical, Manchester. The primary aim of this work was to confirm the purity of the separated fractions observed using FullereneSep® HPLC columns and to conclusively identify the carbon number of these fractions. The results from these studies are presented in Chapter 4, Section 4.4.3.

There are different methods for the transferral of chromatographic eluents into a mass spectrometer. Each technique requires the removal of all of the chromatographic mobile phase and the transfer of the solute to the ion source without degrading the chromatographic resolution. In our studies, a particle beam interface was used to couple the HPLC to the mass spectrometer. This technique involves nebulising the liquid stream exiting from the column. As the liquid is nebulised, the solute molecules stick together in droplets, while the solvent molecules form an aerosol. The droplets are directed into a beam and pass into a desolvation chamber which is set at a certain temperature where any remaining solvent is removed by heating to leave a beam of the involatile solute particles.

A Kratos Concept 1H magnetic sector mass spectrometer was used for this work. This instrument is of a horizontal, double focusing E-B design. The 90° electrostatic analyser (E sector) is followed by a 60°/685 mm inhomogeneous field magnet (B sector), with field and current control via computer-controlled 18bit D-to-A converters. These are also integrated with internal electronics for manual override and repetitive field scanning. High field stability is ensured by water cooling of the magnetic analyser and reference electronics. A physically separate, but electrically integrated console incorporates the computer and microprocessors for control, acquisition and data processing. The instrument uses an off-axis post-acceleration detector. High vacuum is provided by three turbomolecular pumps at the source (360 $l\ s^{-1}$), analyser (150 ls^{-1}) and detector (50 ls^{-1}). A range of ion sources are available,

such as EI, CI and FAB. The source housing design enables multiple inlets to be mounted simultaneously. In our work an EI source was used together with an LC inlet.

The mass range of the instrument is 10-10,00 u at an accelerating potential of 8kV and the scan speed varies from 0.1 sec decade^{-1} to 3,000 sec decade^{-1}. The maximum resolution of the instrument is 80,000 and the mass measurement accuracy is better than 5 ppm.

The HPLC system employed for these on-line LC-MS studies was interfaced to the mass spectrometer using a Kratos particle beam interface. The liquid flow from the column is transferred into a heated concentric flow nebuliser and sprayed into a heated desolvation chamber. the droplets evaporate and any dissolved analyte then transferred via a two stage separator into the EI source, where final evaporation and ionisation occurs. The interface is a probe based system, complete with required pumping and temperature control electronics.

In our experiments the nebuliser and desolvation chamber of the particle beam interface were maintained at a temperature of 80°C. The spectra were recorded with the electron impact source at an electron energy of 80eV. The spectra were run by scanning from 1000 to 100 u at 3 sec dec^{-1} at a resolution of 1000. In view of the low volatility of the fullerenes , the ion source of the mass spectrometer was maintained at 350°C which was the maximum temperature for this instrument. The spectra obtained are discussed in Chapter 4, Section 4.4.3.

Chapter 4

Experimental Results on Extraction, Separation and Characterisation of Fullerenes

4.1 Introduction

As discussed in the previous chapter the process of isolating and characterising fullerenes from soot consists of several stages involving a number of techniques. In this chapter the experimental results obtained using the techniques described in Chapter 3 are presented. These include Soxhlet and ultrasound extraction of soot with different solvents and the investigation and optimisation of separation by HPLC on different stationary phases. Studies on the effects of mobile phase composition, temperature and column length on retention and separation of fullerenes were also carried out. Chromatographic studies on the relationship between capacity factors and molecular weight and calculations of the change in enthalpy on adsorption are reported. The separation of fullerenes by competitive complexation with $AlCl_3$ has also been investigated. Finally results on the characterisation of fullerenes using various laser desorption mass spectrometry techniques are discussed as well as the use of mass spectrometry in conjunction with HPLC for monitoring the formation and degradation of aziridinofullerenes.

4.2 Extraction of Soot for Isolation of Fullerenes

The extraction of soot for isolation of fullerenes was carried out using two methods, Soxhlet extraction and ultra-sound extraction.

It has already been mentioned that the choice of solvent and technique of extraction are extremely important, since they are selective for the type of fullerenes to be extracted from the soot. There is some evidence to suggest that the nature of the binding of the fullerenes to the soot matrix is temperature dependent. In order to investigate this possibility Soxhlet extraction was carried out using toluene, (b.pt. 110°C), 1,4-dichlorobenzene, (1,4-DCB, b.pt. 173°C) and 1,2,4-trichlorobenzene (1,2,4-TCB, b.pt. 214°C).

C_{60} has been found to have high solubility in CS_2 [124],but it decreases over a certain transition temperature (around 285K) [128][129]. In order to solubilise the maximum amount of C_{60} in the solvent, and thus for the extraction to be most efficient, it must be carried out at relatively low temperatures. Obviously, the technique of Soxhlet extraction is of limited use since it requires the solvent to be boiling, unless it is modified to include a cooling fluid exchanger around the main part of the extraction chamber. To overcome the need for this, a second technique, ultra-sound extraction, was employed.

4.2.1 Soxhlet Extraction

The apparatus was set-up as shown in Figure 3.1. Approximately 400ml of solvent was placed in the RB flask and about 50ml in the extraction chamber. The system was connected *via* the top of the condenser to a nitrogen bubbler which acted as a pressure release. The soot was placed in a pre-weighed thimble and the thimble and contents weighed and placed in the extraction chamber. (NOTE: The soot had been previously stored under an argon atmosphere in an air-tight container). The apparatus

was filled with argon and the heating mantle turned on. The extraction was left running continuously until the solvent in the extraction chamber became clear, the characteristic red/brown colour of dissolved fullerenes having disappeared (*ca* 4h.). The solvent in the RB flask, which was a deep red colour, was then transferred to a smaller, preweighed RB flask and the solvent removed by evaporation on a high vacuum system. The flask and contents were weighed and the percentage yield of fullerenes calculated.

As discussed in section 3.2 the solubility of C_{60} in different solvents is rather unpredictable. When Ruoff *et al* [124] compared experimental values of C_{60} solubility in 47 different solvents to values predicted on the basis of polarizability, solvent polarity and molecular size they failed to show any real correlation. Although the Soxhlet extractions of fullerene-rich soot with toluene, 1,4-DCB and 1,2,4-TCB were carried out primarily to determine whether temperature effects played a role in the quantity and type of fullerenes extracted, the effect of the different polarity of the solvents employed will also be discussed.

A sample of fullerene-rich soot (ca. 80g) was extracted with toluene, b.pt. 110°C, (ca. 450ml) until no further change in the colour of the solution in the extraction chamber was seen, *i.e.* no more fullerenes were being extracted. This yielded 3.7g of fullerenes (4.54% by weight of soot). The same sample was then Soxhlet extracted with 1,4-DCB, b.pt. 173°C, and a further 1.89g, of fullerenes were obtained.

The procedure was then repeated using a fresh sample of soot (ca. 80g). However, once primary extraction with toluene was complete the soot was extracted with 1,2,4-TCB instead of 1,4-DCB. This produced a further 3.38g of fullerenes. In each case extraction with 1,4-DCB or 1,2,4-TCB was continued until the solvent in the extraction chamber was colourless. These results demonstrate that, following extraction with toluene, use of higher boiling solvents can produce a further yield of

Table 4.1: Percentage recovery of fullerenes from soot by Soxhlet extraction with different solvents. The soot samples had previously been Soxhlet extracted with toluene.

Solvent	Wt of soot (g)	Wt fullerene extracted (g)	% fullerene extracted
1,2,4-TCB	78.42	3.38	4.31
1,4-DCB	80.03	1.89	2.36

Table 4.2: Percentage recovery of fullerenes from an 80g sample of soot by the sequential extraction with different solvents in the order toluene, 1,4-DCB, 1,2,4-TCB.

Solvent	B.pt (^{0}C)	Wt fullerene extracted (g)	% fullerene extracted
Toluene	110^{0}C	3.70	4.54
1,4-DCB	173^{0}C	1.92	2.36
1,2,4-TCB	214^{0}C	1.03	1.26

Table 4.3: Percentage content of fullerene mixtures extracted with different solvents.

Solvent	% C_{60}	% C_{70}
Toluene	71.2	28.8
1,4-DCB	62.5	37.5
1,2,4-TCB	61.5	38.5

fullerenes. From Table 4.1 it can be seen that a higher percentage of the remaining fullerenes can be recovered using 1,2,4-TCB compared to 1,4-DCB (4.31% by weight as compared to 2.36% by weight).

To investigate this further, a sample of soot (ca. 80g) was sequentially extracted with the three solvents in the ascending order of boiling point, i.e. toluene, 1,4-DCB, 1,2,4-TCB. The weight of fullerenes extracted and percentage yields are given in Table 4.2. Initial toluene extraction yielded 3.70g of fullerenes (4.54% by weight). Extraction with 1,4-DCB increased this by 1.79g (2.2% by weight) and extraction using 1,2,4-TCB yielded a further 1.03g (1.26% by weight). These results further demonstrate the ability of higher boiling solvents to extract fullerenes from the soot once extraction at lower temperatures is complete.

The fullerene mixtures extracted using the different solvents were examined by HPLC (2.5cm × 25cm ChiralCap® column, stationary phase DNBPG, mobile phase 15% chloroform in hexane, flow rate 9.9ml/min, detection at 254nm) to determine their exact composition. The results, shown in Table 4.3, indicate an increase in the percentage of C_{70} in the extract when using higher boiling solvents (28.8% C_{70} in the toluene extract rising to 38.5% when extracted with 1,2,4-TCB).

4.2.2 Effect of Temperature on Extraction of Fullerenes

The results shown in Table 4.1 demonstrate that following extraction with toluene, use of higher boiling solvents can produce a further yield of fullerenes. The yield is greater when a higher boiling solvent is used. Following toluene extraction, extraction with 1,2,4-TCB yielded 4.31% fullerenes by weight whereas extraction with 1,4-DCB produced 2.36% fullerenes.

This is supported by the results shown in Table 4.2, which further demonstrate the ability of higher boiling solvents to extract fullerenes from the soot once extraction at lower temperatures is complete. Thus, after extraction with toluene was complete,

extraction with 1,4-DCB yielded a further 1.79g fullerenes (2.2% by weight). On completion of this, extraction of the soot remaining with 1,2,4-TCB yielded a further 1.03g (1.26% by weight).

Since these studies were conducted the temperature dependence of C_{60} has been studied in detail. Ruoff *et al* [128][129] have found an unusual effect of temperature on C_{60} solubility. In a variety of solvents C_{60} solubility was found to increase with temperature up to a threshold value of around 280K, after which the solubility decreased. Because of this development Soxhlet extractions should now include some sort of cooling device for the extraction chamber to ensure the maximum solubility temperature range.

However, temperature effects are not limited to solubility they also play a role in the extraction kinetics. The results shown in Tables 4.1 and 4.2 demonstrate that extraction at higher temperatures increases the yield of fullerenes obtained. This indicates that the fullerenes may be bound in different environments within the soot matrix. Increasing the extraction temperature could cause increased diffusion of the solvent into the soot matrix or aid adsorption into pores, thus fullerenes which were previously buried too deep to be extracted may be reached. Applying this to the solvents used in these studies, toluene extraction removes "loose" fullerenes, extraction with 1,4-DCB removes species which are more tightly bound and extraction with 1,2,4-TCB removes those fullerenes buried deeper still within the soot.

The fact that 1,4-DCB (a non-polar solvent) can recover fullerenes after extraction with toluene (a polar solvent) is complete and that C_{60} solubility is actually decreased at higher temperatures shows that the important effect in these extractions is that of temperature on the extraction kinetics.

A further feature of these extractions is evident from chromatographic examination of the extracts that are obtained with different solvents. The percentage C_{60}/C_{70}

composition of the different extracts is given in Table 4.3. The C_{60}:C_{70} ratio for toluene extracted soot was found to be 2.6:1, (71.2% C_{60}: 28.8% C_{70}) this changes to 2.2:1(62.5% C_{60}: 37.5% C_{70}) when using 1,4-dichlorobenzene and 1.6:1(61.5% C_{60}: 38.5% C_{70}) with 1,2,4-trichlorobenzene. The increase in amount of C_{70} extracted as the boiling point of the solvent is raised is clearly evident. A possible explanation of this is that the temperature dependence of C_{60} and C_{70} solubility differ, with C_{70} being more soluble at the higher temperatures. This is supported by experimental observations made by Xihuang *et al* [165], who found C_{70} solubility to increase with temperature with no threshold over which solubility decreased, as is the case for C_{60}.

4.2.3 Effect of Solvent Polarity on Soxhlet Extraction of Fullerenes

The polarity of the different solvents as a factor affecting extraction yields has also been considered. The solvents used in this work in order of increasing polarity are 1,4-DCB (non-polar), toluene, 1,2,4-TCB. The solubility of C_{60} has been measured by Ruoff *et al* [124] in toluene as 2.8mg/ml and in 1,2,4-TCB as 8.5mg/ml. There was no data available for the solubility in non-polar 1,4-DCB, however the increased solubility in 1,2,4-DCB than toluene might suggest that polarity is an important factor in C_{60} solubility. If this was the case and temperature effects were not important 1,4-DCB would not be expected to extract any fullerenes once extraction with toluene was complete. The fact that it does shows the unpredictable nature of C_{60} solubility and the importance of temperature effects on reaction kinetics.

4.2.4 Ultrasound Extraction

The solvents used in these extractions were toluene and Carbon Disulphide (CS_2). C_{60} has been found to have a high solubility in CS_2 (7.9 mg/ml) which due to its volatility may be easily removed from the extract to yield the fullerenes. This overcomes the problem of removing solvent encountered previously when the high boiling solvents 1,4-DCB and 1,2,4-TCB were used in the Soxhlet extractions. These

solvents are difficult to remove completely even when using a high vacuum rotary evaporator.

Details of the ultrasound bath used in these studies have been given in Chapter 3, Section 3.3.2. Practical details were as follows. Approximately 100ml of solvent was added to the 250ml RB flask containing the raw soot, which had been previously well-ground with a mortar and pestle. A condenser was attached and the apparatus was lowered into the ultrasound bath until the level of the water in the bath was above the level of the solvent in the RB flask. The bath was then switched on. After 20min. the remaining soot was filtered-off and the solvent removed by rotary evaporation.

Ultra-sound extraction with toluene produced on average 7% by weight of fullerenes whereas extraction using CS_2 yielded 9% fullerenes. For extractions with both solvents it was found that the percentage of fullerenes extracted decreased if the extraction process was continued for too long, extractions lasting in excess of 20 minutes caused the solvent to be heated over 280K and so to lead to a detrimental effect on solubility.

Comparison of toluene extraction for the Soxhlet and ultrasound techniques shows the increased yield that is obtained by sonication. This is most likely due to increased diffusion into the soot matrix allowing extraction of fullerenes buried deeper within the soot.

The increased yield obtained by ultrasound extraction with CS_2 and the ease by which the extracted fullerenes may be recovered are major advantages over the techniques previously used. The process is simple to implement and is completed within 20 minutes. This compares very favourably to the 4 hours typical of Soxhlet extraction with toluene.

4.2.5 High Yield Extraction of Fullerene Soot

To try and achieve a more complete extraction of the soot a combination of ultrasound and Soxhlet extraction was tried. A sample of soot (20g) was first extracted by sonication with toluene. The extract was removed and the resulting residue Soxhlet extracted with toluene (500ml). The combined yield using this process was 2.3g of fullerenes (12% by weight from soot).

4.3 Separation of Fullerenes by Flash Chromatography

First attempts at the separation of fullerene mixtures in the solvent extracts involved flash chromatography down a column of neutral alumina. A preparative column was prepared by gradually pouring the alumina (500g, neutral, activity grade 1) into a glass cartridge which was agitated continually. This procedure ensured that the alumina was packed uniformly. The soluble extract (2.3g), produced by ultra-sound extraction with CS_2 followed by Soxhlet extraction of the residue with toluene, was dissolved in carbon disulphide (500ml) and adsorbed onto anhydrous magnesium sulphate (100g) by rapid evaporation of the solvent. The resulting magnesium sulphate/fullerite mixture, a dry mobile brown powder, was loaded onto the top of the neutral alumina column (500g). A condenser was fitted to the column and the system eluted with boiling hexane for approximately four days using the technique described by Wudl [166]. The solvent eluting from the bottom of the alumina column was monitored by HPLC (System 4, 4.6mm × 250mm FullereneSep® column). The first fraction, a purple band, was seen to elute after 24 hours, and after a further 24 hours a red band eluted from the column.

A yield of pure C_{60} (1.4g, 61%) was obtained after 24 hours and a fraction containing C_{60} and C_{70} in the ratio of 1:1(0.6g) was collected after a further 24 hour collection

period. Elution was then discontinued and the remaining material on the column (0.1g) was obtained by sectioning the column into two lengths and extracting the separate fractions with toluene. All four fractions were then subjected to analysis by HPLC.

The chromatograms obtained for the different fractions eluted from the column are shown in Figures 4.1 and 4.2. The separations were carried out using the Merck-Hitachi HPLC system (for details see Section 3.6) with automatic data collection. The stationary phase used was FullereneSep® (3μ), column, dimensions 250mm × 4.6mm (see section 4.4) with a mobile phase of 100% hexane, flow rate 2ml/min and detection wavelength of 254nm. Figure 4.1a) shows the chromatogram for the first fraction, F1, that eluted from the column. This fraction consists predominantly of one component, C_{60}, eluting at a retention time of 6.13 min.

Figure 4.1b) shows the second fraction, F2, that eluted from the column, This fraction was composed of C_{60} (71.5%) eluting at 6.37min, together with a large proportion of C_{70} (28.5%) eluting at 11.83 min. These percentages are calculated from the peak areas provided by the integrator output of the HPLC system.

Fractions F3 and F4 were obtained after the elution of the second fraction was complete by dividing the column into two lengths and extracting each length with toluene. Fraction F3 was extracted from the lower half of the column while F4 was obtained from the upper section, The chromatogram of fraction F3 is shown in Figure 4.2a), it clearly shows in addition to the C_{60} and C_{70} peaks three peaks at longer retention times due to higher fullerenes. The negative ion mass spectrum of the sample F3 is shown in Figure 4.3. This was obtained on the Kratos Kompact MALDI III instrument, averaged over 50 shots operating in the linear mode. The spectrum shows peaks at m/z 720 C_{60}, m/z 840 C_{70}, m/z 912 C_{76}, m/z 936 C_{78} and m/z 1008 C_{84}. From the mass spectral data the three peaks eluting after C_{70} in fractions F3 were assigned as C_{76}, C_{78} and C_{84} respectively in order of increasing retention time.

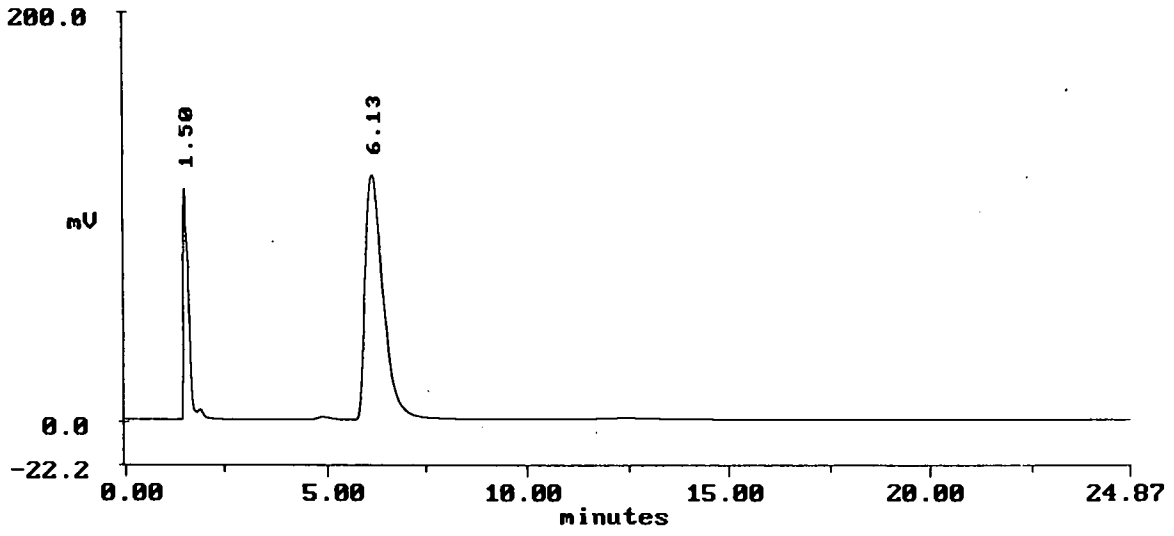

a

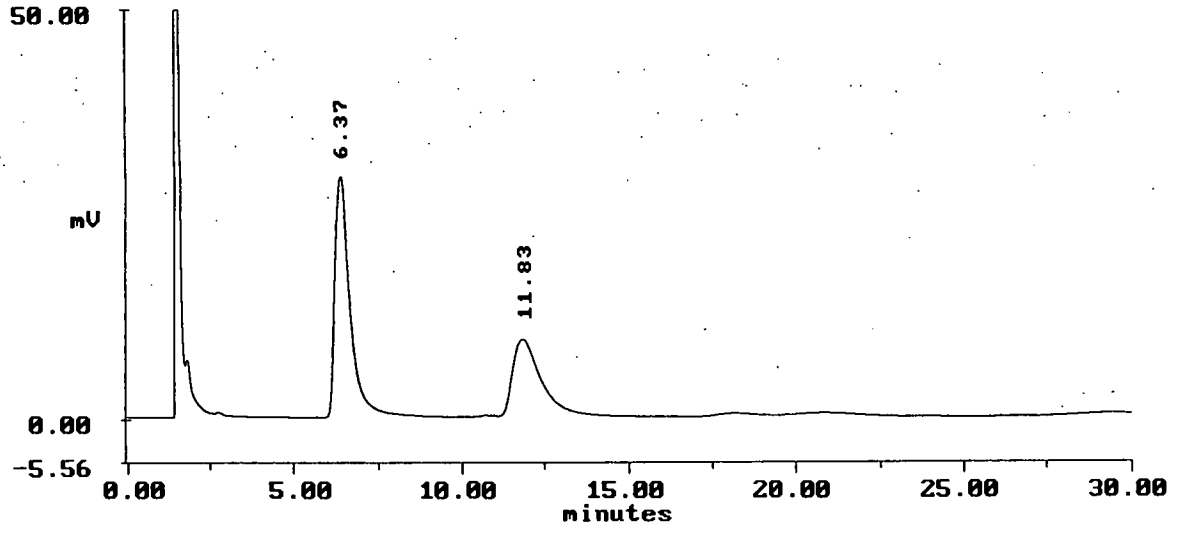

b

Figure 4.1a) Chromatographic trace of fullerene fraction F1 **b)** Chromatographic trace of fullerene fraction F2. (FullereneSep®column, 250mm × 4.6mm, mobile phase 100% hexane, flow rate 2ml/min detection wavelength 254nm.

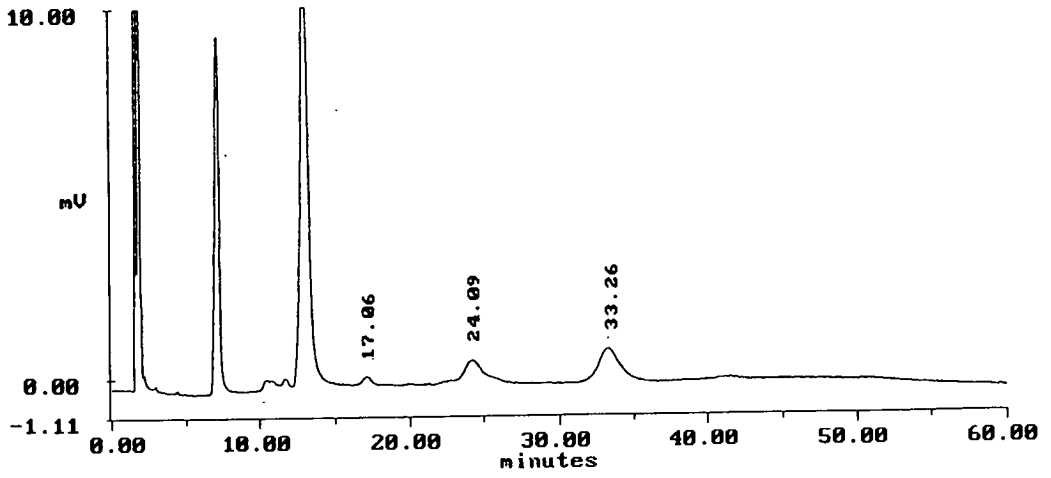

a

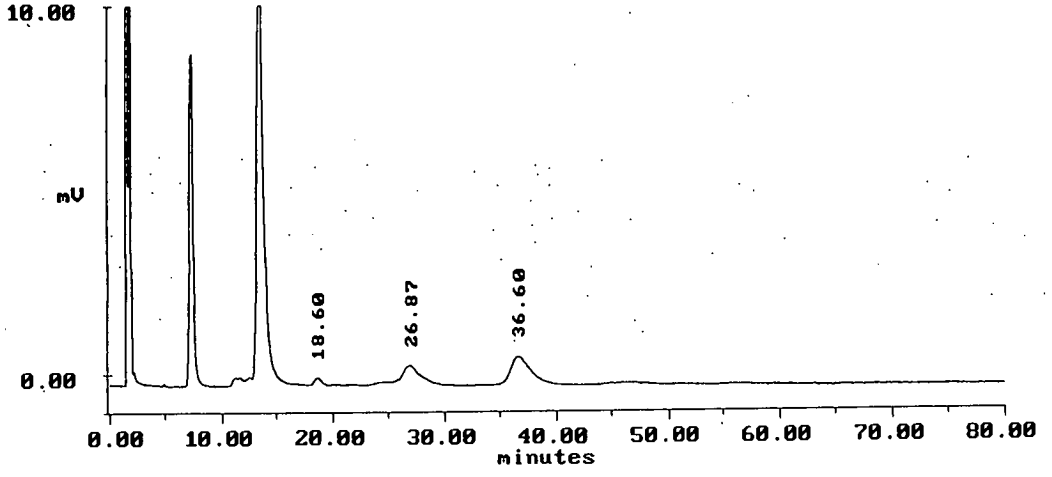

b

Figure 4.2a) Chromatographic trace of fullerene fraction F3 **b)** Chromatographic trace of fullerene fraction F5 (FullereneSep®column, 250mm × 4.6mm, mobile phase 100% hexane, flow rate 2ml/min detection wavelength 254nm. The fractions were obtained by sectioning the lower and upper parts of the column respectively and extracting with CS_2.

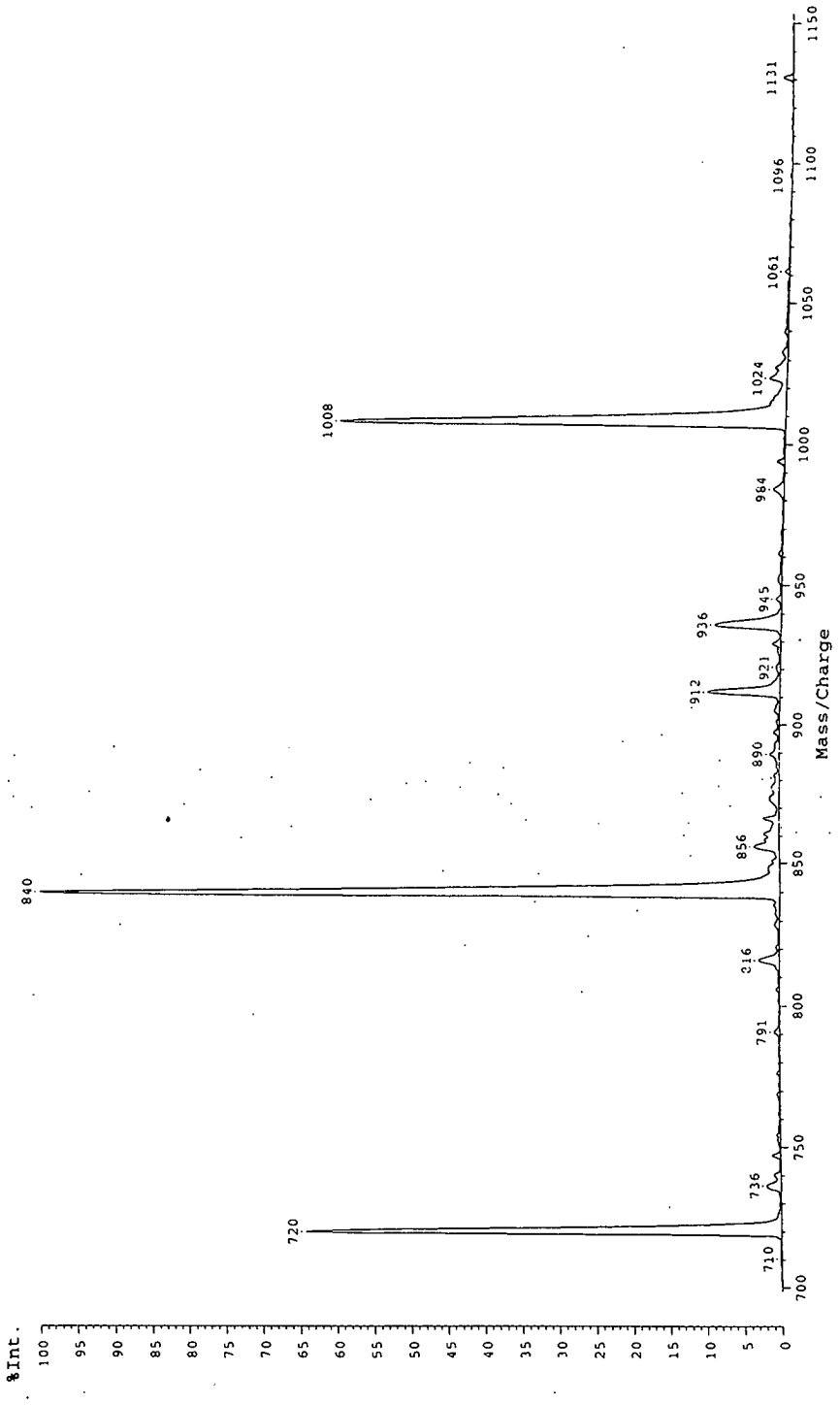

Figure 4.3: Negative ion mass spectrum of fullerene fraction F3 obtained on Kratos Kompact III instrument averaged over 50 shots in the linear mode.

In addition to the presence of higher fullerenes, fraction F3 shows a marked increase in the percentage of C_{70} present. This has now become the largest component in the fullerene mixture, 54.1%, with only 36.1% C_{60} and 9.8% higher fullerenes.

Figure 4.2b) shows the chromatogram of fraction F4. This was obtained from the extraction of the upper part of the column and contains the species that have travelled the least distance. The Chromatogram shows the presence of C_{60}, C_{70}, C_{76}, C_{78} and C_{84}. Examination of the peak areas shows the fraction contains 57.3% C_{70}, 31.5% C_{60} and 11.2% higher fullerenes. This is a further increase in the relative amounts of C_{70} and the higher fullerenes relative to C_{60}.

4.4 HPLC Studies

These studies were carried out using a range of HPLC instrumentation. For full descriptions of these, see section 3.6.

4.4.1 Separation of Fullerenes on ChiralCap® Column

Investigations of separation of fullerene mixtures by HPLC were carried out on a semi-preparative ChiralCap® column (2.5cm × 25cm, 10μm (R)-DNBPG, flow rate 9.9ml/min, detection wavelength 254nm). Samples of fullerene-rich soot extracted with toluene were manually injected onto the column *via* a Rheodyne 7125 injector with a loop volume of 100μl. Initial separation was achieved using a mobile phase of 100% hexane. The results shown in Table 4.4 show that good separation is achieved, (the selectivity factor, a measure of the separating power of the column $\alpha = 2.14$, see Section 3.5 for definition of separation factors). However, the retention times are prohibitively long, C_{60} taking 60 min to elute and C_{70} 110 min (at a flow rate of 9.9ml/min this means that over 1 litre of hexane is required to elute C_{70}, in addition the peaks obtained show considerable broadening, see Figure 4.4. To try to obtain workable retention times, the effect of adding to the mobile phase varying fractions

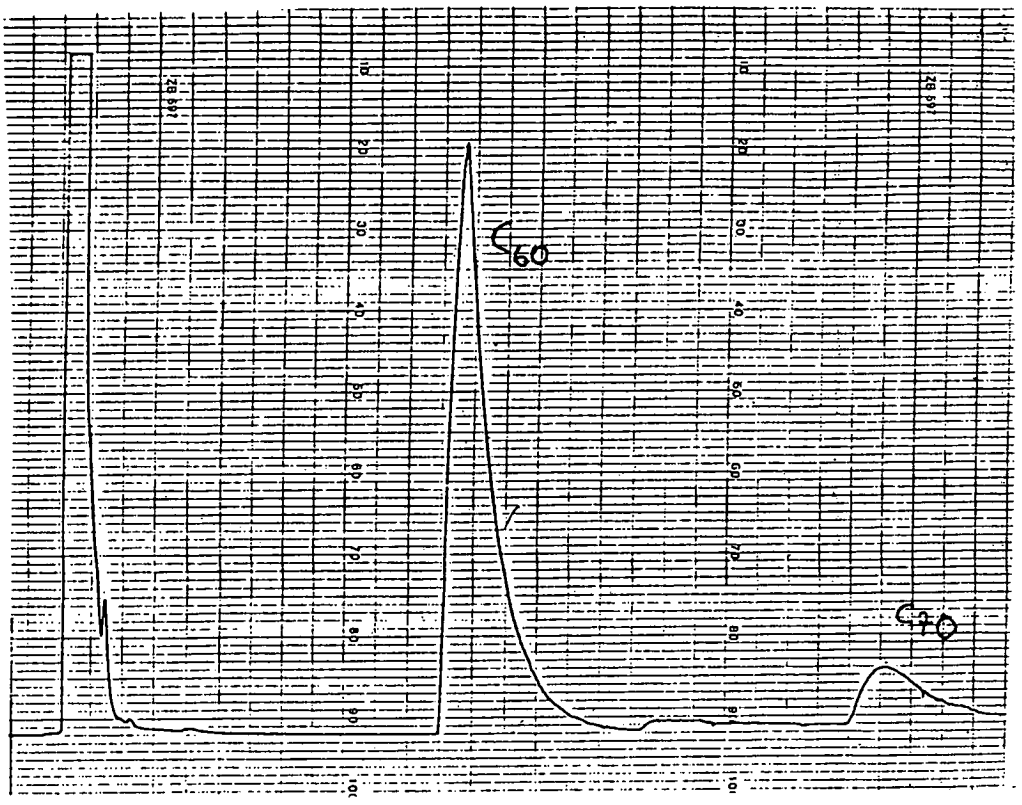

Figure 4.4: Chromatographic trace of C_{60} and C_{70} separated on ChiralCap® column, 2.5cm × 25cm, flow rate 9.9ml/min, mobile phase 5% chloroform in hexane, detection at 254nm.

Table 4.4: The effect on retention time (R.T.) and separation factor of varying the percentage of chloroform in the hexane mobile phase.

% chloroform	**R.T. for C_{60} (mins)**	**R.T. for C_{70} (mins)**	**α**
o	60	110	2.25
5	29	56	2.08
10	24	39	1.94
15	20	30	1.83
20	17	23	1.77
50	16	18	1.52

of chloroform, a polar solvent was investigated.

Mobile phases containing different percentages of hexane and chloroform, from 100% hexane to 50% hexane/50% chloroform were prepared and de-gassed. A series of injections of C_{60}/C_{70} mixtures using the different mobile phases was carried out. The effects on separation and retention times are summarised in Table 4.4

The results show there is a large decrease in the retention of C_{60} and C_{70} when only a small fraction of chloroform is added to the mobile phase. Addition of 4% chloroform halves the retention times of C_{60} and C_{70}. The retention times continue to drop as the percentage of chloroform in the mobile phase is increased; using 50% chloroform the retention of C_{60} decreases to 16min. However, there is a corresponding decrease in the separation (α=1.52). Additionally C_{60} and C_{70} fractions did not show baseline separation with this concentration of chloroform. It was found that use of a mobile phase containing 15% chloroform provides workable retention times (20 min for C_{60} and 30 min for C_{70}) while the peaks remain separated sufficiently from each other to be identified easily.

The reduction in the retention time resulting from the addition of chloroform to the mobile phase is caused by competition between the chloroform and the fullerenes for the stationary phase. The polar chloroform is strongly attracted to the stationary phase and attaches itself. This leaves less area for the fullerenes to interact with and so they are eluted quicker, with the least polarisable, C_{60}, coming off first.

Although C_{60} is more soluble in chloroform than in hexane the reduction in retention time does not appear to be a simple solubility effect as striking reductions are observed even on addition of a very small proportion of chloroform to the mobile phase, furthermore similar effects are observed on the addition of other polar solvents such as acetonitrile or ether even though C_{60} is insoluble in these solvents. These results seem to point conclusively to a direct interaction between the added solvent and the stationary phase.

4.4.2 Separation of Fullerenes on a FullereneSep® Column

Separations of fullerene mixtures were carried out on the novel stationary phase FullereneSep® to determine its separating ability and compare this with other commercially available columns. The different fractions exiting the column were characterised by on-line liquid chromatography mass spectrometry (this technique is described in detail in Section 3.10.3).

A full description of the HPLC system (system 2) used in this study is given in section 3.6. The column used consisted of a 150 × 4.6mm ID cartridge packed with a novel material, FullereneSep® (3μ), developed in collaboration with Capital HPLC Specialists, Bathgate, Scotland. The mobile phase used was *n*-hexane (Rathburn Chemicals Ltd) which was dried with anhydrous sodium sulphate, saturated with argon and filtered before use. Before use the column was equilibrated for one hour at a flow rate of 2 ml/min with *n*-hexane as the mobile phase. All separations were carried out at ambient temperature. Further details of the running conditions are given in the figure captions of the individual chromatograms. Figure 4.5 shows an HPLC trace for the crude toluene-soluble fullerene extract prior to preliminary column chromatography on neutral alumina. Based on the integrated intensities of the bands, C_{60} and C_{70} are present in this sample in the ratio of 100:15 (see figure caption for details) and are separated by a wide margin. Figure 4.6 shows an HPLC trace for a later fraction from the neutral alumina column, which is substantially enriched with the higher fullerenes C_{76}, C_{78} and $C_{82/84}$. Particularly gratifying is the excellent resolution achieved for separation of the higher fullerenes, especially C_{76} and C_{78}, under these non-optimised conditions.

Table 4.5 summarises the separation ability of FullereneSep® as measured in terms of the separation factor, or relative retention value (α), which can be expressed as the

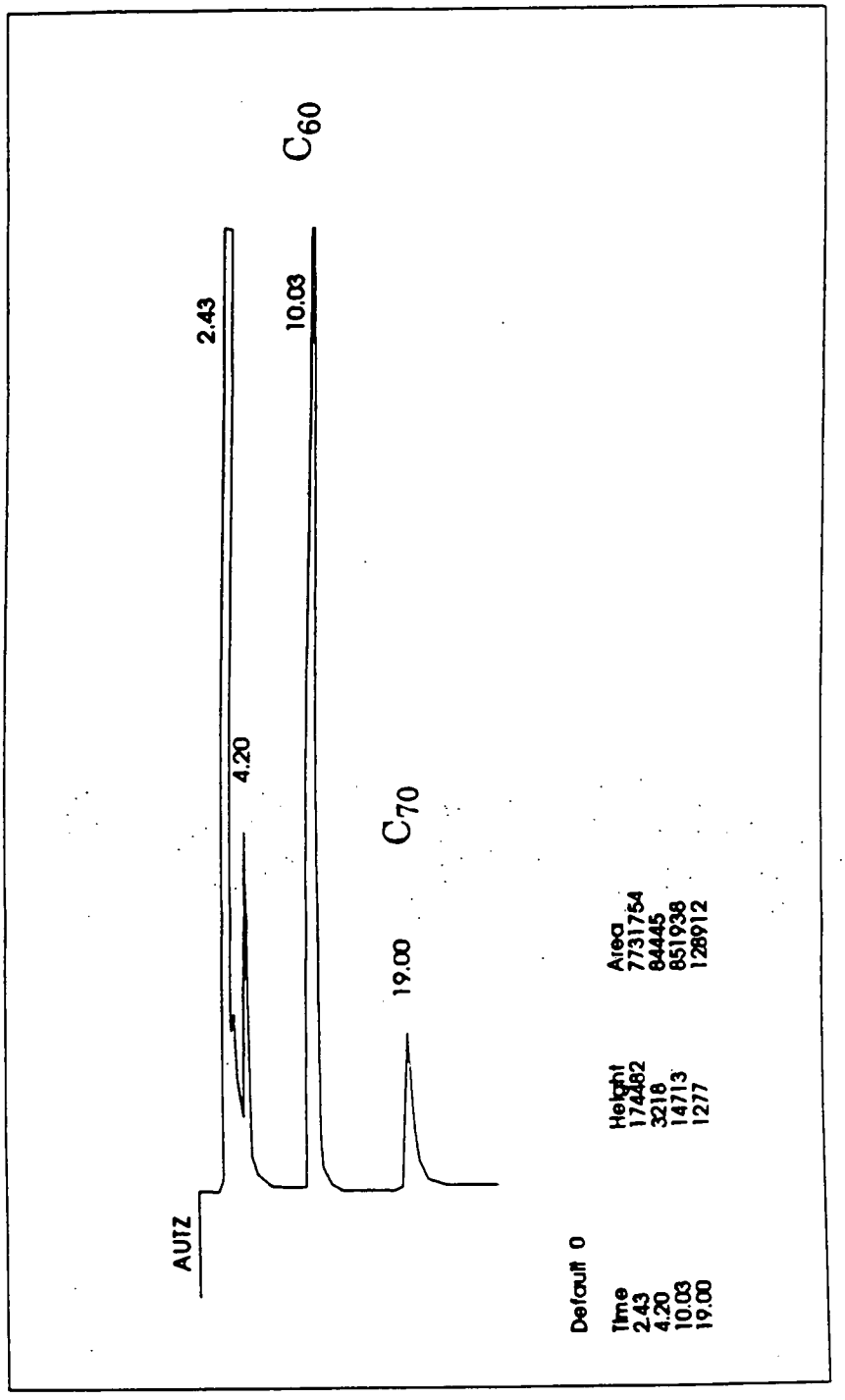

Figure 4.5: HPLC profile of C_{60}/C_{70} mixture on FullereneSep® column; particle size, 3 micron; column dimensions, 150mm × 4.6mm; eluant, 100% hexane; pressure, 800psi; flow rate 1.0 ml/min; UV detection at 254nm, 0.1AUFS.

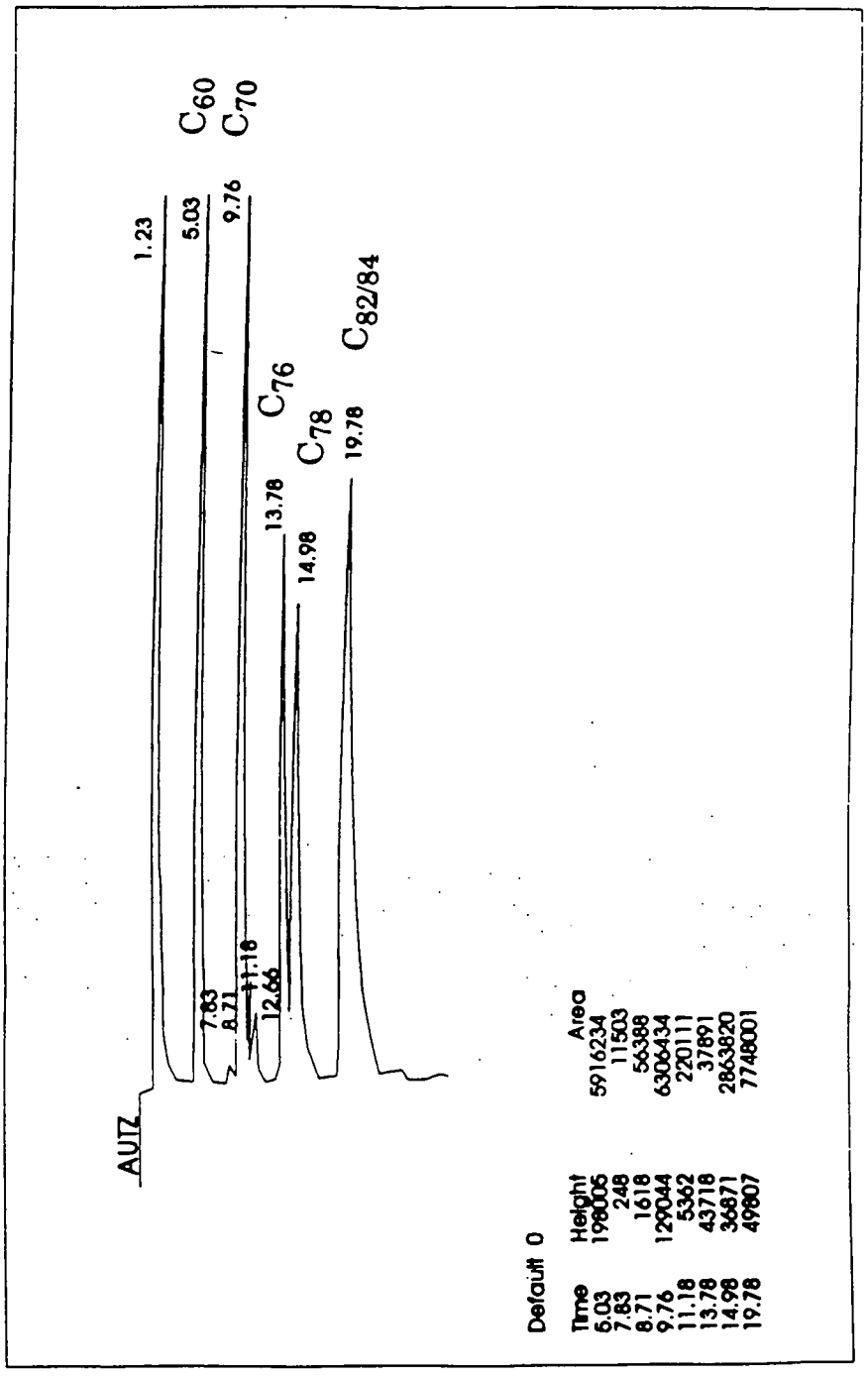

Figure 4.6: HPLC profile of $C_{60}/C_{70}/C_{76}/C_{78}/C_{82/84}$ mixture on FullereneSep® column; particle size, 3 micron;column dimensions, 150 × 4.6mm; eluant, 100% hexane; pressure 300psi; flow rate, 2.0 ml/min; UV detection at 254nm, 0.02 AUFS.

Table 4.5: Capacity factors k′ and separation factors (α) of fullerene fractions relative to C_{60} on FullereneSep®.

Chromatogram	**Peak**	**Flow rate ml/min**	**k′**	**α**
Figure 4.5	C_{60}	1	3.13	1
Figure 4.5	C_{70}	1	6.82	2.2
Figure 4.6	C_{60}	2	3.09	1
Figure 4.6	C_{70}	2	6.93	2.2
Figure 4.6	C_{76}	2	10.2	3.3
Figure 4.6	C_{78}	2	11.18	3.6
Figure 4.6	$C_{82/84}$	2	15.08	4.9

ratio of capacity factors k′ [167]. The pronounced separation of C_{60} and C_{70} (α = 2.2) compares very favourably with that reported for other stationary phases used in fullerene separations, including several that are commercially available [168], [169], although it is not as great as that reported for the tripodal π acidic column [168].

The peak profiles obtained with FullereneSep® are of high quality with little or no evidence of tailing. The relative performance of this column compared to those recently reported by Welch and Pirkle [169] is difficult to compare since no chromatograms are presented in their paper which was limited to C_{60}/C_{70} mixtures.

4.4.3 Characterisation of Fractions Using On-Line Liquid Chromatography Mass Spectrometry

Conclusive identification of the different fullerene fractions eluting from the FullereneSep® column, up to C_{78}, was obtained using on-line particle-beam mass spectrometry (see section 3.10.3).

Figures 4.7-4.11 show the electron-impact mass spectra of the fullerene components eluted from the column. In each case, the region of the chromatogram from which the mass spectrum was obtained is indicated on the accompanying total-ion chromatogram (TIC) profile. The mass spectrum corresponding to the C_{60} component, shown in Figure 4.7, contains the $[C_{60}]^+$ molecular ion at m/z 720, together with its characteristic fragment ions, $[C_{58}]^+$, $[C_{56}]^+$, $[C_{54}]^+$, etc. Intense peaks due to the doubly and triply charged C_{60} ions are also present at m/z 360 and 240, respectively, accompanied by the corresponding daughter ions, which are particularly intense for the doubly charged ion. The quadruply charged ion $[C_{60}]^{4+}$ can also be seen at m/z 180.

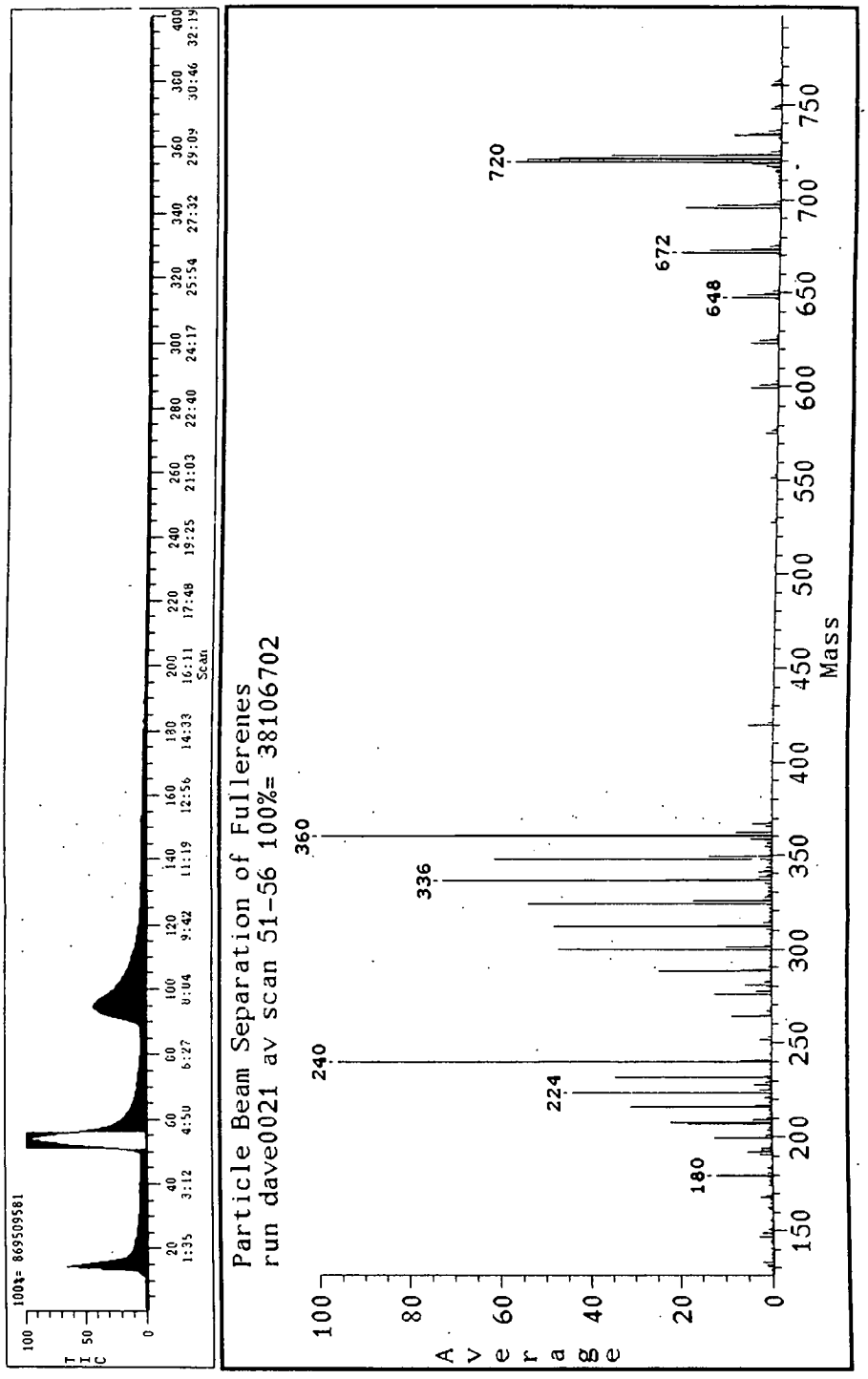

Figure 4.7: EI mass spectrum of C_{60}. The accompanying total ion chromatogram, see top trace, shows the time period over which the EI mass spectrum was accumulated.

The mass spectrum corresponding to the C_{70} component, shown in Figure 4.8, similarly exhibits peaks due to the singly-, doubly- and triply-charged C_{70} molecular ions and their corresponding fragments. A weak peak at m/z 210 corresponding to the quadruply charged ion $[C_{70}]^{4+}$ can also be seen in this spectrum. The signal at m/z 720 in the spectrum is due to daughter ions arising from fragmentation of C_{70} and is not due to the overlap of the C_{60} and C_{70} fractions. This was made clear by monitoring the intensity of the 720 and 840 mass peaks as a function of retention time. Figure 4.9 shows such an LC-MS ion chromatogram. It can be seen that the intensity of the 720 mass peak falls as C_{60} elutes from the column and then rises in parallel with the 840 mass peak as C_{70} elutes.

Figure 4.10 shows the mass spectrum for the next component, eluting after the C_{70} peak, corresponding to C_{76}; both singly- and doubly-charged ions can be seen at m/z 912 and 456, respectively. The somewhat lower signal intensity observed here is presumably due to the lower volatility of C_{76}. The final mass spectrum, shown in Figure 4.11, provides clear evidence of elution of C_{78} (*cf.*[170]); the singly- and doubly-charged C_{78} molecular ions can be seen at m/z 936 and 468, respectively. There is some overlap with the previous eluting peak, as can be seen from the peak tailing in the total ion chromatogram (TIC) at the top of the figure, which accounts for the presence of the peaks at m/z 912 and 456 corresponding to the singly- and doubly-charged ions of C_{76}.

Unfortunately, due to the increasingly low volatility of successively higher fullerenes it was not possible to obtain mass spectral data with sufficiently high signal-to-noise ratio for the later eluting peak which can be clearly seen in Figure 4.6. However, by comparison with results published by Kikuchi *et al* [171] the next peak eluted is assigned as a mixture of $C_{82/84}$.

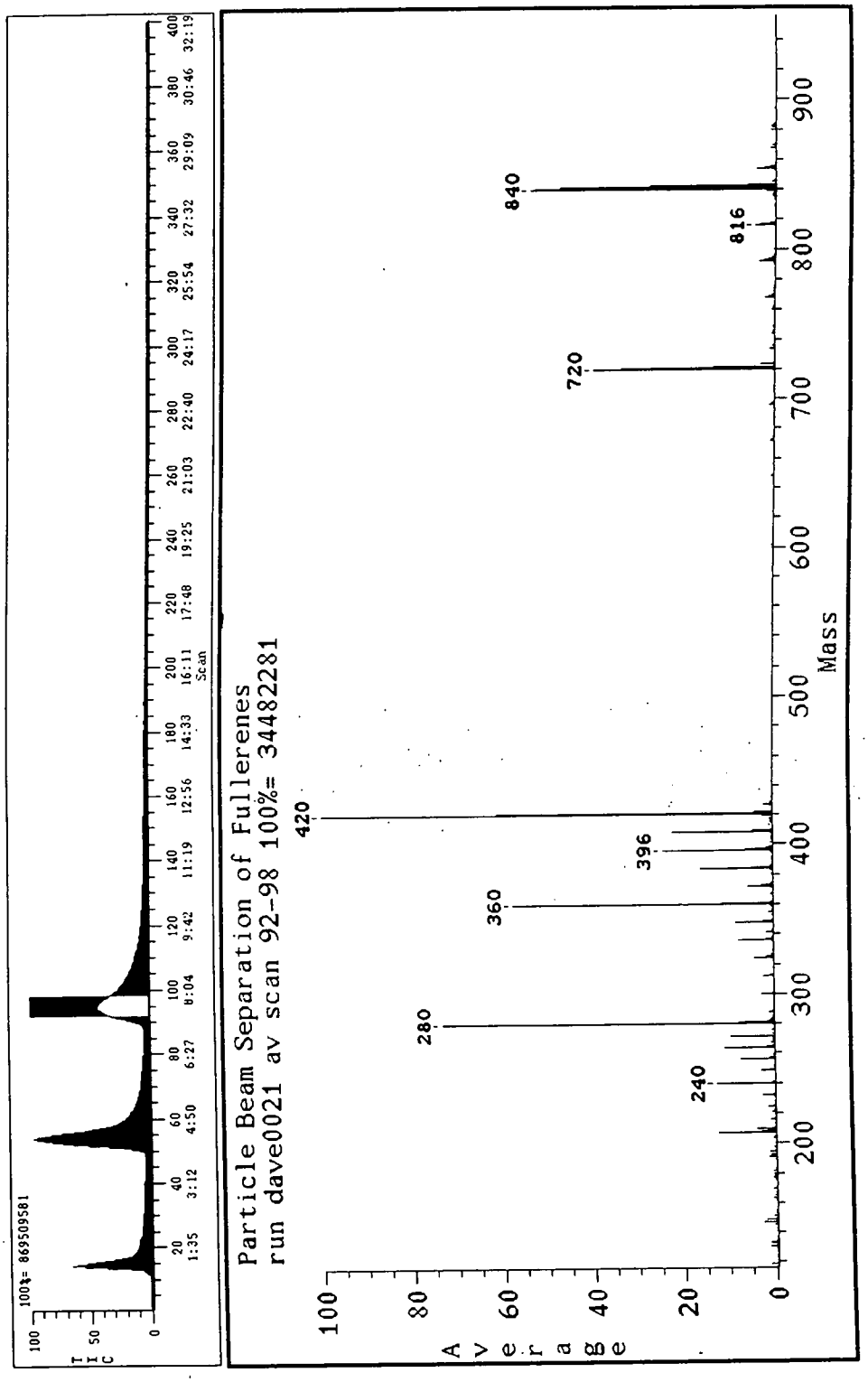

Figure 4.8: EI mass spectrum of C_{70}.

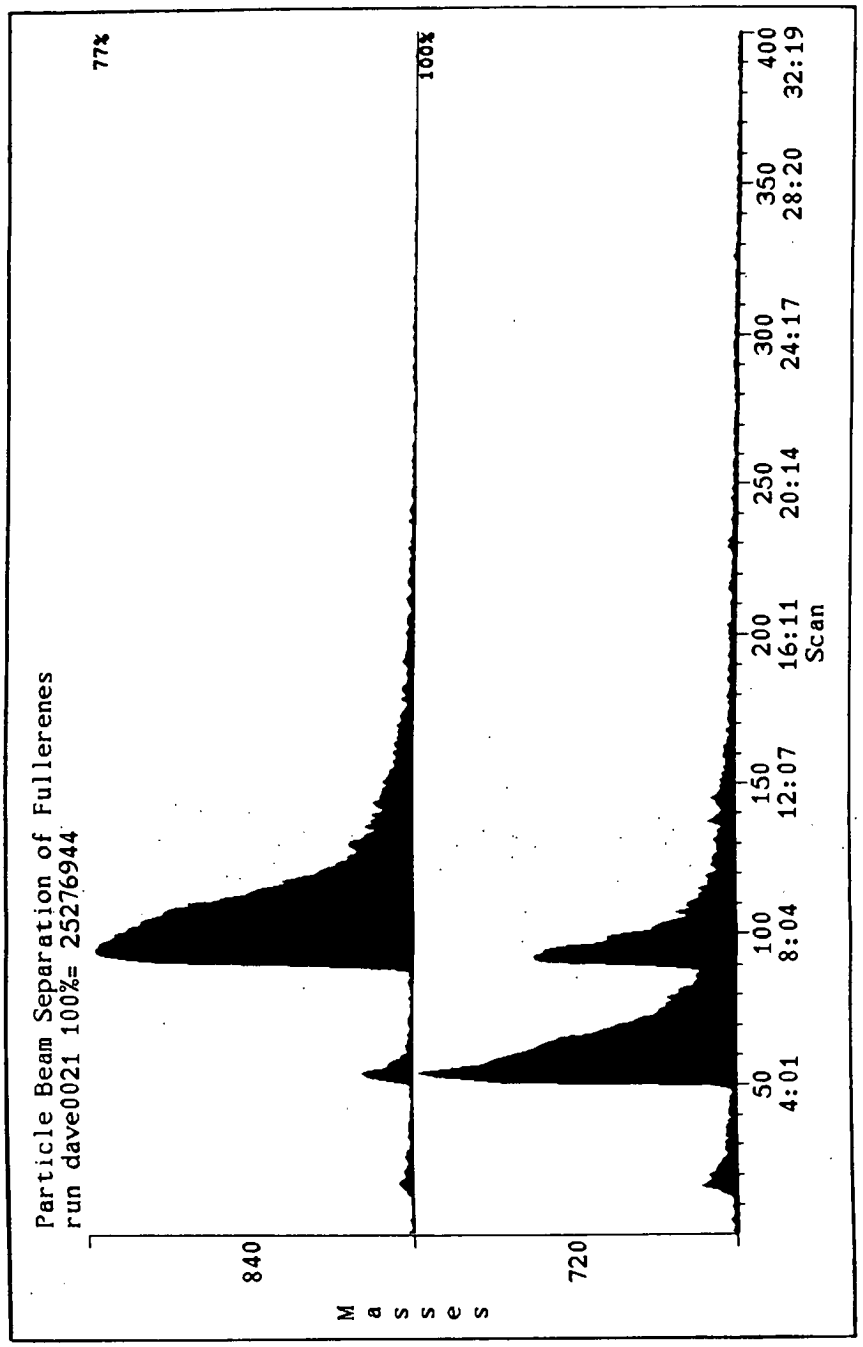

Figure 4.9: LC-MS ion chromatogram recorded at 841 and 720 amu. The trace shows clearly that the prominent peak at 720 amu in the EI mass spectrum of C_{70} (Figure 3.23) is due to fragmentation of C_{70}, and not due to overlap of the C_{60} and C_{70} fractions.

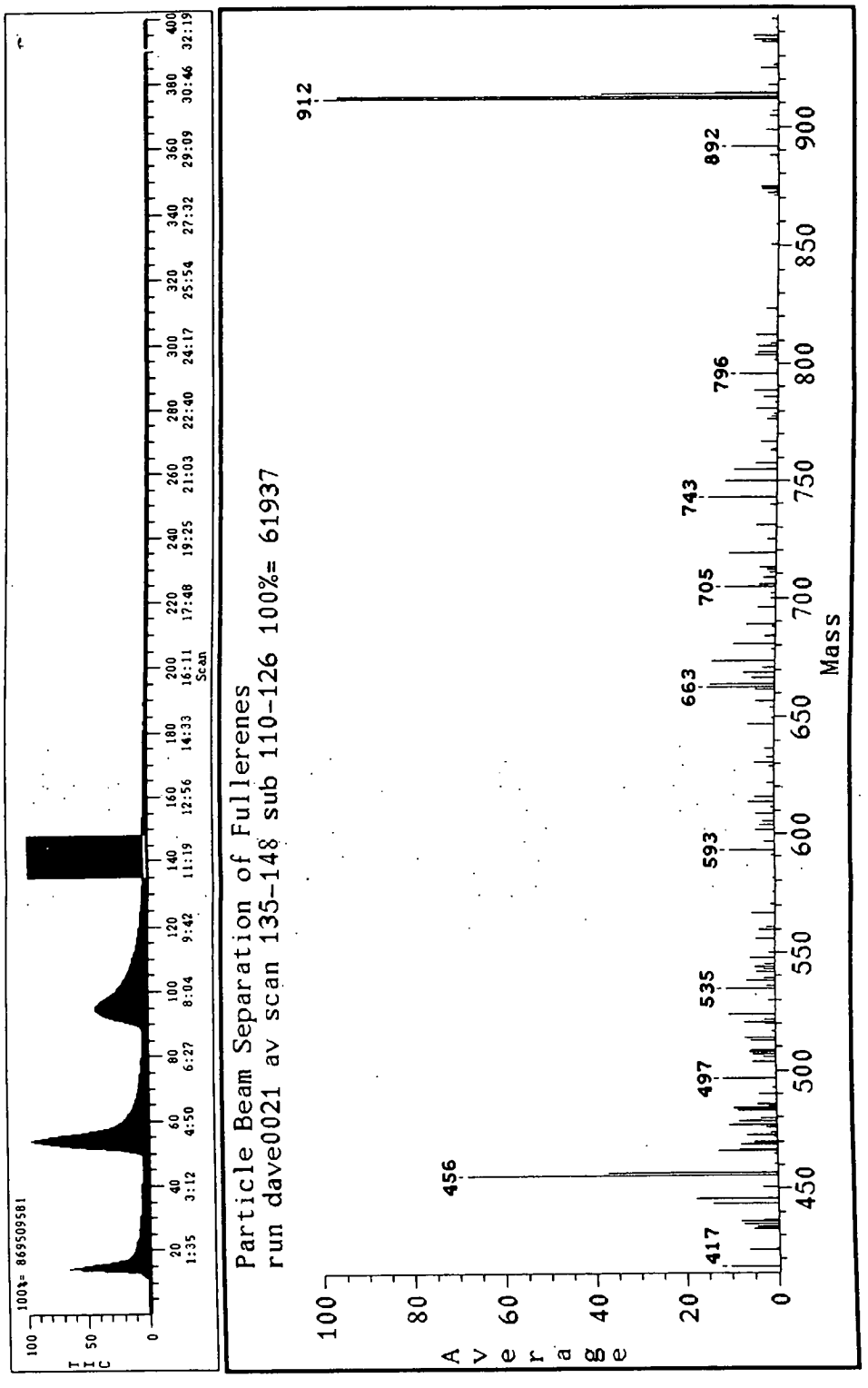

Figure 4.10: EI mass spectrum of C_{76}.

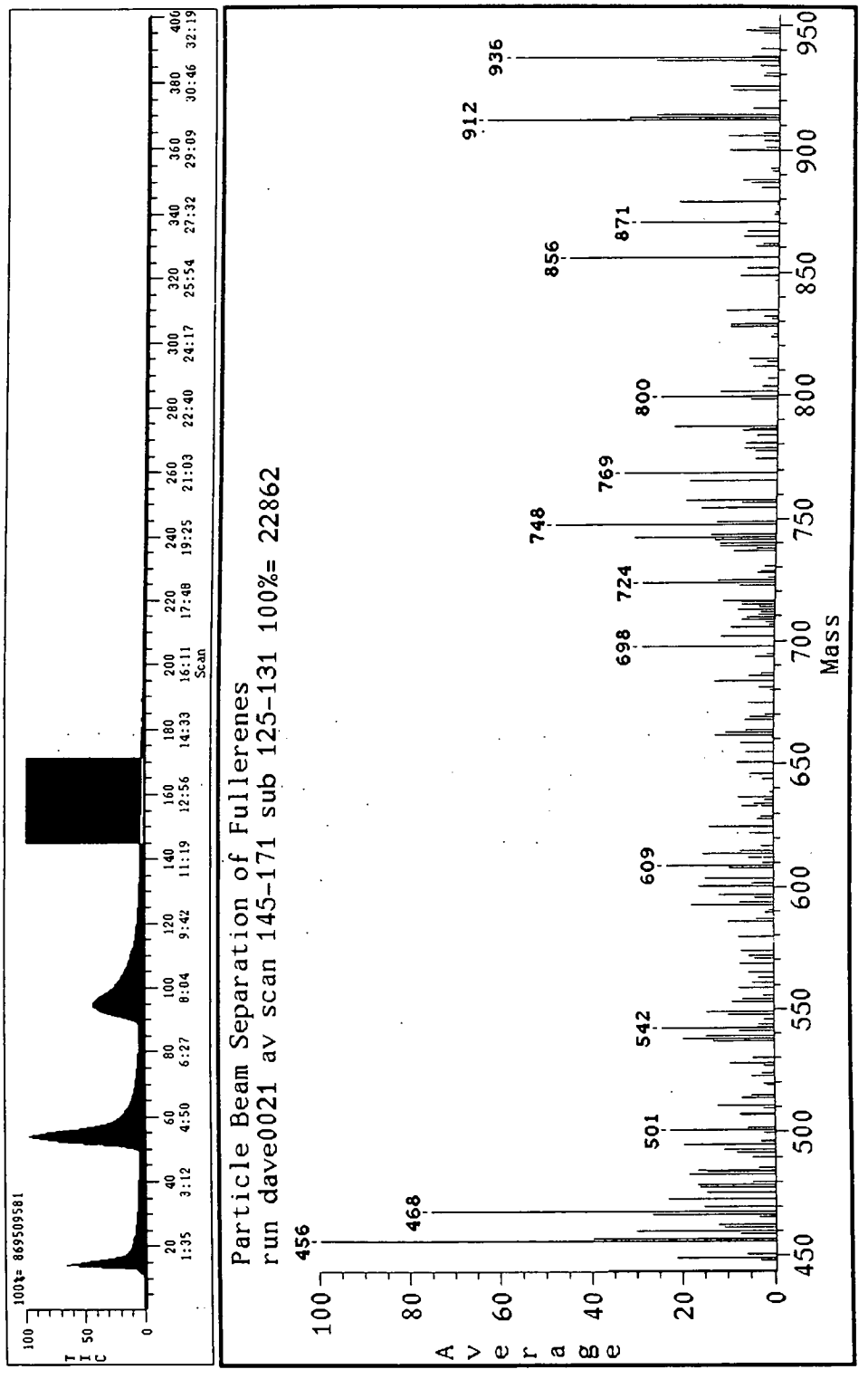

Figure 4.11: EI mass spectrum of C_{78}.

4.4.4 Fullerene Detection at Different Wavelengths

For most of the chromatographic studies carried out in this work species eluting the column were detected using optical absorbance measurements. The mobile phase passes from the column into a flow cell where it is illuminated with light of a specified wavelength and the intensity of absorption measured. The volume of the flow cell is kept to a minimum to reduce the effect of extra column band broadening. The absorbance of molecules in the UV/vis varies considerably. Thus, it is important to choose a wavelength for detection at which all the molecules being separated will absorb to a similar degree.

The Spectra Physiks SpectraSYSTEM™ HPLC (system 3 see section 3.7 for details) equipped with a UV2000 detector was used in this study. This system is equipped with an analytical flow cell of volume 2.4µl. The UV2000 detector has spectral scanning capability enabling peak separation to be examined at multiple wavelengths. Figure 4.12 shows the chromatograms obtained for a sample of fullerenes extracted by ultra-sound sonication with CS_2 and recorded at increments of 5nm in the wavelength range 250nm-380nm (C_{60} absorption is known to decrease at wavelengths below 250nm).

The peaks at R.T. 7.09 min and 11.84 min represent C_{60} and C_{70}, respectively while those at R.T. 15.51min, 17.51min and 22.84 min are due to higher fullerenes, most likely C_{76}, C_{78} and C_{84}. The decrease in absorption of C_{60} as the wavelength of the detector is increased is shown by the decrease in the size of the peak particularly between 250nm-280. There is a corresponding but less marked decrease in the absorption of C_{70} up to 380nm. The higher fullerene peaks show maximum absorption between 250nm-260nm. The absorption decreases dramatically as the wavelength increases so that although the peak at 15.51min may just be seen at 380nm those for the two later eluting peaks have disappeared at a wavelength of 300nm.

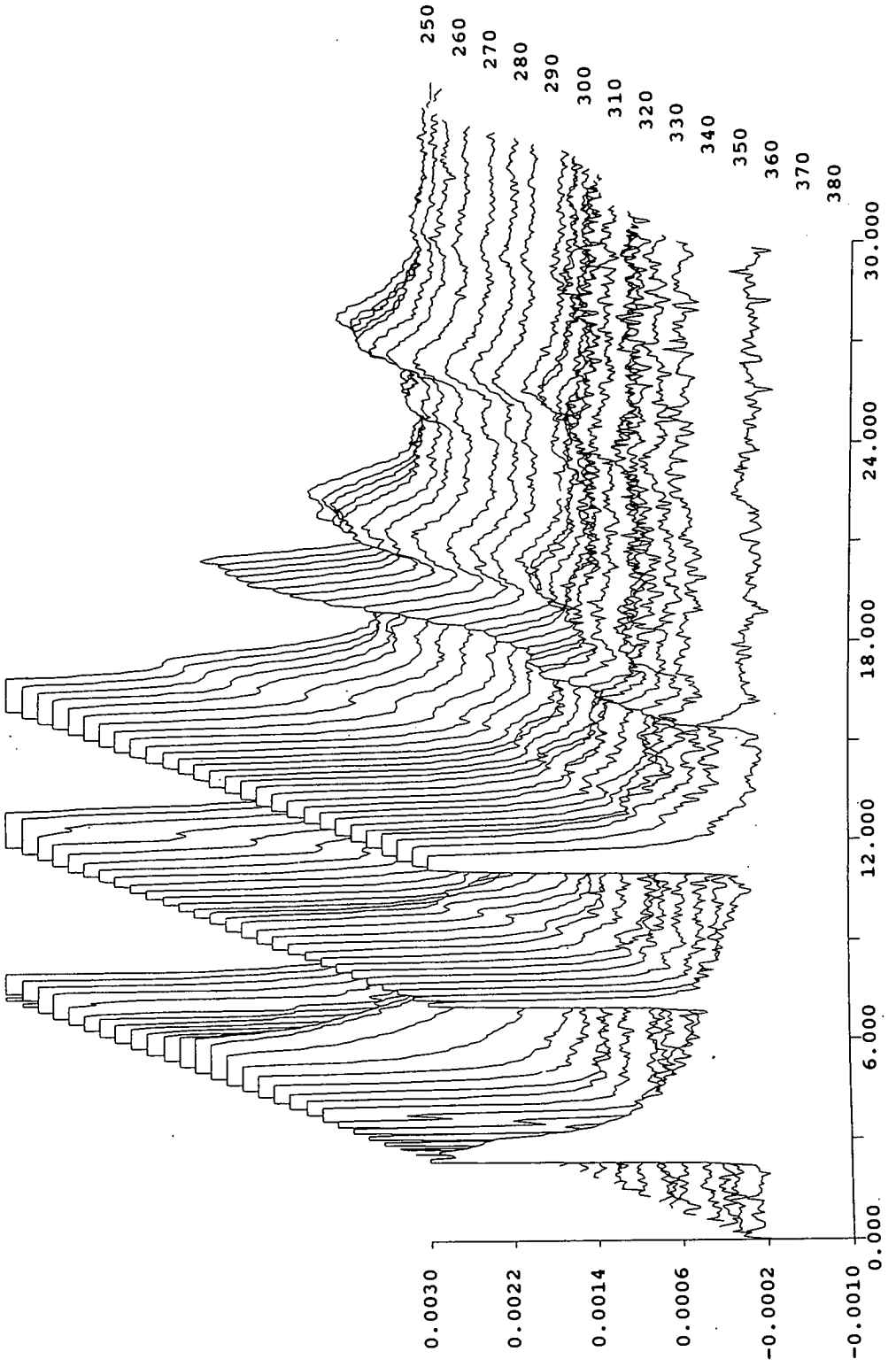

Figure 4.12: Separation of fullerenes, detection wavelengths are indicated on the trace.

From examination of the spectra presented in Figure 4.12 it can be seen that wavelengths in the range 250-260nm were optimum for detection of a range of fullerenes.

4.4.5 Effect of Variation in Mobile Phase Composition Upon Separation Using FullereneSep®

Initial investigations of FullereneSep® demonstrated the utiliy of this stationary phase for separating fullerene mixtures. Further experiments were undertaken to try and optimise separation by variation of the mobile phase.

The effect that adding ether to the hexane mobile phase had on retention times and separation was investigated. Samples of C_{60} and C_{70} were separated on a FullereneSep® column (250mm × 4.6mm, Flow rate 2ml/min, detection wavelength 254nm) using a mobile phase of hexane containing different percentages of ether, ranging from 0 to 10%. The results, shown in Figure 4.13 and in Table 4.6, show there is a decrease in the retention time as the percentage of ether in the mobile phase increases. Figure 4.13a) shows the peak for C_{60} eluting at 6.77 min with a mobile phase of 100% hexane. The retention time has dropped to 2.49 min for a mobile phase of 90% hexane 10% ether as shown in Figure 4.13d). From Table 4.6 it can be seen that the greatest separation occurs using 100% hexane mobile phase ($\alpha = 2.11$), but the retention times are also the greatest, R.T. C_{60} 6.77 min, C_{70} 12.51 min. Addition of 2% ether to the mobile phase causes a significant decrease in the retention times without much effect on the selectivity (R.T. C_{60} 5.23 min, C_{70} 9.52 min, $\alpha = 2.07$).

The results described here are similar to the separations on the ChiralCap® column when chloroform was added to the mobile phase and are again due to competition between the added polar constituent of the mobile phase and the fullerenes to coat the

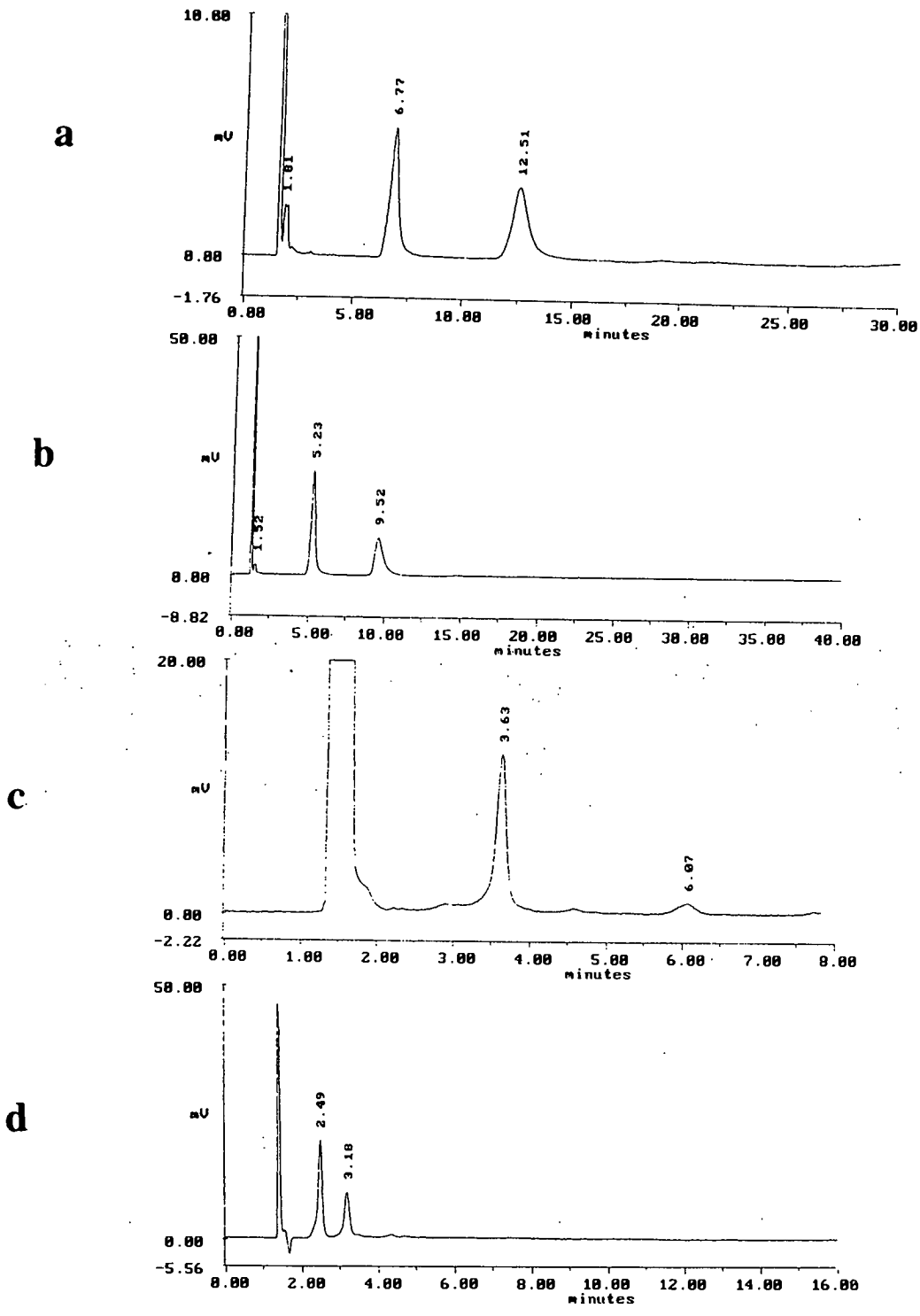

Figure 4.13: Separation of fullerene mixture on FullereneSep® column (250mm × 4.6mm, Flow rate 2ml/min, detection wavelength 254nm) with mobile phases containing different percentages of ether **a) 0%, b) 2%, c) 5%, d) 10%.**

Table 4.6: The effect on retention time (R.T.) and separation factor (α) of varying the percentage of ether in the hexane mobile phase.

% ether	R.T. for C_{60}	R.T. for C_{70}	α
0	6.77	12.51	2.11
2	5.23	9.52	2.07
5	3.63	6.07	1.67
10	2.49	3.18	1.28

Table 4.7: The effect on retention time (R.T.) and separation factor (α) of varying the column length.

Column length (cm)	R.T. for Tol (min)	R.T. for C_{60} (min)	R.T. for C_{70} (min)	α
15	0.75	2.58	4.37	1.97
25	1.03	3.67	6.43	2.05
50	2.43	8.52	14.83	2.04
65	4.02	12.04	20.06	2.00

surface of the stationary phase. Thus as more ether is added there is less stationary phase available for the fullerenes and therefore retention is decreased. The effect is again seen when adding acteonitrile to the hexane mobile phase.

4.4.6 Effect of Column Length Upon Separation

In order to further optimise the separation of fullerenes using the FullereneSep® stationary phase experiments were carried out to examine the effect of varying the column length on both retention time and selectivity. These studies involved the comparison of 15cm and 25cm columns. Columns were then joined in series to make overall lengths of 50cm and 65cm. The mobile phase used was 2% ether in hexane at a flow rate of 2ml/min.

The results are shown in Table 4.7. There is an initial slight improvement in selectivity upon going from a 15cm to a 25cm column (α=1.97 for a 15cm column, 2.05 for 25 cm column). The coupling of columns in series did not increase the selectivity as might have been expected, two 25cm columns in series gave separation α=2.04. This is presumably because the selectivity of the overall column is dictated by the selectivity of an individual column. Thus the joining in series of two 25cm columns and one 15 cm column (α=2.00) shows only marginally greater separating ability than the 15cm column (α=1.97). This minor increase in selectivity is not justified by the much greater retention times that result from the use of the longer columns.

4.4.7 Preparative HPLC on FullereneSep®

Preliminary attempts at preparative scale HPLC using a FullereneSep® stationary phase were carried out on a 2.5cm × 50cm column. Due to financial constraints the column was fabricated and packed in-house at Edinburgh University. The chromatograms of standard C_{60} samples were recorded, however they showed extremely broad peaks even with low sample loading. This effect was caused by poor packing of the column. Unfortunately the cost of preparing sufficient material and

having it commercially packed was prohibitive although the potential for the large scale separation of fullerenes using this stationary phase is evident.

4.5 Determination of Thermodynamic Parameters of Adsorption

In evaluating new stationary phases chromatographic separations obtained as a function of temperature are sometimes measured to determine the thermodynamic parameters of adsorption. Pirkle *et al* [172] have reported an interesting effect of temperature on the chromatographic behaviour of Buckminsterfullerene. Usually in chromatography an increase in column temperature corresponds to a decrease in the relative adsorption of any compounds on the column; thus as fewer compounds are adsorbed the retention is lowered. Pirkle *et al* [172] found for C_{60} and C_{70} that the reverse is true, there is an increase in C_{60} and C_{70} retention times at higher temperatures using a π acidic stationary phase. With the possibility in mind of exploiting this effect for improved separations, a series of separations of fullerene mixtures on a FullereneSep® column were carried out as a function of temperature. The Merck-Hitachi HPLC system (system 4) was used for these experiments as it was equipped with a thermostatted column oven capable of maintaining any temperature in the range ambient-100^{0}C. The temperature range in these separations was limited by the boiling point of ether. At temperatures in excess of 338K separations became impossible due to the ether boiling on the column. This was evidenced by extreme variations in the pressure at this temperature. Five separate runs were carried out, starting at 298K and incrementally increasing the temperature of the column oven by 10K for each successive run.

Figure 4.14 shows the chromatograms obtained at three temperatures (298K, 318K, 338K) for the injection of a sample of $C_{60/70}$ on a 25 cm FullereneSep® column

(mobile phase 4% ether in hexane, flow rate 2ml/min, detection wavelength 254nm). As can be clearly seen the retention times increase at higher temperatures.

The data for the complete range of temperature measurements are given in Table 4.8, comprising the retention times of the components, their capacity factors (k') and the separation factors (α). As can be seen, the retention time for C_{60} increases from 4.11min at 298K to 4.87 min at 338K. Similarly C_{70} is retained over a minute longer at 338K (8.13 min) than at 298K (7.04 min). There is also a slight increase in the separation factor (α) at higher temperature; 1.92 at 298K increasing to 1.96 at 338K. These results for separations on FullereneSep® confirm the unusual behaviour of C_{60} and C_{70} observed by Pirkle *et al* [172].

To try to understand this unusual behaviour it is necessary to consider the thermodynamic processes that occur on adsorption.

The fraction of solute in the mobile and stationary phase can be related to the retention on the column by equation 4.1. The capacity factor or phase capacity ratio k′, which can be determined from a chromatogram (equation 3.2), measures the degree of retention of a solute by the adsorbent in the column and can be given by the expression 4.1:

$$k' = q_s / q_m \qquad 4.1$$

where q_m is the quantity of solute in the mobile phase q_s is the quantity of solute in the stationary phase.

The variation of k′ with temperature then depends upon the heat of transfer of the solute from the mobile to the stationary phase and follows the van't Hoff equation:

$$d\ln k'/ dT = \Delta H_{(m \rightarrow s)} / RT^2 \qquad 4.2$$

where $\Delta H_{(m \rightarrow s)}$ is the enthalpy of transfer of the solute from the mobile to the stationary phase, R is the gas constant and T is the temperature.

Normally in chromatography a loss in entropy accompanies exothermic adsorption (on adsorption both the enthalpy and entropy values are negative). Thus, an increase in column temperature lessons retention.

The unusual behaviour of the fullerenes could then be due to an unusual enthalpy change in moving from the mobile to the stationary phase. The change in enthalpy on adsorption can be easily calculated using the van't Hoff equation (4.2) and by plotting ln k′ against 1/RT. Table 4.9 shows the values of ln k′ for C_{60} and C_{70} which are plotted against 1/RT in Figures 4.15 and 4.16.

Integration of Equation 4.2 gives:

$$\ln k' = -\Delta H / RT + c \qquad 4.3$$

Thus plotting ln k′ against 1/RT will yield a straight line with gradient equal to -ΔH, the change in enthalpy on adsorption.

From Figure 4.14 and from the results shown in Table 4.8, it can be seen that both C_{60} and C_{70} are retained for longer periods as the temperature is increased. From the plots of ln k′ against 1/RT shown in Figures 4.15 and 4.16, the change in enthalpy on adsorption, for both C_{60} and C_{70} is positive (4.7 kJ mol^{-1} and 5.2 kJ mol^{-1}). Thus, the adsorption is an endothermic process, *i.e.* retention increases as temperature is raised. This agrees with the findings of Pirkle *et al* [172]. This behaviour indicates that some process detrimental to analyte adsorption is being reversed as the temperature is being raised.

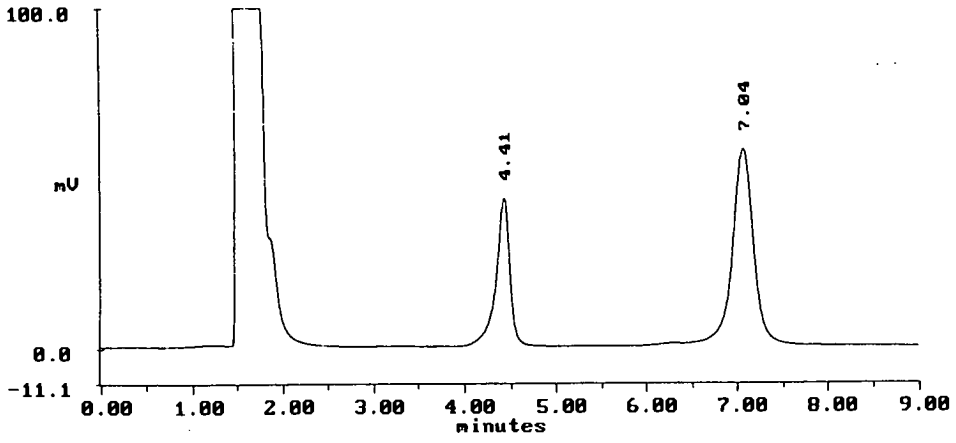

a

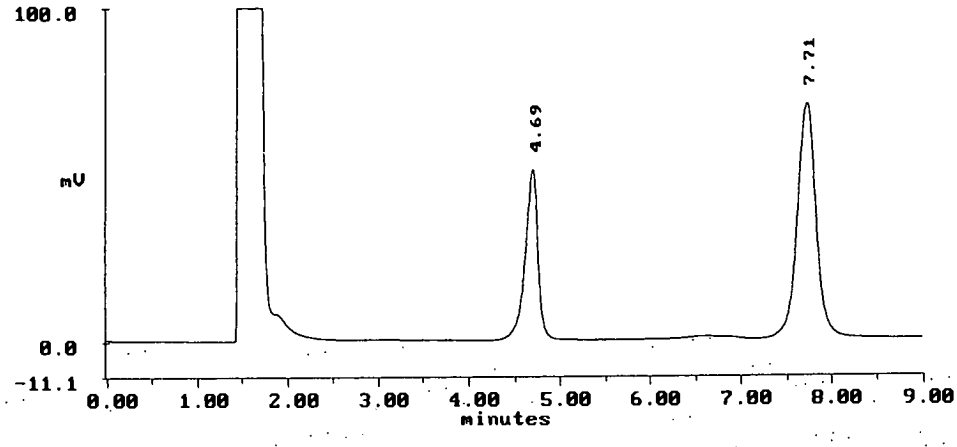

b

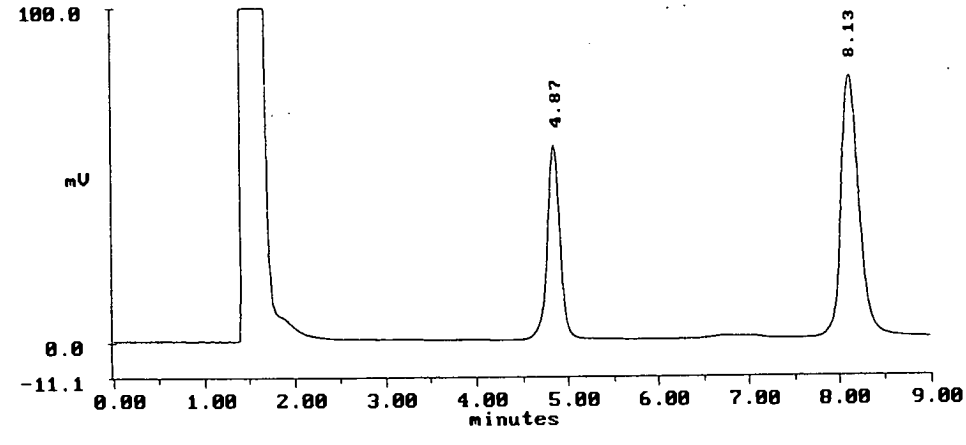

c

Figure 4.14: Chromatogram of C_{60}/C_{70} mixtures at **a)** 298K, **b)**318K and **c)**338K on a 25cm FullereneSep® column (mobile phase 4% ether in hexane, flow rate 2ml/min, detection at 254nm).

Table 4.8: The effect of variation in column temperature on retention time (R.T.) and separation factor (α).

Temperature (K)	R.T. for C_{60} (mins)	R.T. for C_{70} (mins)	k′ C_{60}	k′ C_{70}	α
298	4.41	7.04	1.83	3.51	1.92
308	4.58	7.42	1.95	3.79	1.94
318	4.69	7.71	2.05	4.04	1.95
328	4.80	7.97	2.19	4.29	1.96
338	4.87	8.13	2.27	4.46	1.96

Table 4.9: Values of ln k′ for C_{60} and C_{70} at different temperatures.

Temperature (K)	ln k′ C_{60}	ln k′ C_{70}	1/RT ($\times 10^{-4}$)
298	0.604	1.256	4.036
308	0.670	1.332	3.924
318	0.713	1.396	3.801
328	0.784	1.456	3.684
338	0.820	1.495	3.581

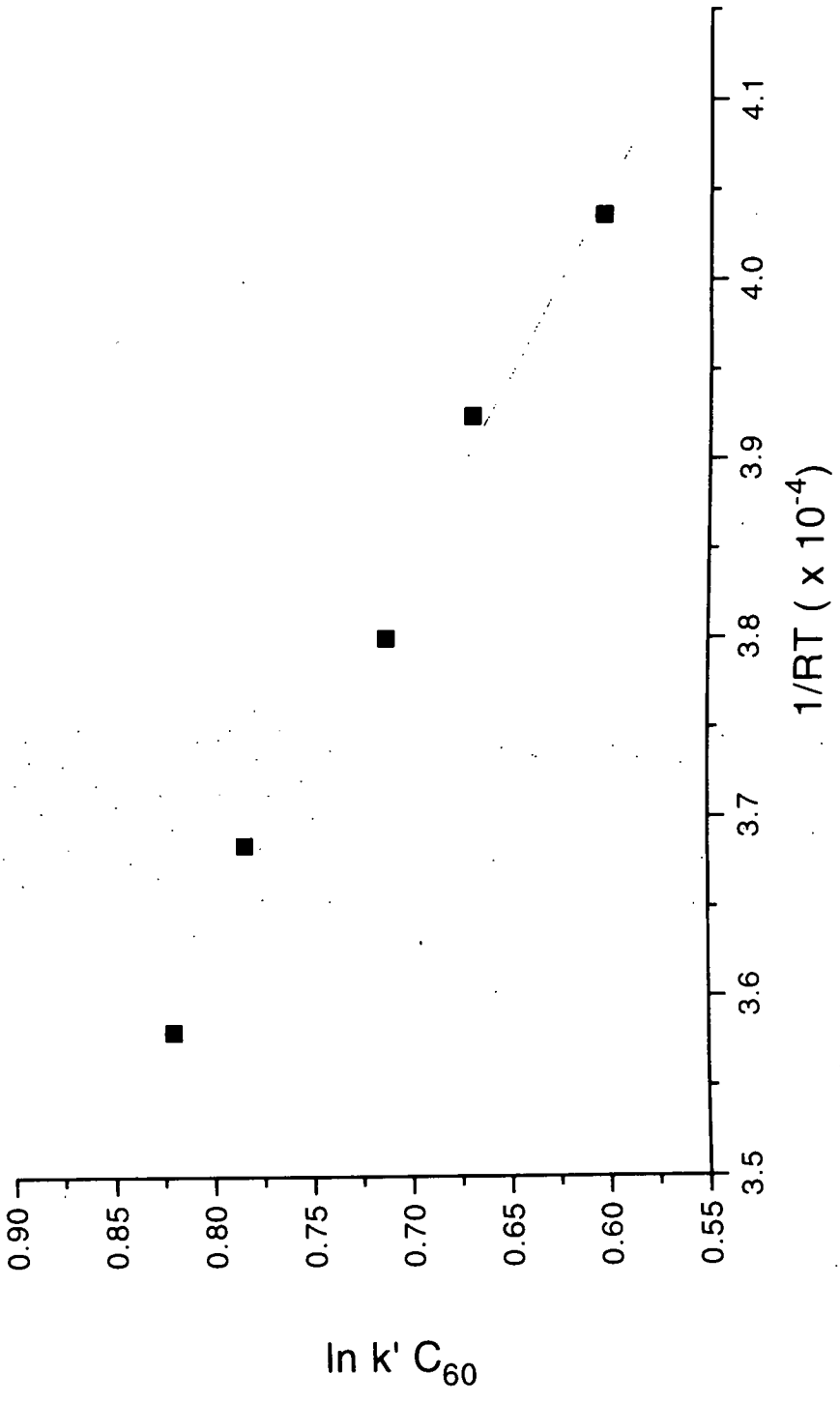

Figure 4.15: Plot of ln k′ (C_{60}) against 1/RT.

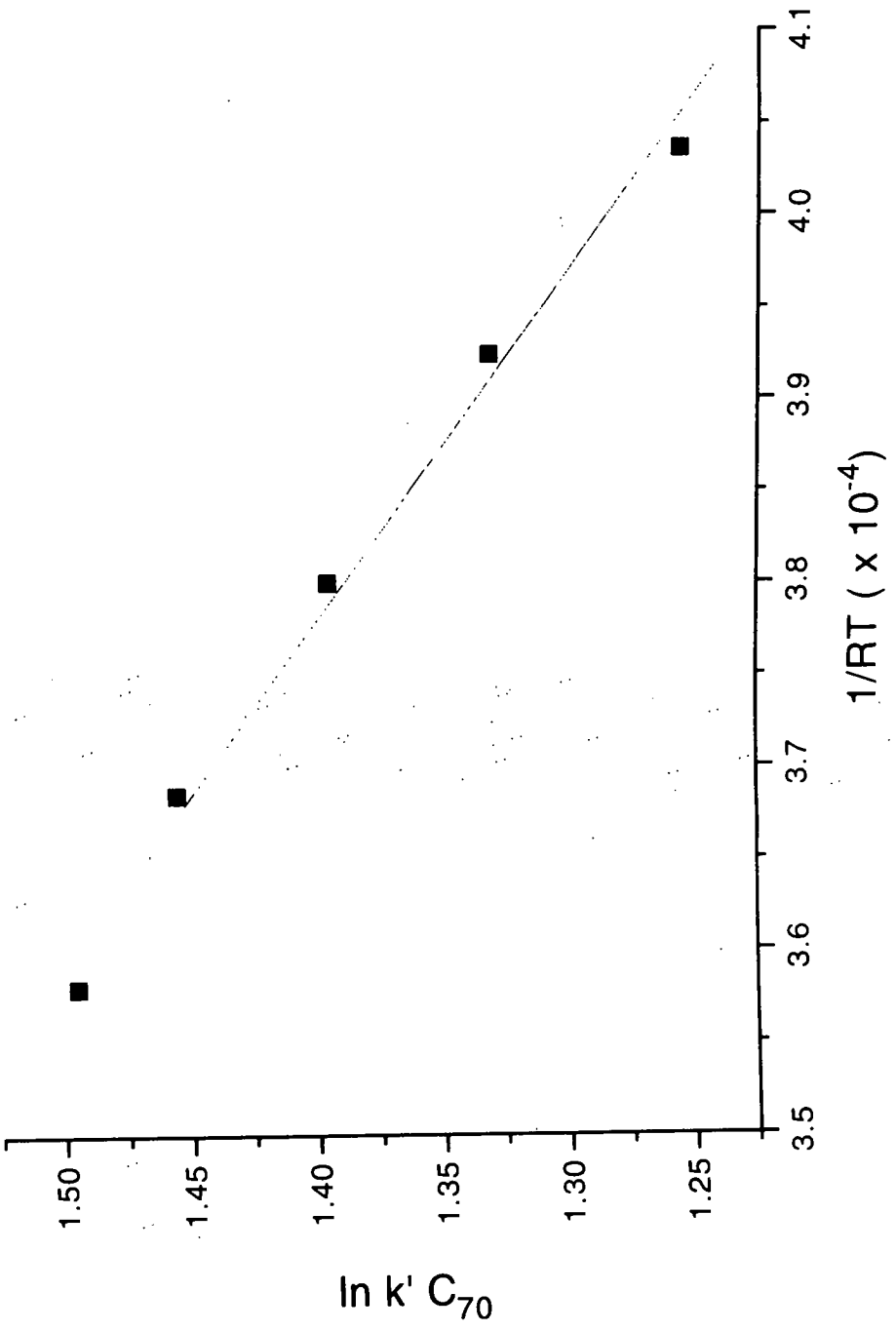

Figure 4.16: Plot of ln k′ (C_{70}) against 1/RT.

A possible reason for the behaviour is the decrease in solubility of C_{60} with increased temperature, *i.e.* ΔH_{sol}, the enthalpy of solvation increases (becoming less negative) as the temperature is raised. This means the affinity of C_{60} for the mobile phase decreases. Although the effect of increased temperature on the enthalpy of adsorption of the solute onto the stationary phase is unknown, the effect of the decreased affinity of the solute for the mobile phase would lead to greater separation, which is governed by the relative affinity of the solute for the mobile and stationary phases. In addition, the high pressure of the system elevates the boiling points of the solvents allowing their use at a higher temperature range.

4.6 Investigation of the Relationship Between Capacity Factors and Molecular Weight for Fullerenes.

In any homologous family of straight-chain carbon molecules there is a relationship between the number of carbon atoms in the species and log k′. A plot of log k′ against the number of carbon atoms for each species in the series will give a straight line. By using this relationship it is possible to predict the number of carbons, and consequently molecular weight, that a species will have from its retention time. In this study the retention times of a series of fullerenes (characterised by on-line LCMS or LDI mass spectrometry) were used to determine whether there was a corresponding relationship for the fullerenes and moreover if this relationship could be used to characterise unknown fullerene species from chromatographic data.

As described previously (see Section 3.4) the capacity factors are a measure of the degree of retention of a solute by a column. They can be calculated easily provided that the retention time of the sample and that of an unretained solute are known (equation 3.2). In order to investigate the relationship between the number of carbons

(molecular weight) of a series of fullerenes and its retention time, it was necessary to obtain chromatograms in which each peak had been characterised. This was achieved initially by using on-line particle beam LCMS (section 3.10.3, see Figures 4.5 and 4.6). On the basis of these results attempts were made to predict the molecular weight of uncharacterised peaks in the chromatograms of other samples which are rich in higher fullerenes.

Retention time data for a series of fullerenes (see Figure 4.6) which were characterised by on-line particle beam HPLC-MS was used to calculate the capacity factors for the different species. The increasingly low volatility of higher fullerenes meant it was not possible to obtain a sufficiently high signal-to-noise ratio to characterise the peak eluting at 19.78 min. in Figure 4.6. However, by comparison with mass spectral data obtained on other instruments of samples prepared in the same way which routinely show a signal for C_{84} and not for C_{82}, this peak was assigned as C_{84}. The capacity factors for the different peaks were calculated. The results are shown in Table 4.10. A plot of log k′ against molecular weight for C_{60}, C_{70}, C_{76}, C_{78} and C_{84} was constructed, which is shown in Figure 4.17.

The plot confirms there is a linear relationship (correlation coefficient 0.993) between log k′ and molecular weight for the fullerenes, similar to that for straight chain hydrocarbons. Initial examination of the plot suggested the possibility of a quadratic relationship between log k' and molecular weight.

To investigate this further the chromatogram of another fullerene mixture obtained on a FullereneSep® column (4.6mm × 150mm, mobile phase 100% hexane, 2ml/min, detection at 254nm) shown in Figure 4.18 was analysed. Mass spectral analysis of this sample was carried out on the Kratos Kompact III instrument, Figure 4.19 shows the resulting negative ion mass spectrum (50 shot average) showing peaks at m/z 720 (C_{60}), 840 (C_{70}), 912 (C_{76}), 936(C_{78}) and 1008 (C_{84}). On the basis of this mass spectrum the peaks in the chromatogram were assigned as C_{60} (R.T. 4.61

Table 4.10: Molecular weights and values of log k′ for the series of fullerenes shown in Figure 4.17.

Fullerene	Molecular Wt	log k′
C_{60}	720	0.489
C_{70}	840	0.841
C_{76}	912	1.009
C_{78}	936	1.048
C_{84}	1008	1.178

Table 4.11: Molecular weights and values of log k′ for the series of fullerenes shown in Figure 4.20.

Fullerene	Molecular Wt	log k′
C_{60}	720	0.404
C_{70}	840	0.736
C_{76}	912	0.921
C_{78}	936	0.969
C_{84}	1008	1.115

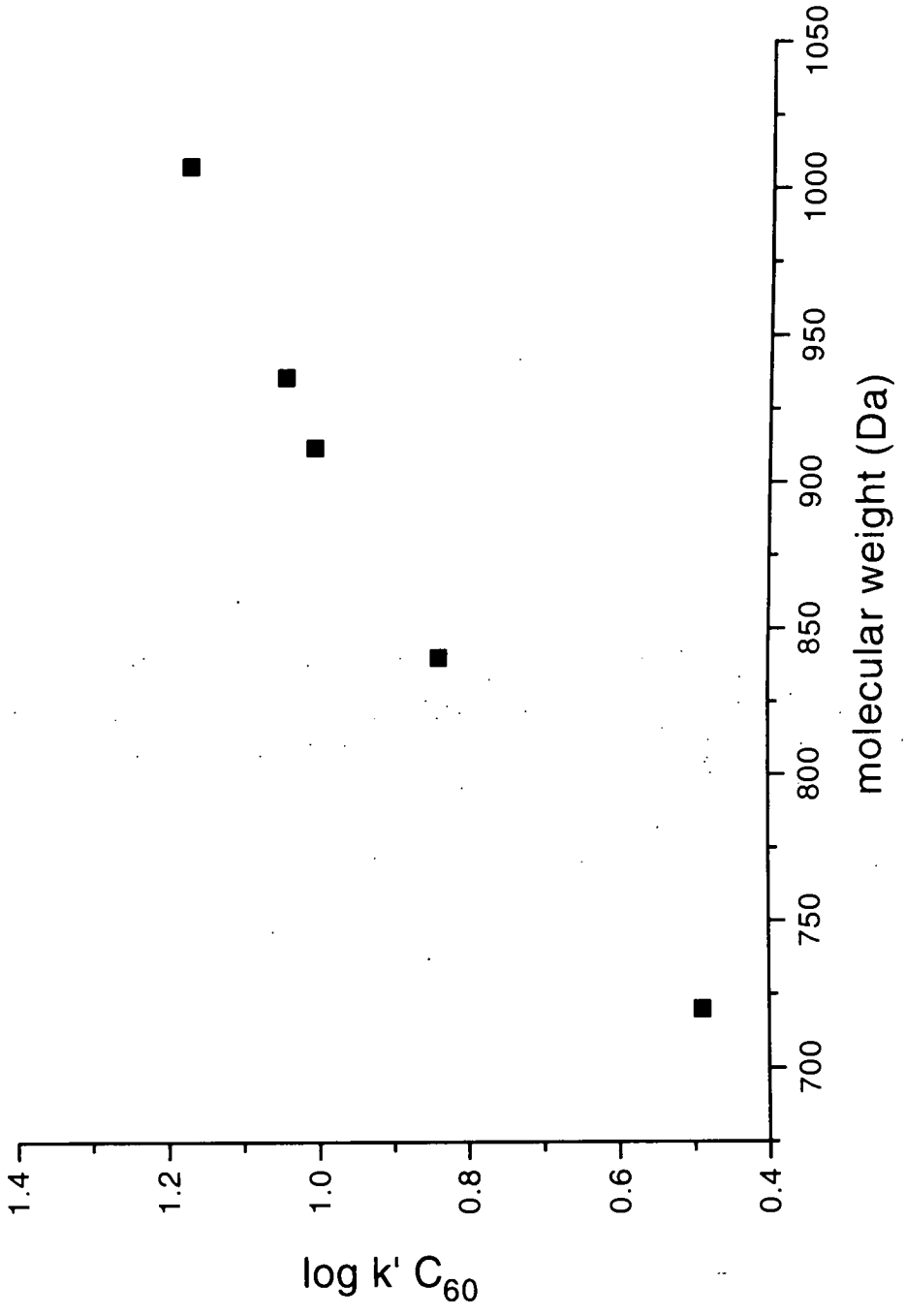

Figure 4.17: Plot of log k′ against molecular weight for fullerene series. k′ values calculated from retention time data in Figure 4.6.

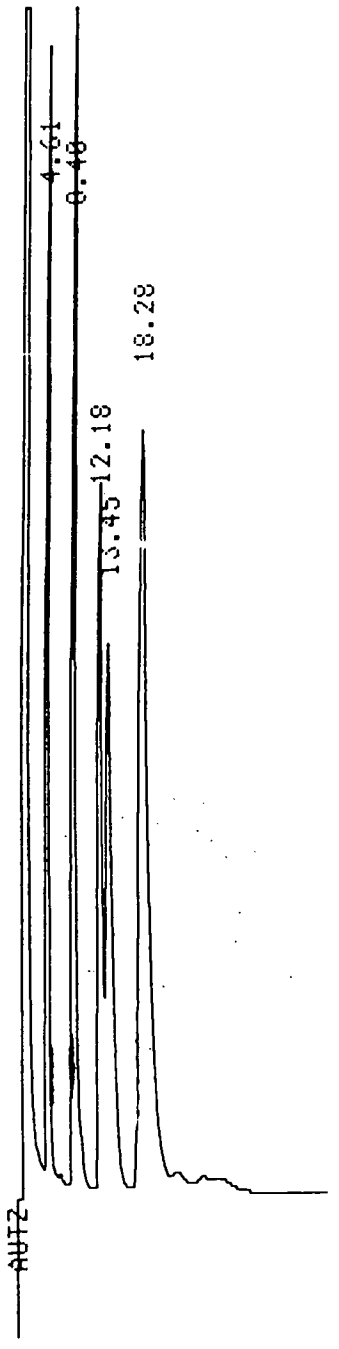

Figure 4.18: Chromatographic trace of a series of fullerenes separated on 4.6mm × 150mm FullereneSep® column 100% Hexane, Flow rate 2ml/min detected at 254 nm.

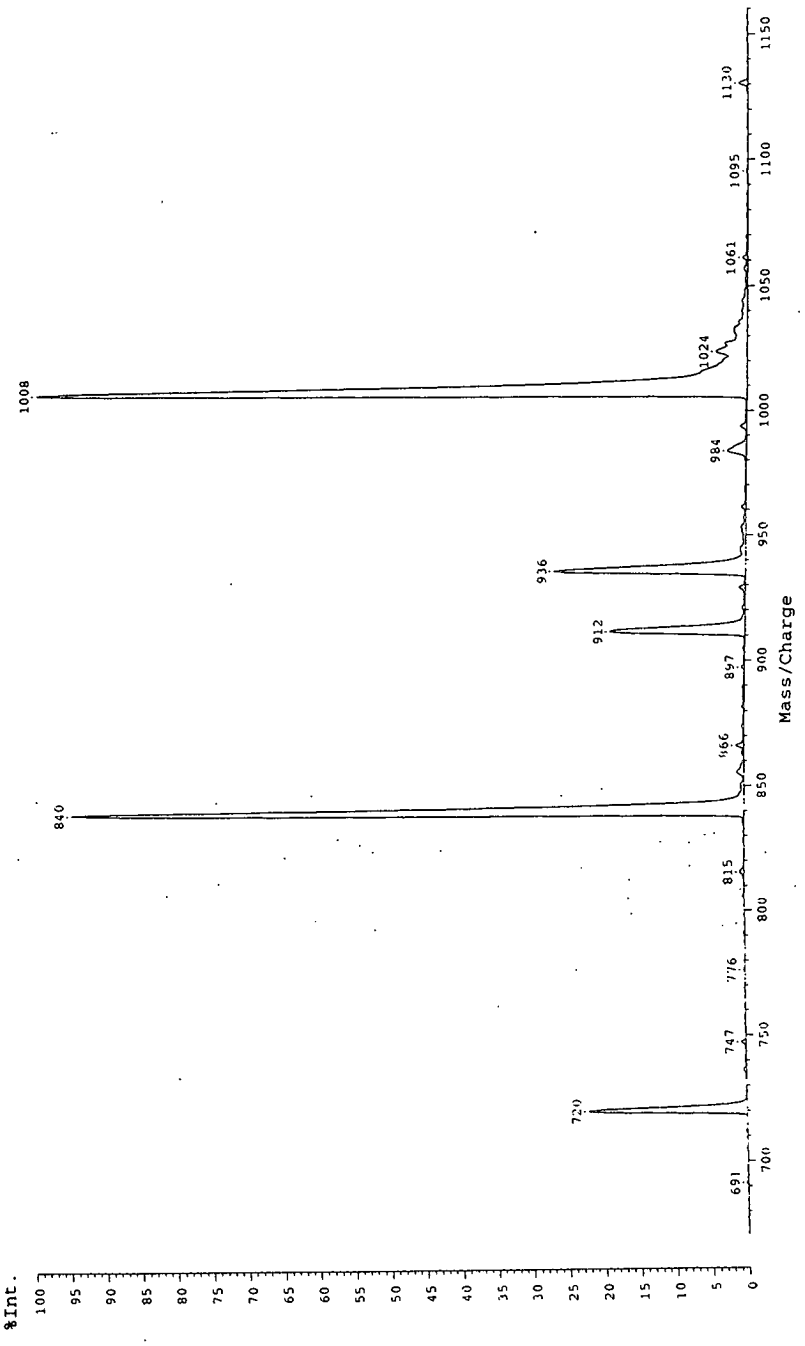

Figure 4.19: Negative ion mass spectrum, averaged over 50 shots in the reflectron mode obtained on the Kratos Kompact III mass spectrometer of the fullerene series shown in Figure 4.18.

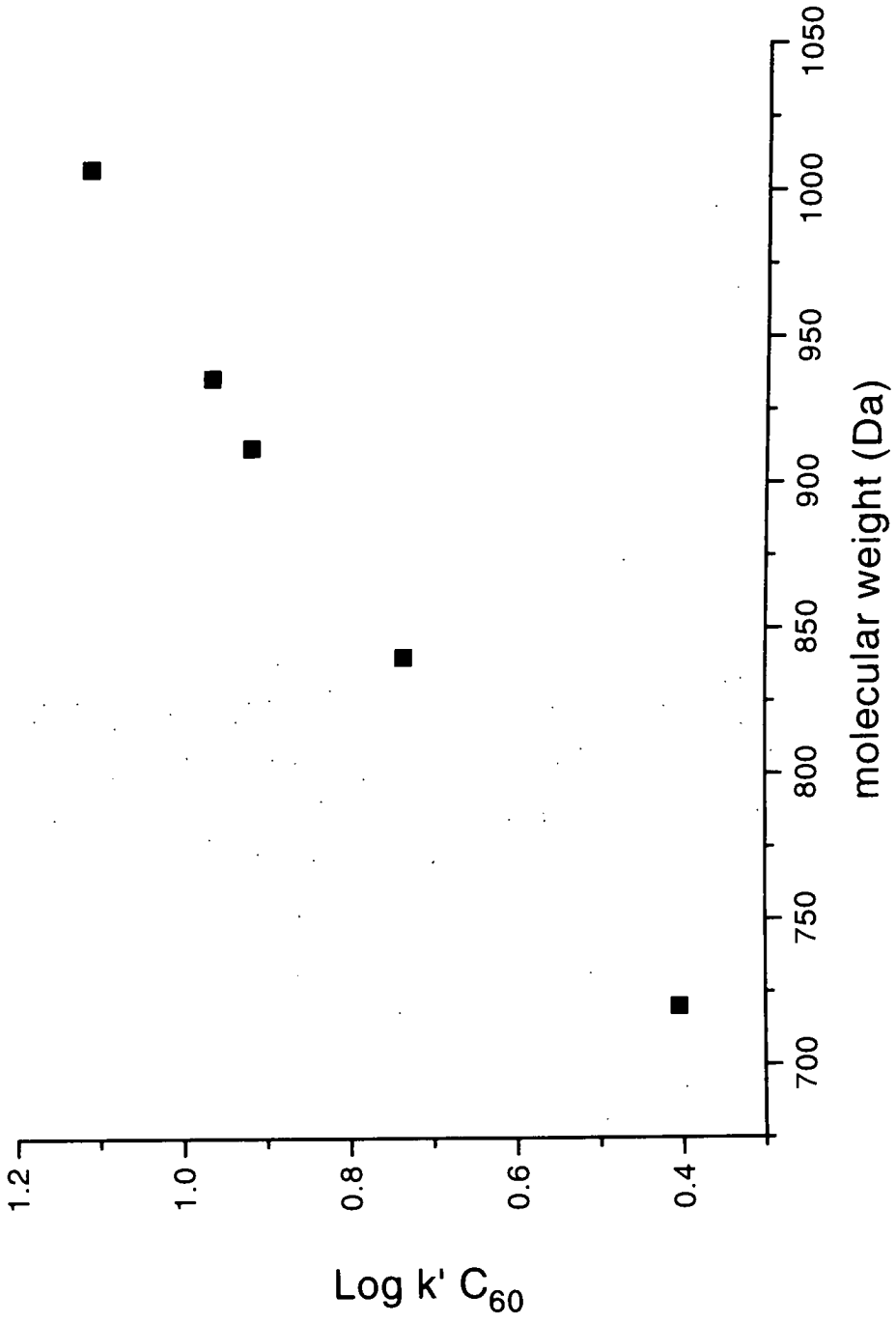

Figure 4.20: Plot of log k′ against molecular weight for fullerene series. k′ values calculated from retention time data in Figure 4.18.

min), C_{70} (R.T. 8.40 min), C_{76} (R.T. 12.18 min), C_{78} (R.T. 13.45 min) and C_{84} (R.T. 18.28 min). Capacity factors for the peaks were calculated, which are given in Table 4.11, and a plot of log k′ against molecular weight was constructed. The plot is shown in Figure 4.20 and confirms the linear relationship (correlation coefficient 0.997)

The question of whether this relationship could be used to predict molecular weights of higher fullerenes from their retention times was then investigated. Figure 4.21 shows the chromatogram obtained on a FullereneSep® column (4.6mm × 150mm, mobile phase 100% hexane, 2ml/min, detector wavelength 254nm) for a sample found to be rich in higher fullerenes. Capacity factors for the peaks up to R.T. 32.68 min were calculated. The first five peaks at R.T 3.90 min, 6.68 min, 9.66 min, 10.90 min and 14.16 min, were assigned as C_{60}, C_{70}, C_{76}, C_{78} and C_{84}, respectively. From these values, listed in Table 4.12 a plot of log k′ against molecular weight was constructed. The resulting equation of the best fit straight line was then used to predict molecular weights for the remaining peaks in the chromatogram. Comparison of predicted values with molecular weights of fullerene structures led to the assignment of each peak in the chromatogram to a fullerene. The comparison between these predicted molecular weights and those for the nearest matching fullerenes are shown in Table 4.13). Finally, Figure 4.22 shows a plot of the molecular weights for this larger data set of the assigned fullerenes against log k′.

Confirmation of the assignment of the molecular weights was achieved by mass spectral analysis of the sample. The negative ion mass spectrum was recorded using a Kratos Kompact III instrument. The spectrum shown in Figure 4.23 (50 shot average) was recorded in the reflectron mode. The peaks at m/z 1032, 1056, 1080, 1104, 1128 and 1152 are in agreement with those predicted from Figure 4.22. These results establish unequivocally the relationship between the retention of a fullerene on the chromatography column and its size, and that this relationship may be useful in the characterisation of fullerene mixtures.

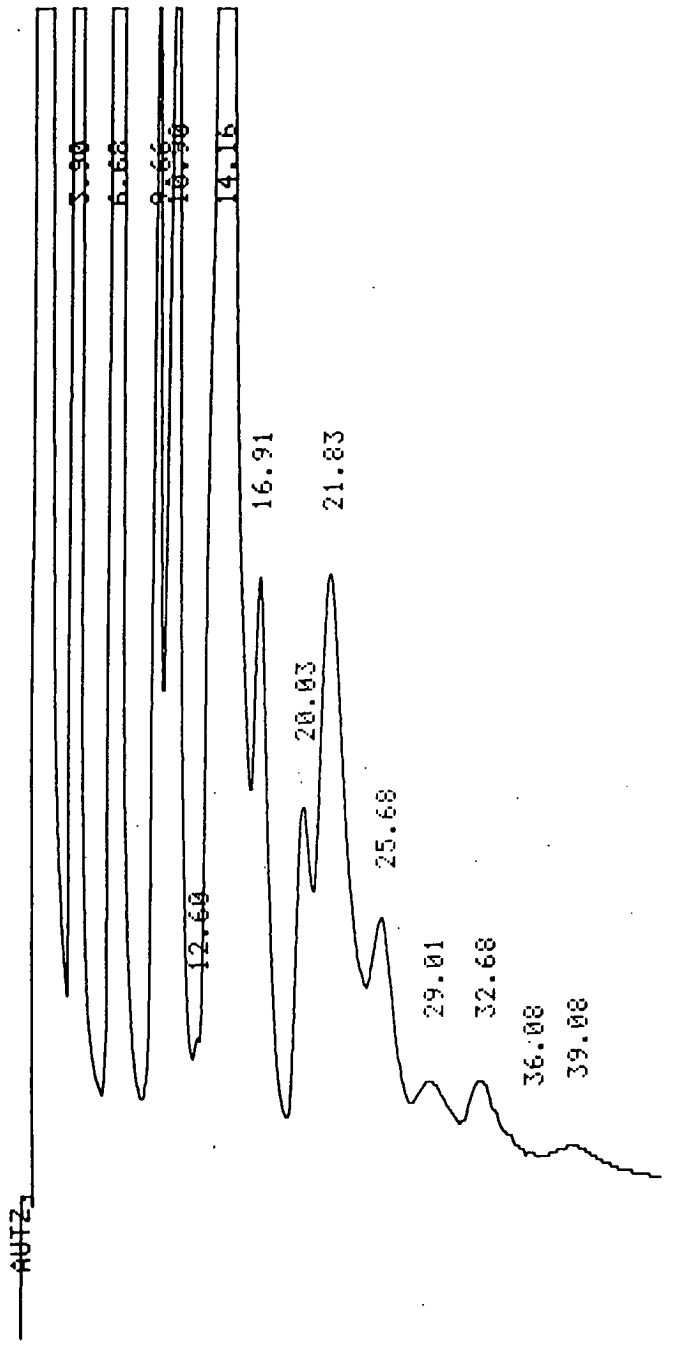

Figure 4.21: Chromatographic trace of a sample enriched in higher fullerenes separated on 4.6mm × 150mm FullereneSep® column 100% Hexane, Flow rate 2ml/min detected at 254 nm.

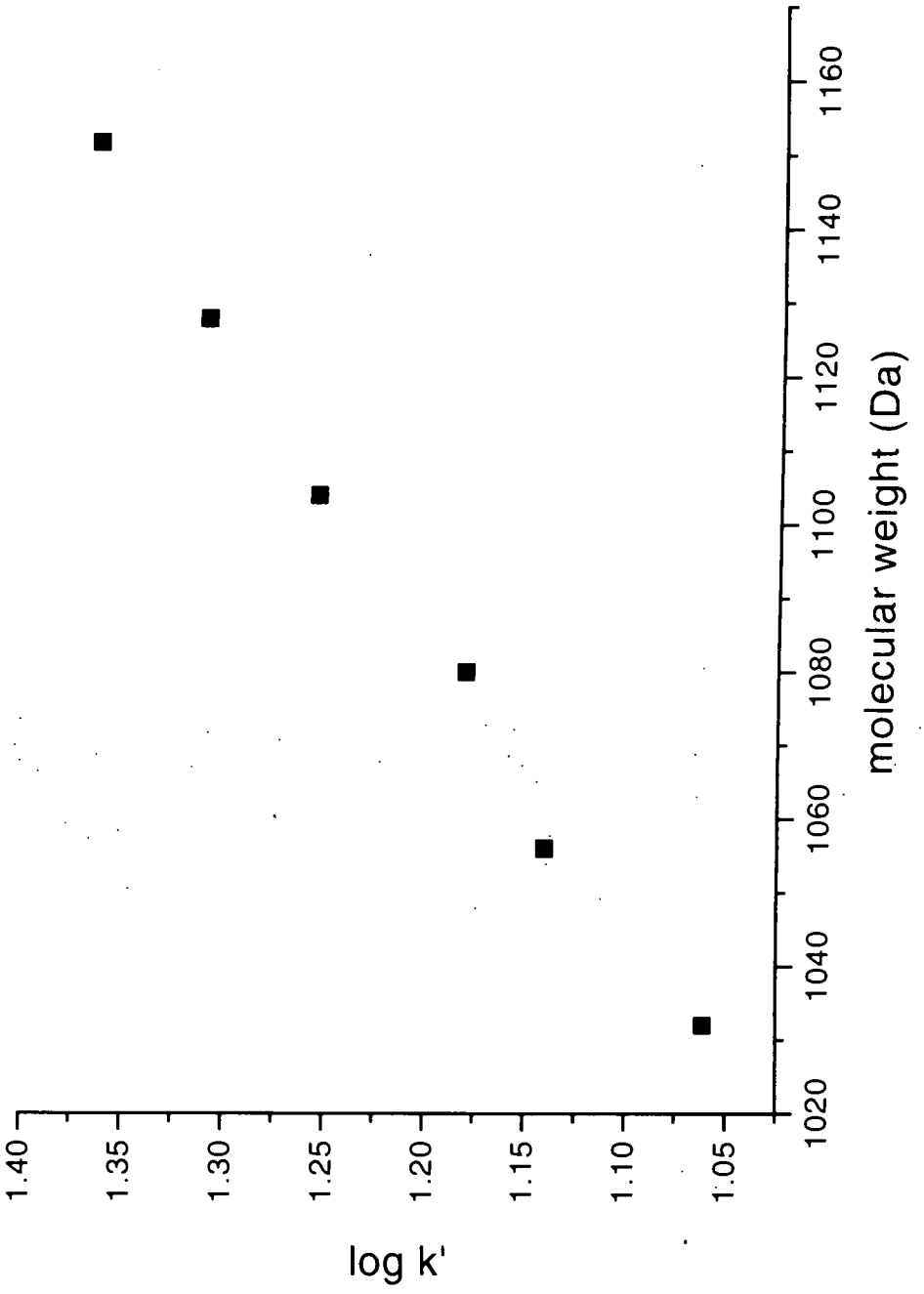

Figure 4.22: Plot of log k' against assigned molecular weight for series of higher fullerenes shown in Figure 4.21. The molecular weights were assigned from values predicted by the equation of the straight line attained using the first four peaks in the chromatogram.

Table 4.12: Molecular weights and values of log k′ for the series of fullerenes shown in Figure 4.21.

Fullerene	Molecular Wt	log k′
C_{60}	720	0.275
C_{70}	840	0.596
C_{76}	912	0.789
C_{78}	936	0.849
C_{84}	1008	0.977

Table 4.13: The predicted molecular weights for the series of fullerenes shown in Figure 4.21.

k′	log k′	Predicted Molecular Wt	Assigned Molecular Wt	Fullerene
11.51	1.061	1030	1032	C_{86}
13.82	1.140	1061	1056	C_{88}
15.15	1.180	1078	1080	C_{90}
17.99	1.255	1108	1104	C_{92}
20.46	1.311	1130	1128	C_{94}
23.17	1.365	1152	1152	C_{96}

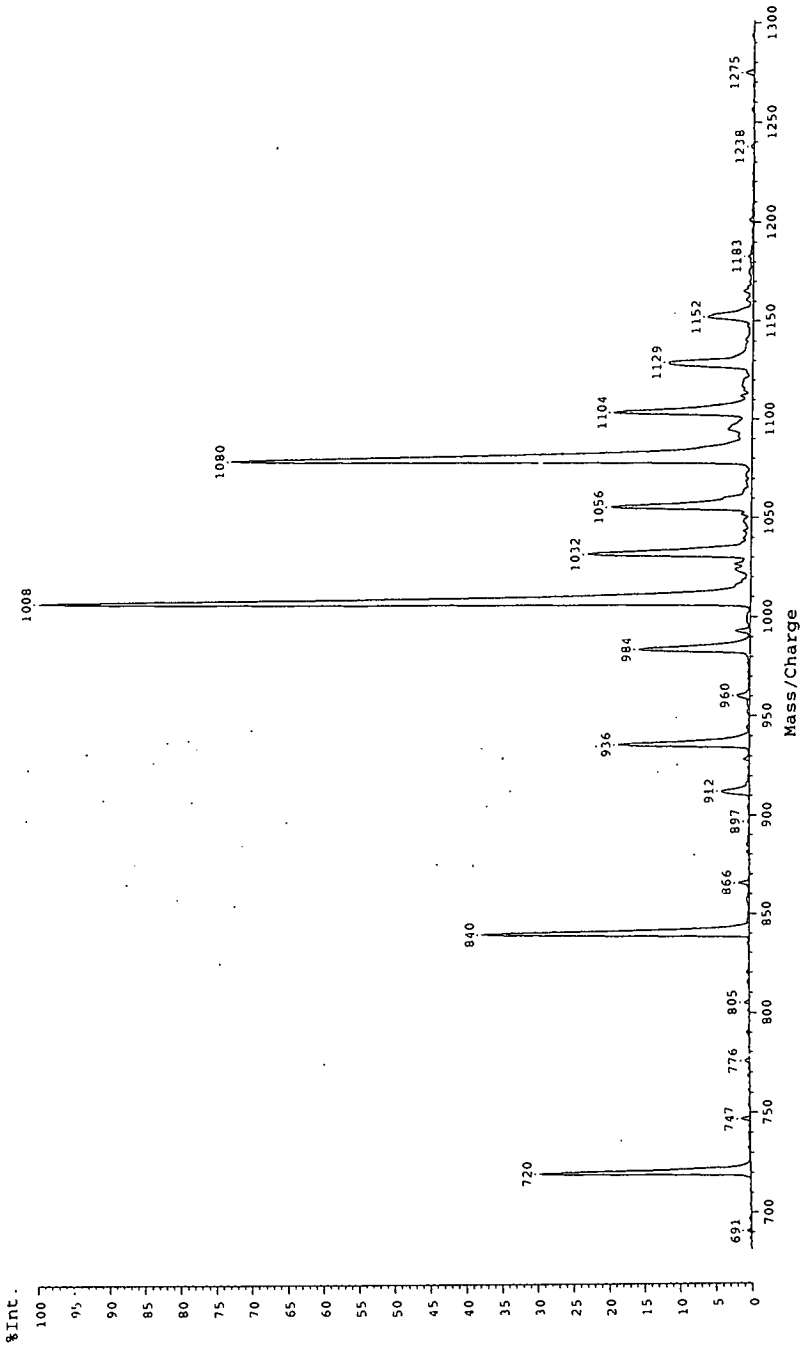

Figure 4.23: Negative ion mass spectrum of sample enriched in higher fullerenes, chromatogram shown in Figure 4.21, obtained on Kratos Kompact III instrument (50 shot average) recorded in the reflectron mode.

A similar study has been carried out by Klute *et al* [173] using a 25cm × 1cm analytical column packed with C_{18} coated 5μ silica with a 55:45% dichloromethane acetonitrile mobile phase running at 1ml/min. In these studies fullerenes up to C_{106} were assigned to peaks in the chromatogram. There was however, no mass spectral information given that could confirm these predictions. In addition there was a large deviation from linearity in the value of log k′ for C_{60}.

4.7 Separation of Fullerenes by Competitive Complexation with $AlCl_3$.

During this work the separation of fullerenes based on their different reactivities was investigated using competitive complexation with $AlCl_3$. The reaction was monitored by chromatographic and mass spectrometric techniques.

Raw soot was subjected to ultrasound extraction with CS_2 for 30 minutes and the resulting fullerene mixture analysed by HPLC (system 4, 4.6mm × 250mm FullereneSep®, mobile phase 4% ether in hexane, flow rate 2ml/min, detection wavelength 254nm). The one step laser desorption/ionisation negative ion mass spectra of the sample were recorded on the Edinburgh instrument. The samples were deposited onto the sample probe from CS_2 solution.. To a 0.5g sample of the fullerene mixture in 100ml CS_2 was added 15g $AlCl_3$ in the presence of two drops of H_2O to initiate the reaction, and the mixture further monitored by HPLC (details given above) over 15 minutes. After 15 minutes the solid material comprising fullerenes that had complexed with $AlCl_3$ was filtered off leaving a solution of unreacted C_{60} and C_{70}. This solution was examined by HPLC and the components characterised from their negative ion mass spectra obtained on the Edinburgh instrument. The solid material was transferred to a separating funnel (500ml) containing 250ml ice water. A vigorous reaction occurred. After the reaction subsided the aqueous solution was extracted four times with CS_2 (100ml portions),

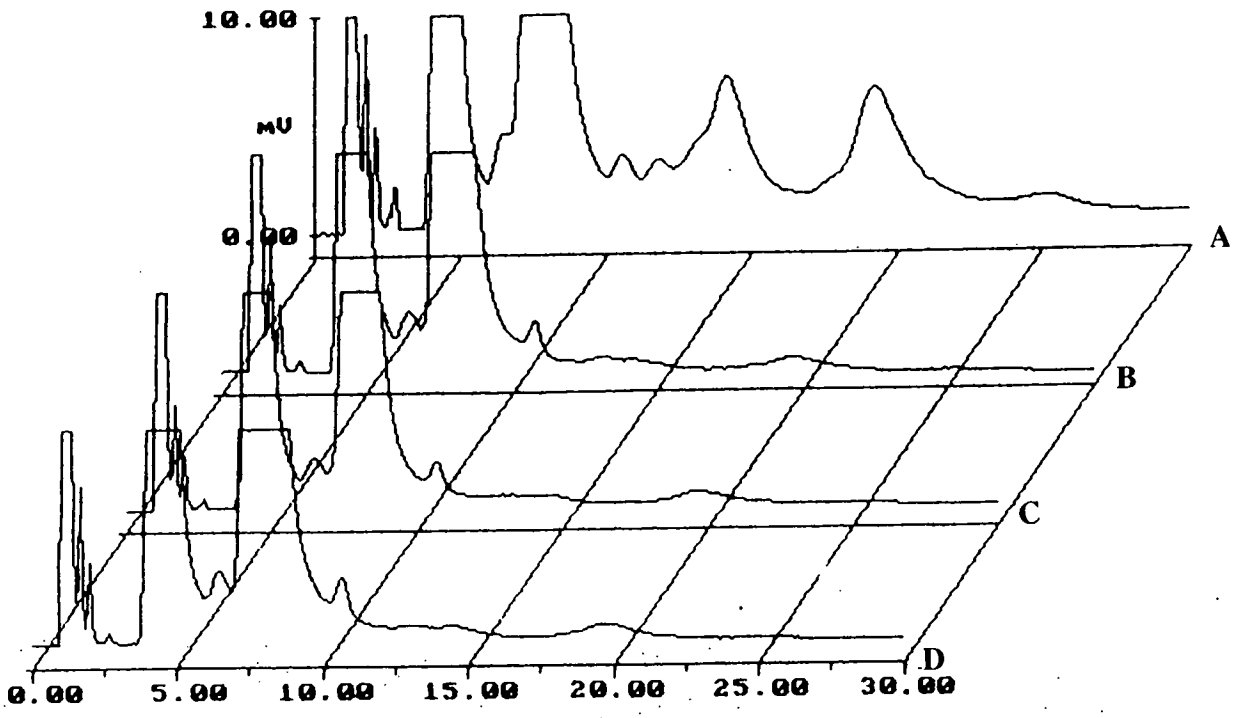

Figure 4.24: Chromatographic monitoring of the reaction between $AlCl_3$ and the fullerene mixture with time. Chromatogram A represents the initial reaction mixture, chromatogram B was taken 5 minutes after the $AlCl_3$ was added and chromatograms C and D at subsequent 5 minute intervals. NOTE: All chromatograms in this study were run on a FullereneSep® column 4.6mm × 250mm Fullerenesep®, system 4, mobile phase 2% ether in hexane, flow rate 2.5 ml/min, detection wavelength 254nm.

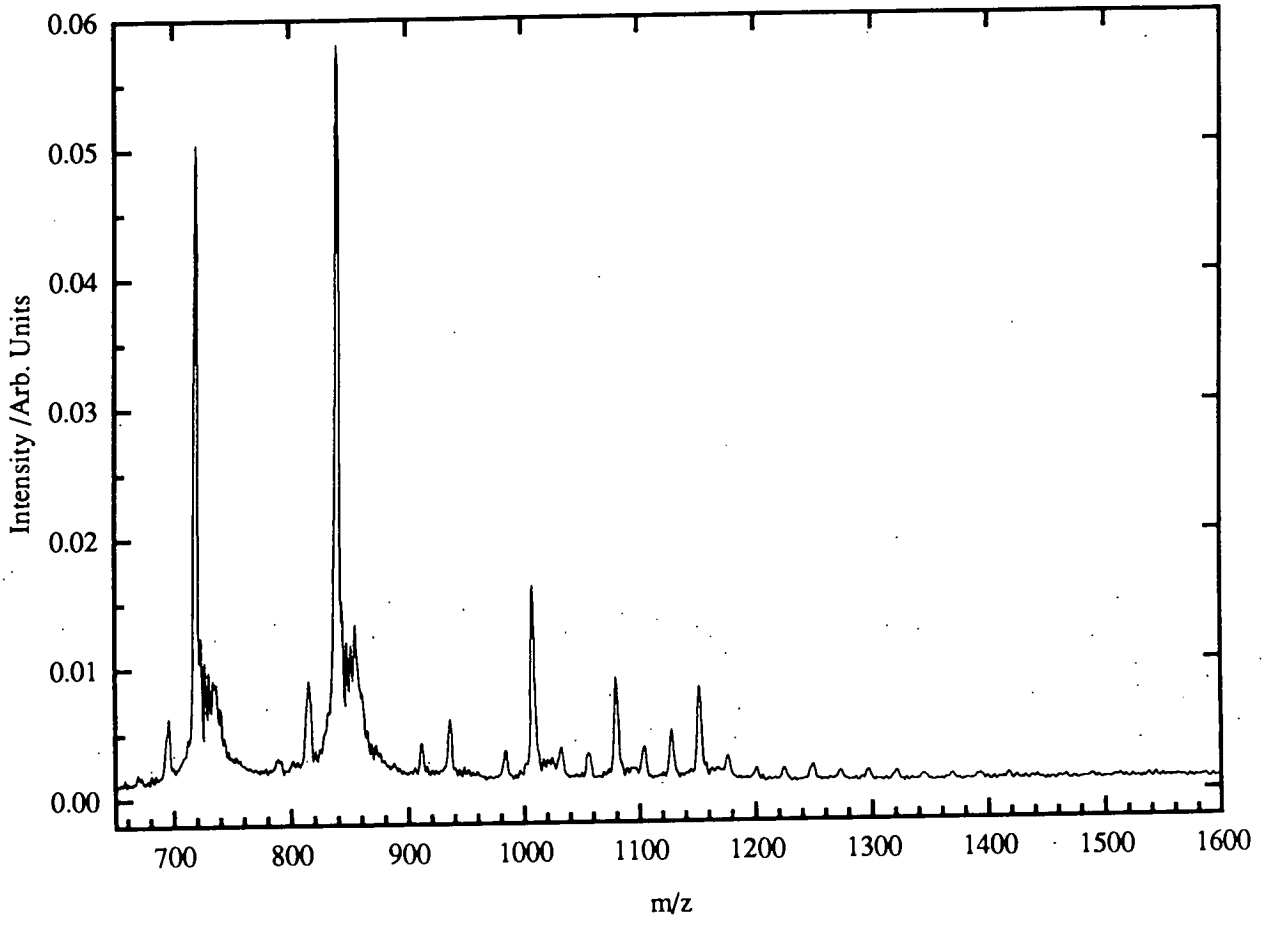

Figure 4.25: LDI negative ion mass spectrum of initial fullerene sample.

the final extract showing no colour in the organic layer. The accumulated extract was then dried over $MgSO_4$ and samples of the dried solution examined by HPLC and characterised by laser desorption/ionisation mass spectrometry. This solution comprises those fullerenes that had reacted with the $AlCl_3$ after the initial 15 minutes.

The solution of fullerenes which had failed to react after the initial 15 minutes, containing primarily C_{60} with some C_{70}, had $AlCl_3$ added a second time and the reaction monitored over a further 5 hours.

Figure 4.24 shows a series of HPLC chromatograms recorded after increasing elapsed time in order to monitor the extent of the reaction between the fullerenes and $AlCl_3$. The chromatograms a), b), c) and d) were recorded after 0, 5, 10 and 15 minutes respectively. The negative ion LDI mass spectrum of the initial fullerene sample recorded on the Edinburgh instrument is shown on Figure 4.25. From examination of the mass spectrum the peaks in the chromatogram were assigned as C_{60}, C_{70}, C_{78}, C_{84} and C_{90} in order of increasing retention time. Integration of the peaks shows the initial sample to contain fullerenes in the ratio C_{60} (71.4%), C_{70} (23.2%) and higher fullerenes (5.4%).

From Figure 4.24 the rapid reaction between the higher fullerenes and the $AlCl_3$ is evident from the disappearance of the peaks at R.T. 10.5 min, 14.5 min and 19.5 min as the reaction proceeds. The reaction between the higher fullerenes and the $AlCl_3$ is essentially complete within 5 min. as evidenced by the disappearance of the peaks due to these species over this time (see Figure 4.24, chromatograms **a** and **b**).

After the fullerenes had been allowed to react with $AlCl_3$ for 15 min. the solid material which had complexed with the $AlCl_3$ was removed and the fullerenes extracted. The chromatogram of this reacted material is shown in Figure 4.26. There

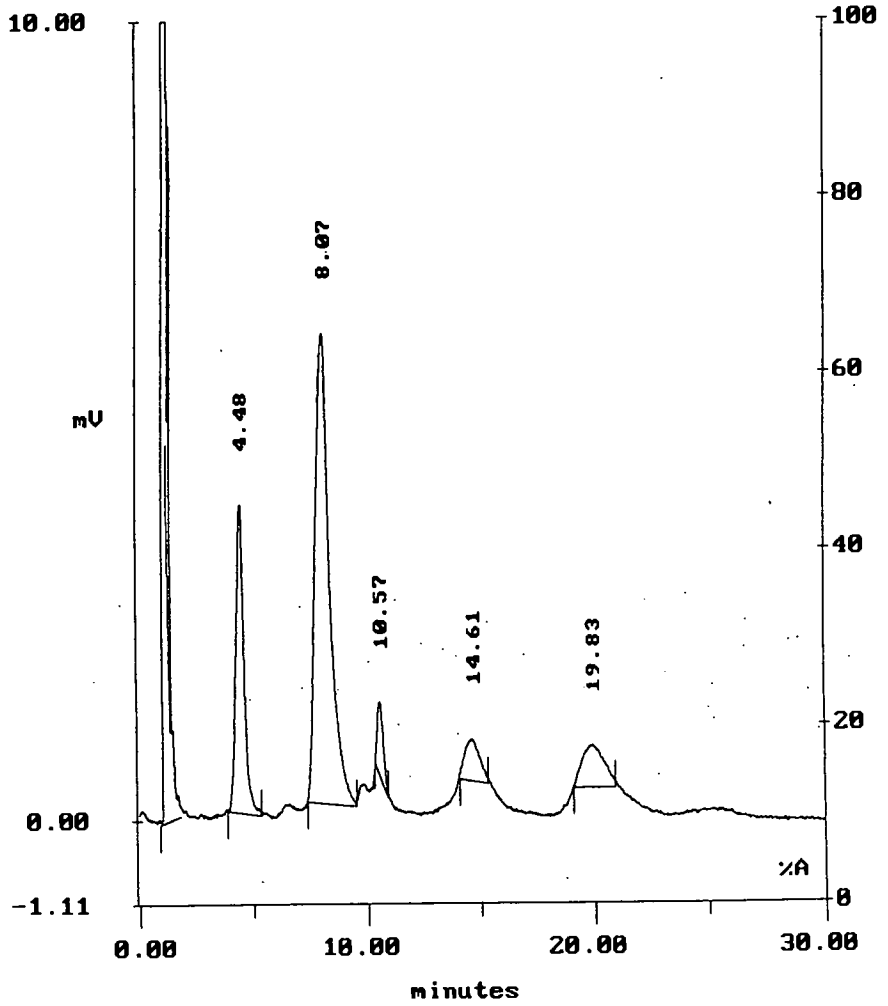

Figure 4.26: Chromatogram of the mix of fullerenes reacted with $AlCl_3$ after the initial 15 minutes. The chromatogram shows C_{60}, C_{70} and a range of higher fullerenes, however there is a strong depletion in the amount of C_{60} and C_{70} present in relation to the higher fullerenes from the initial reaction mixture

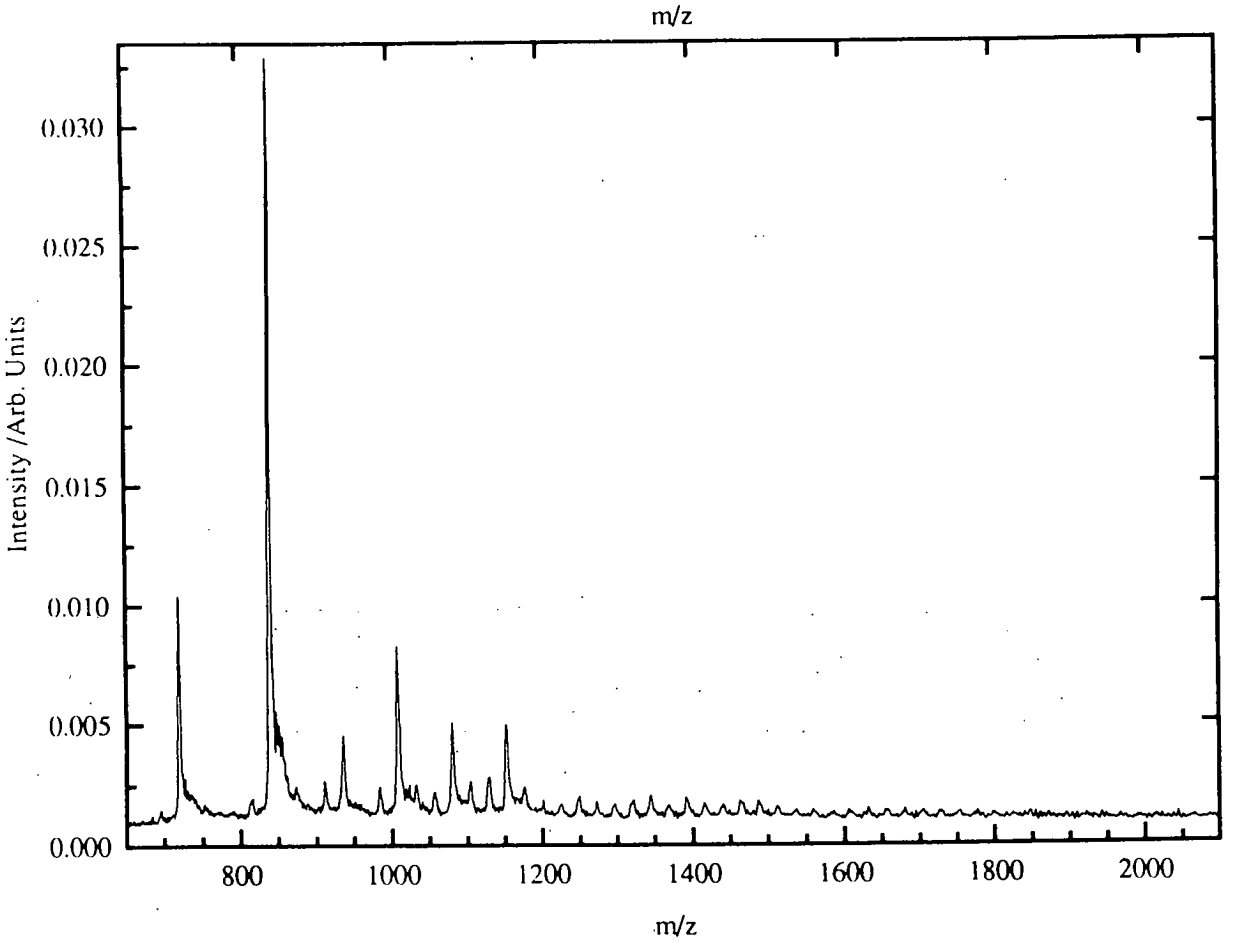

Figure 4.27: Mass spectrum of the reacted fullerenes after the initial 15 minutes. Spectrum shows the presence of C_{60}, C_{70}, C_{78}, C_{84}, C_{90}, and C_{96}

is a marked depletion in C_{60} content compared to the initial sample. From integration of the peaks this sample contains C_{60} (22.3%), C_{70} (61.4%) and higher fullerenes (16.3%). The accompanying LDI negative ion mass spectrum for this sample is shown in Figure 4.27. The spectrum shows a depletion in the peak at m/z 720 (C_{60}) corresponding to that seen in the HPLC chromatogram.

The chromatogram of the fullerenes which failed to react after the initial 15 min. is shown in Figure 4.28. The chromatogram shows the presence of C_{60} and C_{70} with no peaks due to higher fullerenes. This is confirmed by the LDI negative ion mass spectrum shown in Figure 4.29. These results clearly show that the reaction between C_{60} and C_{70} and $AlCl_3$ occurs at a slower rate than the reaction between $AlCl_3$ and higher fullerenes. It should be noted that this sample contains only unreacted C_{60} and C_{70} despite the presence of $AlCl_3$ in large excess.

The chromatogram of the C_{60}/C_{70} mixture taken 85 min. after $AlCl_3$ was added is shown in Figure 4.30. The unreacted fullerenes now consist of 91.1% C_{60} and 8.9% C_{70}. This again illustrates the increased reactivity of the more polarisable higher fullerenes, as the fraction of C_{70} has further decreased while there remains a large amount of unreacted C_{60}.

The exact nature of the $AlCl_3$/fullerene complex is difficult to deduce. However, some inferences may be made. The addition of a small amount of water caused the reaction to proceed vigorously and suggests the complexing agent may be the conjugate acid of $AlCl_3$ rather than the $AlCl_3$ itself. $AlCl_3$ actually exists as a dimer Al_2Cl_6 with bridging between the chlorines. The addition of water breaks the bridging bonds and leaves $AlCl_3(H_2O)$ which easily dissociates to give $AlCl_3(OH)^-$ + H^+, the conjugate acid. A complex of this nature is constantly losing and replacing the OH group. However as the reaction is carried out in the presence of fullerenes it may be that the fullerene attaches itself to the $AlCl_3$ when the OH falls off. This group is then very difficult to remove as it is so bulky. Therefore, even though thermodynamic considerations would appear to suggest a complex with the OH is

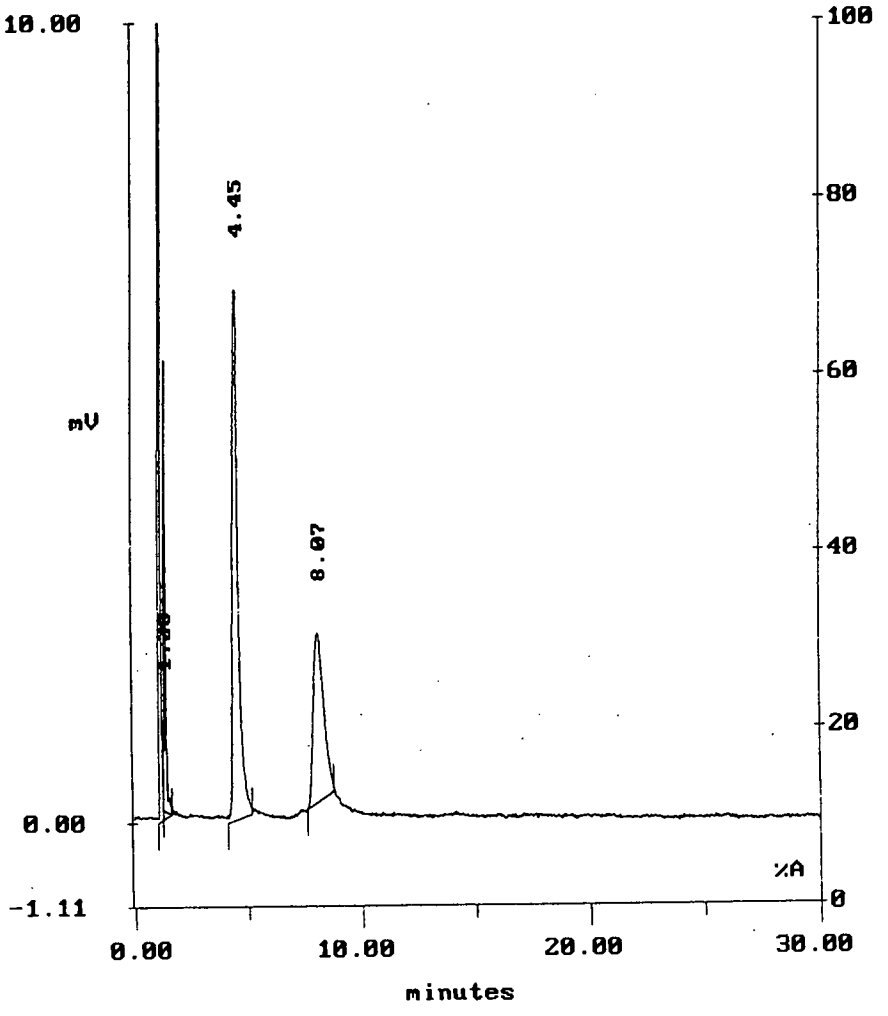

Figure 4.28: Chromatogram of the fullerene mixture which failed to react with $AlCl_3$ after 15 minutes. The chromatogram shows the presence of unreacted C_{60} and C_{70} only.

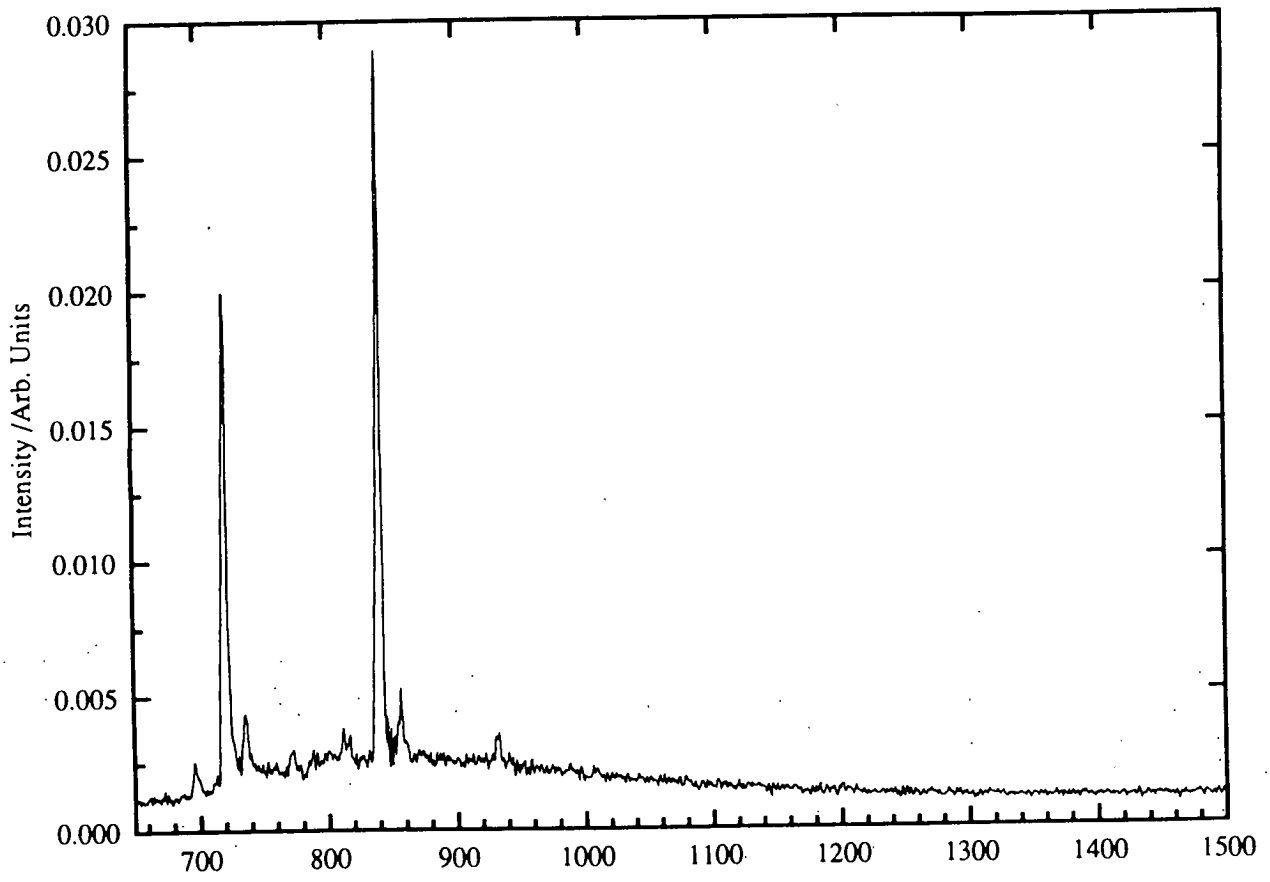

Figure 4.29: Mass spectrum of the unreacted fullerene mixture after the initial 15 minutes. Spectrum shows the presence of C_{60} and C_{70} at m/z 720 and 840, respectively along with trace amounts of their oxides.

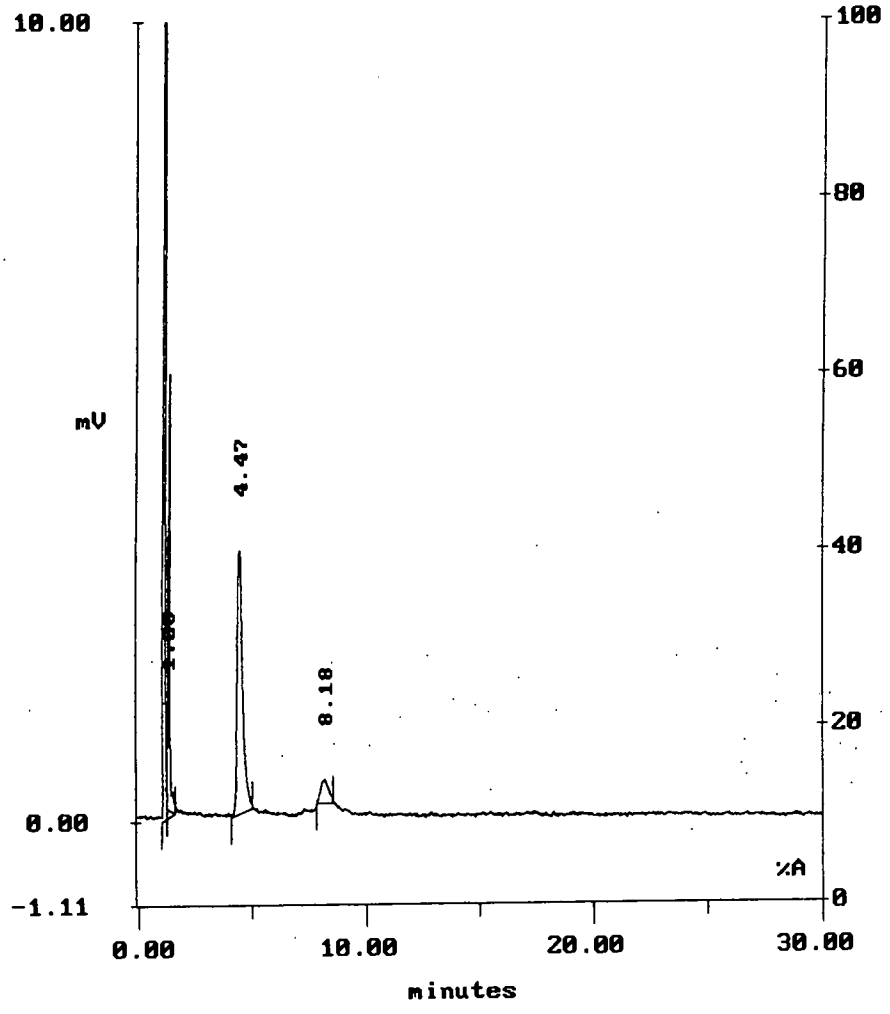

Figure 4.30: Chromatogram of the C_{60}/C_{70} mixture 85 minutes after the $AlCl_3$ had been added for the second time.

more stable, a complex with the fullerenes would actually form in preference if the fullerenes are present in sufficient excess over H_2O.

By using these mass spectral and chromatographic techniques to monitor the reaction with $AlCl_3$ it has been possible to rapidly obtain highly purified samples of both C_{60} and C_{70} and samples greatly enriched in higher fullerenes. With a more detailed study of the initial reaction and monitoring over shorter time periods, it should also be possible to produce samples further enriched in the various higher fullerenes simply by stopping the reaction at the appropriate time.

4.8 Mass Spectrometric Characterisation of Fullerenes and Fullerene Derivatives

As can be seen from the results already presented in this chapter mass spectrometry has played an extremely useful and powerful role alongside the chromatographic measurements when used both on-line as well as off-line.

4.8.1 On-line LCMS

As described earlier this technique was employed to conclusively identify peaks eluting from a FullereneSep® HPLC column (3μ, 4.6mm × 150mm) using a particle beam interface and a Kratos concept 1H high resolution double focusing mass spectrometer. Details of the instrument are given in Section 3.10.3. The characterised peaks were used to determine the selectivity of the novel stationary phase FullereneSep®, and enabled a linear relationship between the phase capacity factors and the molecular weight of the eluting fullerenes to be established. The mass spectra were discussed in detail in Section 4.4.3.

The LCMS technique was of particular value when examining the ability of the column to separate higher fullerenes. C_{60} and C_{70} are often easily identifiable from the chromatograms as they are by far the most abundant species produced, and occur in similar relative amounts using the majority of production and extraction techniques. The distribution of the higher fullerenes, however, is much more difficult to predict and the assignment of peaks in the chromatograms is not always obvious. This difficulty can be overcome to a certain extent using LC-MS technique, which allows the unambiguous identification of the carbon number of peaks eluting in the chromatogram. One drawback, however, of the technique is the limited mass range accessible due to the involatility of the higher fullerenes. As descibed below, laser desorption ionisation (LDI) and matrix assisted laser desorption ionisation (MALDI) provide extremely powerful off-line mass spectrometric techniques for the characterisation of fullerenes and fullerene derivatives. Samples can be rapidly loaded into these time-of-flight mass spectrometers and spectra obtained in a matter of minutes. The multi-position sample stages allow a very large number of samples to be processed and the mass range accessible is very high.

4.8.2 Laser Desorption Ionisation Studies of Fullerene Mixtures

Mass spectrometric characterisation of fullerene samples produced in this study was achieved mainly using laser desorption ionisation techniques. The different experimental techniques are described in detail in chapter 3. In this section some of the results obtained using LDI are presented.

One of the first considerations was whether to examine the positive or negative ions that are produced by laser desorption. Figure 4.31 shows both the positive and negative ion mass spectra of a sample containing a mixture of fullerenes obtained by LDI. The spectrum was recorded on the instrument constructed in house at Edinburgh university (for details see section 3.10.2). The sample was deposited onto the sample

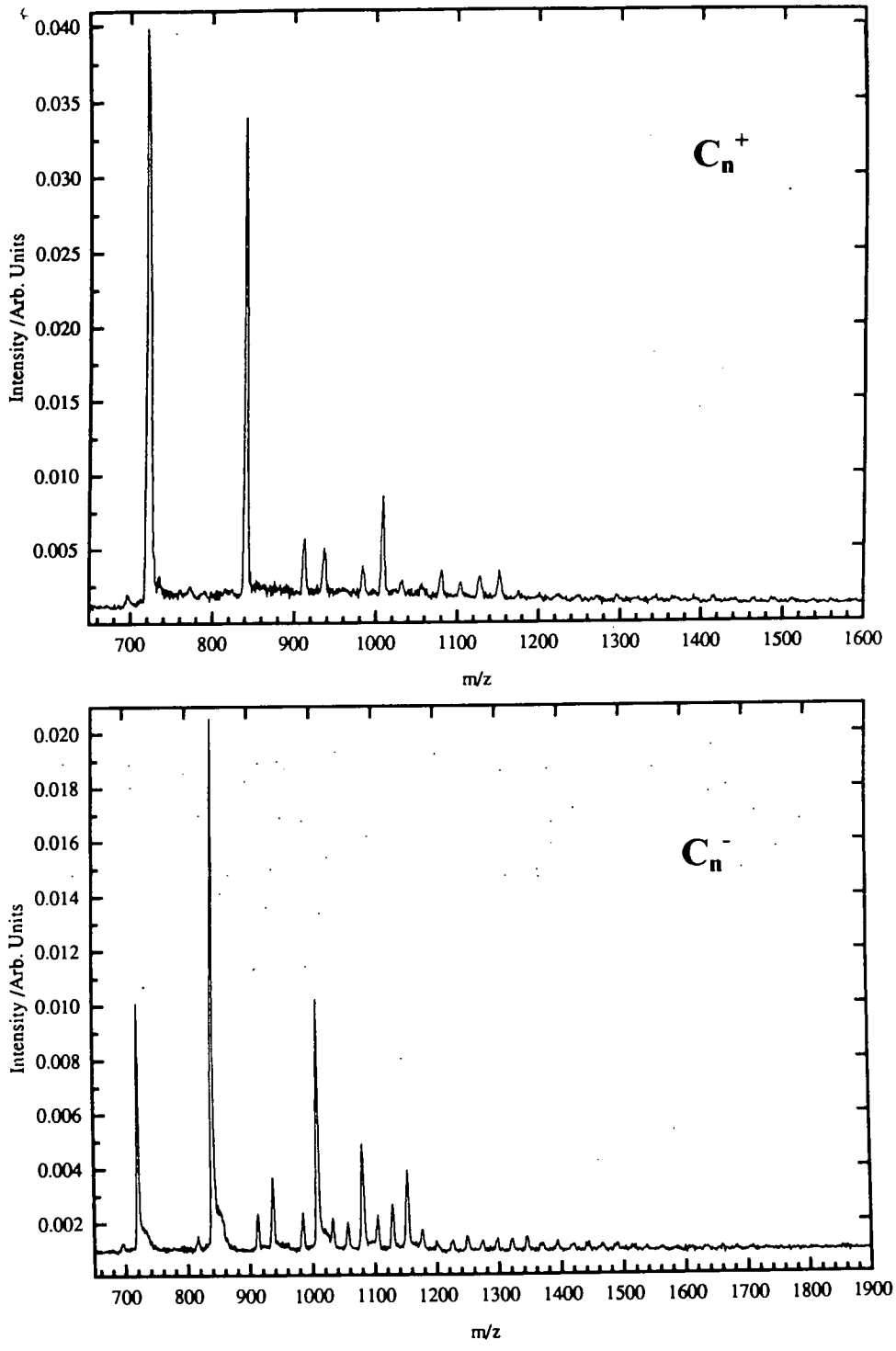

Figure 4.31: Mass spectra of a fullerene mixture recorded using the one step laser desorption/ionisation technique (Edinburgh instrument). The upper spectra is of positive ion distribution and the lower negative ion.

probe from toluene solution. Both spectra show the presence of C_{60}, C_{70} and a range of other higher fullerenes. However, from comparison of the positive with the negative ion mass spectra, there are noticeable discrepancies in the signal intensities. In the negative ion spectra, the relative intensities of C_{70} and the other higher fullerenes compared to the C_{60} signal are much greater than in the positive ion spectra.

Discrepancies between the positive and negative ion spectra could arise for a number of reasons. In the positive ion spectra, a high laser fluence could lead to fragmentation of the fullerenes, which would be greater in the less symmetric, less stable C_{70} and higher fullerene structures than in C_{60}. Thus, the signal intensity of C_{60} would increase compared to that of the other species.

Any possible fragmentation of C_{70} could also increase the amount of C_{60} detected. The fragmentation of fullerene species occurs by the loss of C_2 units to form the next available closed cage structure. C_{70} could thus lose the excess energy gained in the desorption/ionisation process by ejection of successive carbon units until the extremely stable C_{60} structure is reached. Consequently this process would again provide an artificially high value for the C_{60} signal. However, the positive ion spectrum shows little evidence of such fragmentation.

An additional problem affecting the positive ion spectra is the reaggragation of species fragmented by desorption to form new fullerene species not present in the original sample. These growth processes occur particularly for the fragmentation of C_{60} and C_{70} and the reaggregation of the species to give higher fullerenes. Thus there would be a relative decrease in the signal for C_{60} and C_{70} and an increase in the signal for higher fullerenes.

Although these processes may occur for positive ion mass spectra examination of Figure 4.31 shows they are not happening at this laser fluence. As mentioned fullerenes fragment by loss of C_2 units, this leaves a characteristic fragmentation

pattern to low mass. The absence of such a feature in the positive ion mass spectra shown in Figure 4.31 shows this process is not occurring at the laser fluence used. Only a very small peak 24 mass units below that for C_{60} can be seen, and there is no evidence of fragment ions in the mass range between C_{60} (m/z 720) and C_{70} (m/z 840).

As the energy required for fragmentation is greater than that required to detach the extra electron on the negative ion, hot species will lose an electron and therefore not be detected in the negative ion mass spectrum. Similarly, species formed from growth processes, as discussed earlier, will likewise lose an electron and not be detected. Thus, in general, the negative ion mass spectrum would be expected to be more representative of what the sample actually contains since such spectra should be less susceptible to both fragmentation and growth processses. In essence, it should be only the least energetic and thus the most representative ions that are detected.

However, the spectra may be affected by other factors. For example, the amount of ions that may be formed will depend on the electron capture cross section of each species.

Given the number of processes occurring that could affect the intensities of the signal in both the positive and negative ion mass spectra, it is difficult to state with certainty the relative amounts of each species which may have been present in the original samples.

Nonetheless, LDI has been found to be extremely useful for the identification of species in fullerene mixtures. The appearance of different species in the positive and negative ion mass spectra are a result of the different processes that occur. It seems reasonable to conclude therefore that species observed in both spectra are present in the extract and are not a product of laser conditions. The spectra may be easily and rapidly obtained and are of particular value in the identification of higher fullerene

species. As can be seen in both the positive and negative ion spectra in Figure 4.31, species up to C_{96} are clearly present.

A possible experiment to examine the effect of the different processes occurring in the positive and negative spectra on the relative sample intensities would be to examine an equimolar mixture of fullerene species. For example, mass spectra of C_{60},C_{70} and C_{76} could be taken and the different intensities observed to give useful information on the degree of fragmentation or the ability of the various species to form negative ions.

A Comparison of the mass resolution which can be obtained is shown in Figure 4.32. These spectra were recorded on the VG TofSpec instrument. The upper spectrum was recorded in linear mode and the lower spectrum recorded in reflectron mode. The reflectron lens assembly is located in front of the linear detector (see Figure 3.5) and reflects the ions back along the instrument axis to an annular microchannel plate (MCP) before they reach the linear MCP detector. This has the effect of doubling the flight path of the ions, and the reflectron itself compensates for the small random energy differences between the ions as they emerge from the source. These two factors have the combined effect of producing better resolved data with a mass accuracy of 0.02% compared to the 0.2% mass accuracy achieved in the linear mode.

The higher degree of mass resolution and accuracy achieved in the reflectron mode can be easily seen. The ^{13}C isotope distribution can be resolved in the reflectron mode. Natural carbon contains 1.1% of the ^{13}C isotope, thus the mass spectrum of C_{60} and C_{70} show peaks to higher mass due to the incorporation of ^{13}C. The relative intensities of the different mass peaks are called the isotopic fingerprint.

The ability to record spectra over a wide mass range is using LDI is illustrated by the spectrum shown in Figure 4.33. The figure shows the negative ion mass spectrum of the CS_2 extract of a sample enriched in higher fullerenes. This spectrum was also recorded on the VG TofSpec, operating in the reflectron mode, and covers a range

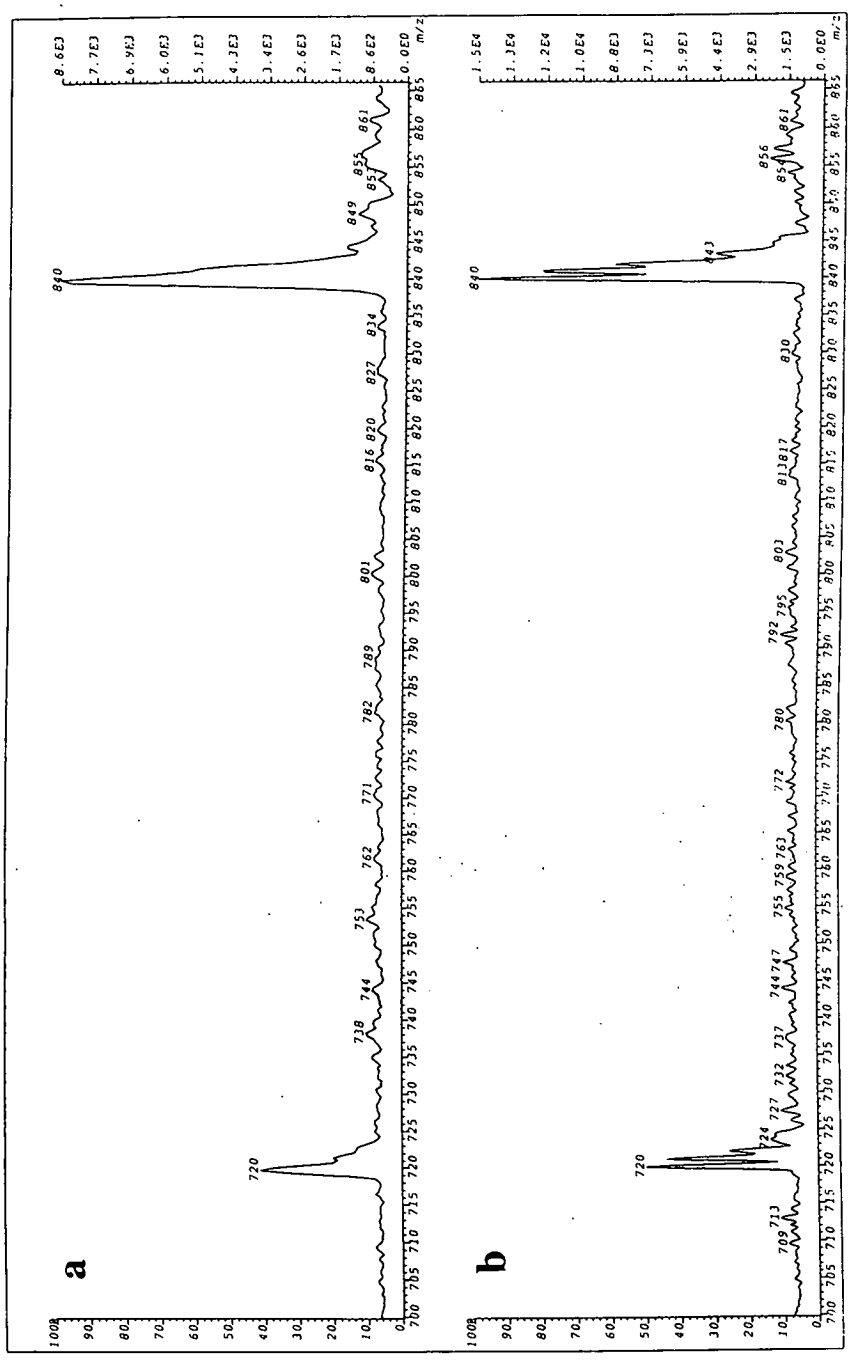

Figure 4.32: LDI negative ion mass spectra averaged over 25 shots in **a)** linear, **b)** reflectron mode recorded on the VG TOFSPEC instrument. The higher degree of mass resolution obtained in the reflectron mode is evident from the isotopic profile.

m/z 600 to m/z 2700. The spectrum shows the presence of fullerenes to high mass. Of interest is the distribution of fullerene species. The peaks at low mass show the characteristic presence of C_{60} (m/z 720), C_{70} (m/z 840), C_{76} (m/z 912), C_{78} (m/z 936) and C_{82} (m/z 984). For molecular weights higher than this there is a peak corresponding to a fullerene for every even numbered carbon species. The absence of peaks at m/z 960 corresponding to C_{80} or between m/z 840 and m/z 912 (C_{70} to C_{76}) is a characteristic of fullerene distributions.

A further example of this characteristic fullerene distribution is shown in Figure 4.34. The figure shows the negative ion mass spectrum of a sample enriched in higher fullerenes obtained on the Kratos Kompact III instrument operating in the reflectron mode. The spectrum shows the presence of higher fullerenes up to C_{96}.

Figure 4.35 shows the mass spectrum of a sample of purified C_{84}. The mass spectrum was also recorded on the Kratos Kompact III instrument, operating in the reflectron mode. The sample was produced as follows. A fraction enriched in higher fullerenes was obtained by passing the ultrasound extract of CS_2 down a neutral alumina flash chromatography column continuously eluting with boiling hexane for two days and extracting the upper part of the column with CS_2. The resulting fractions were then separated by HPLC (system 4 FullereneSep® 4.6mm × 250mm column mobile phase 2% ether in hexane, 2ml/min, detector wavelength 254nm). The sample shown in Figure 4.35 was obtained by continuous injection of the fraction from obtained by flash chromatography and pooling of the collected fractions.

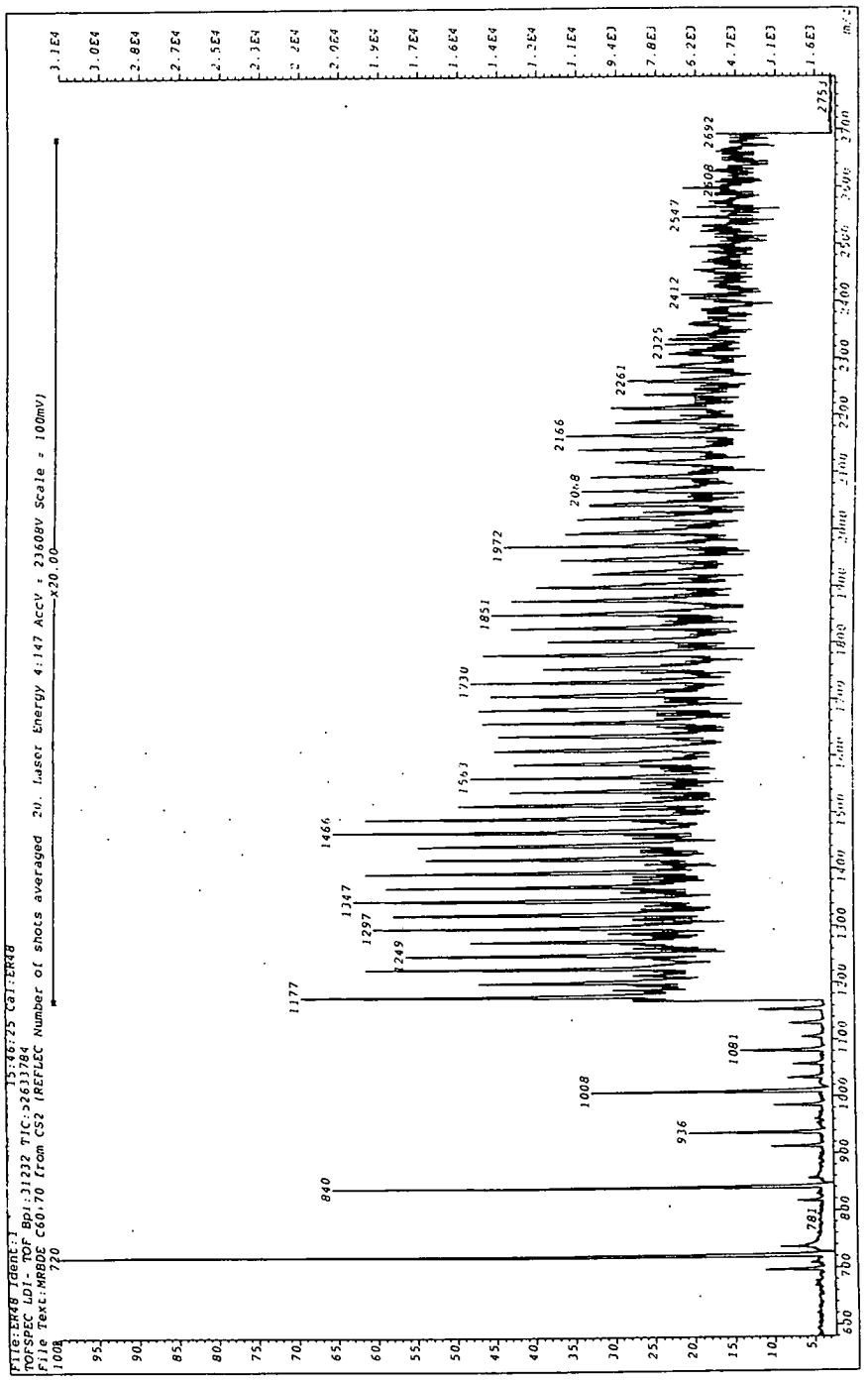

Figure 4.33: LDI Negative ion mass spectrum averaged over 20 shots in the reflectron mode obtained on the VG TofSpec instrument. The figure shows the wide mass range which may be covered.

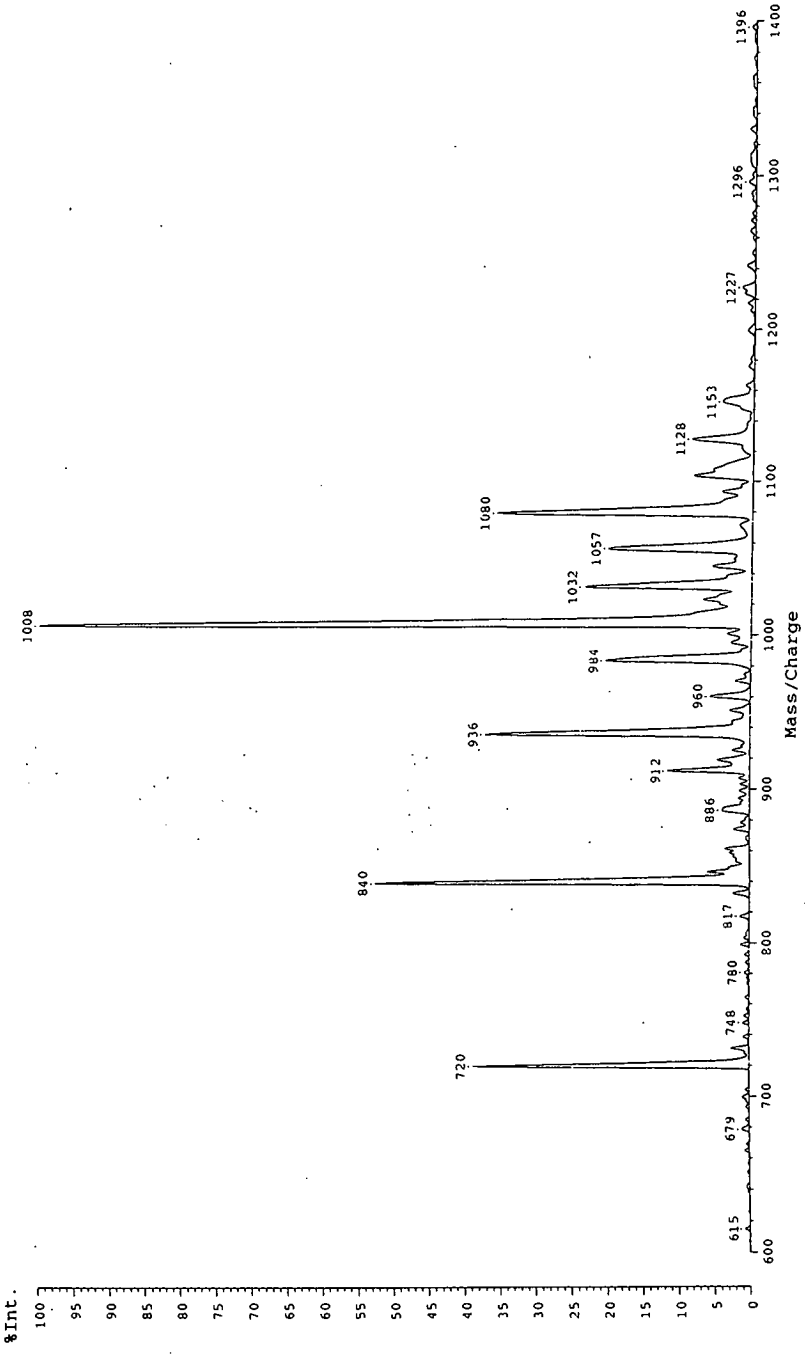

Figure 4.34: LDI mass spectrum of a fullerene sample averaged over 50 shots in the linear mode obtained on the Kratos Kompact III instrument. The spectrum shows the characteristic fullerene distribution pattern.

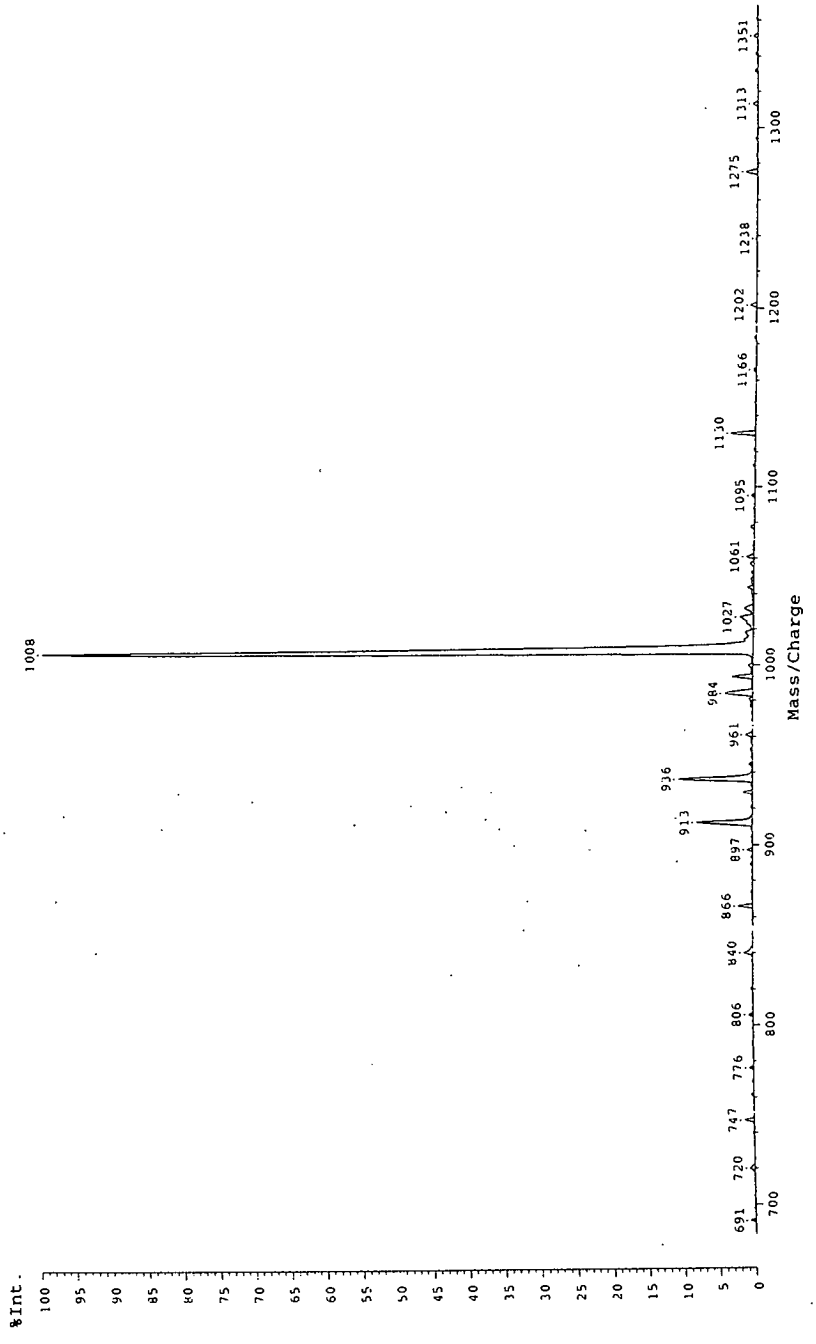

Figure 4.35: LDI negative ion mass spectrum averaged over 50 shots in the reflectron mode obtained on the Kratos Kompact III instrument.

4.9 Formation and Degradation of Aziridinofullerenes Monitored Using HPLC and MALDI

Currently there is considerable interest in the chemistry of C_{60}. Many groups working on the synthesis and characterisation of novel chemical derivatives of C_{60}. In order to understand the chemistry of fullerenes properly, it is helpful to be able to monitor their reactivity. In this work the HPLC and mass spectrometric techniques already described were used to study one such reaction, namely the formation and chemical degradation of aziridinofullerenes. This work was carried out in collaboration with MRB in this Department, who had an active programme of chemical derivatisation of C_{60}, but required fast analytical methods to monitor the progress of his reactions and to identify the eventual reaction products.

It has been shown that N-*tert*-butoxycarbonylaziridino[2',3':1,2]fullerene can be produced by either of two methods [174] (Figure 4.36). The first involves the stepwise addition of *tert*-butylazido formate to a solution of C_{60} in boiling TCE. This reaction leads to the elimination of nitrogen and the formation of the fullerene adduct by *in situ* trapping of the intermediate nitrene (*tert*-BuO_2CN) with C_{60}.

The same result may also be achieved under much milder conditions by base-induced α-elimination of *O*-4-nitro phenylsulfonyl *tert*-butylhydroxamic acid in the presence of C_{60} under phase-transfer conditions at room temperature.

Heating of the fullerene adduct (**4** in Figure 4.36) in TCE (5 h.) leads to the sequential elimination of isobutene and CO_2 to form aziridinofullerene.

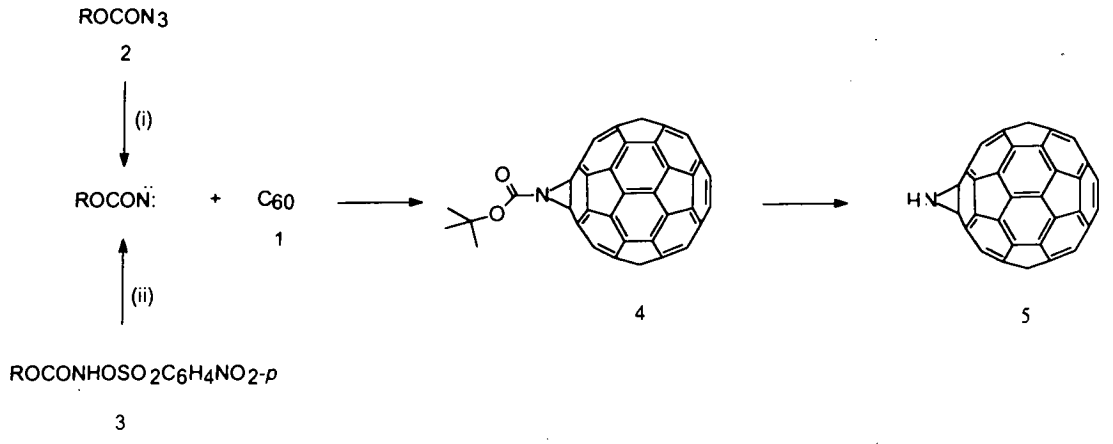

Reagents and conditions: (i) TCE, 147°C; (ii) $NaHCO_3$, $BzEt_3NCl$, H_2O/TCE/DCM, 20°C

Figure 4.36: The formation of n-*tert*-butoxycarbonylaziridino[2',3':1,2]fullerene and its thermal degradation to aziridinofullerene.

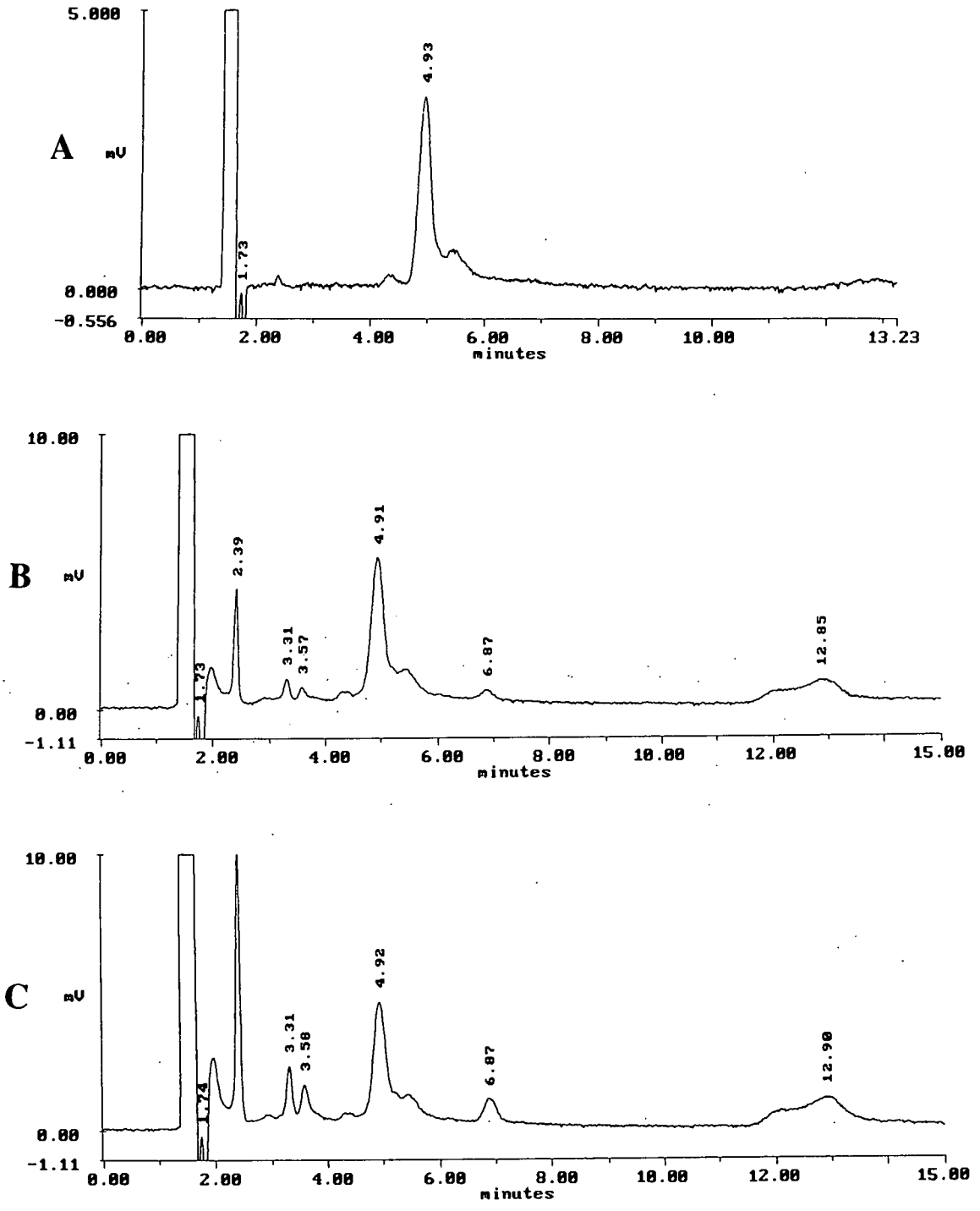

Figure 4.37: Chromatographic monitoring of the reaction mixture. The Figure shows chromatograms at time intervals of **a)** t = 0 (initial reaction mixture), **b)** t = 42 mins and **c)** t = 62 mins.

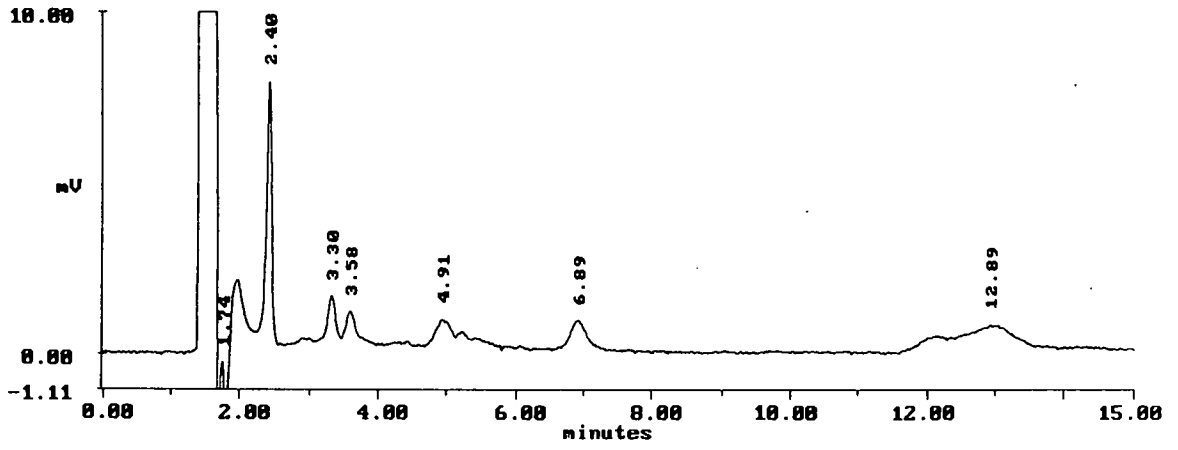

A

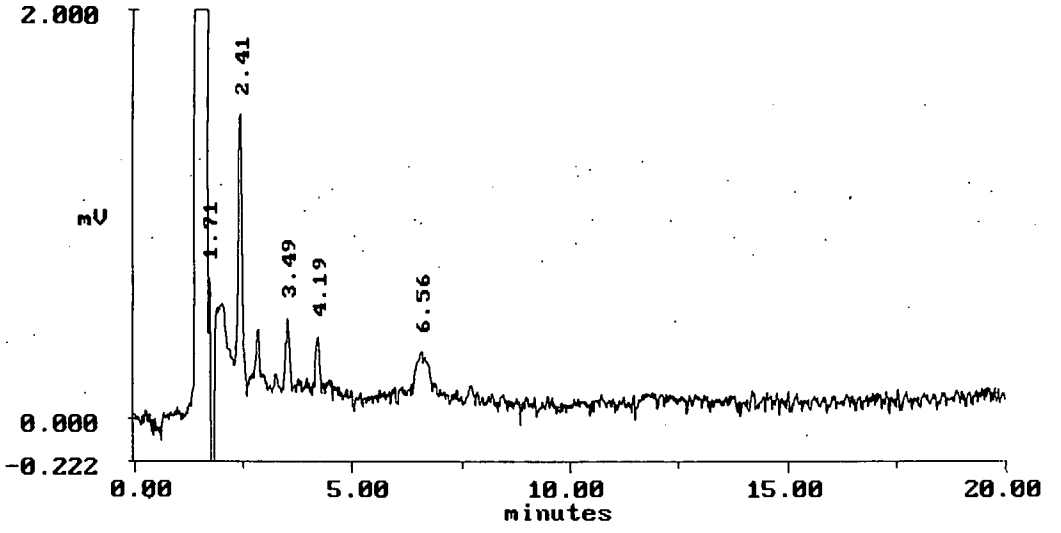

B

Figure 4.38: Chromatograms of reaction mixture at time **a)** t = 150 mins, **b)** t = 420 mins.

The butoxycarbonylaziridinofullerene adducts were prepared as outlined above and heated with TCE for 7 hours. Samples were taken at regular intervals and analysed by HPLC (system 4, 4.6 mm × 150mm FullereneSep® column, flow rate 2ml/min, mobile phase 2% ether in hexane, detection at 254nm) and by matrix assisted laser desorption ionisation (MALDI) mass spectrometry. The MALDI mass spectra were recorded on the Bruker Reflex instrument operating in linear mode. All the spectra shown are negative ion spectra. The samples for MALDI were prepared as follows. Each sample was taken up in CS_2. The matrix used was 0.1M dithranol in dichloromethane. An equal volume of sample and matrix solution was well mixed and then applied to the sample probe and allowed to dry.

Figures 4.37-4.42 show the chromatograms and the mass spectra of the reaction mixture heated in TCE for different times. By comparison of the relative intensities of the peaks as the reaction proceeds a reaction pathway was deduced, which is illustrated in Figure 4.43. As can be seen in Figure 4.37a) the initial reaction mixture contains only one peak at R.T. 4.93 min. due to formation of *bis*-butoxycarbonylaziridinofullerene (6 in Figure 4.43). After 42 min. (see Figure 4.37b), five further peaks have appeared due to the degradation of the *bis*-butoxycarbonylaziridinofullerene. These peaks occur at R.T. 3.31 and 3.58 min. (*bis*-aziridinofullerene-2 isomers, 8 Figure 4.43), at R.T. 12.85 mins (the partially degraded *bis* adduct, 7 Figure 4.43), at R.T. 6.87 mins (the mono-substituted aziridinofullerene adduct, 5 Figure 4.43) and at R.T. 2.39 min (C_{60}). The degradation is seen to be proceeding as evidenced by the chromatogram of the reaction mixture after 62 min. (see Figure 4.37c). The peak at R.T. 4.92 min. due to the starting *bis*-adduct can be seen to have decreased whilst the peaks at R.T. 2.4 mins (C_{60}) and R.T. 6.87 mins (the mono-substituted aziridinofullerene adduct, 5 Figure 4.43) have increased. In addition there are peaks at 3.31 and 3.58 min. (*bis*-aziridinofullerene) and 12.9 min. (partially degraded *bis*-adduct). Figure 4.38a) shows the reaction at a later time. The concentrations of the different reactants can again be seen to be changing from the peak heights. The C_{60} concentration is seen to be

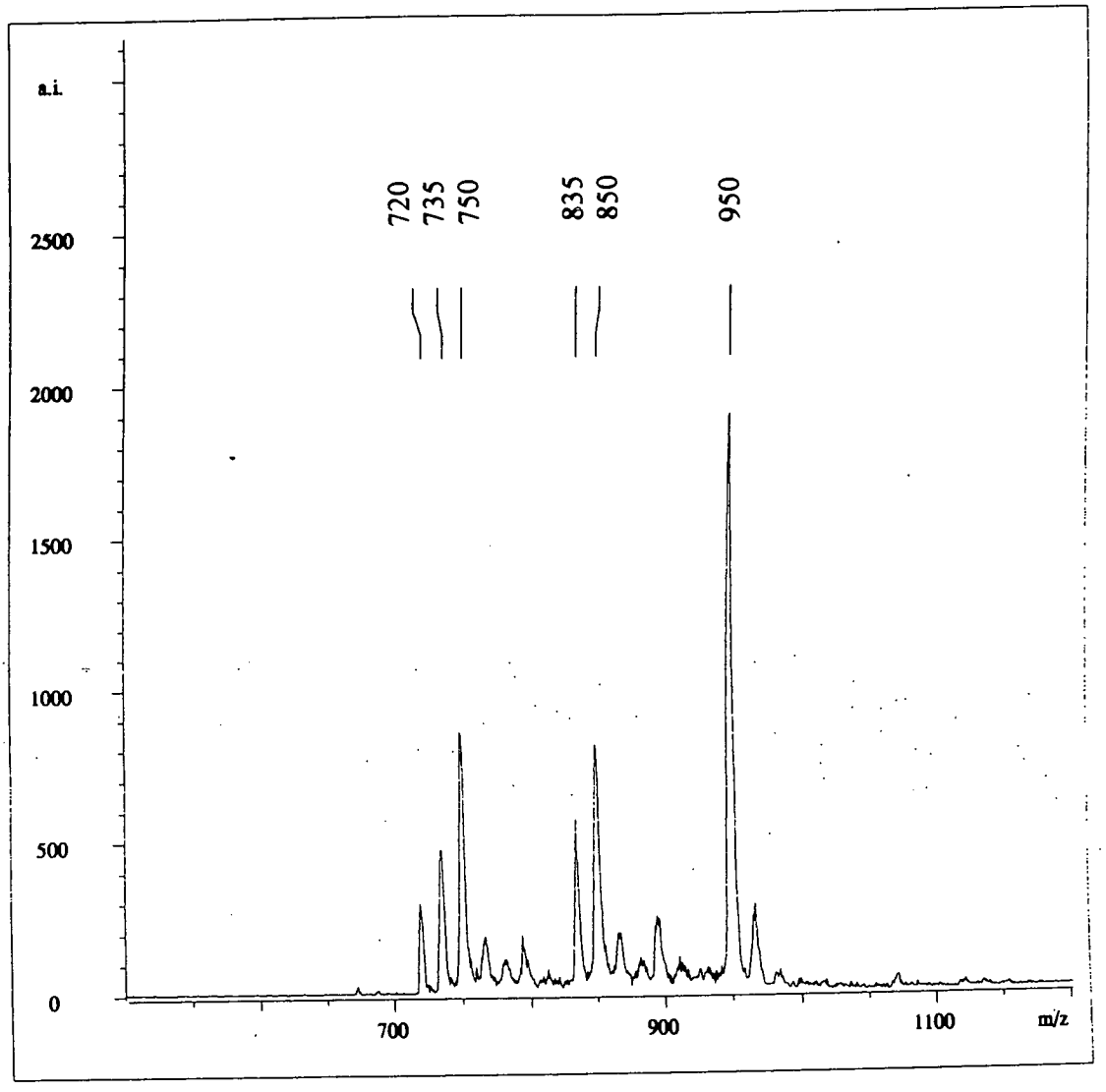

Figure 4.39: Mass Spectrum of reaction mixture after 62 mins.

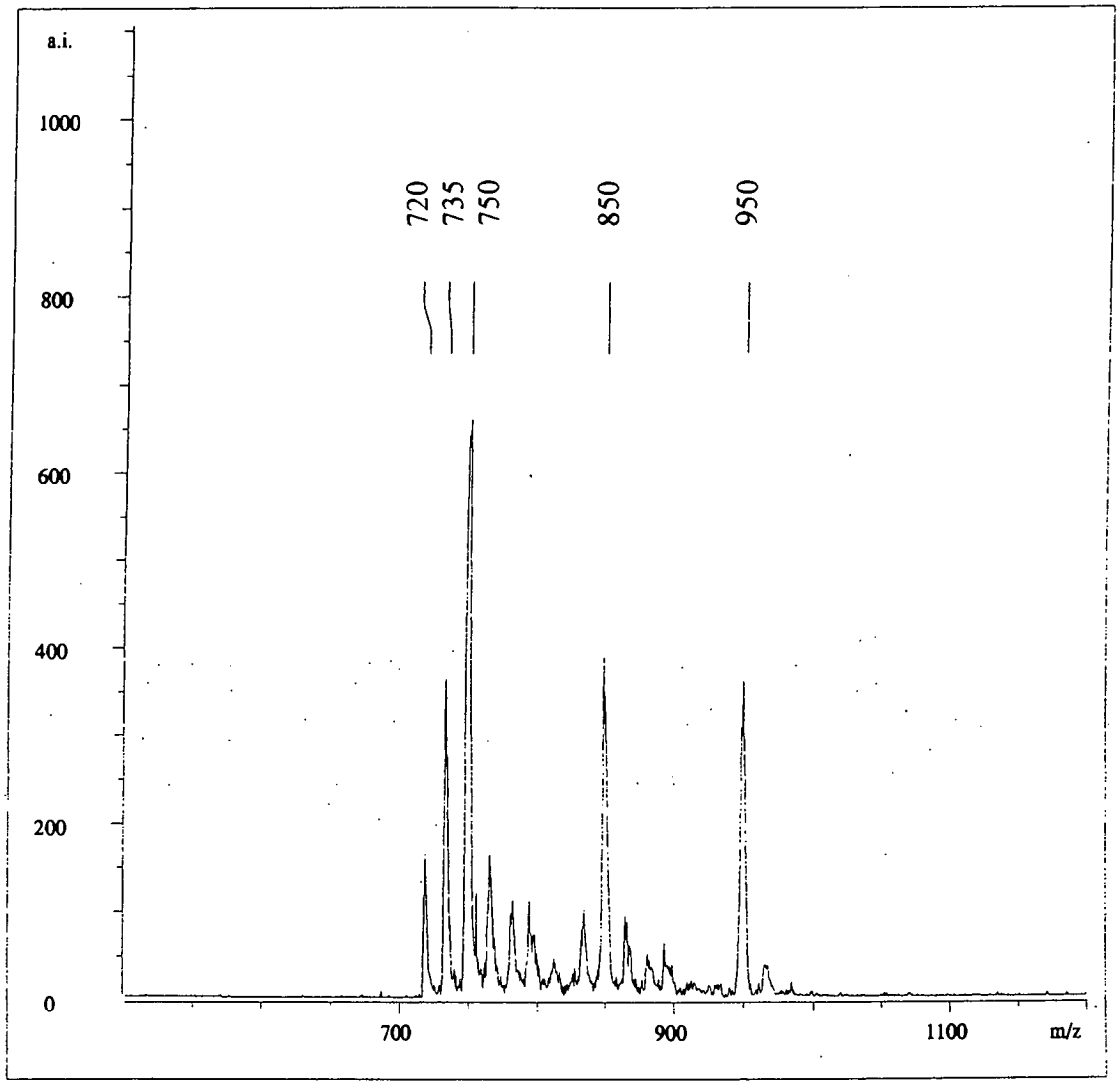

Figure 4.40: Mass Spectrum of reaction mixture after 150 mins.

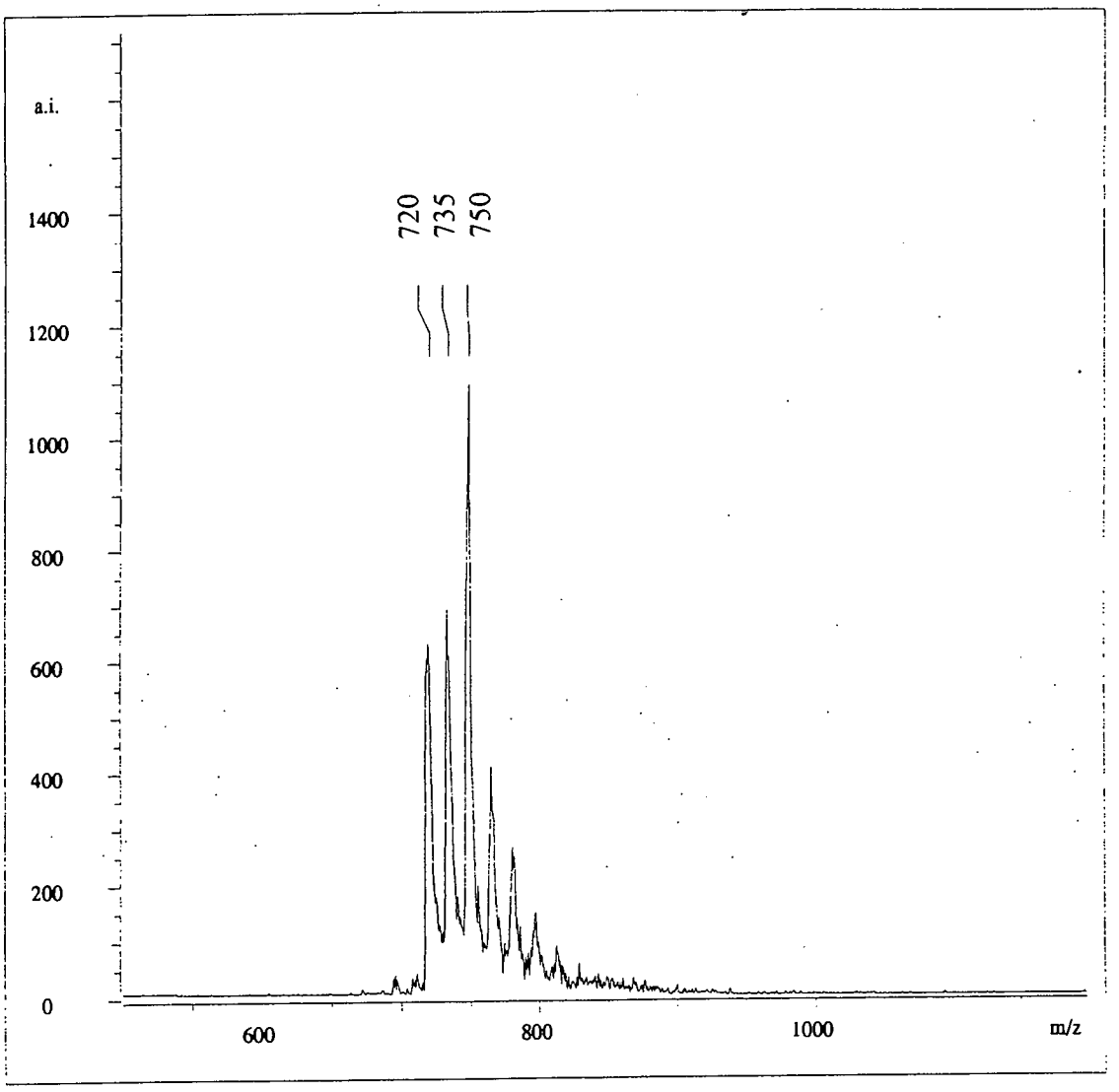

Figure 4.41: Mass Spectrum of reaction mixture after 200 mins.

increasing and there is a corresponding drop in the amount of *bis*-butoxycarbonylaziridinofullerene. The final chromatogram (see Figure 4.38b) shows the presence of C_{60}, and the *mono*- and *bis*-aziridinofullerenes only.

Figure 4.39-4.42 show the mass spectrum of the reaction mixture at different time intervals. The spectrum after 62 mins (Figure 4.39, corresponding to chromatogram 4.37c) shows the presence of *bis*-butoxycarbonylaziridinofullerene (m/z 950), the partially degraded adduct (m/z 850) and *bis*-aziridinofullerene (m/z 750). In addition the analogous mono-adducts are present: N-*tert*-butoxycarbonylaziridinofullerene (m/z 835) and aziridinofullerene (m/z 735) with the peak at m/z 720 showing the presence of C_{60}.

The mass spectrum of the reaction mixture after 150 mins is shown in Figure 4.40. This spectrum corresponds to the chromatogram shown in Figure 4.38a). The data supports the proposed reaction pathway as evidenced by a decrease in peak intensity for the *bis*-butoxycarbonyl adduct (6 Figure 4.43, m/z 950) coupled with an increase in the relative intensity of the *bis*-aziridinofullerene (8 Figure 4.43. m/z 750) after 150 mins see Figures 4.39 and 4.40. There is a parallel effect observed in the degradation of *mono*-substituted adduct (4 Figure 4.43, m/z 835) to aziridinofullerene (5 Figure 4.43, m/z 735) whilst there is no change in the intensity of the peak at m/z 850 the partially degraded *bis*-adduct (7 Figure 4.43). Figure 4.41, the mass spectrum of the reaction mixture after heating with TCE for 200 min, shows there is complete degradation of butoxycarbonyl adducts (4,6,7 Figure 4.43) to aziridinofullerenes (5,8 Figure 4.43) upon further heating. The final mass spectrum taken after 420 mins, corresponding to chromatogram 4.38b) shows these species further degrade to give C_{60} upon prolonged heating.

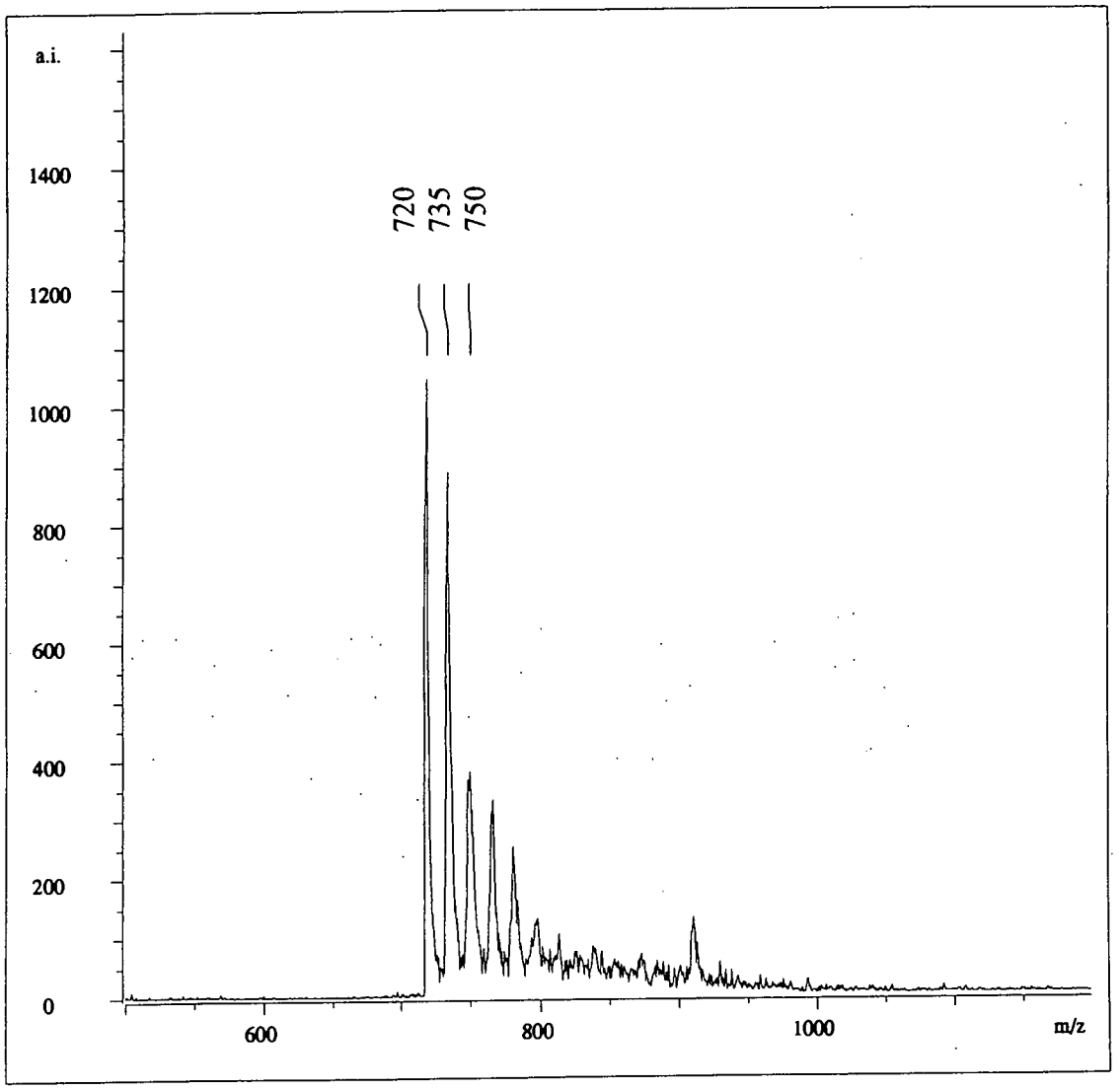

Figure 4.42: Mass Spectrum of reaction mixture after 420 mins.

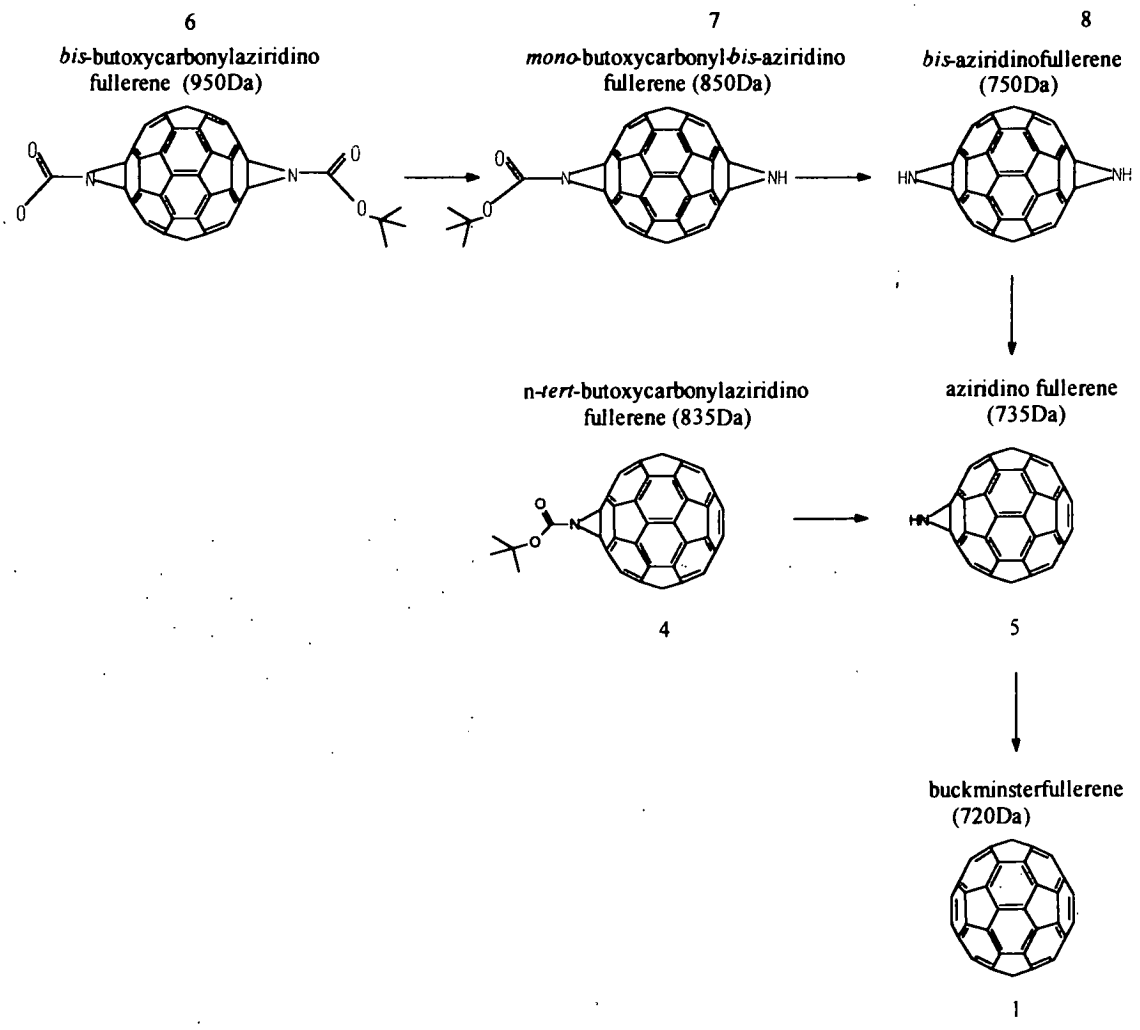

Figure 4.43: Degradation pathway of *mono*- and *bis*-substituted butoxycarbonylaziridinofullerenes.

Chapter 5

Production of Novel Carbon Species

5.1 Introduction

The current intense interest in fullerene research has led to rapid developments within the field and the exploration of new areas as related species have been discovered. Endohedral fullerenes and carbon nanotubes are two examples of these new areas. Both were discovered as a result of fullerene research and both have generated immense interest as scientists have pondered their potential. The speed with which the whole field of fullerene research moves has meant that the goalposts are constantly changing. In this chapter the results of attempts to produce both endohedral fullerenes and carbon nanotubes, using techniques that were initially developed for the production of fullerenes, are described. The aims of the experiments were to determine whether the benchtop reactor described in Chapter 2 could be adapted for the production of these novel materials.

5.1.1 Novel Carbon Species

Endohedral fullerenes are fullerene molecules, of various sizes, which have an atom, usually an alkali metal, trapped inside the carbon cage. The possibility of producing this type of compound was suggested by the detection of fullerenes containing He atoms formed as a by-product of standard fullerene production techniques. Their existence was first proposed by the Rice group [24] following experiments aimed at

proving the proposed truncated icosahedral structure for C_{60}. In these studies, a graphite disk soaked in $LaCl_3$ was laser vaporised and a strong peak for $C_{60}La$ was detected in the cluster mass spectrum.

Recently, other species formed during the fullerene production process have been discovered. The detection of carbon nanotubes, a series of progressively larger hollow carbon tubes, the smaller ones being surrounded by successively larger sizes, was initially reported by Iijima in 1991 [175]. The tubes were closed at each end, ranged from 0.7nm to 70 nm in diameter and could be up to several microns long. The possibility of the tubes having useful mechanical and electronic properties which might be modified by the introduction of foreign materials inside them has since stimulated much interest. In addition, the detection of single walled tubes has also been recently reported [176].

5.2 Endohedral Fullerenes

As mentioned above, the possibility of producing fullerenes with atoms trapped inside was first proposed in attempts to verify the structure of buckminsterfullerene; the most obvious way of confirming the hollow cage structure being to trap an atom inside it. Although early results [24] claiming to have produced endohedral $C_{60}La$ were questioned [25], a breakthrough came in 1991 when Johnson *et al* [177] reported the formation of lanthanum containing C_{82} in milligram quantities, allowing the first detailed spectroscopic characterisation of an endohedral fullerene [177]. By analogy with alkali-doped metal fullerides, in which electrons are donated to the fullerene cage by interstitial metal atoms [178], the conductivity of solid endohedral fullerenes depends on the nature of the internal dopant. This raised the possibility of some species being superconductors [179] and that others containing small polar molecules could be assembled into useful ferroelectric materials [180]. Studies of the properties of these compounds has been hampered by the difficulty in obtaining pure

samples in bulk. A brief summary of some of the production and purification techniques employed is given below.

Methods of producing endohedral fullerenes have progressed in tandem with those used in standard fullerene production. Macroscopic amounts were produced by Chai *et al* [181] using laser vaporisation of a graphite-metal composite rod in a helium filled tube-oven at high temperature. The breakthrough in producing fullerenes in macroscopic amounts by arc or resistive heating methods has led to the adaptation of these techniques for the production of endohedral species. Numerous metallofullerene species have now been produced by burning carbon electrodes packed with a metal oxide such as La, Sc and Y together with graphite powder and pitch [177][182-187].

Introduction of $Fe(CO)_5$ into the atmosphere of a carbon arc discharge has been reported to lead to the production of bulk quantities of an FeC_{60} complex [188]. A further method for the generation of endohedral fullerenes involves the vaporisation of metal oxides using a plasma torch. This has enabled species such as $Y@C_{82}$, $Y_2@C_{82}$, $Y_2@C_{84}$ to be produced in yields comparable to those obtained with arc techniques [189].

In addition fullerenes containing rare gas atoms have been detected [190] and large fullerenes, *i.e.* those with more than 100 carbon atoms in the cage, containing up to 3 or 4 lanthanum atoms have been isolated [191].

In general, however, the production of endohedral fullerenes has been an inefficient process. Although a range of species may be detectable in the soot, the amount that are actually recovered is invariably very low; typically less than a few weight per cent of the total extractable fullerenes (or less than 0.001% of the soot) are recoverable endohedral species.

The amount that may be extracted is limited chiefly by two factors; the reactivity and the solubility of the endohedral species. The use of metal carbides as the source of the metal, rather than metal oxides, has been shown to increase the yield of some endohedral fullerenes because of their oxophilicity. Similarly for these species anaerobic preparation and extraction leads to an increase in the amount recovered [192][193]. A general trend for all species is that increasing the overall metal loading increases the amount of endohedral species produced, although there is a concomitant fall in the fullerene yield [194]. However, even under optimum conditions the fraction of metal atoms encapsulated inside a fullerene is very low.

The solubility of endohedral fullerenes also greatly limits the amount that can be extracted. The exact solubilities depends on the species encapsulated but as most are contained within higher fullerenes their solubilities are generally similar to those of the higher fullerenes themselves, which are more soluble in pyridine and CS_2 than in toluene [195][196].

A further problem in producing isolated samples of endohedral fullerenes is the difficulty in separating them from their empty cage analogues due to the similarity in size and shape. Separations of conventional fullerenes have shown that these species elute in order of increasing size on most HPLC columns, with the resolution decreasing with increased cage diameter [197][198]. The preparative separation of higher endohedral fullerenes faces the same problems as the separation of conventional higher fullerenes. The presence of different isomers also means that it is difficult to achieve good separation [199].

Recently a chromatographic technique for the large scale isolation of endohedral fullerenes has been developed [194]. After extraction of the soot with solvent, typically CS_2, a preparative column is run at very high loading to remove the lower, empty fullerenes, which make up the majority of the sample. Once the highly abundant C_{60} and C_{70} species have been removed, the endohedral fullerenes can then be separated from the remaining empty fullerenes on a second column.

This technique has made possible much new research on endohedral fullerenes allowing the characterisation of pure samples of metallofullerenes such as La@C_{82}, Y@C_{82}, Sc_2@C_{84} [196][200][201] using techniques such as ESR, X-ray absorption fine structure measurements and scanning tunnelling microscopy. Recently, endohedral fullerenes for other lanthanide elements such as Gd of the type M@C_{82} have been isolated, [202] along with di-scandium, [194] tri-scandium [203] and di-lanthanum fullerenes [204].

5.2.1 Models for Formation of Endohedral Metallo-fullerenes

The mechanism for formation of endohedral fullerenes is a matter of debate. Such species have been found, like their fullerene analogues, to form under a variety of conditions and time-scales. Different mechanisms have been proposed to account for these observations. However, no one mechanism has received universal acceptance; in fact it may be that endohedral fullerenes are formed through several different pathways. A brief description of proposed formation mechanisms is given below.

Early laser vaporisation studies of composite metal/oxide graphite substrates conducted by Chi *et al* [205] and McElvany *et al* [206] led to the suggestion that mono-, bi- and tri- endohedral metallofullerene species were produced by (M@C_n)-(M@C_n) coalescence reactions in the bulk, induced by the laser irradiation [205][206].

In a different type of experiment, endohedral complexes with helium and neon atoms have been formed by accelerating ionised fullerenes and impacting them with the target atoms in the gas phase. Although this produces endohedral fullerenes, the high collision energy means the complexes are unstable [207]. Production is improved by heating the fullerene soot with the species to be inserted present in the gas phase. The mechanism proposed argues that the heating process leads to the distortion of C-C

bonds in the surface of the fullerenes temporarily opening a "window" in the cage [208].

In their investigations into fullerene formation Bowers *et al* [108] have performed ionic mobility experiments which have shown fullerenes could be synthesised by annealing polycyclic polyyne rings (see Chapter 2). To investigate whether such a mechanism is possible for endohedral fullerenes Clemner *et al* [209] performed similar experiments with LaC_{60}^{+}.

The technique employed is known as gas-phase ion chromatography [113]. In the experiments performed by Bowers *et al* [108] a pulse of C_{39}^{+} ions generated by laser vaporisation were mass selected and injected into a high pressure helium drift cell under the influence of a weak electric field. The different structural isomers (mono-, bi- and tri-cyclic rings) contained in the pulse each take a characteristic time to drift through the cell and reach the detector. Bowers *et al* found that as the injection energy of the pulse was increased a threshold for isomerisation was crossed leading to structural rearrangement; thus bi-cyclic and tri-cyclic rings would rearrange to form mono-cyclic structures or, if they had sufficient energy, fullerenes.

The studies by Clemner *et al* [209] with LaC_{60}^{+} show that the clusters are initially present as a variety of polycyclic polyyne rings. When the injection energy is increased the clusters anneal as the kinetic energy is thermalised by collisions with the buffer gas. During the annealing process it was found that nearly all of the different ring isomers (over 98%) convert spontaneously into endohedral fullerenes. This indicates there must be a mechanism by which the lanthanum atom is trapped inside the annealing fullerene. From the drift time distributions, the LaC_{60}^{+} ions become more compact on annealing. This contrasts with the behaviour of pure C_{60}^{+} on annealing, where the clusters become larger as the polycyclic rings open to produce bi- and monocyclic rings prior to rearranging to form fullerenes. The mechanism proposed by Clemner *et al* [209] to account for these observations is that the La^{+} ion acts as a nucleation centre with the carbon rings arranging themselves

around the La^+ ion, so that when they anneal the lanthanum atom is encapsulated within the fullerene cage.

5.3 Attempted Production of Endohedral Metallo-fullerenes

In the present work attempts to produce endohedral fullerenes were carried out using the benchtop fullerene reactor described in detail in Chapter 2. High purity graphite rods 3mm dia., were drilled out to a depth of 35mm and packed. In initial experiments these rods were simply packed with a mixture of graphite powder and powdered metal oxide that had been previously ground together with a mortar and pestle. The metal oxides used were cerium oxide (CeO_2) and lanthanum oxide (La_2O_3), obtained from Sigma. To investigate the effect of metal concentration, the percentage by weight of metal oxide in the metal oxide/graphite powder mix was varied from 50% to 80%.

In later experiments the rods were baked under vacuum at high temperature to convert the oxide to carbide prior to use in the reactor. Bandow *et al* [187] have shown that the yield of lanthanum fullerenes increases tenfold when using the metal carbide rather than the oxide. After the graphite rods had been packed with the metal oxide/graphite mixture they were baked at a temperature of 1200°C at a pressure of 10^{-5} torr for five hours. Upon retrieval from the oven the composite rods were stored under argon until use.

These studies were initially carried out in the reactor using a helium buffer gas pressure of 130 torr, which had been found to be optimum for production of fullerenes (see Chapter 2). Subsequently the pressure of the buffer gas was considered as a factor that may effect endohedral fullerene formation and studies were undertaken at a range of pressures between 50 and 200 torr. Extraction of the soot was carried out by ultrasound with CS_2 or pyridine in which the higher

fullerenes and endohedral species appear to have good solubility. The exact experimental procedure was as follows.

5.3.1 Experimental Procedure

High purity graphite rods 3mm dia., obtained from Erodex Ltd (Unocal Poco 76), were drilled out to a depth of 35mm using a 1mm bore drill bit. The pre-weighed drilled rods were packed with a graphite powder:metal oxide mixture and reweighed so the quantity of metal consumed could be calculated.

Arc burning of the rods was carried out in the bench top fullerene generator described in Chapter 2 operating in the dc mode. The 3mm dia. composite rod was attached to part A of the reactor (see Figure 2.10) and placed through the copper guide hole at B so that it rests on the lower 6mm dia. electrode. Prior to use the reactor was purged five times by helium filling cycles to evacuate any oxygen. The discharge arc current was set at 55 amps and the reactor brought to the desired pressure of helium. The thinner composite rod was consumed sacrificially as before. After 2 minutes the part of the rod containing the metal oxides had been consumed, the reactor was brought up to atmospheric pressure of helium and allowed to cool for 5 minutes. To minimise the exposure to air the soot was collected at the end of each run and immediately stored under argon in a preweighed container. The rods were weighed and the amount of graphite and metal consumed was calculated. After 5 rods had been burned and the soot collected and weighed a sample was analysed using LDI time-of-flight mass spectrometry (instrument A, see Chapter 3). The remainder was extracted by sonication with CS_2 or pyridine and the extracts also examined by LDI time-of-flight mass spectrometry. Prior to examination the samples were stored under argon.

The mass spectra of the samples produced using both lanthanum and cerium oxides failed to show any peaks that could be attributable to endohedral fullerenes. In view of the known pronounced oxophilicity of lanthanides, the use of lanthanum oxide as a starting material was initially thought to account for this. Use of lanthanum carbide

as a starting material was therefore investigated. However, baking the rods to convert the oxides into carbides as well as increasing the metal content of the mix, also failed to produce any detectable endohedral fullerene species in either the soot or the extract obtained with CS_2 or pyridine.

The pressure of buffer gas in the reactor as a factor affecting production of endohedral fullerenes was also investigated. The first report of the production of an endohedral fullerene, La@C_{82}, in milligram quantities by Johnson *et al* [187] involved a carbon arc reactor with a helium pressure of 200 torr. Other workers have since produced these species using pressures of helium of 50 torr [193].

For this reason attempts to produce endohedral fullerenes from rods that had been baked to convert the metal oxide to carbide were carried out at helium pressures of 50, 100, 130 and 200 torr. However, these again failed to show any peaks that could be attributable to endohedral fullerenes.

5.3.2 Results and Discussion

Failure to produce endohedral fullerenes under these optimised conditions led to examination of the technique for inherent problems. Although the rods were kept under an inert atmosphere prior to use, the reactor design meant some exposure to air was inevitable as they were inserted into the reactor prior to burning. Some exposure of the soot to the air was also unavoidable during the retrieval and extraction process. The use of a glove bag to overcome this problem was considered but was impracticable. Although exposure to air could have caused any endohedral fullerenes to react with atmospheric oxygen, the effect on the overall yield would probably not have been that great. It has been reported that the lanthanofullerenes are generally less air-sensitive than most other organolanthanide complexes [210]. For example, species such as La@C_{82} and Y@C_{82} have been shown to react only slowly with atmospheric oxygen to give insoluble products [211]. Since the retrieval and extraction processes were carried out as quickly as possible, the length of time any

endohedral fullerenes would have been exposed was minimal, and therefore the decrease in the yield would not be expected to have been great.

The failure to produce endohedral fullerenes can most likely be attributed to a problem in the actual running of the reactor. Leakage of air into the reactor caused by imperfect vacuum seals leading to the presence of oxygen at relatively high concentrations during the arc-burning process would prohibit endohedral fullerene production. This effect would be far greater than any subsequent exposure of the products to air. The reactor was known to give an imperfect vacuum, which although sufficient for standard fullerene production seems to affect the formation of the endohedral species to a far greater extent. This suggests that the formation of endohedral fullerenes requires stringent reactor conditions.

The presence of oxygen from incomplete conversion of metal oxide into carbide during the baking process is not an important factor in lowering the yield of metallofullerenes, since endohedral fullerene species can be synthesised starting from metal oxides.

Interpretation of the effect on endohedral fullerene formation of reactor conditions is severely hampered by the lack of understanding of the formation processes. Although high yields of endohedral fullerenes have been reported in carbon arc reactors under widely varying conditions, this may suggest not that these species form readily under different conditions, but that the conditions required are specific to the reactor design. As discussed in Chapter 2 the optimum conditions for fullerene production vary when using different reactors. Considerations of possible formation processes for fullerenes (discussed in Chapter 2) suggest that the temperature of the arc and the length of time the growing structure is close enough to it to allow annealing are critical factors in the formation of fullerenes. These factors will depend on operating currents and pressure of buffer gas used, which will in turn be influenced by reactor design. This would account for the often reported difficulty in reproducing successful

preparations of endohedral fullerenes using slightly different experimental arrangements.

5.4 Carbon Nanotubes

Carbon nanotubes, hollow fibre like particles, produced as a by product of fullerene formation, were initially reported by Iijima in transmission electron microscopy studies of the species found inside a standard fullerene generator [175]. The nanotubes he observed were multi-shelled, each being surrounded by a successively larger one; the innermost having a diameter of 1-2nm while the outermost shell could be up to 70 nm across. The nanotubes were found to be closed and rounded at both ends and could be several microns in length.

5.4.1 Methods for Production of Nanotubes

Since the discovery of nanotubes, there have been reports of the synthesis of other nanoparticle structures of carbon related to buckminsterfullerene. These include single-walled nanotubes [212], and nano-encapsulates, carbon nanostructures of varying geometries with metal atoms inside them [213]. The encapsulation of metal seed particles within growing carbon structures has opened up a new field of nano materials and is provoking much interest as the bulk production of these different structures is investigated.

Although research into nanotubes and nanoencapsulates is still very much in its infancy, with the investigation of the properties of these new materials only beginning, there is tremendous potential for growth. The major areas for future work are likely to involve developing a fuller understanding of the growth process parameters in order to direct growth towards a desired type of structure and, more importantly, understanding the physical properties of these novel materials which may render them of significant commercial value. Already there is the possibility of

using nanoscale encapsulation in the engineering of other novel materials with different properties. At present studies of the properties of different nanotube species are hampered by the lack of a suitable method of separating them from the soot matrix.

5.4.2 Formation Mechanism of Carbon Nanotubes

Since their discovery, nanotube research has centred on improvements in techniques for their production. From optimisation of the reactor operating parameters, conditions for producing multi-walled nanotubes in macroscopic amounts have been found [214].

The major factor affecting the yield of nanotubes has been found to be the helium pressure in the reactor. When the pressure is increased from that used for fullerene production, say 130 torr, the yield of the nanotubes rises, with a maximum at around 500 torr. Under these conditions around 75% of the consumed graphite is converted into a cylindrical deposit which forms on the larger non-consumed graphite electrode. This deposit consists of two distinct areas, an outer grey metallic hard shell and an inner black core. When examined using electron microscopy, the inner core is found to be rich in nanotubes, which are often found to be of similar size and aligned in the same direction. The grey region consists of a mixture of tubes occurring in disordered bundles [214].

The remarkable yields with which both multi- and single-walled nanotubes grow within carbon arcs indicate that their formation is an efficient process. This is surprising in view of the fact that nanoparticles with other geometries which have been observed, such as "onionites", appear to be more thermodynamically stable and should form readily in the arc [215]. The reaction pathway leading to nanotube production must therefore either be kinetically competitive, or alternatively be energetically more favourable under the specific conditions of these experiments.

Observations of nanotube production have led to suggestions of possible formation methods. Smalley *et al* [216] suggested that the mechanism for formation of multi-walled tubes involved open-ended growth in which small carbon species from the plasma add on to the reactive dangling bonds of the carbon edge of the nanotube. The parallel open tubes are thought to act as powerful field emitters with concentration of the field at the tips of the tubes. This keeps the nanotubes open and thereby enhances the electron emission from their tips, attracting the positive carbon ions which provide the feedstock for nanotube growth.

This mechanism of growth illustrates the need for a continuous stable arc to be maintained during the production of nanotubes. The tubes grow rapidly only when the tips are open, and this condition can only be sustained in the high-temperature, high-field conditions that occur in the centre of the arc. The production of bundles of nanotubes of the same length can be explained by any drop in the supply of carbon materials caused by inhomogeneity of the arc.

The presence of different layers in the deposit generated by nanotube growth is accounted for by the temperature of the arc. Near the centre of the arc any structures less thermodynamically stable than the nanotubes are immediately evaporated. The tubes in this region grow in parallel due to the flow of electrons that keeps their tips open and ensures a steady supply of C_n^+ species. Further out from the centre of the arc, where the conditions are less extreme, the other less stable nanoparticles may form. This region still consists mainly of nanotubes, but they now occur in tangled bundles and are interspersed with other structures such as "onionites".

The formation of carbon nanotubes may provide some information concerning the processes involved in fullerene formation. There has been relatively little work carried out on the formation mechanism of the tubes, and there is no single mechanism that is universally accepted. The mechanisms that have been suggested, however, propose gradual growth by addition of carbon radicals and their incorporation into a curved hexagon network. The formation of fullerenes, a species

closely related to the nanotubes, may then be expected to proceed *via* a similar mechanism. This would indicate the mechanism involves the addition of carbon radicals to a growing structure as is the case in both the "fullerene road" model proposed by Heath [103] and the "pentagon road" model suggested by Smalley *et al* [102].

The arc burning technique is also used for the production of single-walled carbon nanotubes. However, these species are produced only when metals such as Fe/Ni [217] or Co [218] are incorporated into the anode. A powder of the metal(s) is mixed with graphite and packed into a hole drilled in the graphite rod and then inserted into the reactor. The operating conditions in the reactor differ depending on the metal(s) used. For Fe or Ni the technique is the same as that used for the production of multi-walled tubes (500 torr He), whereas when Co is used the optimum conditions are similar to those used in fullerene production (130 torr). Unlike multi-walled tubes, those with single walls are found to be present in the soot rather than in a deposit on the cathode. Their formation is believed to involve a catalytic interaction between the metal and the growing carbon species on the atomic level, although no direct mechanism has yet been proposed.

5.5 Production of Carbon Nanotubes

In the present work experiments were undertaken to determine whether it was possible to produce carbon nanotubes in the simple benchtop reactor originally designed for fullerene production. As discussed below this was successfully accomplished. The technique used to produce carbon nanotubes involved a similar procedure to that employed for fullerene generation and the attempted production of endohedral fullerenes. Briefly, this involved the consumption of 3mm dia. high purity graphite rods, obtained from Erodex Ltd (Unocal, Grade Poco 76), by the resistive heating from a contact arc. The only difference in the technique from that used in

fullerene production involved the pressure of the buffer gas. The optimum pressure for the production of fullerenes in the reactor had been found to be 100 torr (see Chapter 2) whilst Ebbesen *et al* [214] have reported 380 torr (500 mbarr) helium to be optimum for the production of the nanotubes. However, as optimum conditions may vary from reactor to reactor it was decided to investigate a range of helium pressures from 100 torr to 450 torr. As no method of separating the tubes from the soot was known, samples of raw soot were taken from various positions within the reactor, *i.e.* around the electrodes and their supports or from the reactor walls, and examined for their nanotube content using high resolution transmission electron microscopy (HRTEM). As discussed further below, carbon nanotubes were successfully produced using this benchtop reactor and some good quality TEM images were obtained.

5.6 High Resolution Transmission Electron Microscopy (HRTEM)

An electron microscope uses a beam of electrons rather than a beam of light (as in an optical microscope) to form an image of an object. The instrument basically consists of a column kept under high vacuum comprising a system of electron lenses with an electron source at one end, a viewing and recording system at the other and means for mounting the specimen to be examined, in between them. In a transmission electron microscope (TEM), the sharply focused electron beam passes through a very thin metallized specimen onto a fluorescent screen, where a visual image is formed which can be photographed. This technique differs from the scanning electron microscope (SEM), which is used with thicker specimens, and forms a perspective image. In SEM, a beam of primary electrons scans the specimen and those that are reflected, together with any secondary electrons emitted, are collected. This current is used to modulate a separate electron beam in a TV monitor, which scans the screen at the same frequency, consequently building up a picture of the specimen.

A simplified diagram of a transmission electron microscope similar to the one employed in the present work is shown in Figure 5.1. The TEM column consists of three main components: 1) illuminating system-electron source and condenser lenses, 2) imaging system and specimen translation stage, and 3) image-viewing and recording system.

The column is generally mounted vertically with the electron source at the top and the imaging system at the bottom for reasons of mechanical rigidity. The column needs a high degree of rigidity and freedom from vibration if it is to produce high resolution images, (*e.g.* if an object is to be resolved to 2Å then the image must remain stationary to less than 1Å).

5.6.1 The Illuminating System

The first part of the illuminating system consists of an electron 'gun' which generates and accelerates the electrons used to illuminate the specimen. The design and performance of the electron gun is of great importance in the construction of an electron microscope; on it depends the intensity of illumination of the image and hence its visibility. The stability of the image also depends on the stability of the gun.

The second part of the illuminating system is the condenser lens. The purpose of the condenser lens is to collect and direct the illuminating electrons onto the specimen with the minimum loss of energy. By adjustment of both the electron gun and the condenser lens together, the output and the focus of the electron beam can be varied and hence the image brightness and exposure time can be controlled. Adjustment of the condenser lens also controls the area of the sample which will be illuminated.

Below the illuminating system there is a stigmator lens. This applies an equal and opposite field to the beam so that the illuminating electrons can be formed into a circular spot of maximum brightness and not be dissipated into an ellipse. Similarly

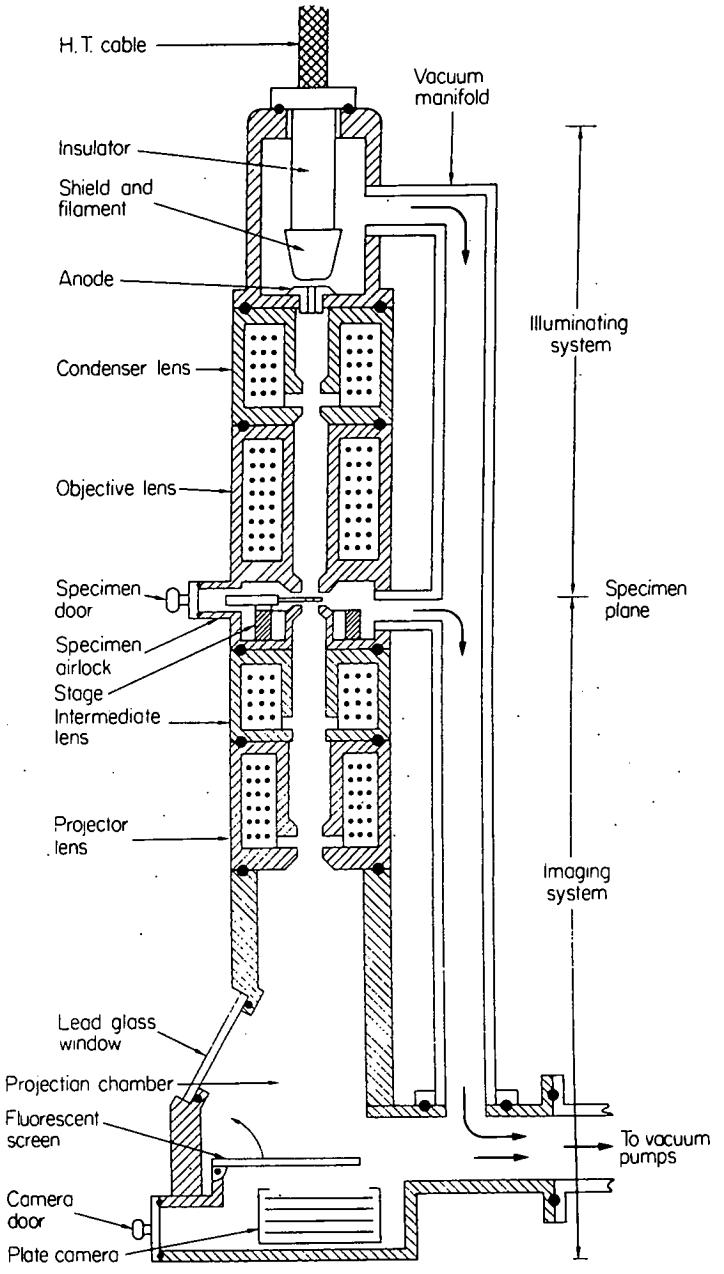

Figure 5.1: A simplified diagram of a transmission electron microscope (TEM). The TEM column consists of three main components: 1) illuminating system-electron source and condenser lenses, 2) imaging system and specimen translation stage, 3) image-viewing and recording system.

there is a further stigmata lens positioned just beneath the objective lens in the image forming system.

5.6.2 Imaging System and Specimen Translation Stage

The single most important component in an electron microscope is the objective lens. This is the first magnifying lens. The overall magnification of the sample in the electron microscope is the product of a system of three lenses, the objective, intermediate and projector lens (see Figure 5.2). Consequently, any defect in the objective lens will be magnified by the rest of the optical system.

The ray path diagram illustrated in Figure 5.2 shows how the final image is formed in a three-lens magnifying system such as is found in most electron microscopes. The range of overall magnification covered is generally from about × 10 000 to × 200 000. Final magnification is changed by altering the strength of the intermediate lens from about × 1 to about × 20. This alters the position of the object plane of the intermediate lens, and consequently the current in the objective must also be changed to compensate when the magnification is changed. This operation is also called 'focusing'.

The system shown in Figure 5.2 is used for high magnification. Two of the lenses are of high power, while the central intermediate lens is a weak lens of variable power and is used to control overall magnification. The current in the intermediate lens is controlled by the position of a step-wise 'magnification control' on the operator's desk. As the power of the intermediate lens is changed, the power of the objective lens must also be altered in order to keep the plane of the first real image, formed by the objective, coincident with the object plane of the intermediate lens. This focusing must be performed every time the magnification is changed.

The specimen itself, mounted on a suitable carrier (a thin plastic membrane supported on a copper grid), must be held rigidly in place at the exact object plane. It is possible to move the specimen in two mutually perpendicular directions whilst

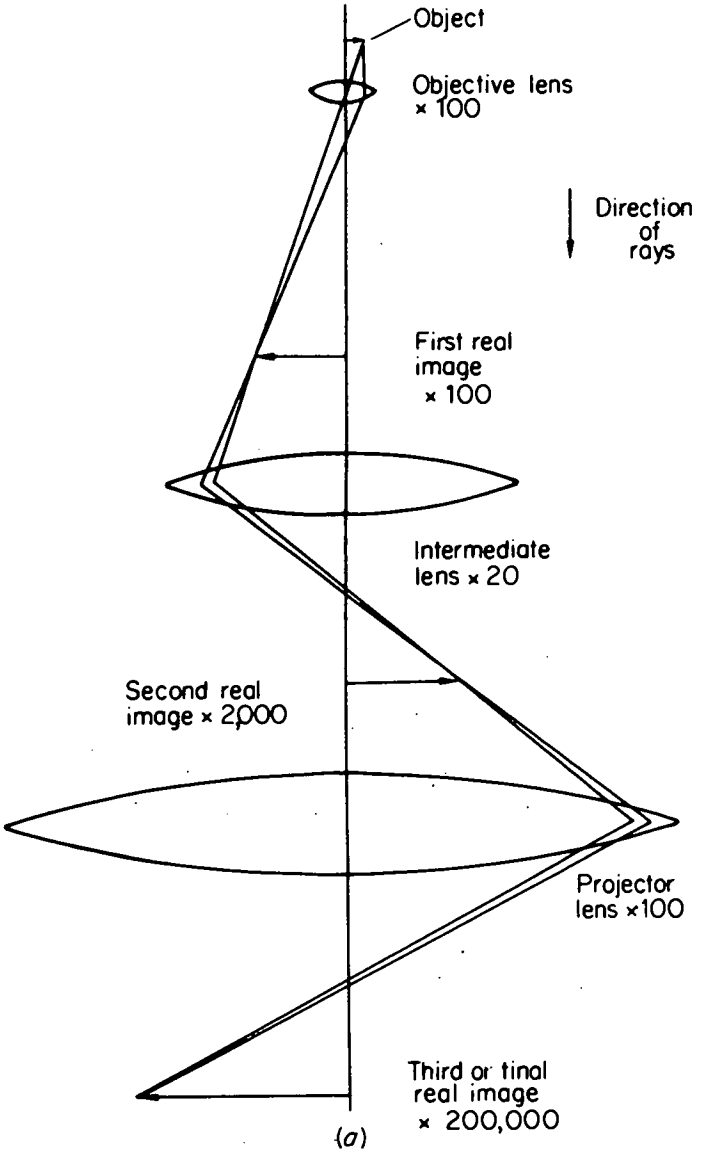

Figure 5.2: Schematic diagram of typical three-lens imaging system for TEM, comprising objective, intermediate and projector lens. The ray path diagram shows how the final image is formed

keeping it exactly in the object plane. The specimen translation stage allows reproducible movements to within ±10nm. As the column itself is operated under high vacuum, the specimen is transferred onto the specimen stage through an air-lock.

5.6.3 Image Viewing and Recording System

A real image of the specimen, that is visible to the eye, is formed below the projector lens on a screen covered with a material which fluoresces when bombarded with electrons. The material fluoresces green since this is the colour to which the dark adapted eye is most sensitive. This makes it easier to focus the image at the low brightness encountered at high magnifications. The screen can be viewed through a binocular telescope in order to see the image in more detail. The main advantage of magnifying the image in this way is that little image brightness is lost. The final image is obtained by photographing the screen.

5.7 Characterisation of Carbon Nanotubes using Transmission Electron Microscopy

Soot samples were produced by burning 3mm dia. high purity graphite rods in the benchtop reactor as described before (see section 2.4.2). Experiments were carried out at helium buffer gas pressures of 100 torr, 200 torr, 300 torr, 380 torr and 450 torr. After two production runs at each pressure samples of soot were taken from different locations inside the reactor and examined by HRTEM. Care was taken to remove any soot remaining in the reactor prior to the next run.

Samples were examined using a JEOL 100S transmission electron microscope with 100 KV accelerating voltage. Prints were taken on Kodak SO 163 film and developed in D19. Computer-based image analysis was carried out using Optimas 6 (Optimas UK Ltd.) image analysis software. The samples were prepared and handled as follows. The soot (ca. 0.3g) was dispersed in acetone (4ml) and spotted onto a copper

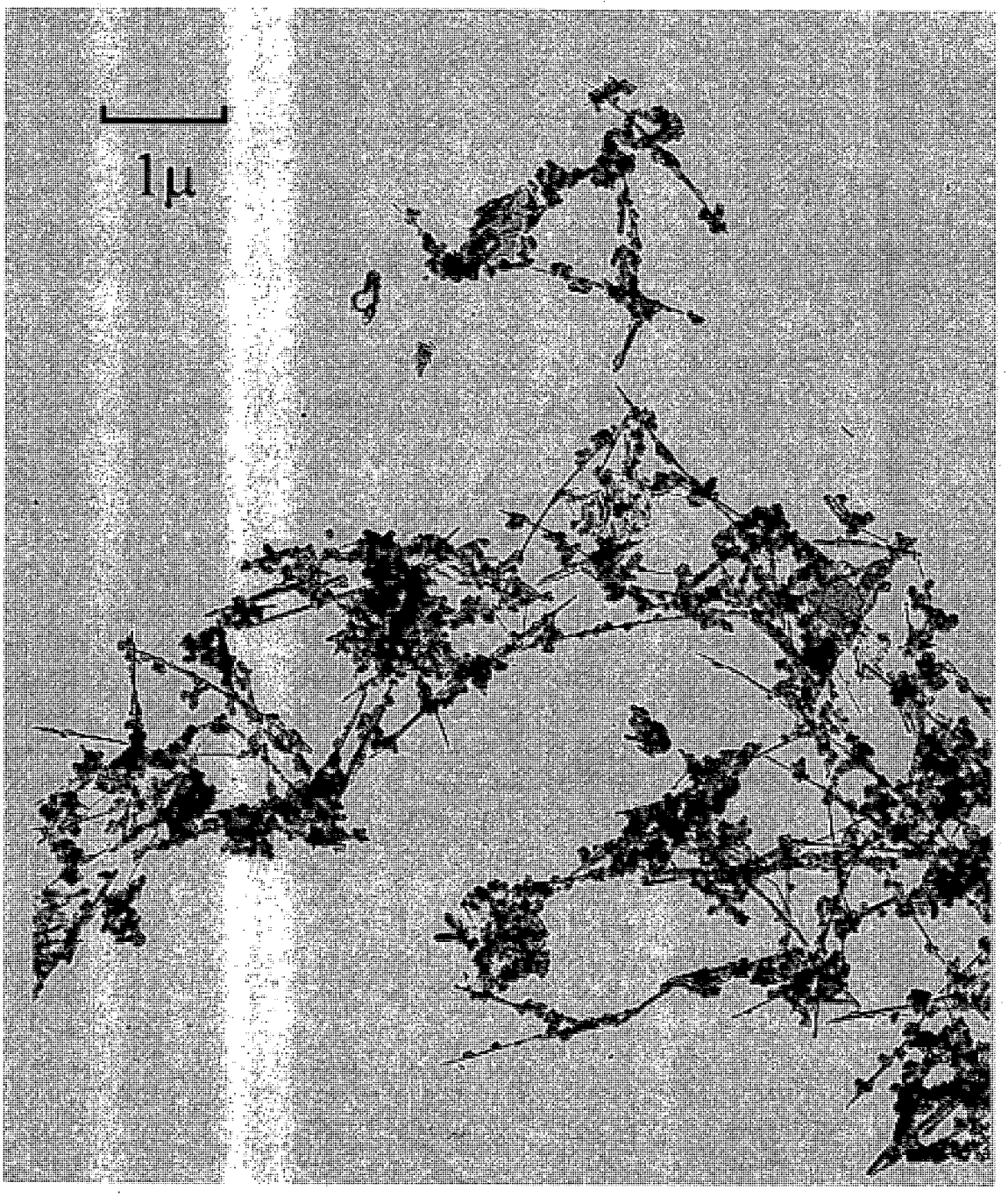

Figure 5.3: Transmission electron micrograph image of multi-walled nanotubes. Magnification × 250 000. Sample obtained from electrodes; reactor buffer gas pressure 300 torr.

Figure 5.4: Transmission electron micrograph image of multi-walled nanotubes. Magnification × 250 000. Sample obtained from electrodes; rector buffer gas pressure 380 torr.

grid covered in a thin (2nm) plastic membrane or carbon support film. The grid was transferred into the column of the microscope *via* the air-lock and examined at a range of different magnifications. Care was taken when approaching the higher magnifications that the power of the beam did not result in melting of the plastic membrane. When the image on the screen was sufficiently resolved a photograph was taken.

Electron micrographs of the carbon nanotubes produced in the reactor at magnifications between × 250 000 and × 500 000 are shown in Figures 5.3-5.9. Examination of the nanotubes revealed them to be multi-walled species of various lengths occurring in disordered bundles.

The images in Figures 5.3 and 5.4 show clusters of nanotubes at a magnification of × 250 000. The sample in Figure 5.3 was produced using a helium pressure of 300 torr, compared to a helium pressure of 380 torr for the sample shown in Figure 5.4 380. In each case the samples were taken from around the electrodes near the centre of the arc. Both show a large distribution of non-aligned multi-walled nanotubes of varying lengths.

Figure 5.5 shows an image of more isolated nanotubes at a magnification of × 250 000. This sample was taken from soot on the walls of the reactor, generated using a helium pressure of 300 torr.

Figures 5.6 and 5.7 show bundles of non-aligned multi-walled nanotubes at a magnification of × 312 000. These samples were both taken form soot on the reactor electrodes, which had been generated using a helium pressure of 380 torr. In Figure 5.6 the diameter of the innermost tube is visible in a number of the nanotubes, as the lighter area in the centre of the tube.

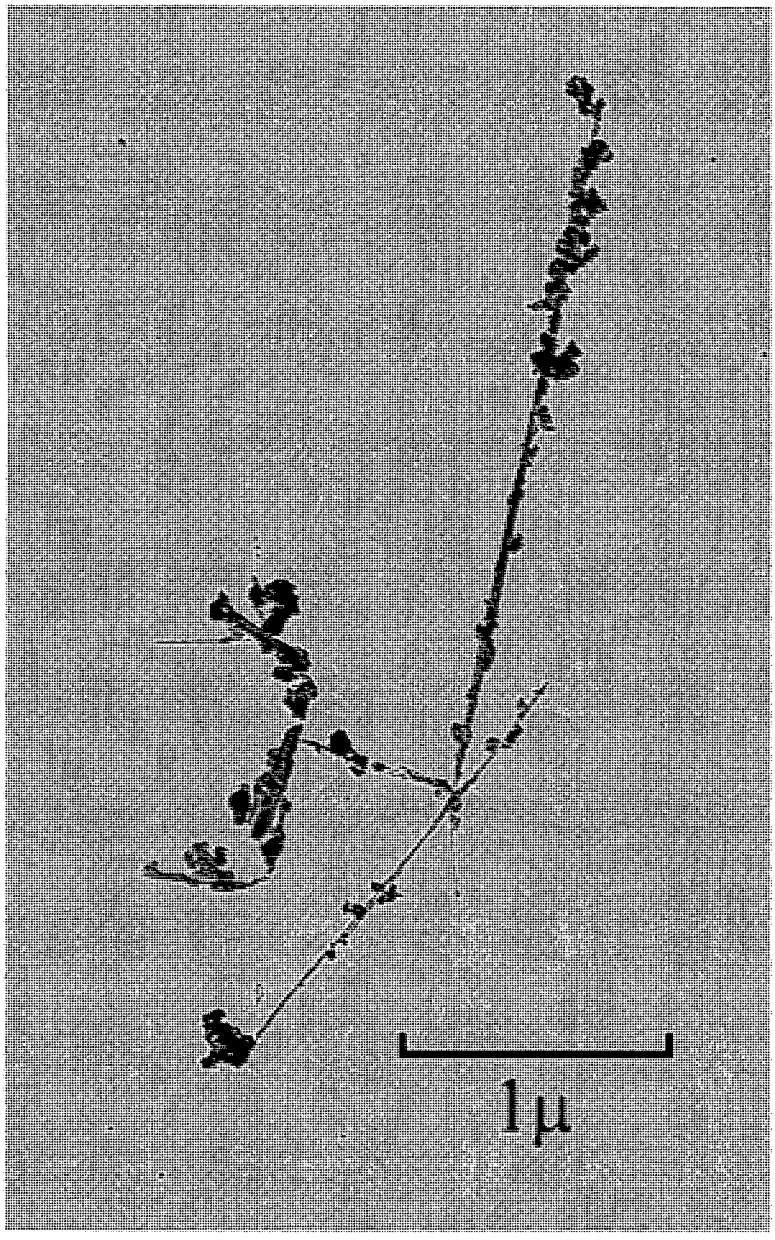

Figure 5.5: Transmission electron micrograph image of nanotubes. Magnification × 250 000. Sample obtained from walls of reactor; reactor buffer gas pressure 300 torr.

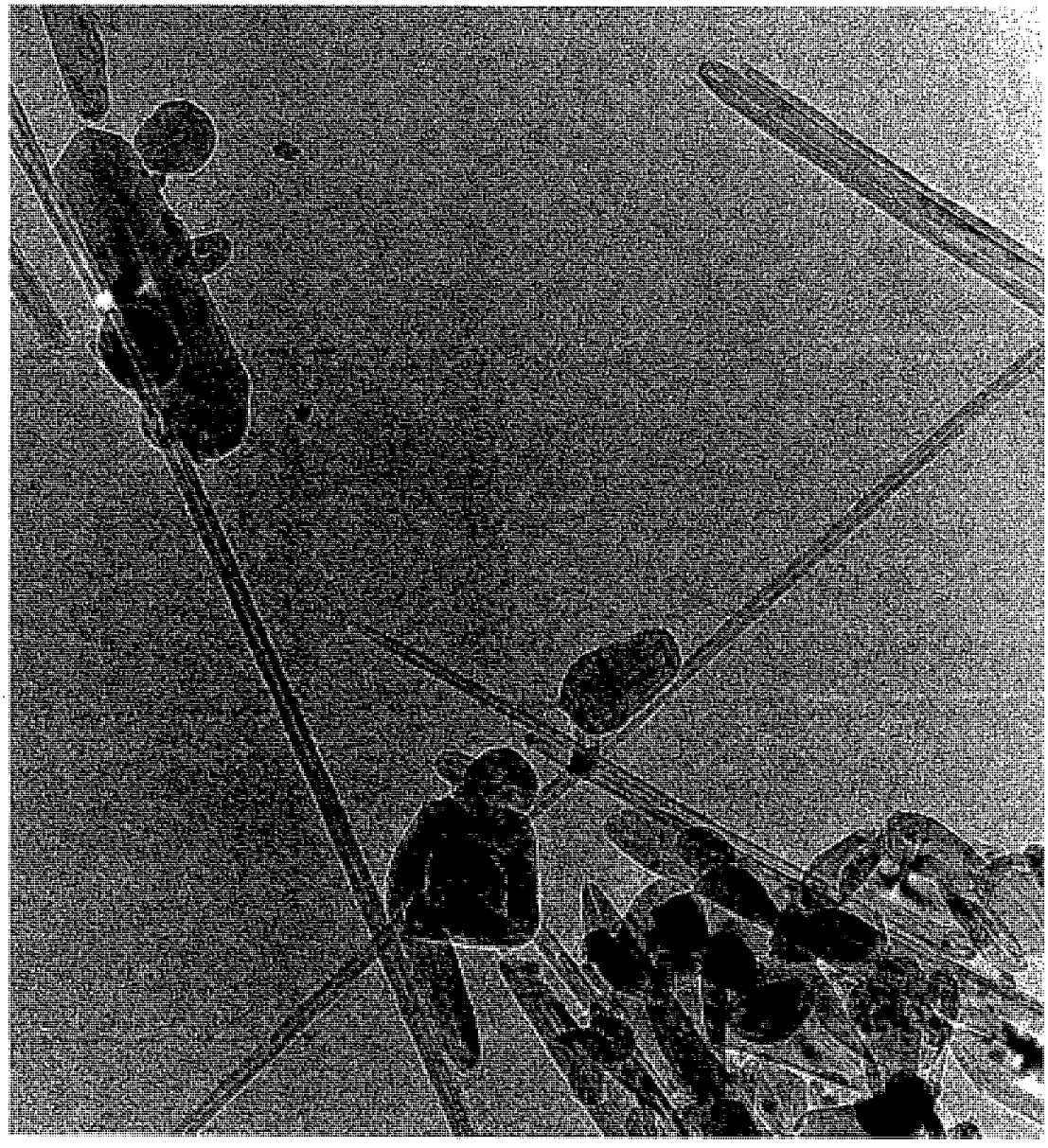

Figure 5.6: Transmission electron micrograph image of bundles of multi-walled nanotubes. Magnification × 312 000. Sample obtained from soot on the electrodes of the reactor; buffer gas pressure 380 torr.

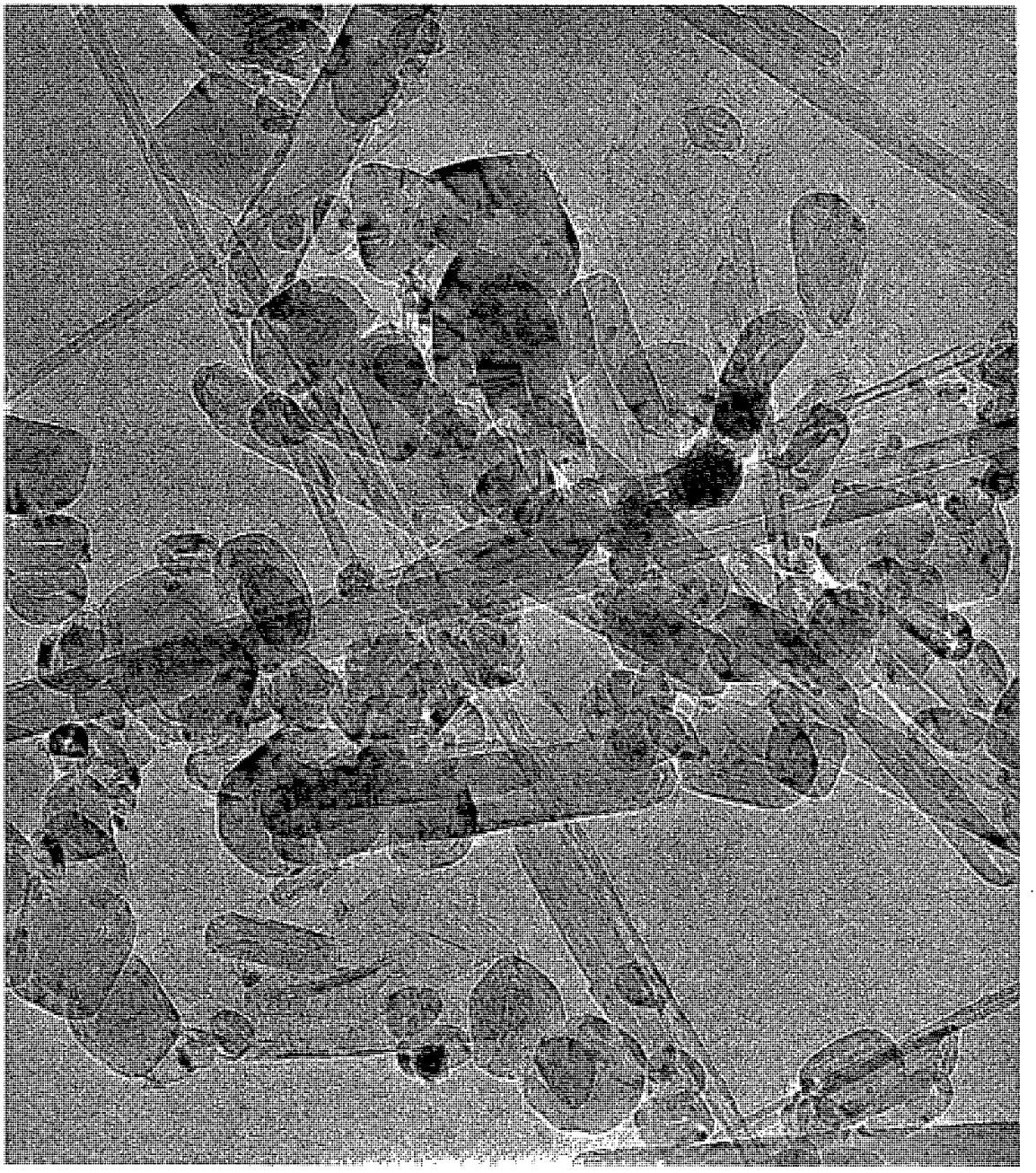

Figure 5.7: Transmission electron micrograph image of bundles of multi-walled nanotubes. The diameter of the innermost tube is visible in a number of the nanotubes. Magnification × 312 000. Sample obtained from soot on electrodes of the reactor; reactor buffer gas pressure 380 torr.

Figure 5.8 shows nanotubes at a higher magnification × 400 000. The nanotube in the centre of the figure has a slightly crooked geometry possibly due to the fusion of two tubes.

Figure 5.9 shows an image of a multi-walled nanotube at the highest magnification employed × 500 000, (scale 1.5mm:1nm). The diameters of the innermost and outermost tubes can be estimated from the superimposed scale. The innermost tube is shown corresponds to the lighter coloured area in the centre of the structure bordered by heavier grey lines. From the scale, the diameter of the innermost tube is ca. 7.5nm while that of the outer most is ca. 34nm.

Figure 5.10 shows the image of a multi-walled nanotube obtained from a soot sample generated using a helium pressure of 500 torr. The internal dimensions of the tube were examined using the Optimas 6 image analysis software. The diameter of the innermost tube was found to be 11.4nm, the distance measured is represented by the vertical indicator line **4** on the image. It can be seen that the outer diameter of the tube is not uniform. This may be due to incomplete formation of inner tubes. The diameter of the outermost tube was measured at 2 points on the image, corresponding to the two vertical indicators **6** and **7,** and found to be 83.4nm and 85.8nm ,respectively. Similarly, the distance between the outermost tube and the next one in succession was measured at three points on the image, corresponding to vertical indicators **1, 2** and **3,** and three different values were found 6.6nm, 8.4nm and 7.83nm, respectively.

Although the lack of a suitable method for separating the nanotubes from the soot matrix makes a quantitative assessment of the optimum conditions for their production impossible, qualitatively the yield of nanotubes was found to be highest with the reactor buffer gas pressure at 380 torr He. This result is based on examination of the soot produced using TEM. At a reactor pressure of 100 torr He no evidence of carbon nanotubes could be found, but as the pressure was increased, the quantity of tubes present also increased. At 200 torr the nanotubes were first

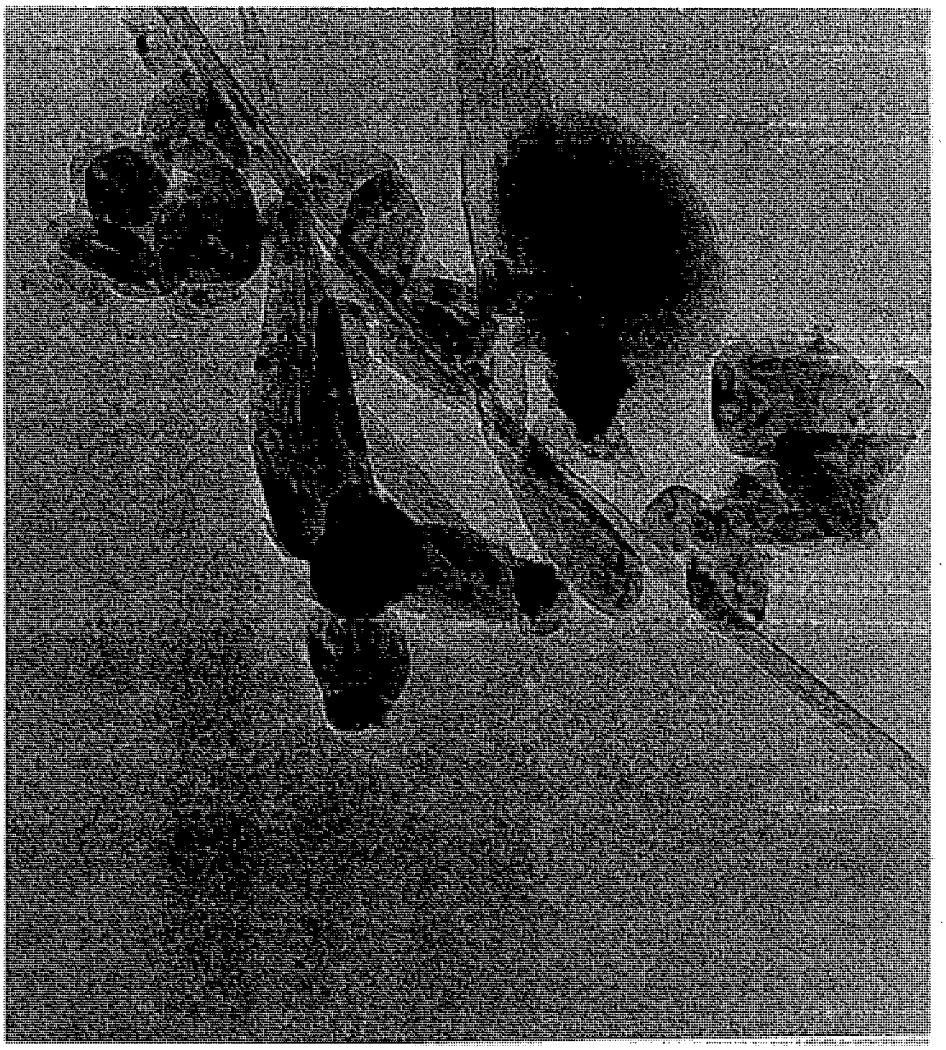

Figure 5.8: Transmission electron micrograph image of nanotube sample. Magnification × 400 000.

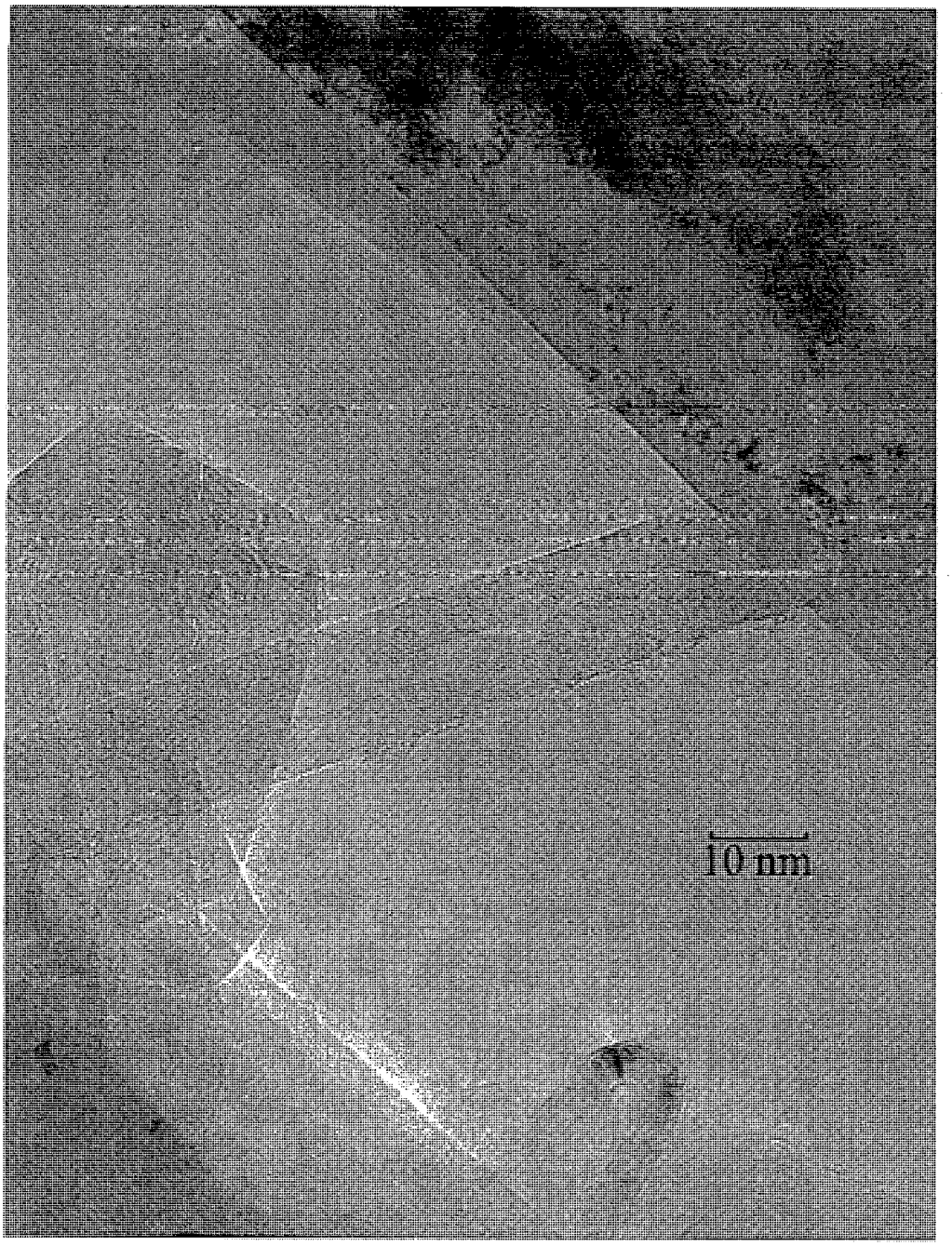

Figure 5.9: Transmission electron micrograph image of multi-walled nanotube sample, Magnification × 500 000. For the nanotube in the centre of the image the diameter of the innermost tube is ca. 7.5nm while that of the outer most is ca. 34nm.

observed in the electron micrographs. However, they occurred as individual tubes rather than being present in large clusters. With a helium pressure of 300 torr the tubes were more abundant and reached a maximum at a reactor pressure of 380 torr, above which there did not appear to be a significant change. It should be stressed, however, that this result was based purely on qualitative observations on the samples made while being examined by TEM.

Once it had been asserted that nanotube production was greatest at helium pressures around 380 torr, further rods were burned at this pressure and samples taken from different locations inside the reactor. The samples were examined by TEM and the amount of tubes present compared to determine whether there was any variation in the yield of nanotubes from different locations. Samples were taken from the reactor walls, which are at a distance of around 100mm from the centre of the arc, and from the electrodes and their supports, which are close to the centre.

The TEM micrographs showed that the samples from around the electrodes contained the most nanotubes. The hard grey deposit that had formed on the bottom electrode during production was also examined but no nanotubes were found.

The relevance that these results have to the formation scheme of the nanotubes is unclear, although a few basic inferences may be made. The greater yield of nanotubes at the higher reactor buffer gas pressures indicates that the buffer gas has a role in preventing the reacting carbon species from migrating from the centre of the arc. This is supported by the fact that a larger number of nanotubes are found at the centre of the arc compared to the periphery. Two factors that may be involved are the higher concentration of reacting species, to add onto any growing structure in the region of the arc, and the greater heat available for annealing of any structure.

The fact that the tubes occur in disordered bundles may be due to the inhomogeneity of the arc. The gravity feed mechanism for the upper sacrificial carbon rod has led to

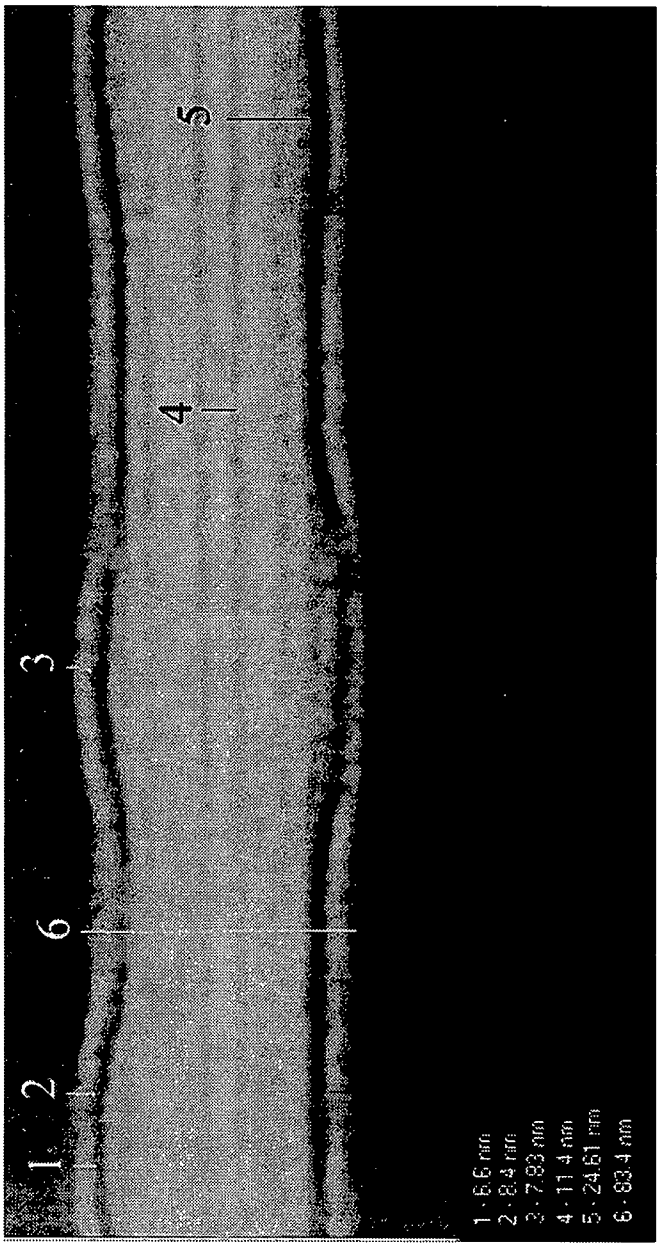

Figure 5.10: Measurement of internal diameters of a multiwalled nanotube using transmission electron microscopy and image analysis software. Several diameters along the length of the nanotube are shown by the vertical indicators. The dimensions obtained are listed at the bottom left hand side of the image.

problems with maintaining electrical contact, which is sufficient for the production of fullerenes and nanotubes, but causes the arc to sputter. This sputtering could have caused the tubes to form in disordered bundles rather than being aligned in close proximity.

5.8 Conclusions

The initial aim of the work described in this chapter was to determine whether the benchtop carbon arc reactor described in Chapter 2 and successfully used for the generation of fullerenes could be employed for production of the related species, endohedral fullerenes and carbon nanotubes. It was found that carbon nanotubes could be produced readily using a variety of conditions. Endohedral fullerenes, however, were not detected despite intensive investigations of the conditions and modifications to the procedure aimed at optimising the yield. These optimisations, involving preparation of the rods, buffer gas pressure, sample handling and extraction, were based on conditions used for successful high yield preparations reported in the literature.

The failure to detect endohedral species led to the examination of the reactor design for possible causes. The unavoidable exposure to air leading to reaction with atmospheric oxygen both before and after production was one possible cause, although the presence of oxygen during the formation process due to an imperfect vacuum was a more serious concern. The use of a glove bag to overcome this problem was considered but was impracticable. In order to completely overcome this problem the whole process would have to be carried out in a dry box.

The effect of minor variations in design between reactors is a further complication when attempting to produce endohedral fullerenes. Production of these species by carbon arc evaporation has been reported under a variety of conditions. However , several research groups have reported difficulty in reproducing these experiments

[219]. Conditions for optimum fullerene production are known to be specific to the reactor used (see Chapter 2) and the production of endohedral fullerenes would be expected to be also. The production of these species under different conditions may therefore be a result of different reactor designs. The failure to produce the endohedral fullerenes in a reactor used successfully for fullerene production indicates the need for more stringent reactor conditions for endohedral fullerene production.

In comparison with the problems encountered trying to produce endohedral fullerenes, the production of carbon nanotubes was found to be a much more facile process, and could be achieved under a variety of buffer gas pressures. The nanotubes were found to be multi-walled and of various lengths occurring in disordered bundles. They were first observed in samples produced using a reactor buffer gas pressure of 200 torr helium. The amount of nanotubes in the sample increased as the buffer gas pressure was raised, reaching a maximum at 380 torr.

The increased yield at higher pressures, along with the fact that a larger quantity of nanotubes were observed near the centre of the arc than at the periphery indicates the buffer gas prevents the carbon species from migrating from the centre of the arc, thereby increasing the time the species have to anneal and ensuring the growing structure is kept close to the supply of reactive carbon species from the arc.

Chapter 6

Concluding Remarks

The degree of interest generated in the fullerenes since their production in macroscopic amounts was first announced by Kratschmer *et al* [2] means this area is one of the "hot" topics in current scientific research. The field has attracted workers from a variety of different scientific backgrounds and now spans such seemingly diverse areas as astrophysical phenomena, high temperature superconductors, molecular wires and inhibitors of the HIV protease. The breadth of interest in the field and the speed with which it has moved has meant the emphasis of this project has changed as new areas have opened up. This chapter will summarize the work described earlier, the advances made and how developments in the wider fullerene field affected the course of the research. In addition I will give suggestions as to areas in which I would like the work to progress in the future.

The original aims of this project were to construct and develop a reactor whereby macroscopic amounts of fullerenes could be produced with the maximum of efficiency in terms of the greatest yield in the shortest time. Chapter 2 describes how this was achieved. A design was chosen and the reactor constructed. The operating parameters were investigated so that conditions were found under which the yield of fullerenes produced was optimised. This characterisation of the reactor is an important process as optimum conditions for production will differ from reactor to reactor due to any small difference in design. The productivity was measured not only by the percentage yield of fullerenes from the soot, but the time taken to produce each sample and the ease by

which the soot could be retrieved. The pressure of the buffer gas was found to be a controlling factor in the fraction of fullerenes the soot contained.

Other factors that were considered were the output current and the dissipation of the heat produced. Increased currents lead to faster production runs but considerably longer turnaround times. The optimisation of the reactor involved finding conditions which gave the maximum possible yield of fullerenes in the shortest time.

During the initial experiments, the need for certain modifications to be made to the reactor design became evident. The resulting changes to the internal geometry of the reactor greatly effected the yield of fullerenes produced., illustrating not only the importance of convection processes, but how the particular internal dimensions of the reactor may effect the yield of fullerenes. This again highlighted the importance of characterising a new reactor as small changes in design have a large effect on production.

After the characterisation process was completed experiments aimed at increasing the yield and understanding the formation mechanisms were carried out. The use of larger graphite rods resulted in a higher percentage yield of fullerenes, but the increase in power required to burn these rods meant that the overall productivity of the reactor was reduced. Further experiments involving the seeding of the graphite rods with an organic substrate tri-indane, had no noticeable effect on the yield of fullerenes although there was some difference in the C_{60}/C_{70} ratio.

The benchtop reactor provided a valuable source of the fullerene rich soot at a time when macroscopic quantities of fullerenes were extremely rare. The series of experiments by which the reactor was characterised led to the development of a set of running conditions that allowed production of between 0.5g and 0.75g fullerenes per day. In addition the

reactor was used for a series of more speculative experiments aimed at further increasing the yield and probing the formation mechanism.

The rate at which the fullerene field has developed however meant that it became financially viable to purchase commercially produced soot. This meant the emphasis of the project changed with attention now being paid to the best methods of isolating the fullerenes in high yields. However this did not mean the benchtop reactor became redundant, rather the nature of the experiments changed. As research into the fullerenes revealed the existence of novel related species the benchtop reactor was used in attempts at their production.

The experiments conducted in the production of fullerenes not only gave an insight into the factors affecting their formation but provided useful experience for the later experiments aimed at producing related species. The system of characterising the reactor and optimising production conditions was basically the same no matter what species the experiments were designed to produce.

Chapter 3 presents the techniques by which isolated, characterised fullerenes were produced. This process has many different stages, and in each stage there is a choice of techniques that may be employed. The results obtained using different protocols are given in Chapter 4.

Initial experiments involved Soxhlet extraction of the fullerene rich soot at different temperatures. The increased yields obtained with higher boiling solvents demonstrated that temperature had an effect on extraction kinetics. This effect was amplified by the findings of Ruoff *et al* [128][129] that C_{60} solubility decreases with temperature over 280K.

The unusual temperature dependence of C_{60} solubility led to the use of another extraction technique. Sonication of the soot in an ultrasound bath could be performed at ambient temperature and produced higher yields than the corresponding Soxhlet extraction. Although the sonication itself caused the solvent to heat up, the temperature could be controlled to maximise the solubility of C_{60} by limiting the time of the extraction. The use of CS_2 as extraction solvent further increased the yield.

Separation of the fullerene mixtures by a range of chromatographic techniques was investigated. Initial separations to break the extracts down into more convenient fractions was achieved by flash chromatography on a neutral alumina column. Although this technique provided both pure C_{60} samples, and samples enriched in higher fullerenes, it was an extremely lengthy and complicated process, the final fractions being obtained by extraction of the column itself.

As a result of this an alternative method of separation was investigated. Competitive complexation of fullerene mixtures with $AlCl_3$ provided a means by which large quantities of fullerene mixtures could rapidly be broken down into more convenient fractions. The various fullerene species were found to react at different rates with the $AlCl_3$ depending on their degree of polarisability, which is in turn determined by their geometry. Stopping the reaction at a particular time and retrieving the species that have reacted allows fractions enriched to various degrees in the different species to be collected. The use of HPLC to monitor the reaction allows the composition of the fractions collected to be determined. The ease and speed of this method of producing separated fullerenes meant it was used in preference to flash chromatography.

Attempts to separate the fullerenes by HPLC were first carried out on a ChiralCap® semi-preparative chromatography column, with a DNBPG stationary phase. Successful separation of C_{60} and C_{70} was achieved, however the retention times with a 100%

hexane mobile phase were found to be prohibitively long. Addition of chloroform to the mobile phase caused the retention time to decrease, however there was a corresponding fall in selectivity. The use of such a column which contains a π acidic stationary phase for the separation of fullerenes was first investigated because of the success of these stationary phases in separating similarly π electron rich polycyclic aromatic hydrocarbons [154].

The success of this interaction in separating fullerenes led to the design and development of FullereneSep® a novel stationary phase specifically for the separation of fullerenes. FullereneSep® was designed so as to maximise the π acidity whilst minimising any other effects that may inhibit interaction with the fullerenes. The ability of this stationary phase to separate fullerenes was investigated using LC-MS to characterise the different fractions. It was found to achieve excellent separation of a variety of fullerenes and give low retention times with excellent peak profiles. The success of FullereneSep® meant it was used for all future separations.

Optimised conditions for separation were found by studies on FullereneSep® under a variety of conditions. Investigation of the effect of temperature on fullerene separation revealed an interesting increase in retention at higher temperature. Calculation of the change in enthalpy on adsorption of C_{60} and C_{70} showed the process to be endothermic.

Further investigation of chromatographic parameters were undertaken when the relationship between capacity factors and molecular weight was examined. These studies found there was a linear relationship between log k′ and carbon number (molecular weight) for the fullerenes similar to that for a homologous family of straight chain carbon compounds. The use of this relationship in predicting the molecular weight of uncharacterised peaks in the chromatogram of a series of fullerenes from their retention times was demonstrated and the predictions confirmed by LDI mass spectrometry.

The combination of these techniques, the high yield extraction with CS_2 to produce the fullerene mixture, preliminary separation of the mixture into convenient fractions by competitive complexation with $AlCl_3$ and the optimised conditions for chromatographic separations on the novel stationary phase FullereneSep®, provided a means by which the fullerenes could rapidly be isolated.

The isolated fullerene samples produced in this study were characterised for the most part using single step LDI TOF mass spectrometry. The value of this technique was illustrated by a series of mass spectra. Probably the major advantage of LDI is the speed of analysis; the samples require no special preparation and simple fullerenes may be run without the use of a matrix and the spectra rapidly obtained.

The processes that may lead to discrepancies between the positive and negative ion spectra of the same sample were discussed. These discrepancies were demonstrated in the spectra of a sample containing a mixture of fullerenes. Examination of the processes that may occur for each type of ion lead to the conclusion that the negative ion mass spectra were more representative of what the sample actually contains.

The versatility of the LDI technique was demonstrated by the wide mass range that can be examined and the value of the ability to acquire data in the reflectron mode demonstrated by the ^{13}C isotopic fingerprint studies of C_{60} and C_{70}.

Finally the use of MALDI mass spectrometry in conjunction with HPLC provided a means by which the degradation of a fullerene derivative could be followed and the exact pathway deduced.

The use of the benchtop reactor in attempts to produce the related novel species endohedral fullerenes and carbon nanotubes is described in Chapter 5. Production of the

endohedral species was attempted under a variety of conditions. Extensive modifications to the technique based on the conditions for high yield production reported in the literature were implemented however no endohedral species were detected.

The failure to produce them lead to the examination of the technique for possible inherent defects. Factors such as the unavoidable exposure to air when loading and unloading the reactor were considered as was the possible presence of oxygen in the reactor chamber during production. Although the production of such species has been reported under a wide variety of experimental conditions the difficulty of reproducing these results has been reported by other groups. From the experiments carried out earlier for the production of fullerenes, it is known that small changes in reactor design can have a major effect on fullerene yields. It was therefore suggested that the reported formation of endohedral species under a range of experimental parameters could be due to the different highly specific conditions required in each particular reactor. From the results described here it certainly seems that formation of the endohedral species requires a much more stringent set of conditions than the formation of fullerenes.

In contrast the production of carbon nanotubes was found to occur under a variety of conditions with maximum yields at higher gas pressures (380 torr) than those used for fullerene production. The nanotubes produced were found to be multi-walled and occurred in disordered bundles.

6.1 Future work

The field of fullerene research is still expanding rapidly. New areas such as the carbon nanotubes are provoking the same interest C_{60} did when it was first detected, yet some of the initial problems such as how these structures can form in such high yields out of rapidly condensing carbon vapour, have yet to be solved. There is a need for further improvement to extraction and isolation protocols. As discussed the C_{60} solubility has

been found to decrease at higher temperatures, however C_{70} does not show corresponding behaviour [165]. The difference in the solubility behaviour with temperature of C_{60} and C_{70} offers a means by which fractions enriched in C_{70} may be extracted simply by carrying out the extractions at higher temperatures. Study of the solubility of higher fullerenes species as a function of temperature is also required for the possibility of developing a protocol by which different molecular weight fullerenes may be selectively extracted.

The separation of fullerenes by chromatography may be further refined. The FullereneSep® stationary phase has been shown to be able to separate fullerenes, however the separation might be improved if the number of points where the fullerene may interact with the stationary phase is increased. The design of a molecule that would act as a "cup" for the fullerenes with their unique geometry to sit in would allow such a multi-point interaction.

The area that currently provokes the greatest attention are the carbon nanotubes. The ease by which these structures may be produced has helped fire this interest. Single-walled species have been produced by the catalytic addition of metal powder into graphite rods which are subsequently combusted in the reactor. Recently Smalley *et al* [220] have reported the synthesis of single-walled nanotubes in high yields and with structural uniformity and have demonstrated the potential of these structures as molecular wires by electrical transport measurements on individual tubes. The confirmation of the potential of these species means research in this area will continue to increase in the future.

Bibliography

1. Kroto, H.W., Heath, J.R., O'Brien, S.C., Curl, R.F, Smalley,R.E., *Nature,***318**, 162, (1985).

2. Kratschmer, W., Lamb, F.D., Fostiropoulos, K., Hoffman D.R., *Nature*, **347**, 354, (1990).

3. Jones, D.E.H., *New Sci.* **32**, 245, (1966).

4. Osawa, E, Kagaku, *Kyoto*, **25**, 854, 1970 (in Japanese); *Chem. Abstr*, **74**, 75698v (in reference *Chem. Rev*, **91**, 1213, (1991).

5. Yoshida, Z., Osawa, E., Aromaticity Kagakudojin: *Kyoto* 174, (1971) (in Japanese) (in reference *Chem. Rev.* , **91**, 1213, (1991).

6. Bochvar, D.A., Gal'pern E.G., Dokl. *Akad. Nauk SSSR* **209**, 610, (1973); *Proc. Acad. Sci. USSR* **209**, 239-241(1973) (English Translation) (in reference *Chem. Rev.*, **91**, 1213, (1991).

7. Davidson, R.A., *Theor. Chim. Acta* **58**, 193, (1981).

8. Douglas, A.E., *Nature, (London)*, **269**, 130, (1977).

9. Kroto, H. W., *Chem. Soc. Rev.* **11**, 435 (1982).

10. Heath, J.R., Zhang, Q., O'Brien, S.C., Curl, R.F., Kroto, H.W., Smalley, R.E., *J. Am. Chem. Soc.*, **109**, 359, (1987).

11. Kroto, H.W., Heath, J.R., O'Brien, S.C., Curl, R.F., Smalley, R.E., *Astrophys, J.*, **314**, 352, (1987).

12. Rohfling, E.A., Cox, D.M., Kaldor, A., *J.Chem. Phys.* **81**, 3322, (1984).

13. Cox, D.M., Trevor, D.J., Reichmann, K.C., Kaldor, A., *J. Am. Chem. Soc.*, **108**, 2457, (1986).

14. Hahn, M.Y., Honea, E.C., Paguia, A.J., Schriver, K.E., Camarena, A.M., Whetten, R.L., *Chem. Phys. Letts.*, **126**, 215, (1986).

15. Bloomfield, L.A., Geusie, M.E., Freeman, R.R., Brown, W.L., *Chem. Phys. Lett.*, **121**, 33, (1985).

16. Schmaltz, T.G., Seitz, W.A., Klein, D.J., Hite, G.E., *Chem. Phys. Letts.*, **130**, 203, (1986).

17. Zhang, Q.L., O'Brien, S.C., Heath, J.R., Liu, Y., Curl, R.F., Kroto, H.W., Smalley, R.E., *J. Phys. Chem.*, **90**, 525, (1986).

18. McElvany, S.W., Nelson, H.H., Baronavski, A.P., Watson, C.H., Eyler, J.R., *Chem. Phys. Letts.* **134,** 214, (1987).

19. Weiss, F.D., Elkirid, J.L., O'Brien, S.C., Curl, R.F., Smalley, R.E., *J. Am. Chem. Soc.*, **110**, 4464, (1988).

20. Rohlfing, E.A., *J. Chem. Phys.*, **93**, 7851, (1990).

21. Hallet, R.A., McKay, K.G., Balm, S.P., Allat, A.W., Kroto, H.W., (in reference *Chem. Rev.*, **91**, 1213, (1991)

22. Doverstal, M., Lindgren, B., Sassenburg, U., Yu. H., (in reference *Chem. Rev.*, **91**, 1213, (1991)

23. Kroto, H.W., *Nature*, **329**, 529, (1987).

24. Heath, J.R., O'Brien, S.C., Zhang, Q.L., Liu, Y., Curl, R.F., Kroto, H.W., Smalley, R.E., *J. Am. Chem. Soc.*, **107,** 7779, (1985).

25. Cox, D.M., Trevor, D.J., Reichmann, K.C., Kaldor, A., *J. Am. Chem. Soc.*, **108,** 2457, (1986).

26. O'Brien, S.C., Heath, J.R., Curl, R.F., Smalley. R.E, *J. Chem. Phys.* **88**, 220, (1988).

27. Weiss, F.D., O'Brien, S.C., Elkind, J.L., Curl, R.F., Smalley, R.E., *J. Am. Chem. Soc.* **110**, 4464, (1988).

28. Fowler, P.W., Steer, J.I., *J. Chem. Soc. Chem. Commun.*, 1403, (1987).

29. Hosoya, H., *Comp. Maths. Appl.*, **12,** 271, (1986).

30. Brendsdal, E., Cynn, S.J., *Theochem*,, **57**, 55, (1989).

31. Schmaltz, T.G., Seitz, W.A., Klein, D.J., Hite, G.E., *J. Am. Chem. Soc.* **110**, 1123, (1988).

32. Luthi, H.P., Almof, J. *Chem. Phys. Lett.*, **135**, 357, (1987).

33. Halę, P.D., *J. Am. Chem. Soc.*, **108**, 6087, (1986).

34. Stanton, R.E., Newton, M.D., *J. Phys. Chem.*, **92**, 2141, (1988).

35. Disch, R.L., Schulman, J.M., *Chem. Phys. Letts.*, **125**, 465, (1986).

36. Elser, V., Haddon. R.C., *Nature*, **325,** 792, (1987).

37. Fowler, P.W., Lazzaretti, P., Zanasi, R., *Chem. Phys. Lett.*, **165**, 79-86, (1990).

38. Fowler, P.W., Lazzaretti, P., Malagoli, M., Zanasi, R., *Chem. Phys. Lett.* **179,** 174, (1991).

39. Taylor, R., Hare, J.P., Abdul-Sada, A.K., Kroto, H.W., J. Chem. Soc. Chem. Commun. 1423, (1990).

40. Parker, D.H., Wurz, P., Chatterjee, K., Lykke. K.R., Hunt, J.E., Pellin, M.J., Hemminger, J.C., Gruen, D.M., Stock, L.M., *J.Amer. Chem. Soc* **113,** 7499, (1991).

41. Howard, J.B., Lafleur, A.L., Makarowsky, Y., Mitra, S., Pope, C.J., Yadav, T., *Carbon,* **30(8)**, 1183, (1992).

42. Alexakis, T., Tsantrizos, Y.S., Meunier, J.L., Tsantrizos, P.G. in *Recent Advances in the Chemistry and Physics of Fullerenes and Related Materials* eds Kadish, K.M., Ruoff, R.S., (The Electrochemical Society, Pennington, NJ, **vol 95-10**, 32, 1995).

43. Tohji, K., Saito, K., Matsuoka, I., Sogabe, T., Nagasawa, K., *Fullerenes:Recent Advances in the Chemistry and Physics of Fullerenes and Related Materials* (eds Kadish, K.M., Ruoff, R.S.,The Electrochemical Society, Pennington, NJ, **vol 94-24**, 132, 1994).

44. Fields, C.L., Pitts, J.R., Lewandowski, A., in *Recent Advances in the Chemistry and Physics of Fullerenes and Related Materials* eds Kadish, K.M., Ruoff, R.S., (The Electrochemical Society, Pennington, NJ, **vol 95-10,** 1, 1995).

45. Khemani, K.C., Prato, M., Wudl, F., *J. Org. Chem.*, **57**, 3254, (1992)

46. Chatterjee, K., Parker, D.H., Wurz, P., Lykke, K.R., Green, D.M., Stock, L.M., *J. Org. Chem.* **57**, 3253, (1992).

47. Selegue, J.P., Shaw, J.P., Guarr, T.F., Meier, M.S., in *Recent Advances in the Chemistry and Physics of Fullerenes and Related Materials* eds Kadish, K.M., Ruoff, R.S., (The Electrochemical Society, Pennington, NJ, **vol 94-24,** 1274, 1994)

48. Banks, M.R., Gosney, I., Jones, A.C., Jones, D.S., Langridge-Smith, P.R.R., M^{c}Quillan, R.J., Thorburn, P. *Chromatographia,* **35**, 631, (1991).

49. Anderson, T., Nillson, K., Sundahl, M., Westman, G., Wennerstrom, O. *J. Chem. Soc. Chem. Commun.* 604, (1992).

50. Atwood, J.L., Koutsantonis, G.A., Raston, C.L., *Nature,* **368**, (1994).

51. Rao. A.M., Zhou, P., Wang, K.A., Hager, G.T., Holden, J.M., Wang, Y., Lee, W.T., Bi, X.X., Eklund, P.C., Cornett, D.S., Duncan, M.A., Amster, I.J., *Science,* **259,** 955, (1993).

52. Iwasa, Y., Arima, T., Fleming, R.M., Siegrist, T., Zhou, O., Haddon, R.C., Rothberg, L.J., Lyon, K.B., Carter, H.K., Jr., Hebard, A.F., Tycko, R., Dabbagh, G., Krajewski, J.J., Thomas, G.A., Yagi, T. *Science*, 264, 1570, (1994).

53. Nunez Regueiro, M., Béthoux, O., in *Recent Advances in the Chemistry and Physics of Fullerenes and Related Materials* eds Kadish, K.M., Ruoff, R.S., (The Electrochemical Society, Pennington, NJ, , **vol 94-24,** 519, 1994).

54. Vaughan, G.B.M., Heiney, P.A., Fischer, J.E., Luzzi, D.E., Ricketts-Foot, D.A., McGhie, A.R., Hui, Y.W., Smith, A.L., Cox, D.E., Romanow, W.J., Allen, B.H., Coustel, N., McCauley, J.P., Smith, A.B., *Science.* **254**, 1350 (1991).

55. Zhu, Q., Cox, D.E., Fischer, J.E., Kniaz, K., McGhie, A.R., Zhou, O., *Nature,* **355**, 712 (1992).

56. Birkett, P.R., Christides, C., Hitchcock, P.B., Kroto, H.W., Prassides, K., Taylor, R., Walton, D.R.M., *J. Chem. Soc. Perkin. Trans.* **2,** 1407 (1993).

57. Roth, G., Adelmann, P., *Appl. Phys. A*, **56,** 169, (1993).

58. Douthwaite, R.E., Green, M.L.H., Heyes, S.J., Rosseinsky, M.J., Turner, J.F.C., *J. Chem. Soc. Chem. Commun.,* 1367, (1994).

59. Crane, J.D., Hitchcock, P.B., Kroto, H.W., Taylor, R., Walton, D.R.M., *J. Chem. Soc. Chem. Commun.,* 1764, (1992).

60. Tanigaki, K., *Nature,* **352,** 222, (1991).

61. Hirosawa, I., Prassides, K., Mizuki, J., Tanigaki, K., Gevaert, M., Lappas, A., Cockcroft, J.K., *Science*, **264,** 1294, (1994).

62. Paul, P, Xie, Z., Bau, R., Boyd, P.D.W., Reed, C.A., *J. Am. Chem. Soc.* **116,** 4145, (1994)

63. Prassides, K., Christides, C., Thomas, I.M., Mizuki, J., Tanigaki, K., Hirosawa, I., Ebbesen T.W., *Science,* **263**, 950, (1994).

64. Andreoni, W. in *Physics and Chemistry of the Fullerenes,* Editor Prassides, K., Kluwer, Dordrecht, p169.

65. Hawkins, J.M., Meyer, A., Lewis, T.A., Loren, S., Hollander, F.J., *Science* **252,** 312, (1991).

66. Balch, A.L., Catalano, V.J., Lee, J.W., Olmstead, M.M., Parkin, S.R., *J. Am. Chem. Soc.* **113**, 8953, (1991).

67. Balch, A.L., Ginwala A.S., Lee, J.W., Noll, B.C., Olmstead, M.M., *J. Am. Chem. Soc.* **116**, 2227, (1994).

68. Balch, A.L., Costa, D.A., Lee, J.W., Noll, B.C., Olmstead, M.M., *Inorg. Chem.,* **33,** 2071, (1994).

69. Crane, J.D., Hitchcock, P.B., Kroto, H.W., Taylor, R., Walton, D.R.M., *J. Chem. Soc. Chem. Commun.* 1764, (1992).

70. Wang, Y., West, R., Yuan, C-H., *J. Am. Chem. Soc.,***115**, 3844, (1993).

71. Peicaud, A., Hsu, Y., Reed, C.A., Koch, A., Khemani, K.C., Allemand, P.M,, Wudl, F., *J. Am. Chem. Soc.*, **113,** 6698, (1991).

72. Bossard, C., Rigaut, S., Astruc, D., Delville, M-H., Felix, G., Fevier-Bouvier, A., Amiell, J., Flandrois, S., Delhaes, P., J. *Chem. Soc. Chem. Commun.* **333,** (1993).

73. Haufler, R.E., Conceicao, J., Chibante, L.P.F., Chai, Y., Byrne, N.E., Flanagan, S., Haley, M.M., O'Brien, S.C., Pan, C., Xiao, Z., Billups, W.E., Ciufolini, M..A., Hauge, R.H., Margrave, J.L., Wilson, L.J., Curl, R.F., Smalley, R.E., *J. Phys. Chem.,* **94**, 8634, (1990).

74. Allemand, P.M., Koch, A., Wudl, F., Rubin,Y., Diederich, F., Alvarez, M.M., Anz, S.J., Whetten, R.L., *J. Am. Chem. Soc.,* **113**, 1050, (1991).

75. Haddon, R.C., Brus, L.E., Raghavachari, K., *Chem. Phys. Letts.* **125,** 459, (1986).

76. Dubois, D., Kadish, K.M., Flanagan, S., Haufler, R.E., Chibante, L.P.F., Wilson, L.J., *J. Am. Chem. Soc.,* **113,** 4364, (1991).

77. Dubois, D., Kadish, K.M., Flanagan, S., Wilson, L.J., *J.Am. Chem. Soc.,* **113**, 7773, (1991).

78. Jehoulet, C., Bard, A.J., Wudl, F., *J. Am. Chem. Soc.* **113,** 5456, (1991).

79. Xie, Q., Arias, F., Echegoyen, L., *J. Am. Chem. Soc.* **115**, 9818, (1993).

80. Suzuki, T., Li, Q., Khemani, K.C., Wudl, F., Almarsson, O., *Science,* **254,** 1186, (1991).

81. Suzuki, T., Li, Q., Khemani, K.C., Wudl, F., Almarsson, O., *J. Am. Chem. Soc.,* **114**, 1103, (1992).

82. Suzuki, T., Li, Q., Khemani, K.C., Wudl, F., *J. Am. Chem. Soc.,* **114,** 7301, (1992).

83. Shi, S, Khemani, K.C., Li, Q.C., Wudl, F., *J. Am. Chem. Soc.*, **114**, 10656, (1992).

84. Prato, M., Li, Q.C., Wudl, F., *J. Am. Chem. Soc.*, **115,** 1148, (1993).

85. Suzuki, T., Maruyama, Y., Akasaka, T., Ando, W., Kobayashi, K., Nagase, S., *J. Am. Chem. Soc.,* **116,** 1359, (1994).

86. Maggini, M., Karlsson, A., Scorrano, G., Sandona, G., Farnia, G., Prato, M., *J. Chem. Soc. Chem. Commun.,* 589, (1994).

87. Echegoyen, L., in *Recent Advances in the Chemistry and Physics of Fullerenes and Related Materials* eds Kadish, K.M., Ruoff, R.S., (The Electrochemical Society, Pennington, NJ, **vol 94-24,** 979, 1994)

88. Haddon, R.C., Brus, L.E., Raghavachari, K., *Chem. Phys. Lett.* **125**, 459, (1986).

89. Xie, Q., Pérez-Cordero, E., Echegoyen, L., *J. Am. Chem. Soc.,* **114,** 3978, (1992).

90. Bausch, J.W., Prakash, G.K.S., Olah, G.A., Tse, D.S., Lorents, D.C., Bae, Y.K., Malhotra, R., *J. Am. Chem. Soc.* **113**, 3206, (1991).

91. Miller, G.P., unpublished results from Exxon laboratory see Chem. and Engineering News, Dec. 16, (1991).

92. Christie, K.O., Wilson, W.W., Paper presented at the Flourine Division, 203rd American Chemical Society Meeting, San Francisco, CA (1992), Paper No. 66.

93. Bausch, J.W., Prakash, G.K.S., Olah, G.A., Tse, D.S., Lorents, D.C., Bae, Y.K., Malhotra, R., ***J. Am. Chem. Soc.*** **113,** 3206, (1991).

94. Koch, A., Khemani, K.C., Wudl, F., *J. Org. Chem..*, **56,** 4543, (1991).

95. Kroto, H.W., McKay, K.G., *Nature*, **331**, 328, (1988).

96. Gerhardt, P.H., Loffler, S., Homann, K.H., *Chem. Phys. Lett.,* **137**, 306, (1987).

97. Parker, D.H., Wurz, P., Chatterjee, K., Lykke, K.R., Hunt, J.E., Pellin, M.J., Hemminger, J.C., Gruen, D.M., Stock, L.M. *J. Am. Chem. Soc.* **113,** 7499-7503, (1991).

98. Bunshah, R.F., Jou, S., Prakash, S., Doerr, H.J., Isaacs,L., Wehrsig, A., Yeretzian, C., Cynn, H., Diederich, F. *J. Phys. Chem.* **96**, 6866, (1992).

99. Taylor, R., Langley, G.J., in *Recent Advances in the Chemistry and Physics of Fullerenes and Related Materials* eds Kadish, K.M., Ruoff, R.S., (The Electrochemical Society, Pennington, NJ, **vol 95-10**, pp1-10, (1995)

100. Creasy, W.R., Brenna, J.T., *Chem. Phys.,* **126,** 453, (1988)

101. Lineman, D.N., Somayajula, K.V., Sharkey, A.G., Hercules, D.M., *J. Phys. Chem.* **93,** 5025, (1989).

102. Smalley, R.E. *Acc. Chem. Res.*, **25,** 98, (1992).

103. Heath, J.R., *Fullerenes: Synthesis, Properties and Chemistry of large Carbon Clusters* (eds Hammond, G.S. and Kuck, V.J. 1-23 American Chem. Soc. Washington DC 1991)

104. Haufler R.E., Chai, Y., Chibante, L.P.F., Conceicao, J., Jin, C., Wang, L.S., Maruyama, S., Smalley, R. E., *Mat. Res. Soc. Symp. Proc.* **206,** 627, (1991).

105. Weiske, T., Bohme, K., Hrusak, J., Kratschmer, W., Schwarz, H., *Angew. Chemie. Int. Ed. Engl.* **30 No.7**, 884, (1991).

106. Wakabayashi, T., Achiba, Y., *Chem. Phys. Lett.* **190,** 465, (1992).

107. Broyer, M., Goeres, A., Pellarin, M., Sedlmayr, E., Vialle, J.L., Woste, L., *Chem. Phys. Lett.* **Vol 198 No 1,2** , 128. (1992).

108. Helden, G.V., Gotts, N.G., Bowers, M.T., *Nature*, **363**, 60, (1993).

109. Chelikowsky, J.R., *Phys. Rev.* **B45,** 12062, (1992)

110. Hunter J.M., Fye, J., Roskamp, E.J., Jarrold, M.F., *J. Phys. Chem.* **97**, 3460, (1993).

111. Zyss, J. Chermla, D.S., *Nonlinear Optical Properties of Organic Molecules and Crystals* Vol 1 (eds Chemla, D.S., and Zyss, J.,) 23-192, (Academic press)

112. Jongerius, M.J., Drenten, R.R., Droste, R.B.J., Phillips, *J., Res.* **42,** 231. (1992).

113. Kemper, P.R., Bowers, M.T. *J. Phys. Chem.*, **95,** 5134, (1991).

114. Ashwell, J.G., Hargreaves, R.C., Baldwin, C.E., Bahra, G.S., Brown, C.R., *Nature,* **357,** 393, (1992).

115. Clays, K., Persoons, A., *Phys. Rev. Letts.,* **66,** 2980, (1991).

116. Granestrand, P., *Electron Letts.*, **50,** 816, (1987).

117. Parker, D.H., Chatterjee, K., Wurz, P., Lykke, K.R., Pellin, M.J., Stock, L.M., Hemminger, J.C., *Carbon,* **30**, 1167, (1992)

118. Haufler, R.E., *Fullerenes:Recent Advances in the Chemistry and Physics of Fullerenes and Related Materials* (eds Kadish, K.M., Ruoff, R.S.,The Electrochemical Society, Pennington, NJ, **vol 94-24,)** p50, 1994)

119. Suito, Y., Inagaki, M., Shinohara, H., *Chem. Phys. Lett.*, **200,** 643

120. Scrivens, W.A., Tour, J.M., *J. Org. Chem.* **57**, 6932, (1992).

121. De Vries M.S., Wendt, H.R., Hunziker, H., Peterson, E., Chang, S., *Proceedings of the XXII Lunar and planetary Sciences Conference,* 315 (1991).

122. Wilson M.A., Pang, L.S.K., Quezada, R.A., Fisher, K.J., Dance, I.G., Willett, G.D., *Carbon* **31**, 393, (1993)

123. Sivaraman, N., Dhamodaran. R., Kaliappan, I., Srinivasan, T.G., Vasuveva Rao, P.R., Mathews, C.K., J. Org. Chem. , **57**, 6077 (1992)

124. Ruoff,R.S., Tse, D.S., Malhotra, R., Lorents, D.C. *J. Phys. Chem.* **97**, 3379, (1993).

125. Beck, M.T., Mandi, G., Keki,S., in *Recent Advances in the Chemistry and Physics of Fullerenes and Related Materials* eds Kadish, K.M., Ruoff, R.S., (The Electrochemical Society, Pennington, NJ, **vol 95-10**, 1511, 1995).

126. Dhamodaran, R., Kaliappam, I., Sivaraman. N., Srinivasan, T.G., Vasuveva Rao. P.R., Mathews, C.K., *Indian. J. Chem* **31A&B**, F32 (1992).

127. Parker,D.H., Wurz,P., Chatterjee, K., Lykke, K.R.,, Pellin, M.J., Stock, L.M., Hemminger, J.C., *Carbon,* **30(8)**, 1167, (1992).

128. Ruoff, R.S., Malholtra, R., Huestis, D.L., Tse, D.S., Lorents, D.C., *Lett. Nature,* **362,** 140, (1993).

129. Ruoff, R.S., Olofsson, G., Wadso, I., . Beck, M.T., Mandi, G., Keki,S., in *Recent Advances in the Chemistry and Physics of Fullerenes and Related Materials*

eds Kadish, K.M., Ruoff, R.S., (The Electrochemical Society, Pennington, NJ, **vol 95-10**, 1519, 1995).

130. Smith, A.L., Li, D., King,B., Zimmerman, G., in *Recent Advances in the Chemistry and Physics of Fullerenes and Related Materials* eds Kadish, K.M., Ruoff, R.S., (The Electrochemical Society, Pennington, NJ, **vol 94-24**, 443, 1994)

131. Kumar, S.K., Szleifer, I., Sharp, K., Rossky, P.J., Friedman, R., Honig, B., *J. Phys. Chem.* **99**, 8382, (1995).

132. Hawkins, J.M., Lewis, T.A., Loren, S.D., Meyer, A., Heath, J.R., Shibato, Y., Saykally, R.J., *J. Org. Chem.*, **55**, 6250, (1990).

133. Diack, M., Compton, R.N., Guiochon, G., *J. Choratogr.*, **639**, 129, (1993)

134. Jinno, K., Uemura, T., Nagahima, H., Itoh, K., *Anal. Chem.*, **65**, 2650, (1993).

135. Cox, D.M., Behal, S., Disko, M., Goren, S.M., Greaney, M., Hsu, C.S., Kollin, *J. Am. Chem. Soc.*, **113**, 2940, (1993)

136. Nondek, L., Kuzilek,V., *Chromatographia*, **33,** 344, (1992).

137. Tse, D.S., Ruoff, R.S., Lorents, D.C., Malhotra, R., in *Recent Advances in the Chemistry and Physics of Fullerenes and Related Materials* eds Kadish, K.M., Ruoff, R.S., (The Electrochemical Society, Pennington, NJ, **vol 94-24,** 191, 1994)

138. Herren, D., Thilgen, C., Calzaferri, G., Diedrich, F., *Ibid.*, 644-188-192(1993)

139. Martin, G.B., Xiao,J., Savina, M.R., Wilks, M., Francis, A.H., Meyerhoff, M.E., in *Recent Advances in the Chemistry and Physics of Fullerenes and Related Materials* eds Kadish, K.M., Ruoff, R.S., (The Electrochemical Society, Pennington, NJ, **vol 94-24**, 178, (1994)

140. Anderson, T.H., Nilsson, K., Sundahl, L., Westman, G., Wennersrom, O., *J. Chem. Soc. Chem. Commun.* 604, (1992).

141. Saenger, W. *Angew. Chemie.*, **92**, 343, (1980).

142. Scrivens, W.A., Bedworth, P.V., Tour, J.M. *J. Am. Chem. Soc.*, **114,** 7917, (1992).

143. Scrivens, W.A., Cassell, A.M., Kinsey, K.E., Tour, J.M., in *Recent Advances in the Chemistry and Physics of Fullerenes and Related Materials* eds Kadish, K.M., Ruoff, R.S., (The Electrochemical Society, Pennington, NJ, **vol 94-24,** 166, 1994)

144. Gugel, A., Mullen, K., *J. Chromatogr.* **628,** 23, (1993),Meyer, M.S., Selegue, J.P., Vance, V.K., Guarr, T.F., *J. Chem. Soc. Chem. Commun.* 63, (1993).

145. Meyer, M.S., Selegue, J.P., *J. Org. Chem.* **57,** 1924, (1992).

146. Gugel, A., Becker, M., Hammel, D., Mindach, L., Rader, J., Simon, T., Wagner, M., Mullen, K., *Angew. Chem.* **31(5),** 644, (1992).

147. Gugel, A., Mullen, K., *Chromatographia.* **37(7-8),** 387, (1993).

148. Shinohara, H., Sato, H., Saito, Y., Takayama, M., Izuoka, A., Sugawara, T., *J. Phys. Chem.* **95**, 8449, (1991).

149. Yeretzian, C., Wiley, J.B., Holczer, K., Su, T., Nguyen, S., Kaner, R.B., Whetten, R.I., *J.Phys. Chem.,* **97,** 10097, (1993).

150. Keizer, P.N., Morton, J.R.,Preston, K.F., Sugden, A.K., *J. Phys. Chem.,* **95,** 7117, (1991).

151. Coustel, N., Bernier, P., Aznar, R., Zahab, A., Lambert, J.M., Lyard, P., *J. Chem. Soc. Chem. Commun.*, 1402, (1992).

152. Wan, T.S.M., Leung, G.N.W., Tso, T.S.C., in *Recent Advances in the Chemistry and Physics of Fullerenes and Related Materials* eds Kadish, K.M., Ruoff, R.S., (The Electrochemical Society, Pennington, NJ, **vol 95-10**, 1474, 1995).

153. Jinno, K., Nagashima, H., Itoh, K., Saito, M., Fres Buonoshita, M., *J. Anal. Chem.* **344,** 435, (1992).

154. Nondeck, L., *J. Chromatography,* **373**, 61, (1986).

155. Atwood, J.L., Koutsantonis, G.A., Raston, C.L., *Nature,* **368**, 229, (1994).

156. Rohlfing E.A., Cox D.M., Kaldor, A., *J.Chem. Phys.*,**81**, 3322, (1984).

157. L.Dunsh, U. Kirbach., K. Klostermann *J. Molecular Structure* **348,** 381-384., (1995).

158. Ulmer, G Campbell, E.E.B., Kuhnle,R., Busmann, H-G., Hertel I.V. *Chem Phys letts* **182,** 114, (1991).

159. Bethune , D.S., Meijer., G. Tang,. W.C., Rosen, H.J., *Chem Phys. Lett.* **174,** 219, (1990).

160. Creasy ,W.R, Brenna., J.T., *J. Chem. Phys.* **126,** 453, (1988).

161. Yeretzian., C. Hansen., K. Diederich,F., Whetten, R.L *Nature,* **359,**44, (1992).

162. Yang, S.H., Pettiette, C.L., Conceicao, J., Cheshnovsky, O., Smalley, R.E., *Chem. Phys. Lett.* **139**, 233, (1987).

163. Radi, P.P., Hsu, M-T., Rincon, M.E., Kemper, P.E., Bowers, M.T., *Chem. Phys. Letts.*, **174**, 223, (1990).

164. Mowat, I.A., Donovan, R.J., *Rapid Communications in Mass Spectrometry,* **9,** 82 , (1995).

165. Xihuang, Z., Jianben, L., Yongqing, W., Zhennan, G., Jun, Y., Baohuai, W., Zhifen, L., Youmin, Z. in *Recent Advances in the Chemistry and Physics of Fullerenes and Related Materials* eds Kadish, K.M., Ruoff, R.S., (The Electrochemical Society, Pennington, NJ, **95-10**, 1544 , 1995)

166. F. Wudl, K.C. Khemani, M.Prato, *J. Org. Chem;* **57,** 3254, (1992).

167. Knox, J.H., Ed, *High Performance Liquid Chromotography.* Edinburgh University Press 1978.

168. Hawkins, J.M., Lewis, T.A., Loren, S.D., Meyer, A, Heath, J.R., Shibato, Y., Saykally, R.J., *J. Org. Chem.* **55**, 6250, (1990).

169. Welch, C.J., Pirkle, W.H., *J. Chromatogr.* **89** , 609,(1992).

170. Kikuchi, K., Nakahara, N., Honda, M., Suzuki, S., Saito, K., Shiromaru, H., Yamauchi, K., Ikemoto, I., Kuramochi, T., Hino, S., Achiba, Y., *Chem. Letters,* 1607, (1991).

171. Kikuchi, K., Nakahara, N., Wakabayashi, T., Honda, M., Matsuyima, M., Moriwaki, T., Suzuki, S., Shiromaru, H., Saito, K., Yamauchi, K., Ikemoto, I, Achiba, Y., *Chem. Phys. Lett.* **188**, 177 (1992).

172. Pirkle, W.H., Welch, C.J., *J. Org. Chem.*, **56**, 6973, (1991).

173. Klute, R.C., Dorn, H.C., McNair, H.M., *Journal of Chromatographic Science,* **30,** 438, (1992).

174. Banks, M.R., Cadogan, J.I.G., Gosney, I., Hodgson, P.K.G., Langridge-Smith, P.R. *Tetrahedron letters* **35**, 9067, (1994).

175. Iijima, S. *Nature,* **354**, 56 (1991)

176. Lambert, J.M., Ajayan, P.M., Bernier, P., Planeix, J.M., Brotons, V., Coq, B., Castaing, *J. Chem. Phys. Letts.* **226,** 364, (1994)

177. Johnson ,R.D. de Vries M.S. Salem,J.R. Bethune D.S. Yannoni C.S. *Nature* **355** 239, (1992)

178. Haddon, R.C., Hebard, A.F, Rosseinsky, M.J., Murphy, D.W., Duclos, S.J., Lyons, K.B., Miller, B., Rosamilia, J.M., Fleming, R.M., Kortan, A.R., Glarum, S.H., Makhija, A.V., Muller, A.J., Eick, R.H., Zahurack, S. M., Tycko, R., Dabbagh, G., Thiel, F.A. *Nature* **350** 320 (1991).

179. Hebard, A.F., Rosseinsky, M.J., Haddon, R.C., Murphy, D.W., Glarum, S.H., Pastra, T.T.M., Ramirez, A.P., Kortan, A.R. *Nature* **350,** 600, (1991).

180. Cioslowski, J. *J, Am. Chem Soc.,* **113,** 4139, (1991), Cioslowski,J. Nanayakkara, *A. Phys. Rev. Letts.* **69**, 2871, (1992)

181. Chai, Y. Guo, T., Jin, C., Haufler, R., Chibante, L.P.F., Fure, J., Wang, L., Alford, J.M., Smalley, R.E. *J.Phys.Chem.* **95,** 7564, (1991) .

182. Hoinkis, M., Yannoni, C.S., Bethune, D.S., Salem, J.R., Johnson, R.D., Crowder, M.S., De Vries, M.S., *Chem. Phys. Letts.* **198,** 461, (1992).

183. Suzuki, S., Kawata, S., Shiromaru, H., Yamauchi, K., Kikuchi, K., Kato, T., Achiba, Y. *J. Phys. Chem.* **96**, 7159, (1992).

184. Alvarez, M., *J. Phys. Chem.* **95**, 10561, (1991).

185. Ross, M.M., Nelson, H.J., Callahan, J.H., McElvany, S.W. *J. Phys. Chem.* **96**, 5231, (1992)

186. Shinohara, H., Sato, H., Saito, Y., Ohkochi, M., Ando, Y., *J. Phys. Chem.* **96,** 3571, (1992).

187. Bandow, S., Shinohara, H., Saito, Y., Ohkochi, M., Ando, Y., *J. Phys. Chem.* **97**, 6101, (1993).

188. Pradeep, T., Kulkarni, G., Kannan, K. R., Row T.G. Rao.C. *J. Am. Chem. Soc.* **114,** 2272, (1992).

189. Yoshie, K. Kasuya, K., Eguchi, K. Yoshida,T. *Appl. Phys. Lett.* **61,** 2782, (1992).

190. Saunders M., Jimenez-Vasquez, H.A., Cross,R.J. Poreda,R.J., *Science* **259**, 1428, (1993)

191. Smalley R.E. in *Fullerenes: Properties and Chemistry of Large Carbon Clusters* (eds Hammond G,Kuck, V.) 141-159 (Am. Chem. Soc., Washington D.C. 1992)

192. Bandow.,S. Kitagawa, H., Mitani, T., Inokuchi, H., Saito, Y, Yamaguchi, H., Hayashi, N., Sato, H., Shinohara, H., *J. Phys. Chem.* **96,** 9609, (1992)

193. Shinohara, H., Yamaguchi, H., Hayashi, N sato, H., Ohkohchi, M., Ando, Y., Saito, Y. *J. Phys. Chem.*, **97,** 4259, (1993).

194. Gillan E.G. Yeretzian, C., Min, K.S., Alvarez, M.M., Whetten, R.L., Kaner, R.B. *J.Phys. Chem.* **96**, 6869, (1992).

195. Ross, M.M. Nelson H.J., Callahan, J.H. Mcelvany,S.W. *J. Phys. Chem.* **96**, 5231, (1992).

196. Shinohara,H., Sato,H. Saito.Y., Ohkohchi, M. Ando,Y., *J. Phys. Chem.* **96**, 3571, (1992).

197. Diack, M. Hettich,R.L., Compton,R.N., Guiochon,G. *Anal. Chem,* **64**, 2143, (1992).

198. Kimata,K.,Hosoya,.K.Araki.T.,Tanaka,N. *J. Org. Chem.*, **58,** 282, (1993).

199. Anacleto, J.F., Quilliam, M.A., *Anal. Chem.*, **65**, 2236, (1993)

200. Kikuchi, K., Nakao, Y., Achiba, Y. in *Recent Advances in the Chemistry and Physics of Fullerenes and Related Materials* eds Kadish, K.M., Ruoff, R.S., (The Electrochemical Society, Pennington, NJ, , **vol 94-24**, 1300, (1994)

201. Wang, X.D., Xue, Q.K., Hashizume, T., Shinohara, H., Nishina, Y., Sakurai, T., *Physical Review B*, **48, No 20**, 15 492

202. Kikuchi, K., Kobayashi, K., Sueki, S., Suzuki, S., Nakahara, H., Achiba, Y., Tomura, K., Katada, M., *J. Am. Chem. Soc.* **116,** 9775, (1994).

203. Shinohara, H., Inakuma, M., Hayashi, N., Sato, H., Saito, Y., Kato, T., Bandow, S., *J. Phys. Chem.*, **98,** 8597, (1994).

204. Alvarez, M.M., Gillan, E.G., Holczer, K., Kaner, R.B., Min, K.S., Whetten, R.L., *J. Phys. Chem.* **95**, 10561, (1991).

205. Chai,Y., Guo,T., Jin,C., Haufler,R.E., Chibante,L.P.F., Fure,J., Wang,L., Alford,J.M., Smalley,R.E., *J.Phys.Chem.*, **95,** 7564, (1991)

206. McElvany,S.W., *J.Phys.Chem.*, **96,** 4935, (1992).

207. Wan. Z., Christian.J.F., Anderson,S.L., *J.Chem. Phys.*,**96**, 3344, (1992).

208. Moran-Lopez,J.L., Cabrera-Tujillo, J.M., Dorantes-Davilla,J., *Solid State Communications* **96, No.7,** 452, (1995).

209. Clemner, D.E., Shelimov, K.B., Jarrold, M.F. *Nature*, **367,** 718, (1994).

210. Weaver,J.H., Chai,Y., Kroll,G.H., Jin,C.,Ohno.,J.R., Haufler.,R.E., Guo.,T., Alford,J.M., Conceicao.J., Chibante.,L.P.F., Jain.A., Palmer.,G., Smalley,R.E., *Chem. Phys. Letts.* **190,** 460, (1992).

211. Kikuchi,K., Nakao,Y., Suzuki,S., Achiba,Y., Suzuki,T., Maruyama.,Y., *J.Am. Chem.Soc.*, **116**, 9367, (1994)

212. Iijima, S., Ichihashi, T., *Nature* **363**, 603, (1993),Bethune, D.S., Kiang, C.H., de Vries, M.S., Gorman,G., Savoy, R., Vazquez, J., Beyers, R., *Nature* **363**, 605, (1993).

213. Ruoff, R.S., Lorents, D.C., Chan, B., Malhotra, R., Subramoney, S., *Science,* **259,** 346, (1993).

214. Ebbesen, T.W., Ajayan, P.M., *Nature*, **358,** 220, (1992).

215. Ugarte,D *Nature* **359,** 707, (1992).

216. Colbert, D.T., Zhang, J., McLure, S.M., Nikolaev, P., Chen, Z., Hafner, J.H., Owens, D.W., Kotula, P.G., Carter, C.B., Weaver, J.H., Rinzler, A.G., Smalley, R.E. Science, **266,** 1218, (1994).

217. Seraphin, S. in *Recent Advances in the Chemistry and Physics of Fullerenes and Related Materials* eds Kadish, K.M., Ruoff, R.S., (The Electrochemical Society, Pennington, NJ, , **vol 94-24**, 1433, (1994)

218. Bethune, D.S. Kiang, C.H., de Vries, M.S., Gorman, G., Savoy, R., Vasquez, J., Beyers, R. *Nature* **363**, 605, (1993).

219.a) Kroto, H.W., Private communication, **b)** Shinohara, N., Private communication

220. Tans, S.J., Devoret, M.H., Dai, H., Thess, A., Smalley, R.E., Geerligs, L.J., Dekker, C., *Nature*, **386**, 474, (1997).